Establishment and Characterisation of Chemoresistant Osteosarcoma Cell Lines by Single and Multi-Agent Induced Strategies

A thesis submitted to Middlesex University in partial fulfilment of the requirements for the Degree of Doctor of Philosophy

Kaan Low

M00514680

Faculty of Science and Technology

Department of Natural Sciences

Middlesex University London

May 2022

Abstract

Osteosarcoma is a rare malignant bone tumour that occurs primarily in adolescents and young adults. Prior to the adoption of chemotherapy in mid 1970s, more than 85% if post-surgery osteosarcoma patients developed metastasis. Nowadays, standard osteosarcoma treatment of osteosarcoma includes neo-adjuvant chemotherapy followed by surgical removal and adjuvant multi-drug chemotherapy. The combination of cisplatin, doxorubicin and high-dose methotrexate is the standard treatment for most patients. Surgery combined with chemotherapy has improved the survival rate for osteosarcoma patients to 60% - 70%. However, most of the patients with metastatic or recurrent osteosarcoma have poor prognosis due to the development of chemotherapeutic drug resistance.

Developing drug-resistant cancer cell models is one approach to study the mechanisms of chemoresistance in cancer cells. In this study, clinically relevant chemoresistant osteosarcoma cell models were developed from the cell lines MG-63 and HOS-143B. One of the strategies used the current study includes a multiple drugs combination approach, where cisplatin, doxorubicin, and methotrexate are combined in one treatment. The purpose of this method is to simulate a similar experience with osteosarcoma patients who are receiving clinical chemotherapy treatment and therefore, to establish a clinically relevant osteosarcoma-resistant model to study the mechanisms of drug resistance.

Cisplatin, doxorubicin, and methotrexate were used as single agents and in triple combination. The highest level of resistance to cisplatin was observed in MG-63/CISR8 (3.56 ± 0.43-fold; $p=0.001$), doxorubicin in HOS-143B/DOXR8 (1.99 ± 0.20; $p=0.0002$), and methotrexate in HOS-143B/MTXR8 (3.77 ± 0.90-fold; $p=0.046$). The MG-63/TRIR8

and HOS-143B/TRIR8 triple-resistance models showed lower levels of resistance, 2.28 ± 0.63-fold (p=0.032) and 2.17 ± 0.13-fold resistant (p=0.0004) to combination treatment; and were not resistant to the drugs individually. Apoptosis assays suggest that the resistance in MG-63/TRIR8 is mainly from cisplatin and methotrexate and not doxorubicin. In contrast, the resistance in HOS-143B/TRIR8 is mainly from doxorubicin and methotrexate instead of cisplatin. Upregulation of P-glycoprotein was seen in all resistant models except those developed with single-agent methotrexate. The P-glycoprotein inhibitor elacridar reversed the resistance of doxorubicin on MG-63/DOXR8 (0.36 ± 0.06-fold, p=0.003), MG-63/TRIR8 (0.72 ± 0.07-fold, p=0.04), HOS-143B/CISR8 (0.47 ± 0.09-fold, p=0.009), and HOS-143B/TRI (0.45 ± 0.03-fold, p=0.0005). The migration rate of the MG-63 resistant models was significantly increased by 2.12 – 2.46-fold, their invasion rate tended to increase, and RT-PCR showed a switch from epithelial to mesenchymal gene signalling. In contrast, a significant decrease in migration was seen in HOS-143B resistant models with 0.39 – 0.43-fold, their invasion rate tended to decrease and a switch from mesenchymal to epithelial gene signalling occurred.SPHK1 and HIF1A were upregulated in most of the resistant models from the PCR array analysis and SPHK1 protein level was also determined to increase in MG-63/CISR8 (2.03 ± 0.08-fold, p=0.034), MG-63/DOXR8 (1.77 ± 0.24-fold, p=0.02), and HOS-143B/CISR8 (3.55 ± 0.84-fold, p=0.0459). A strong correlation (r=0.726) was shown between the gene expression of SPHK1 and HIF1A in HOS-143B resistant sublines.

Currently, there is also a lack of effective treatments for patients who experience relapsed osteosarcoma. One treatment for relapsed patients is gemcitabine and docetaxel combination chemotherapy (GEMDOX). A systematic review was performed in this study to investigate the efficacy of combination therapy of gemcitabine and docetaxel on

relapsed osteosarcoma patients. The results showed the age and gender of the patients would have a prognostic effect on the GEMDOX regimen as the second-line treatment for relapsed osteosarcoma, whereas the GEMDOX therapy was determined to have a higher efficacy on male patients and with age <18. There was no difference in toxicities between different doses (675 mg/m^2 and 1,000 mg/m^2) of the GEMDOX regimen, age, or gender of patients. A preclinical in vitro study was performed by investigating the sensitivity of GEMDOX therapy on the established resistant sublines. The established resistant osteosarcoma sublines were used to investigate the efficacy of the GEMDOX treatment in the relapsed setting. Out of 8 of the resistant models, MG-63/DOXR8 was significantly resistant to gemcitabine (2.44 ± 0.26-fold, p=0.001) compared to MG-63 and HOS-143B/MTXR8 was significantly resistant to docetaxel (2.32 ± 0.17-fold, p=0.005) compared to HOS-143B. These two resistant sublines were also significantly resistant to the combination of gemcitabine and docetaxel with 2.50 ± 0.53-fold (p=0.04) and 2.09 ± 0.32-fold (p=0.017) respectively. However, the rest of the 6 resistant sublines were not resistant to GEMDOX treatment, which indicates GEMDOX regimen as a potential therapeutic treatment for relapsed osteosarcoma.

This project is the first to develop chemoresistant osteosarcoma cell lines with a triple combination of drugs. The characteristics of these resistant models also provide a better understanding of the resistant mechanisms in osteosarcoma cells. Lastly, these developed single and multi-agents induced clinically-relevant osteosarcoma cell lines could act as an invaluable tool for future studies of drug resistant mechanisms in osteosarcoma cells.

Acknowledgements

First, I would like to thank my supervisors Dr. Britta Stordal, Dr. Helen Roberts and Associate Professor Frank Hills for your support, guidance, time, patience, motivation, and encouragement throughout my PhD journey. This once in a lifetime opportunity has been by far the most challenging but most worthwhile experience of my life. Britta, Helen, Frank have always had faith in me. I very much appreciate Britta's honesty, professionalism, wisdom, humble and ability to connect related experts to help with my projects.

Enormous thanks must go to all the staffs and students in Middlesex University for being such a great group of people who look out for one another and help each other succeed. I have received help and guidance from Dr. Beata Burczynska, Dr. Song Wen, Dr. Nick Kassouf, Dr Eamaan Shafat, Dr. Antia Imeobong, Dr. Milan Vu, Gabriel Rosa, Janice Pereira, and have developed friendships that I value greatly. I would like to especially thank Dr. Eamaan, Dr. Antia and Gabriel for their help in many professional and personal advice. Dr. Eamaan has helped me with the cell culture and cytotoxicity assay. Gabriel has helped me with the molecular study.

I would also like to thank all the postgraduate students in Middlesex University for their help in the laboratory. I would especially thank Dr. Song Wen and Dr. Beata Burczynska for their invaluable molecular expertise and advice in flowcytometry and Western Blotting.

Publications

Scientific Manuscripts

1. Low, K., Hills, F., Roberts, H.C., and Stordal, B., 2022. "Establishment and Characterisation of Signle and Triple-Agent Resistant Osteosarcoma Cell Lines." *Advanced Biology*, p.2200194.
2. Low, K., Hills, F., Roberts, H.C., and Stordal, B., 2022. "The Efficacy of Gemcitabine and Docetaxel Chemotherapy for the Treatment of Relapsed and Refractory Osteosarcoma: A systematic Review and Pre-clinical Study." *Critical Review in Oncology/Hematology*, n/a-n/a. (Under Review)

Conference Proceedings

1. Middlesex University Summer Conference 2018, London, June 2018, Oral presentation. Awarded Best oral presentation.
2. Middlesex University Summer Conference 2019, London, June 2019, Oral presentation. Awarded Best oral presentation.
3. 2019 National Cancer Research Institute Conference, Glasgow, September 2019, Poster. (https://abstracts.ncri.org.uk/abstract/optimisation-of-a-selection-strategy-for-drug-resistance-osteosarcoma-cell-lines/)
4. Middlesex University Summer Conference 2021, London, June 2021, Oral Presentation. Awarded Best oral presentation.

Table of Contents

Abbreviations

3-MA	3-Methladenine
ABC	ATP-Binding cassette
ABCB1	ATP-Binding cassette sub-family B member 1
AF	Area fraction
Akt	Protein kinase B
ALL	Acute lymphoblastic leukaemia
APE-1	Humanapurinic endonuclease
ATCC	American Type Culture Collection
ATG	Autophagy-related proteins
ATM	Ataxia Telengiectasia Mutated
ATP	Adenosine Triphosphate
Bax	Bcl-2-associated X protein
BCD	Actinomycin D
BCL-2	B-cell lymphoma 2
Bcl-2l1	Bcl-2 like protein 1
Bcl-XL	B-cell lymphoma-extra large
BCRP	Breast cancer resistant protein
BER	Base excision repair
BH2	Dihydrobiopterin
BH4	Tetrahydrobiopterin
BrDU	Bromodeoxyudridine
BrdU	Bromodeoxyuridine
BSA	Bovine Serum Albumin
BSO	dl-buthionine-S,R-sulfoximine
CBT	Cognitive behavioral therapy

CCN2	Cellular Communication Network Factor 2
CD39	Ectonucleoside triphosphate dephosphorylase 1
CD73	Ecto-5’-nucluotidase
CDDP	Cisplatin
cDNA	Complementary DNA
CI	Confidence interval
CIS	Cisplatin
CO2	Carbon dioxide
$CoCl_2$	Cobalt chloride
COX-2	Clyclooxygenase
Cq	Comparative cycle threshold
CR	Complete response
CRISPR	Cplstered regularly interspaced short palindomic repeats
C_t	Comparative cycle threshold
CT scan	Computerised tomography scan
CTCAE	Common terminology critria for adverse events
CTGF	Connective tissue growth factor
dFdCDP	Gemcitabine diphosphate
dFdCTP	Gemcitabine triphosphate
DHFR	Dihydrofolate reductase
DilC12	Tetramethylindocarbocyanine perchlorate
DMEM	Dulbecco's Modified Eagle Medium
DMSO	Dimethyl sulfoxide
DNA	Deoxyribonuclic acid
DOX	Doxorubicin
DSBs	Double-stranded breaks

EA	Early apoptotic cells
E-cad	E-cadherin
ECL	electrochemiluminescence
ECM	Extracellular matrix
EDTA	Ethylenediamine tetraacetic acid
EMT	Epithelial to mesenchymal transition
ERCC	Endonuclease non-catalytic subunit
ERK 1/2	Extracellular signal-regulated kinase 1/2
EURAMOS-1	Eurapean and American Osteosarcoma Studies
FACS	Fluorescence-activated cell sorting
FBS	Fetal bovine serum
FDA	Food and Drug Administration
FITC	Fluorescenin Isothiocyanate
FLSs	Firboblast-like synoviocytes
FOXO3	Forkhead box O3
GAPDH	Glyceraldehyde 3 – phosphate dehydrogenase,
gDNA	Genomic DNA
GEMDOX	Gemcitabine and docetaxel regimen
GSH	γ-glutamylcysteinylglycine
GST	Glutathione-S-transferase
GSTP1	Gluthothione S-Transferase Pi 1
H_2O_2	Hydrogen peroxide
HDIFO	High-dose Ifosfamide
HGDC	Human Genomic DNA Control
HGSOS	High-Grade surface osteosarcoma
HIF1A	Hypoxia Inducible Factor 1 Subunit Alpha

HMGB1	High Mobility Group Box 1
HPLC	High performance liquid chromatography
HR	Homonologous recombination
HRO	Horseradish peroxidises
I.V.	Intravenous injection
IC50	Inhibitory concentration of 50% viability
JNK	c-Jun N-terminal kinase
KRAS	Kirsten rat sarcoma virus
LA	Late apoptotic cells
LC3	1A/1B-light chain 3
LI-COR	Licor Odyssey Infrared Imaging System
LNA	Locked-nucleic acid
LOS	Low-grade osteosarcoma
MAP	Mitogen-activated protein kinase
MARK2	Microtubule affinity regulated kinase 2
MDR	Multi drug resistance
MDR1	Multidrug resistance mutation 1
MET	Mesenchymal-to-epithelial transition
miRNA	MicroRNA
MMR	Mismatch repair
MRI	Magnetic resonance imaging
mRNA	Messenger RNA
MSH2	MutS Homolog 2/6
mTOR	Mammalian target of rapamycin
MTX	Methotrexate
NADH	Nicotinamide adenine dinucleptide hydroggenase

NaOH	Sodium Hydroxide
N-cad	N-cadherin
NEAA	Non-essential amino acids
NER	Nucleotide excision repair
NF- κB	Nuclear factor kappa light chain enhancer of activated B cells
NF-Y	Nuclear factor Y
NGS	Next-generation sequencing
NHEJ	Non-homologous end-joining
NHS	National Health Service
NIH	National Institutes of Health
NSCLC	Non-small cell lung carcinoma
NTC	Non-template control
ORR	Overall response rate
PCR	Polymerase chain reaction
PD	Progressive disease
Pen/Step	Penicillin/Streptomycin
PFS	Progression free survival
P-gp	P-glycoprotein
PI3K	Phosphoinositide 3-kinase
PIOS	Periosteal osteosarcoma
PPC	Positive PCR Control
PR	Partial response
pRb	Retinoblastina protein
QC	Quality control
QIC	QuantiNova Internal Control RNA
qPCR	Qualitative Polymerase chain reaction

qRT-PCR	Qualitative Reverse Transcription Polymerase chain reaction
QSR	Qualitative structure activity relationships
Rb	Retinoblastina gene
RB1	Retionoblastoma Protein
RECIST	Response Evaluation Criteria in Solid Tumour
RFC1	Reduced folate carrier 1
RNA	Ribonucleic acid
ROS	Reactive oxygen species
RT-PCR	Reverse Transcription Polymerase chain reaction
S1P	Sphingosine-1-phosphate
SD	Stable disease
SDS-PAGE	Sodium dodecysulphate-polyacrylamide gel electrophoresis
SEER	Surveillance,Epidemiology and End Results
SEM	Standard error mean
SFM	Serum-free media
siRNA	RNA interference
SKI-II	SPHK inhibitor
SKI-V	Sphingosine kinase 1 inhibitor
SKP2	S-phase Kinase Associated Protein 2
SOS	Small-cell osteosarcoma
SPHK1	Sphingosine kinase 1
SPSS	Statistical Package for Social Sciences
TAE	Tris-acetate-EDTA
TFs	Transcription factor
TGM2	Transglutaminase 2 Promote
TK-	Thymidine kinase negative

Tm	Melting temperature
TNF	Tumour necrosis factor
TOP2A	Topiosomerase-II
TOS	Telangiectatic osteosarcoma
WHO	World Health Organisation

List of Figures

List of Tables

Chapter 1: Introduction

1.1 Overview

Osteosarcoma is a rare malignant bone tumour that occurs primarily in adolescents and young adults (Jemal *et al.*, 2011). Osteosarcoma is highly metastatic and the lungs are the most common site of metastases (Huang *et al.*, 2009; Morrow *et al.*, 2018). The standard treatment of osteosarcoma includes neo-adjuvant chemotherapy followed by surgical removal and adjuvant multi-drug chemotherapy (Luetke *et al.*, 2014; Simpson *et al.*, 2017). The combination of cisplatin (CIS), doxorubicin (DOX), and high-dose methotrexate (MTX) are the standard treatment for most patients. The combination of surgery and neoadjuvant chemotherapy has significantly improved the 5-year survival rate for osteosarcoma patients to 60% - 70% (Meyers *et al.*, 2005). However, most of the patients with metastatic or recurrent osteosarcoma have a poor prognosis due the development of drug resistance after treatment with chemotherapy (Kager *et al.*, 2003; Chen *et al.*, 2017).

One of the methods to improve the survival rate of osteosarcoma patients is by overcoming drug resistance (Scotlandi, Picci and Kovar, 2009). The development of drug resistance in osteosarcoma has been studied and several mechanisms demonstrated including genetic alterations (Lønning and Knappskog, 2013), drug-target mutation and amplification (Yamamoto *et al.*, 2009), altered drug accumulation (Derdak *et al.*, 2008), and autophagy (Zhang *et al.*, 2015). The expression of MDR1, which is responsible for producing P-glycoprotein (P-gp), has been widely studied in osteosarcoma (Chou and Gorlick, 2006; Susa *et al.*, 2010). P-gp is a membrane-bound protein which transports doxorubicin and methotrexate out of the cells leading to chemoresistance (Gottesman, Fojo and Bates, 2002; Liu *et al.*, 2016). Furthermore, the ABC transporter family, specifically MRP1, MRP2 and MRP3 also play a major role in the efflux of methotrexate (Kruh *et al.*, 2001). Apart from methotrexate, MRP2 has also been shown to effectively

transport cisplatin and doxorubicin out of cancer cells and consequently cause resistance (Borst *et al.*, 2000).

Developing drug-resistant cancer cell models is one approach to study the mechanisms of chemoresistance in cancer cells. Previous resistant models have been established by using osteosarcoma cell lines such as SOSP-9607 (Han *et al.*, 2014), Saos-2 (Niu *et al.*, 2010), MG-63 (Oda *et al.*, 2000), and U-2OS (Yin *et al.*, 2007). These established osteosarcoma resistant models have increased fold resistant ranges from 6 to 120-fold compared to their parental cell lines. Some of the resistant cell models also exhibit cross-resistance to other chemotherapeutic drugs including ifosfamide, epidoxorubicin, pirarubicin and paclitaxel (Niu *et al.*, 2010).

In this study, clinically relevant chemoresistant osteosarcoma cell models were developed from the cell lines MG-63 and HOS-143B. MG-63, which was established from a 14-years old male with osteosarcoma is marginally metastatic (Pautke *et al.*, 2004); and HOS-143B originally derived from HOS, established from a 13-year-old Caucasian female with a high level of metastasis (Dass *et al.*, 2007). One of the strategies used the current study includes a multiple drugs combination approach, whereas cisplatin, doxorubicin, and methotrexate are combined as a single treatment. This strategy is to develop a novel drug-resistant model by using combination of drugs instead of single drug as shown in those established models before. The purpose of this method is to simulate a similar experience with osteosarcoma patient who is undertaking clinical chemotherapy treatment and therefore, establishing a clinically relevant osteosarcoma-resistant model to study the mechanisms of clinical drug resistance.

1.2 Human osteosarcoma

Human osteosarcoma (OS) is the most frequent primary malignant bone tumour worldwide and the second highest cause of cancer related to death in children and teenagers (Fletcher, World Health Organization and International Agency for Research on Cancer, 2013). The term osteosarcoma was first introduced in the 19th century, and it was derived from the Greek *sarx*, meaning flesh (Peltier, 1985). Osteosarcoma is a highly-aggressive neoplasm typically composed of spindle cells producing osteoid (Klein and Siegal, 2006). Osteosarcoma comprises 2.4% of all malignancies in patients and nearly 20% of all primary bone cancers (Ottaviani and Jaffe, 2009). The annual morbidity of osteosarcoma is approximately 5 million cases worldwide with prevalence towards males at ratio 1.5:1 (Chen *et al.*, 2017). The incidence rates range from 3 to 5 million cases in men and 2 to 4 million cases in women (Mirabello, Troisi and Savage, 2009). The common pathogenic site of osteosarcoma is mainly at the knee joint periphery and the symptoms include dysfunction, pain, swelling, anaemia and weight loss (Pan, Chan and Chia, 2010).

1.2.1 Type of osteosarcoma

Osteosarcoma has been histologically classified by The World Health Organisation (WHO) into central, surface tumours, and intramedullary, with several subtypes under each category (Schajowicz, Sissons and Sobin, 1995). Each type of osteosarcoma is determined by looking at the tumour cells under the microscope. The most common type of osteosarcoma is conventional osteosarcoma, which represents 80% of all osteosarcoma cases. The rest of the subtypes only account for 1% to 5% of the total osteosarcoma cases (Misaghi *et al.*, 2018).

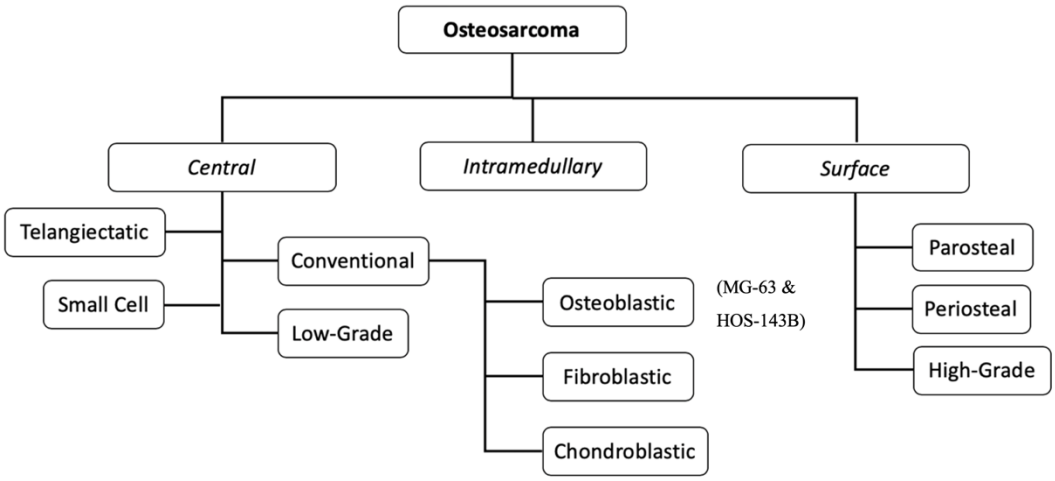

Figure 1.1: Flowchart of the type of osteosarcoma. Osteosarcoma is mainly categorised into three main groups – central osteosarcoma, surface osteosarcoma, and intramedullary osteosarcoma. MG-63 and HOS-143B are conventional subtypes of osteosarcoma. Original diagram developed using (Schajowicz, Sissons and Sobin, 1995).

1.2.2 Central osteosarcoma

1.2.2.1 Conventional osteosarcoma

Conventional osteosarcoma can be further categorised into osteoblastic, chondroblastic, and fibroblastic. Each category can be differentiated by the predominant features of the cells (Misaghi *et al.*, 2018). However, the clinical outcome is the same among these groups (Ozaki *et al.*, 2002). Conventional osteosarcoma is usually high grade and most of the cases occur in the metaphysis of long bone. The metaphysis is the narrow portion of a long bone between the epiphysis (end part of long bone) and diaphysis (central part of long bone). Conventional osteosarcoma can also occur in the diaphysis of long bones and in the axial skeleton (Bielack *et al.*, 2002). Fibroblastic osteosarcoma contains a relatively greater proportion of fibroblastic spindle cells compared to the amount of osteoid (Lin and Patel, 2013). Chrondroblastic osteosarcoma has a greater proportion of chondrocytes and cartilaginous matrix, and osteoblastic is mainly composed of osteoblasts and abundant of osteoid (Lin and Patel, 2013). This study will examine conventional osteosarcoma using cell lines MG-63 and HOS-143B.

1.2.2.2 Telangiectatic osteosarcoma

Telangiectatic osteosarcoma (TOS) contributes for 2% of overall osteosarcoma cases (Turel *et al.*, 2012). TOS is a rare variant of osteosarcoma and the common locations for this tumour are the long tubular bones and femur, followed by tibia and humerus (Turel *et al.*, 2012). TOS is recognised histologically by blood-filled cavities and malignant cells on the septa, which is located between two cavities or masses of softer tissue. Although TOS was believed to have a worse prognosis than the conventional type of osteosarcoma; recent studies have suggested no difference between the two types (Bacci *et al.*, 2001; Weiss *et al.*, 2007).

1.2.2.3 Small-cell osteosarcoma

Around 1% to 2 % of all sarcoma cases are small-cell osteosarcoma (SOS). SOS can be differentiated by the histological features, which is small with round hypochromatic nuclei and little nuclear polymorphism, which is quite similar to Ewing's sarcoma (Devaney, Vinh and Sweet, 1993; Nakajima *et al.*, 1997).

1.2.2.4 Low-grade osteosarcoma

Low-grade osteosarcoma (LOS) has contributed to around 1% to 2 % of overall osteosarcoma cases. LOS generally diagnosed more often in the elderly instead of adolescents (Andresen *et al.*, 2004). LOS is difficult to identify due to its features of low grade and may like fibrous dysplasia, desmoplastic fibroma or periosteal osteosarcoma (Bertoni, Bacchini and Fabbri, 1993). The prognosis of LOS is significantly better than conventional osteosarcoma. However, there is a risk of transformation of LOS to conventional osteosarcoma if LOS is treated with curettage alone, which is a surgical scraping or cleaning of benign tumour by using curette (Unnim, Mcleodm and Pritcharmdd, 1977).

1.2.3 Surface osteosarcoma

Surface osteosarcomas are osteosarcomas which arise to the periosteum or cortex of the bone with no involvement of the medullary cavity. There are different types of surface osteosarcomas which have been characterised by the anatomic location, histologic grade, and dominant type of matrix (Klein and Siegal, 2006). Surface osteosarcoma is categorised into perosteal osteosarcoma, periosteal osteosarcoma, and high-grade surface osteosarcoma.

1.2.3.1 Parosteal osteosarcoma

Parosteal osteosarcoma (PAOS) is a low-grade surface osteosarcoma which arises from periosteum. PAOS generally occurs at the posterior aspect of the distal femur and accounts for 4% to 6% of osteosarcoma (Misaghi *et al.*, 2018). PAOS may effect at other sites such as proximal humerus and proximal tibia (Johnson *et al.*, 1999; Hewitt *et al.*, 2008). Histologically, PAOS contain a streamers of bone trabeculae that exhibit a high degree of parallel orientation, which is similar to what might be spotted in periosteal new bone reaction (Klein and Siegal, 2006).

1.2.3.2 Periosteal osteosarcoma

Periosteal osteosarcoma (PIOS) consists of a matrix component that is mainly cartilaginous, and it is noticeably less common than parosteal osteosarcoma with approximately 25% of all juxtacortical osteosarcomas (Murphey *et al.*, 2004). Periosteal is easily visible on radiographs because PIOS normally occur between the cortex and the cambium layer of the periosteum (Unni, Dahlin and Beabout, 1976). PIOS normally effect the tibial or femoral diaphysis instead of posterior to the metaphysis of the distal femur (Murphey *et al.*, 2004).

1.2.3.3 High-grade surface osteosarcoma

High-grade surface osteosarcoma (HGSOS) usually establishes as a surface lesion on a bone (Wold *et al.*, 1984). HGSOS accounts for less than 1% of all osteosarcoma cases (Misaghi *et al.*, 2018). Local growth and aggressiveness of HGSOS is more accelerated than parosteal osteosarcoma because of its higher-grade lesions. HGSOS may have some degree of localised invasion to the endosteum and cortex considering it has the same malignant potential as conventional osteosarcoma (Klein and Siegal, 2006). HGSOS

exhibits a surface lesion with partial mineralisation and it may also extend to surrounding soft tissues radiographically (Wold *et al.*, 1984).

1.2.4 Epidemiology

Osteosarcoma is considered as an orphan disease, which affects fewer than 200,000 people worldwide, but it is the most frequent primary cancer of bone (Ottaviani and Jaffe, 2009). The incidence rate of osteosarcoma in Europe is 0.2 – 100,000/year (Luetke *et al.*, 2014). The incidence rate is highest in adolescents at the age of 15 to 19 (0.8 – 1.1/100,000/year) and the ratio of male to female is around 1.5:1 (Chen *et al.*, 2017). According to Global Cancer Statistics 2020, the incidence rate was 5.4 per million persons per year in male and 4.0 per million in females (Sung *et al.*, 2021). Although osteosarcoma is a rare cancer disease, it ranked the third most common cancer in adolescence, only after lymphoma and brain tumour in this age group (Ottaviani and Jaffe, 2009). Osteosarcoma is extremely rare in children before the age of 5 years, which only accounts for 2% of overall osteosarcoma patients (Hartford *et al.*, 2006; Kager *et al.*, 2010). Rapid bone growth and osteosarcoma has been suggested to be related based on its highest peak incidence at adolescence and the higher incidence rate in male (Geller and Gorlick, 2010).

Osteosarcoma has been indicated as the most common primary malignant tumour among people of all ages and sexes, resulting for around 35% of cases, followed by chondrosarcoma for 25%, and Ewing sarcoma for 15% (Ottaviani and Jaffe, 2009). There are around 400 new cases of osteosarcoma diagnosed among children and adolescents each year in the United States (Ottaviani and Jaffe, 2009). Figure 1.2 has shown the osteosarcoma incidence by country or region and they mostly have the highest peak of incidence in children between the age of 10 to 20 (Mirabello, Troisi and Savage, 2009).

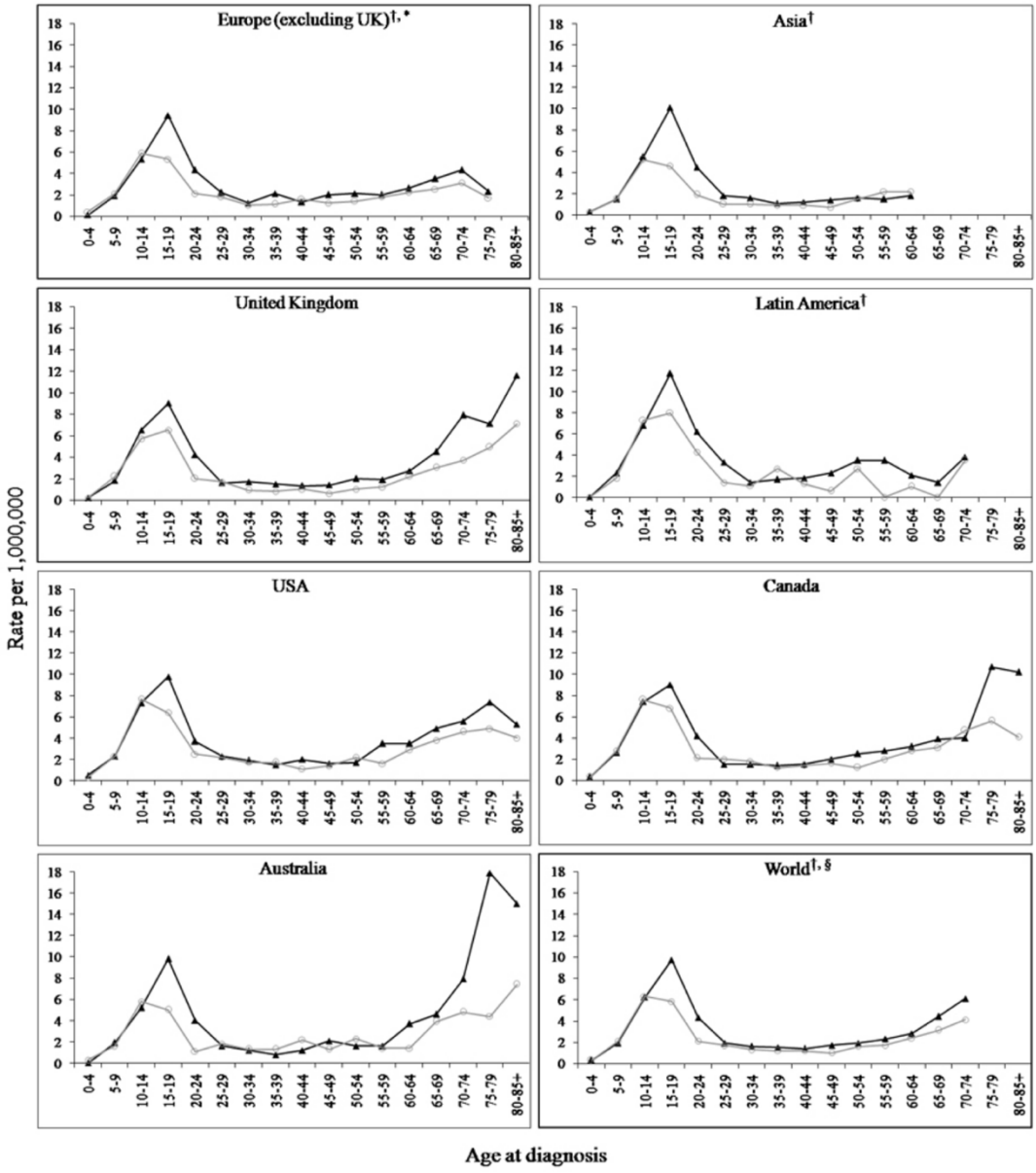

Figure 1.2: Osteosarcoma incidence by country or region. Black triangles are male rates, grey circles are female rates. Adapted from (Mirabello, Troisi and Savage, 2009)

The incidence rate of osteosarcoma rises steadily between age 5 to 10 years, and a sharper rise between age 11 and 15 years, which is believed to associate with the pubertal growth spurt. The overall highest peak incidence of osteosarcoma occurs at the ages between 10 to 14 years, and the rate decrease after which (Eyre *et al.*, 2009). The second peak of the incidence appears in elderly after age 65, in which frequently related to Paget disease (Hansen, Seton and Merchant, 2006; Deyrup *et al.*, 2007).

1.2.5 Tumour site

The most common sites for osteosarcoma are the femur, which accounts for around 42% total cases of osteosarcoma and 75% of them occur in the distal femur. Tibial bone accounts for 19% of the cases and 80% of these are in the proximal tibia. Followed by the humerus for 10%, and 90% of them in the proximal humerus. Other locations are likely to be the jaw or skill, pelvis and the ribs (Marcove *et al.*, 1970). Before 1970, the surgical treatment available for osteosarcoma was only amputation and around 80% of the osteosarcoma patients died of metastatic lung disease (Marcove *et al.*, 1970). The National Cancer Data Base Report described that the relative 5-year survival rate for patients younger than 50 years was 30% (Damron, Ward and Stewart, 2007).

1.2.6 Metastatic disease and local recurrence

Approximately 10% to 20% of osteosarcoma patients present with metastatic disease at the time of diagnosis (Bielack *et al.*, 2002). The metastases develop most commonly in the lungs, around 90%, but it can also develop in bones (8% – 10%), and occasionally in lymph nodes (Bacci, 2003; Bacci *et al.*, 2006). Nevertheless, there are around 80 to 90% of osteosarcoma patients believed to have micro-metastatic disease, which is not possible to detect by using current diagnostic techniques (Geller and Gorlick, 2010). Approximately 30% to 40% of patients with localised osteosarcoma will develop a local

or distant recurrence (Kempf-Bielack *et al.*, 2005) and around 90% of relapses are lung metastases which normally happen in the first 2 or 3 years (Ferrari *et al.*, 2003). However, it is rare to relapse after 5 years of initial treatment of osteosarcoma, which only occurs in 1% to 2% of all osteosarcoma patients (Bacci, 2003). One of the studies had suggested the trend for late relapse arising from osteosarcoma re more likely to arise in chondroblastic subtypes (Hauben *et al.*, 2006). Osteosarcoma recurrences normally have a poor prognosis (Franke *et al.*, 2011). In the cases of osteosarcoma patients who relapsed, the further treatments cured around 31% of those with local recurrence alone. However, in the cases of patients with metastases, only 10% of the patients were being cured as compared to the patients with local recurrence (Luetke *et al.*, 2014). The median interval from first and second recurrence of osteosarcoma was reported to be 9 months, the median interval between subsequent recurrences remained quite constant at around 6 months (Bielack *et al.*, 2009).

1.2.7 Diagnosis and staging

The most typical symptoms of osteosarcoma include pain, localised swelling, and limitation of joint movement (Pan, Chan and Chia, 2010). Typical findings on X-rays and histological examination of tumour needs to be verified by open biopsy to make a definitive diagnosis (Durfee, Mohammed and Luu, 2016). The tumour will be diagnosed as osteosarcoma, by definition, when the tumour is formed by osteoid from the malignant cell population (Geller and Gorlick, 2010). Staging osteosarcoma requires the assessment of osteosarcoma's intramedullary and soft tissue extension and the relation of the tumour to nerves and blood vessels. Magnetic resonance imaging (MRI) is considered the most favourable tools for staging because MRI is capable in assessing the whole bone and the neighbouring joints (Bielack *et al.*, 2009). For systemic staging, most potential metastases sites must be observed as well such as lungs and the skeleton. The assessment includes

CT scan of thorax, complete X-rays scan of chest, and a X-rays or MRI scans of affected bone (Geller and Gorlick, 2010).

1.2.8 Current treatment

The treatment strategy for osteosarcoma before the 1970s was mainly limb amputation and the overall 5-year survival rate was only 10 to 20% at that time (Longhi *et al.*, 2006). The overall survival rates of osteosarcoma and degree of disease-free survival has increased over the past three decades due to the improvement of surgical techniques and the implementation of radiotherapy and/ or systemic chemotherapy (Ferguson and Goorin, 2001). The combination of surgery and postoperative radiotherapy has increased the long-term survival rate to 50% (Ozaki *et al.*, 2002). Once the systemic multi-agent chemotherapy (cisplatin, doxorubicin, and methotrexate) followed by surgery was been introduced, the survival rate of osteosarcoma increased dramatically to approximately 60 to 70% (Ferrari *et al.*, 2005). Currently, the combination of chemotherapy and surgical treatment is the standard treatment of patients with conventional osteosarcoma. During the surgical resection, radiotherapy can be applied along with the treatment program (Ta *et al.*, 2009). Radiotherapy is used as the treatment for osteosarcoma when the lesions are in inaccessible sites (Ta *et al.*, 2009).

1.2.8.1 Surgery

Surgical resection of the tumour remains an essential part of the treatment strategy of all patients with osteosarcoma. Without surgical resection, osteosarcoma is proved to be rarely cured even with effective chemotherapy (Jaffe *et al.*, 2002). The main objective to perform the surgery is to completely remove the tumour to minimise the risk of local recurrence and maximise the chance of overall survival (Ta *et al.*, 2009). A major shift from amputation toward limb-salvage surgery has been due to the advances in imaging

techniques and the positive effects of preoperative chemotherapy (Yasko, 2009). The local recurrence rate has been reported to be slightly higher after limb-salvage surgery (5% – 7%) compared to amputation surgery (2% – 3%). However, there was no significant differences in the survival rate between the two different methods of surgery (Marulanda *et al.*, 2008; Errani *et al.*, 2011). The incidence of local recurrence has been reported to be closely related to the achieved surgical margins, where better removal of tumour lesions leads to better outcomes (Errani *et al.*, 2011).

1.2.8.2 Radiotherapy

Radiotherapy can be used for a local treatment of an unresectable tumour even though it is considered a radioresistant tumour (DeLaney *et al.*, 2005). The effectiveness of local control radiotherapy also reported to be markedly improved with the application of some chemotherapeutic agents such as cisplatin, ifosfamide, and high-dose methotrexate (Errani *et al.*, 2011).

1.2.8.3 Chemotherapy

Historically, chemotherapy was normally administered as single-agent treatment (Saeter *et al.*, 1991). However, combination protocols became favoured and proved by the early studies to be more effective than single-agent treatment (Rosen *et al.*, 1979; Rosen, 1985; Rosen and Nirenberg, 1985). In treating osteosarcoma, up to 60% of relapse-free survival rates were provided by the combination of doxorubicin and methotrexate and it became central to modern chemotherapy treatment regimens (Geller and Gorlick, 2010). Others such as cyclophosphamide, bleomycin, and actinomycin D (BCD) were often administered to patients in the past. However, as the regimens only offered a limited benefit compared to doxorubicin and methotrexate, they were eventually abandoned (Geller and Gorlick, 2010). The cure rate of osteosarcoma by surgery ranges from 15%

to 20% and improves dramatically to 70% in combination with chemotherapy. However, additional chemotherapy is palliative and toxic to approximately 40% of the patients with progression of osteosarcoma after front-line therapy. Moreover, the chances for patients with recurrent disease to be cured is only estimated as less than 30% (Susa *et al.*, 2009).

Currently, the most active chemotherapeutic drugs used against osteosarcoma are cisplatin, doxorubicin, high-dose methotrexate with leucovorin rescue and ifosfamide (Bielack *et al.*, 2009). The duration of chemotherapy treatment for osteosarcoma is generally 6 – 12 months depending on the response of the patients (Carrle and Bielack, 2006). Doxorubicin is the most essential component in most of the regimens compared to other agents. However, because of its high potential of cardiotoxicity, the use of doxorubicin is dose-limiting (Bacci *et al.*, 2002). Cardiac toxicity has been recognised as a serious and potentially fatal complication of doxorubicin since the early 1970s (Janeway and Grier, 2010). Cisplatin as the second most used agent, is also included in most of the regimens for treating osteosarcoma and the third most used agent is high-dose methotrexate with leucovorin rescue to decrease the toxic effects of methotrexate (Carrle and Bielack, 2006). According to EURAMOS-1 (an international randomised study for osteosarcoma), the strongest positive impact on disease-free survival in patients with osteosarcoma is to treated with the combination of cisplatin, doxorubicin, high-dose methotrexate and ifosfamide if the histological response assessment after the surgery and pre-operative chemotherapy is poor (necrosis rate ≤ 90%) (Whelan *et al.*, 2015). If the histological response assessment is good (necrosis rate ≥ 90%), the patients are treated with the same combination without the ifosfamide (Whelan *et al.*, 2015).

The most commonly used range of dosages are shown in Table 1.1. Before the surgery, neoadjuvant pre-operative chemotherapy is normally administered to the patients for a

period of about 8 to 10 weeks. After the surgery, adjuvant post-operative chemotherapy is continued for a period of another 12 to 29 weeks (Carrle and Bielack, 2006).

Table 1.1 Commonly used range of cumulative dose and dose per cycle for osteosarcoma patients.

Drugs	Cumulative dose	Dose per cycle
Cisplatin	480 – 600 mg/m^2	100 – 120 mg/m^2
Doxorubicin	240 – 480 mg/m^2	60 – 90 mg/m^2
Methotrexate	48 – 168 g/m^2	From 12g/m^2
Ifosfamide	30 – 69 g/m^2	6 – 14 g/m^2

Adapted from (Hattinger *et al.*, 2010).

1.2.9 Relapsed osteosarcoma

Patients who experience a recurrence of their cancer following a period of remission which are known to have relapsed disease (Kempf-Bielack *et al.*, 2005). A significant decrease in the long-term survival rates is shown in patients with relapsed osteosarcoma compared to primary disease, with only approximately 30% – 40% of patients surviving for 5 years (Ferrari *et al.*, 2003). The survival rate reduces even further to only 14% for patients with a second recurrence of osteosarcoma disease (Bielack *et al.*, 2009) and the lungs are the most common site of recurrence for osteosarcoma (Luetke *et al.*, 2014). There is currently no standardised treatment guidelines for recurrent osteosarcoma, therefore the treatment remains the same as primary osteosarcoma, which includes surgery removal of detectable tumour and chemotherapy treatment (Bielack *et al.*, 2009; Gerrand *et al.*, 2016). There have been no major successful improvements to the standard of chemotherapeutic approach to osteosarcoma despite the advances in research since the MAP regimen was established in 2001 (Whelan *et al.*, 2015). Therefore, there is no

alternative chemotherapy regimen is currently recommended for patients with relapsed osteosarcoma (Gerrand *et al.*, 2016). Ifosfamide had been suggested as an addition to the MAP regimen, however no significant difference was found in survival rate of the patients whilst increased toxicities occured (D. Yu *et al.*, 2019). To date, there is no established standard second-line chemotherapy regimen for the treatment of relapsed osteosarcoma (Gerrand *et al.*, 2016).

1.2.9.1 Alternative treatment for relapsed osteosarcoma

The lower survival rates for relapsed osteosarcoma patients and the lack of consensus over recommended second-line treatment reflects the need for novel chemotherapeutic agents for this category of patients. Some chemotherapeutic agents have been studied including Interferon α-2b, sorafenib, and etoposide (Y. Zhang *et al.*, 2018).

1.2.9.2 Potential second line regimen

The combination of gemcitabine and docetaxel regimen (GEMDOX) has been demonstrated to be effective for other sarcomas such as leiomyosarcoma, which is a type of soft tissue sarcoma (Maki, 2007; Hensley, 2010). A review study has shown a favourable response rate of 43% and lower incidence of toxicities in GEMDOX regimen in sarcomas and bone sarcomas compared to the standard doxorubicin and ifosfamide regimen which only has a 30% response rate (Leu *et al.*, 2004). However, the side effects associated with docetaxel include hypersensitivity, neutropenia, peripheral neuropathy, and oedema (Baker *et al.*, 2009). Moreover, the side effects associated with gemcitabine include oedema, skin reactions, and myelosuppression (Barton-Burke, 1999). The most severe side effect associated with the combination GEMDOX regimen are haematological, as a result of myelosuppression (Qi *et al.*, 2012).

1.3 Cellular mechanisms of cisplatin

1.3.1 Cytotoxicity of cisplatin

Cisplatin is one of the most potent chemotherapy drugs widely used for cancer treatment. The interest in platinum and other metal containing compounds to use as potential anticancer drugs was triggered by the discovery of cisplatin *cis*-[Pt(II)(NH(3))(2)Cl(2) ($[PtCl_2(NH_3)_2]$ or CDDP (Lippert, 1999). Many patients with different types of cancer have been successfully treated by of cisplatin including cancers of bones, sarcoma, muscles, and blood vessels (Rosenberg, 1980; Desoize and Madoulet, 2002). Though, due to the side effects in normal tissues, the use of cisplatin is dose-limiting (Arany and Safirstein, 2003). The general cell damaging side effects of platinum therapy include nausea, vomiting, myelosuppression, and immunosuppression. Other specific side effects such as nephrotoxicity, neurotoxicity and hearing loss are also linked with cisplatin therapy (Desoize and Madoulet, 2002; Florea and Büsselberg, 2006; Günes *et al.*, 2009; Shah and Dizon, 2009; Tsang, Al-Fayea and Au, 2009).

The anticancer effects of cisplatin include inducing programmed cell death or apoptosis by interacting with DNA (Yoshikawa *et al.*, 1997). After administration of cisplatin into the bloodstream of a patient, the high chloride concentration in the blood plasma of a patient limits the replacement of cisplatin's chloride ligands by water molecules. Cisplatin is vulnerable to attack by protein found in the blood plasma, especially those that contain thiol groups, such as serum albumin and the amino acid cysteine (Alderden, Hall and Hambley, 2006). The intact cisplatin will either diffuse into tumour cells through the membrane or by Cu-transporting proteins. The chloride concentration intracellularly is low thus water is replacing one of the chloro-ligands of the intact cisplatin and a reactive and positively charged cisplatin is formed.

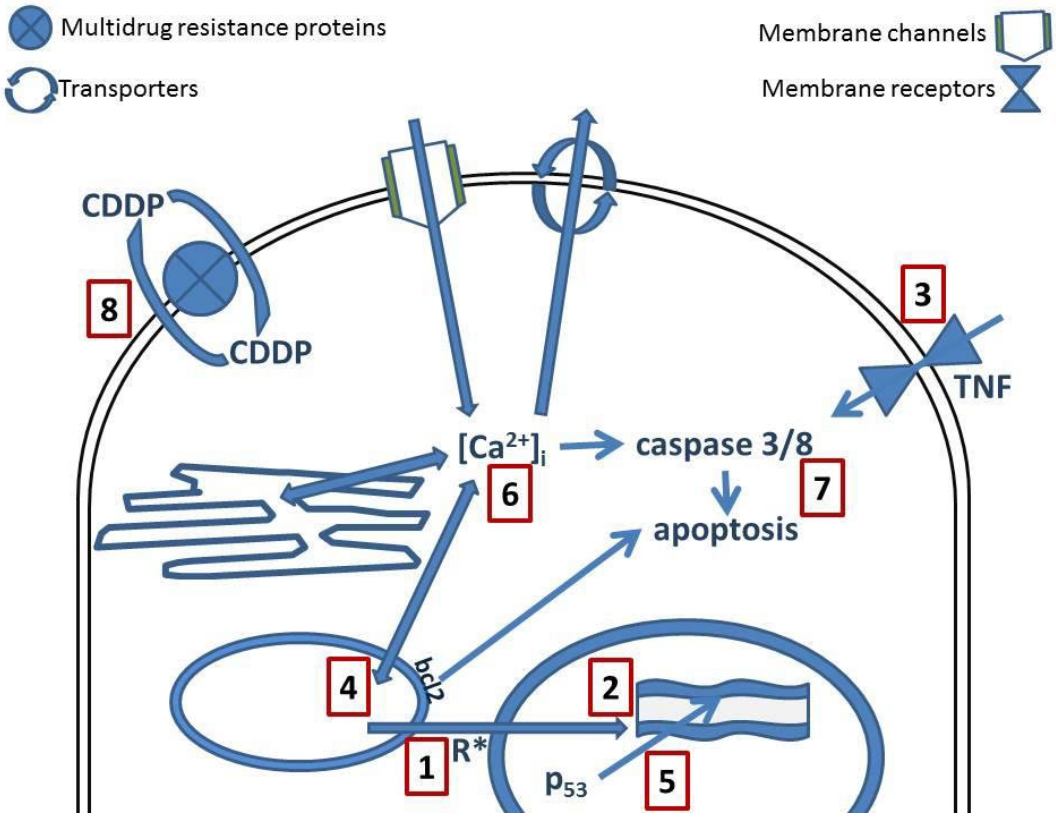

Figure 1.3: Cellular interactions of cisplatin. (1) Reactive oxygen species, (2) DNA, (3) Tumour necrosis factor (TNF), (4) Mitochondria, (5) p53, (6) Calcium signalling. (7) Caspases. (8) Multidrug resistant proteins. Adapted from (Florea and Büsselberg, 2011).

This reactive cisplatin usually reacts with guanine of the DNA and a monofunctional DNA adduct is formed (Florea and Büsselberg, 2011). The DNA binding proteins that can recognise the distortion of the DNA can either initiate DNA damaged repair or signal for apoptosis to be initiated (Alderden, Hall and Hambley, 2006). Tumours can be damaged by the activation of apoptosis through various signal transduction pathways as shown in Figure 1.3.

1.3.2 Mechanisms of cisplatin resistance

The cellular resistant mechanisms of cisplatin are complicated and involves many mechanisms such as: (a) decreased intracellular drug accumulation via drug efflux; (b) inactivation of cisplatin by increased levels of cellular thiols; (c) regulatory proteins; (d) increased nucleotide excision-repair activity; and (e) decreased mismatch-repair activity and evasion of apoptosis (Kartalou and Essigmann, 2001; Brabec and Kasparkova, 2005; Sedletska, Giraud-Panis and Malinge, 2005).

Cisplatin-resistant cell lines frequently have reduced intracellular accumulation of cisplatin due to decreased uptake or increased efflux (Parker *et al.*, 1991; Dempke *et al.*, 1992; Beretta *et al.*, 2004). The exact mechanisms of uptake of cisplatin by the cells is not fully understood to date (Rada *et al.*, 2018). However, there is evidence demonstrating cisplatin uptake is mediated by membrane proteins such as the sodium-potassium pump, and cisplatin uptake was inhibited by sodium-potassium ATPase inhibitor ouabain (Andrews *et al.*, 1988). These results suggest that the cellular uptake of cisplatin is mediated by a carrier-transport system. Apart from decreasing uptake of cisplatin by the cell through membrane proteins, the cellular accumulation of cisplatin could also be decreased by increasing the efflux of the drug from the cells by the ATP-dependent glutathione S-conjugate export pump (Ishikawa, 1992; Fujii *et al.*, 1994) (Figure 1.4).

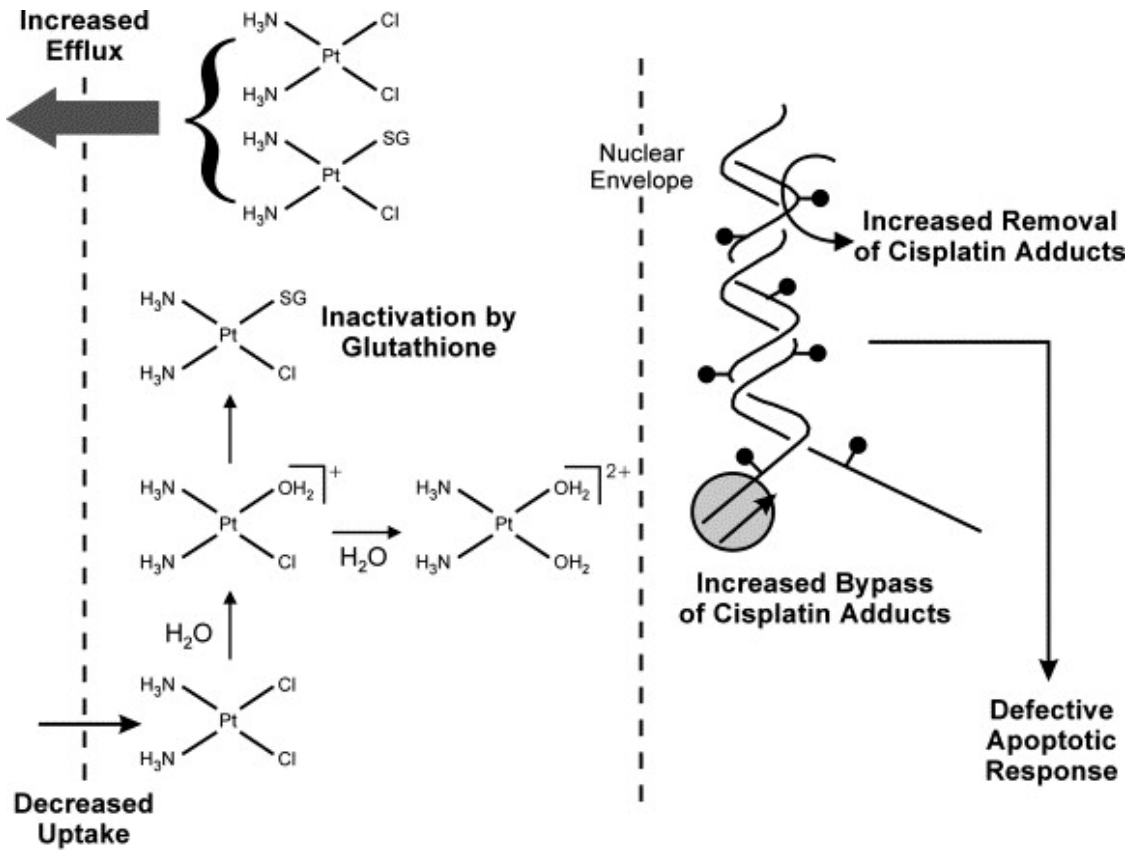

Figure 1.4: Mechanism of resistance to cisplatin. Reduced intracellular drug accumulation by decreased uptake or increased efflux; inactivation by glutathione; increased removal of cisplatin adducts; increased bypass of cisplatin adducts; defective apoptotic response. Adapted from (Kartalou and Essigmann, 2001).

Increased inactivation by intracellular proteins such as glutathione (γ-glutamylcysteinylglycine, GSH) causing resistance to cisplatin also reported by various studies. GSH can be covalently bound to cisplatin and transported out of the cell by ATP-dependent pump (Ishikawa and Ali-Osman, 1993). Moreover, the cytotoxic potential of cisplatin was depleted due to the binding of GSH to cisplatin which prevents the formation of cisplatin-DNA adducts (Eastman, 1987). The use of the inhibitor dl-buthionine-S,R-sulfoximine (BSO) successfully decreased the synthesis of GSH and hence increased cisplatin sensitivity of some cancer cells (Hromas *et al.*, 1987; Mistry *et al.*, 1993). The expression of oncogenes and tumour suppressor genes have also been demonstrated in contributing the cellular resistance to cisplatin due to the pleiotropic effects on cellular homeostasis (Kartalou and Essigmann, 2001).

1.3.3 Detoxification of cisplatin in osteosarcoma

Cisplatin also generates a high level of reactive oxygen species (ROS), which when they accumulate lead to cellular damage (Townsend, Tew and Tapiero, 2003). Osteosarcoma, and all cancer cells have detoxification mechanisms to inactivate drugs such as cisplatin. The main detoxification enzymes include glutathione (GSH) and glutathione-S-transferase (GST), and GSTP-1 enzyme is the main member of GST family (Siddik, 2003). The expression of GSTP1 in osteosarcoma could be linked to a poor prognosis as the patients present with high relapse rate (Wei *et al.*, 2006). Furthermore, suppressing GSTP1 expression has successfully induced apoptosis and DNA damage in osteosarcoma (Huang, Mills and Worth, 2007). GSTP1 could also inhibit apoptosis by inhibiting JNK phosphorylation or activating phosphorylation of extracellular signal-regulated kinase 1/2 (ERK1/2) and p38 MAPK (Adler *et al.*, 1999; Yin *et al.*, 2000; Lu *et al.*, 2004).

1.4 Cellular mechanisms of doxorubicin

1.4.1 Cytotoxicity of doxorubicin

Doxorubicin is an anthracycline drug first discovered in the 1970's extracted from *Streptomyces peucetius var. caesius*. Doxorubicin is commonly used in the treatment of cancers such as lung, ovarian, breast, sarcoma, myeloma, and paediatric cancer (Arcamone *et al.*, 1969; Weiss, 1992; Cortés-Funes and Coronado, 2007). However, the biggest limitation of doxorubicin is the cardiotoxicity, where the toxicity can be predicted by the total cumulative dose (Swain, Whaley and Ewer, 2003; Carvalho *et al.*, 2009).

The main mechanisms of action of doxorubicin in cancer cells involves (a) intercalation within DNA base pair and causing disruption of topoisomerase-II-mediated DNA repair; and (b) generation of free radical-mediated oxidative and their damage to DNA and limiting DNA synthesis (Figure 1.5) (Gewirtz, 1999; Sritharan and Sivalingam, 2021). In general, reactive oxygen species is released in the process where doxorubicin is oxidised to semiquinone and back to doxorubicin. These reactive-oxygen species will then cause cellular membrane and DNA damage, oxidative stress and eventually lead to cell apoptosis (Doroshow, 1986). Those genes capable of oxidative reaction are involve in the modulation of this pathway, such as nitric-oxide synthases, NADH dehydrogenases, and xanthine oxidase (Pawłowska *et al.*, 2003; Fogli, Nieri and Breschi, 2004). Other candidate genes which can deactivate free radical are also involved, such as superoxide dismutase, glutathione peroxidase, and catalase. In addition, DNA damage and induction of apoptosis can also be triggered when topoisomerase-II is inhibited in the nucleus by doxorubicin. (Tewey *et al.*, 1984).

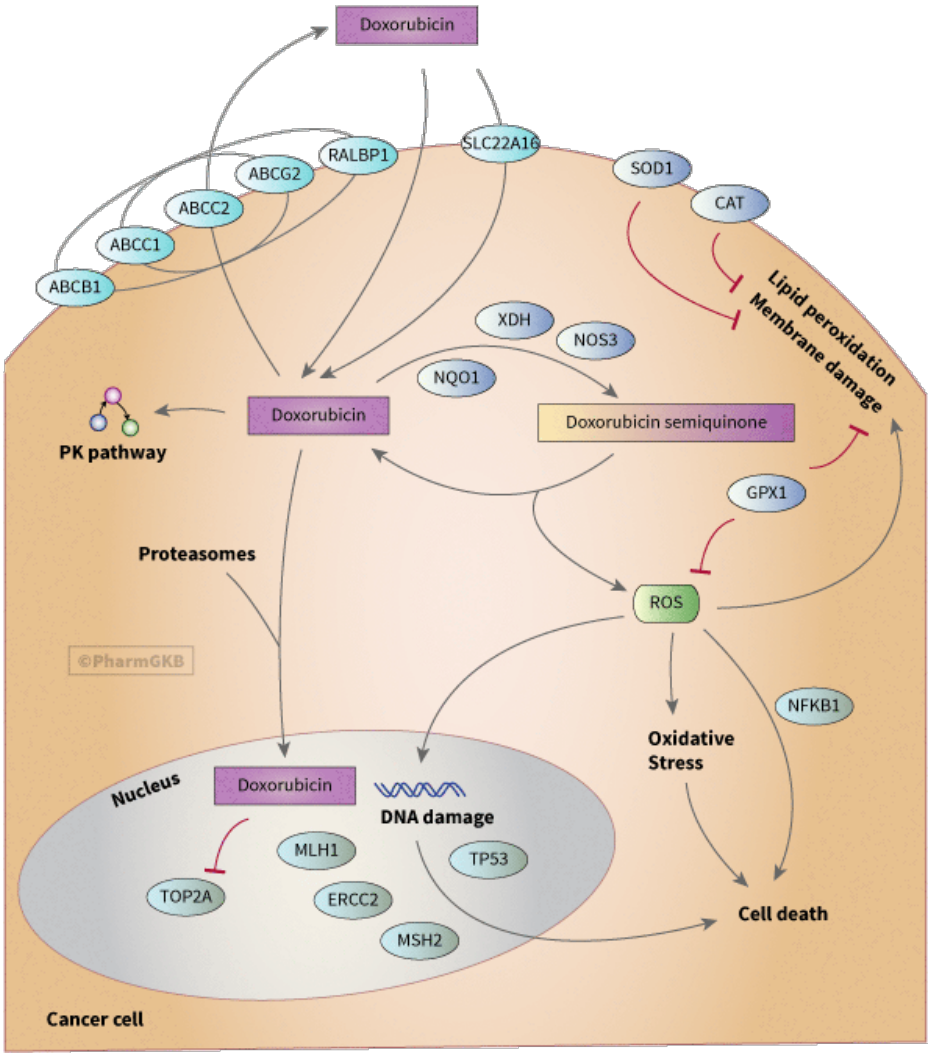

Figure 1.5: Pharmacodynamics of doxorubicin in cancer cells. Genes involved in the modulation of the pathway are capable of oxidative reaction or capable of deactivating free radicals. Adapted from (Thorn *et al.*, 2011).

Cardiotoxicity is one of the major limitations and side effect of doxorubicin, and the proposed mechanisms are (a) iron-related free radicals and formation of doxorubicinol metabolite and (ii) mitochondrial disruption. Generally, doxorubicinol will be formed after the reduction of doxorubicin, which is a metabolite which interferes with iron and calcium regulations and the F0F1 proton pump of mitochondria (Thorn *et al.*, 2011). Metabolism of doxorubicin within the mitochondria can disrupt respiration and finally leads to the release of cytochrome-C initiating apoptosis (Clementi *et al.*, 2003).

1.4.2 Mechanisms of doxorubicin resistance

In general, doxorubicin resistance normally occurs when the drug accumulation decreases in the nucleus and hence decreases the DNA damage and induction of apoptosis. The resistant mechanisms include (a) upregulation of efflux pumps, (b) continued topoisomerase-II (TOP2A) function, and (c) suppression of downstream apoptosis signalling (Cox and Weinman, 2016) (Figure 1.6).

Doxorubicin can pass through cellular membranes independently of specific transporters due to its hydrophobic properties (Alves *et al.*, 2017). However, the accumulation of the drug could be decreased due to the active drug efflux through ATP-dependent efflux transporters (Cox and Weinman, 2016). The ATP-binding cassette (ABC) transporter family were first determined to be an important component of drug transport in different tissues. The increased expression of ABCB1 (MDR1, P-glycoprotein) is believed to contribute to doxorubicin resistance by acting as an ATP-dependent drug efflux pump and resulting in increased drug efflux (Germann, 1996; Germann *et al.*, 1997). Multiple transcription factors including NF-Y and the Sp family are indicated to be controlling the gene expression of ABC proteins (Scotto, 2003).

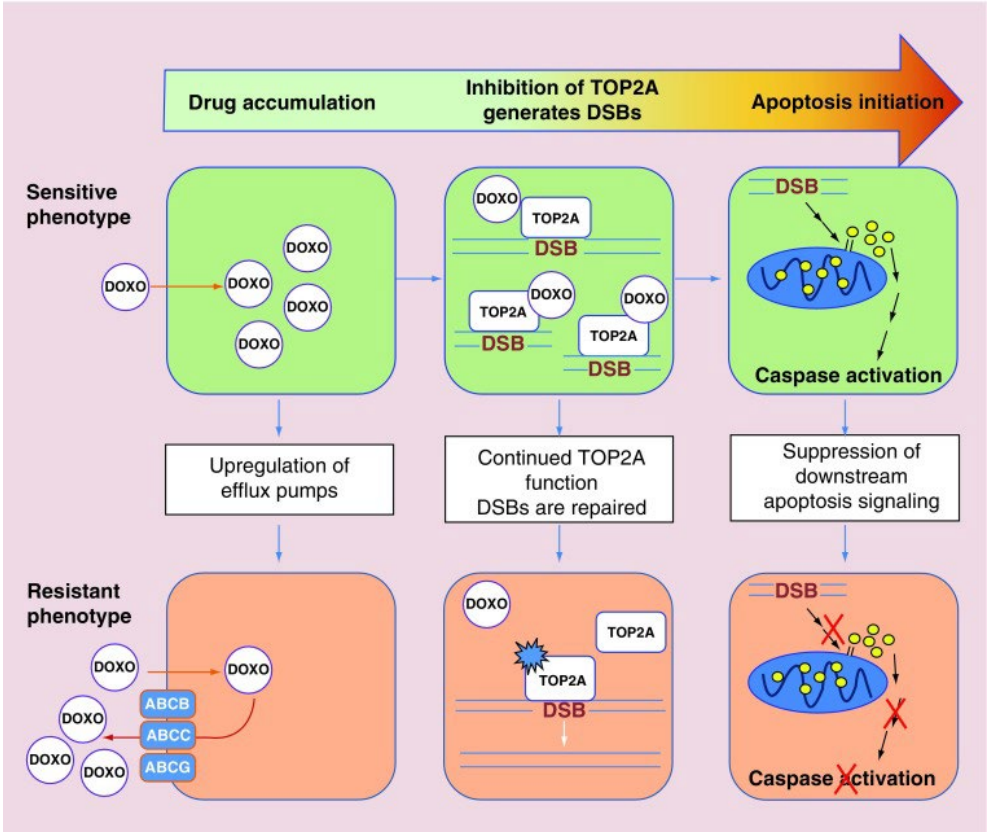

Figure 1.6: Resistant mechanisms of doxorubicin in cancer cells. (a) Accumulation of doxorubicin is inhibited by the upregulation of ABC family efflux pumps. (b) The repair of TOP2A-generated double-stranded DNA breaks are inhibited by doxorubicin. (c) Apoptosis is inhibited by the downregulation of effectors of apoptosis. Adapted from (Cox and Weinman, 2016).

Several transcription factors such as AP-1 and NF- κB have been shown to upregulate the expression of ABC family proteins, whereas p53 is capable of downregulating their expression (Osborn and Chambers, 1996; Johnson, Ince and Scotto, 2001; Kuo *et al.*, 2002). Additionally, P-gp expression has been demonstrated to be influenced by the activity of the enzyme COX-2 as celecoxib, a COX-2 inhibitor, successfully downregulates the P-gp expression in multidrug-resistant HCC liver cancer cells (Fantappiè *et al.*, 2007; Mazzanti *et al.*, 2009).

One of the mechanisms of action of doxorubicin is causing cellular toxicity by topoisomerase-II (TOP2A), leading to protein-bound double-stranded DNA breaks (DSBs) and the subsequent triggering of apoptosis (Nitiss, 2009). One study has demonstrated by showing the sensitivity of doxorubicin is increased through the reduction of TOP2A expression and increasing of the beta isoform of topoisomerase II (Nitiss, 2009). Additionally, another study also indicates that tumours with deletion of TOP2A have increased resistance and tumours with upregulated TOP2A gene have increased sensitivity of doxorubicin (Krishna and Mayer, 2000; Press *et al.*, 2011).

The third proposed mechanisms of doxorubicin resistance is the suppression of downstream apoptosis signalling, such as p53, NF-κB, FOXO3, PI3K/Akt, MAP kinases, sirtuins and microRNAs (Cox and Weinman, 2016). The tumour suppressor p53 is one of the DNA damage sensors and responsible as a transcriptional activator of pro-apoptotic factors (Bartke *et al.*, 2001; Ryan, Phillips and Vousden, 2001). The enhancement of p53 by inhibitor of MDM2-p53 binding, Nutlin-3 has been shown to increase the sensitivity of cancer cells to doxorubicin (Zheng *et al.*, 2010). Moreover, the restoration of p53 expression has promoted the apoptosis activity induced by doxorubicin in HCC cells (Zhao *et al.*, 2007). NF- κB is another transcription factor with multiple and opposing

functions, such as tumour suppression or promotion depending on the cellular context (Fan *et al.*, 2008). Activation of NF- κB signalling by DNA damage leads to variable effect on apoptosis mainly through the regulation of Bcl-XL and XIAP (Fan *et al.*, 2008). When doxorubicin induces double-stranded DNA breaks in DNA, NF- κB will act with an anti-apoptotic effect (Perkins, 2012). The gene FOXO3 also potentially contributes to doxorubicin resistance by activating P-gp in leukemic cells (Hui *et al.*, 2008), and the expression of FOXO3 has been observed to be increased in breast cancer tissue with poor prognosis and doxorubicin-resistant breast cancer cell lines (Chen *et al.*, 2010).

1.4.3 Adenosine triphosphate-binding cassette (ABC) transporter

The expression of a class of energy-dependent efflux pumps known as adenosine triphosphate (ATP)-binding cassette (ABC) transporters are one of the dominant mechanisms of cancer multi-drug resistance (MDR) (Gottesman, Fojo and Bates, 2002; Gillet and Gottesman, 2010). There are 48 members in this protein family in humans, which are responsible for diverse physiological functions such as transporting peptides, ions, toxins, sterols, and lipids (Holland *et al.*, 2003). Several proteins among these members, including P-glycoprotein (P-gp; also known as multidrug resistance protein 1, MDR1; or ABCB1), breast cancer resistance protein (ABCG2 or BCRP), and MDR-associated protein 1 (ABCC1 or MRP1), are indicated to be involved in multidrug resistance (Cole *et al.*, 1992; Doyle *et al.*, 1998; Gottesman and Ling, 2006). The efficiency of the chemotherapeutic drugs is consequently diminished due to these three transporters' broad drug specificity which could transport structurally diverse compounds and therefore causing drug efflux and decreased drug accumulation inside the cells.

1.4.4 P-glycoprotein

P-glycoprotein (P-gp) is the first identified and most studied MDR transporter over 40 years ago and has been recognised as a possible target to overcome multidrug resistance in cancer (Gottesman and Ling, 2006). More than half of the NCI-60 tumour cell lines such as central nervous system tumours and all melanomas express P-gp (Alvarez *et al.*, 1995; Szakács *et al.*, 2004). Poor clinical outcome and reduced chemotherapeutic response has been linked to the increased expression of P-gp in various cancer cells including solid tumours and blood cancers (Sharom, 2011). Moreover, an upregulation of P-gp expression had been found in leukaemia and breast cancer after disease progression following chemotherapy treatment (Leonard, Fojo and Bates, 2003). Various chemotherapeutic drugs are susceptible to P-gp mediated efflux, including taxane-based drug (docetaxel & paclitaxel), tyrosine kinase inhibitors, anthracyclines (daunorubicin & doxorubicin), and others as shown in Figure 1.7 (Ambudkar *et al.*, 1999 ; Eckford and Sharom, 2009; Sharom, 2011).

P-gp is also responsible for normal physiological detoxification by transporting abundant endogenous and exogenous substrates (Szakács *et al.*, 2006). High levels of P-gp are expressed in the epithelial cell surfaces, for example the biliary epithelium of liver, mucosa of the gastrointestinal tract, adrenal cortex, and proximal tubules of kidney (Fojo *et al.*, 1987; Cordon-Cardo *et al.*, 1989; Schinkel *et al.*, 1994). Adrenal and kidney cancer cells with multidrug resistance also have high expression levels of P-gp (Noonan *et al.*, 1990). In addition, hematopoietic progenitor cells of bone marrow are protected by the presence of P-gp effluxing chemotherapeutic agents (van Tellingen *et al.*, 2003). Furthermore, drugs such as paclitaxel has been affected by the P-gp expression in intestinal epithelia due to its capability of modifying tissue absorption and drugs elimination (Sparreboom *et al.*, 1997). Due to all these impacts of P-gp to

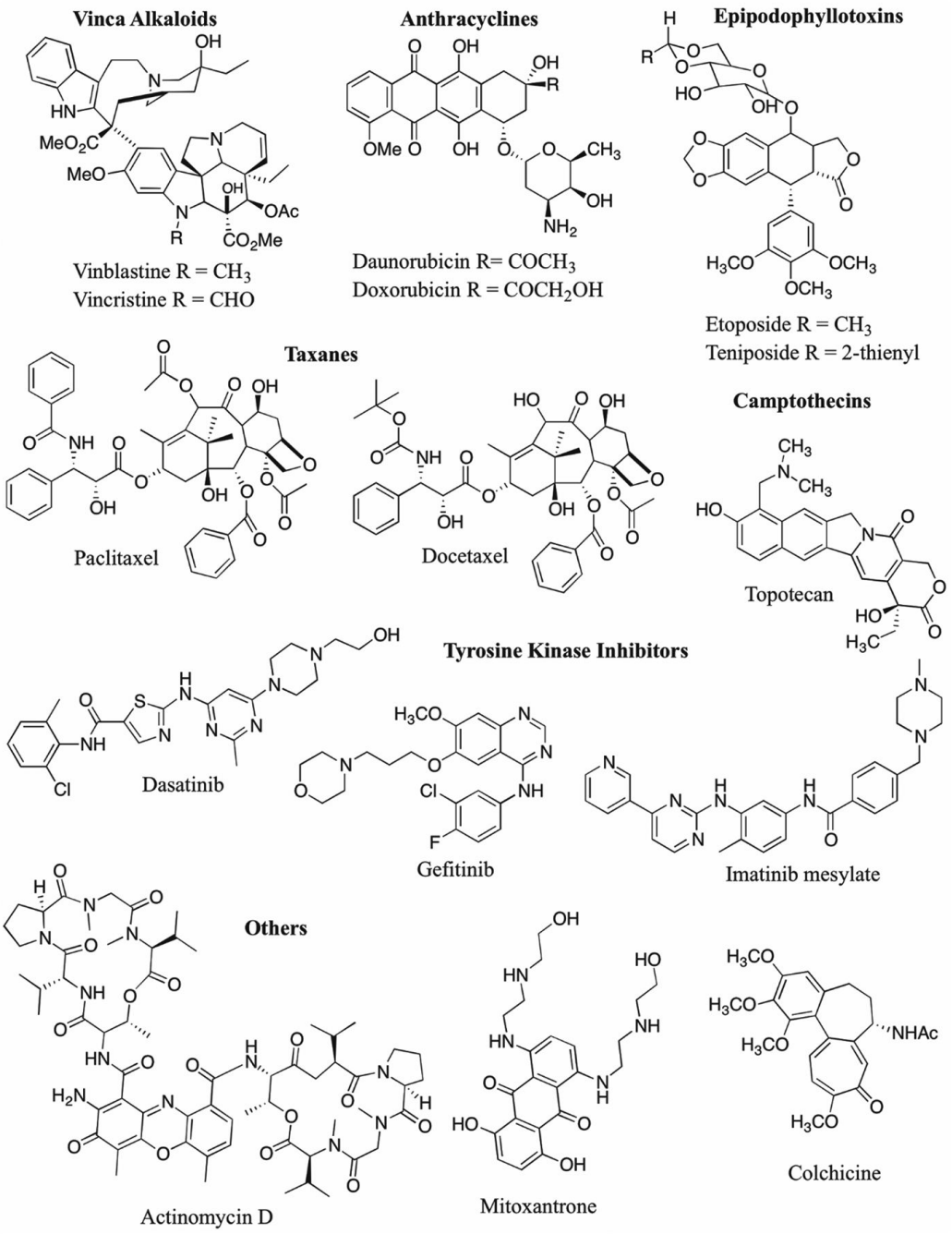

Figure 1.7: Chemotherapeutic cancers which are susceptible to P-gp mediated efflux.

Adapted from (Waghray and Zhang, 2018).

chemotherapeutic drugs as its normal physiological detoxification, the evaluation of P-gp susceptibility during a new drug candidate development has become an important step in the pharmaceutical industry (Borst and Schinkel, 2013).

1.4.5 Development of P-gp inhibitors

The first generation of P-gp inhibitors were defined to have an important effect as inhibition of ABC transporters such as P-gp. The first generation P-gp inhibitors are cyclosporine A (Higgins *et al.*, 1997), quinidine (Callaghan *et al.*, 2008), and verapamil (Lage, 2008). These P-gp inhibitors are the first chemo-sensitiser identified as the substrates for P-gp and the function is to compete with the chemotherapeutic drug compounds for efflux by the P-gp pump. However, these chemo-sensitisers are not highly specific for the P-gp, instead they are substrates for other transporters which result irregular pharmacokinetic interactions with the chemotherapy drugs (Ambudkar *et al.*, 1999). In addition, the level of affinity of P-gp for these first generation of inhibitors are low, and require high doses to increase its efficiency that resulting in undesirable toxicity (Ullah, 2008).

The development of second generation P-gp inhibitors was based on the experience with the first generation modulators, to identify analogues to specifically inhibit P-gp with greater potency and less toxicity (Krishna and Mayer, 2000). Chiral drugs were implemented in most of the second generation of P-gp inhibitors such as dexverapamil, which is the R-enantiomer of first generation verapamil (Wilson *et al.*, 1995). Another type of second-generation inhibitor is the dexniguldipine, which is the R-enantiomer of niguldipine has a lower affinity for calcium channel binding sites but with equally potent in reversing drug resistance via inhibiting P-gp (Höllt *et al.*, 1992). Valspodar or PSC-833 was developed from cyclosporine A by Novartis as a potent MDR modifier with

around 20 fold more potent than cyclosporine A (Kusunoki *et al.*, 1998). However, the major side effect of this compound is it resulted in increased drug toxicity due to the interaction of the associate chemotherapeutic drugs (Chico *et al.*, 2001). In addition, the second generation inhibitors also lacked selectivity of P-gp (Merlin *et al.*, 1994).

The third generation of P-gp inhibitors were developed to overcome the limitations of the second generation P-gp inhibitors by using combinatorial chemistry and quantitative structure activity relationships (QSR) (Krishna and Mayer, 2000). The third generation of inhibitors include elacridar, zosuquidar, tariquidar, ontogen, laniquidar, PGP-4008, DP7, and CBT-1 (Palmeira *et al.*, 2012). Third generation inhibitors were displayed a higher level of specificity to P-gp, however elacridar and tariquidar (XR9576) were found to be also bind to BCRP transporter (de Bruin *et al.*, 1999; Kelly *et al.*, 2011). Despite the discovery and development of third generation of P-gp inhibitors with increased potent and specificity to P-gp, improvements are still needed to be considered as a perfect MDR inhibitor to effectively overcome drug resistance in cancer cells. Poor results were obtained from phase III clinical trials for tariquidar, elacridar, ontogen, zosuquidar, and laniquidar mostly due to high toxicity (Palmeira *et al.*, 2012).

1.5 Cellular mechanisms of methotrexate

1.5.1 Cytotoxicity of methotrexate

Inhibition of the synthesis of purines and pyrimidines required for DNA and RNA synthesis in malignant and non-malignant cells was the mechanism initially proposed during the development of methotrexate. However, other mechanisms of action have been shown in cancer cells, including (a) inhibition of transmethylation reactions, (b) diminished accumulation of polyamines, (c) decreasing of proliferation of antigen-dependent T-cells, and (d) enhanced adenosine release (Tian and Cronstein, 2007) (Figure

1.8). The function of most cell types involved in inflammation are regulated directly or indirectly by methotrexate including T cells, B cells, monocytes, neutrophils, endothelial cells, and fibroblast-like synoviocytes (FLSs) (Cronstein and Aune, 2020). Folate-dependent enzymatic steps in the de novo synthesis of purines and pyrimidines were targeted by methotrexate critically to inhibit the synthesis of DNA and RNA. Patients taking methotrexate normally exhibits decreasing number of circulating leukocytes in the bone marrow (Steffen and Stolzmann, 1969). When methotrexate is used as the treatment of inflammatory disease instead of malignancies, the reduced number of leukocytes cause a toxic reaction for the patients. Patients with rheumatic disease are therefore normally treated with folic acid or folinic acid to prevent the toxic effects of methotrexate (Morgan *et al.*, 1990, 1998; Shiroky *et al.*, 1993; Morgan, 1994).

Dihydrofolate reductase (DHFR) is an enzyme responsible for catalysing the reduction of dihydrofolate to tetrahydrofolate. The formation of methyl donors tetrahydrofolate and 5-methyltetrahydrofolate is diminished when the DHFR is inhibited by methotrexate and hence reducing the synthesis of polyamines such as spermine and spermidine. Polyamines function as cytotoxins that could result in injuring the cells when monocytes hydrolyse polyamines to ammonia and H_2O_2. (Nesher and Moore, 1990). Adenosine is converted by adenine nucleotides via the action of the cell-surface enzymes ectonucleoside triphosphate dephosphorylase 1 (CD39) and ecto-5'-nucluotidase (CD73). The anti-inflammatory effects of methotrexate mediated by adenosine is demonstrated by studies in mice where adenosine release is increased by methotrexate (Cronstein, Naime and Ostad, 1993).

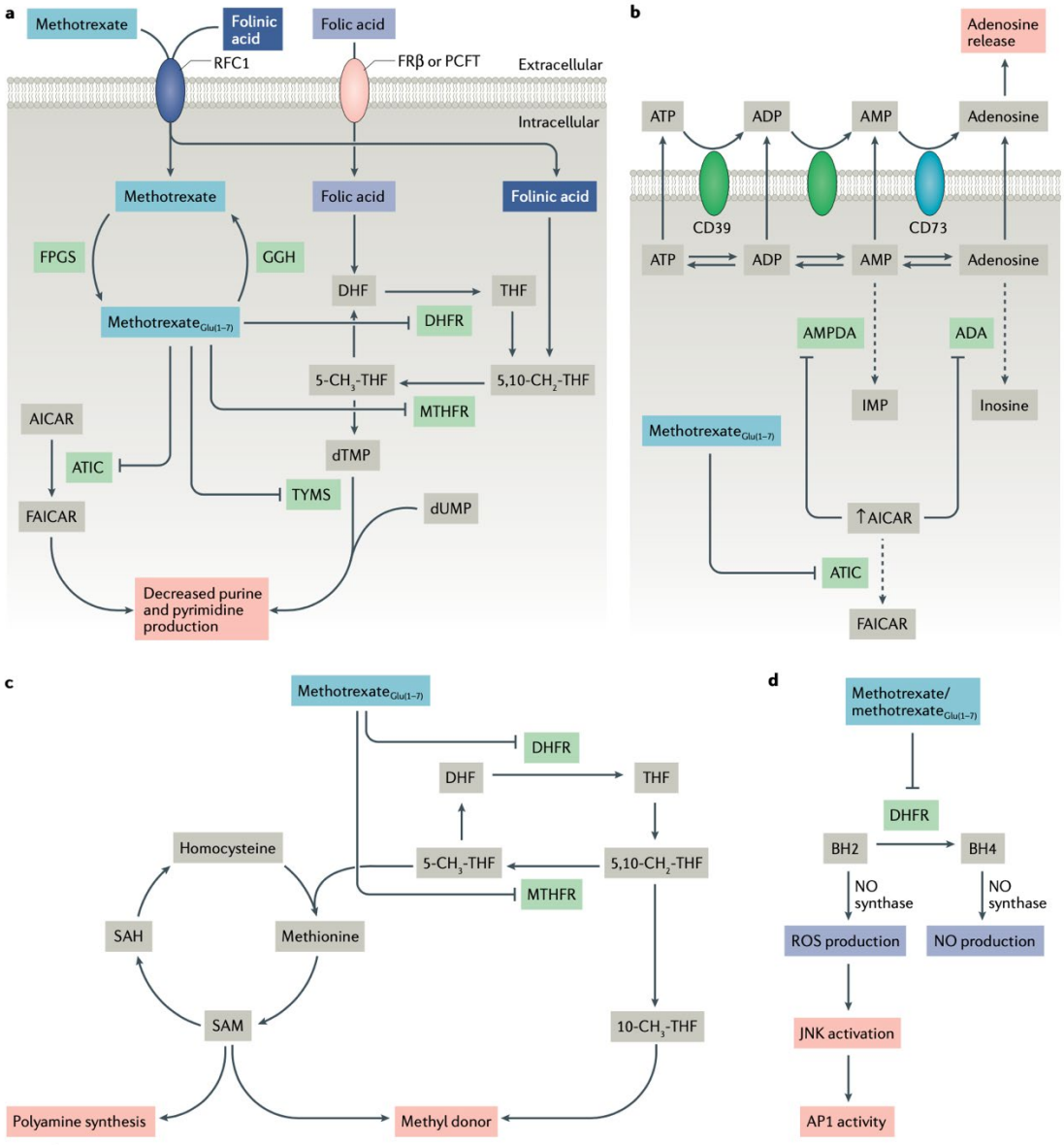

Figure 1.8: Essential biochemical reactions regulated by methotrexate. (a) Inflammation suppresses by methotrexate, (b) enhancement of adenosine release, (c) inhibition of transmethylation reactions, (d) nitric oxide synthase uncoupling. Adapted from (Cronstein and Aune, 2020).

Nitric oxide synthase uncoupling occurs when reactive oxygen species such as hydrogen peroxide is produced instead of nitric oxide by nitric oxide synthases during the absence of tetrahydrobiopterin (BH4). DHFR also catalyses the reduction of dihydrobiopterin (BH2) to BH4, whereas this reduction of both dihydrofolate and BH2 are inhibited by methotrexate. The increased production of reactive-oxygen species then activates the transcription factor JUN serves as a key regulator of apoptosis as well as other cellular processes (Cronstein and Aune, 2020).

1.5.2 Mechanisms of methotrexate resistance

Around 20% to 30% of acute lymphoblastic leukaemia (ALL) patients experiencing methotrexate treatment failure due to drug resistance (Rhee *et al.*, 1993). Methotrexate resistance has been widely studied extensively *in vitro* and *in vivo*. There are five different major resistance mechanisms proposed, including (a) decreased accumulation of drug due to impaired transport, (b) reduction of polyglutamate formation, (c) upregulation of DHFR, (d) mutated DHFR with decreased binding ability to methotrexate, and (e) increased level of γ-glutamyl hydrolase which hydrolyses methotrexate polyglutamates (Wang and Li, 2015)

Resistant mechanisms caused by transport mechanisms are the most common acquired resistance *in vitro* and *in vivo* (Sirotnak, 1987; Schweitzer, Dicker and Bertino, 1990). Due to lack of samples and internal controls, the study of methotrexate transport in patients is limited. An additional challenge in performing a comparative analysis for the assessment of resistance is that pre- and post-treatment samples are required. The methotrexate resistant mechanisms include increased levels of DHFR enzyme due to the overexpression of DHFR gene, and impaired intracellular transport of methotrexate, as a consequence of decreased level of the reduced folate carrier (RFC) in the cell membrane

(Guo *et al.*, 1999). The ABC-family of membrane bound transporters do not only mediate resistance doxorubicin, they have also been shown to play an important role in the efflux of methotrexate out of the cell (Zeng *et al.*, 2001). MRP1, MRP2 and MRP3 in particular have been demonstrated to effectively transport methotrexate out of the cell and play an important role in contributing methotrexate resistance (Kruh *et al.*, 2001). Another study has also found a significant decreased accumulation of methotrexate in cells with overexpressing wild-type P-gp, indicating methotrexate is also one of the substrates of P-gp (Jiang, Yan and Wu, 2019). As elevated levels of MRP1 contributes to the resistance of doxorubicin and elevated levels of MRP2 is contributing to the cisplatin resistance (Guminski *et al.*, 2006), tumours with enhanced levels of these two proteins will lead to a cross resistance in cisplatin, doxorubicin, and methotrexate, which are the most effective chemotherapeutic agents used in treating osteosarcoma patients.

The retinoblastoma gene (Rb), is a tumour suppressor gene, has an influence on DHFR expression (Iida *et al.*, 2003). Methotrexate resistance was observed in human sarcoma cancer cells with absence of retinoblastoma protein (pRb) and resulting increasing DHFR mRNA expression and enzyme activity without gene amplification (Li *et al.*, 1995). Moreover, cancer cells with mutated *p*53 with the association of low-level DHFR gene expression will result in cells that enter the S phase of the cell cycle without repair of DNA damage caused by methotrexate (Göker *et al.*, 1995).

1.5.3 Decreased intracellular accumulation of methotrexate

The most common mechanisms for methotrexate-resistance in tumour cells including osteosarcoma is to decrease drug accumulation in the cells. Osteosarcoma cells could achieve reduction of methotrexate accumulation through reducing number of drug

carriers on the cell surface, increasing drug efflux, and alterations in the expression or structure of target enzyme (He, Ni and Huang, 2014).

Dihydrofolate reductase (DHFR) plays an important key role in the synthesis of de novo DNA and the synthesis of DNA is inhibited by the interaction between methotrexate and DHFR. Reduced folate carrier (RFC) is one of the pathways methotrexate uses to enter the tumour cells (Goldman and Matherly, 1985). RFC was shown to be involved in contributing the resistance mechanisms to methotrexate in osteosarcoma, whereas methotrexate-resistant osteosarcoma cells were present a lower intracellular concentration of methotrexate and decrease expression level of RFC compared to sensitive osteosarcoma cells (Wang and Li, 2014). The association between the reduction in RFC expression and methotrexate resistance in osteosarcoma cells was also demonstrated in the study of Hattinger *et al*. (Hattinger *et al.*, 2003).

Moreover, a correlation study between the histological response to pre-operative chemotherapy and the protein level of RFC has shown a decrease in RFC in samples with poor histological responses (Flintoff *et al.*, 2004). Genetic alterations in RFC proteins have been shown to confer resistance to methotrexate depending to the degree of alteration (Yang *et al.*, 2003). Promoter methylation and polymorphism in 3'UTR of RFC may also be the cause of reduction as decreased RFC expressing was found in samples with heterozygous polymorphism of 2617 C/T or 2582 T/G in the 3' UTR (Yang *et al.*, 2008).

1.6 Other resistant mechanisms in osteosarcoma

The standard treatment regimen for osteosarcoma includes the combination of surgery and chemotherapy. The most common chemotherapeutic drugs used are the combination

of cisplatin (CIS), doxorubicin (DOX), and methotrexate (MTX). All chemotherapeutic drugs have different mechanisms of action to eliminate the tumour cells and one major benefit of applying combination of drugs is the different modes of action increase the chances of targeting the tumour cells at different levels. For example, in the osteosarcoma standard regimen, cisplatin is capable of preventing DNA replication and cell division by inhibiting DNA synthesis; doxorubicin is able to produce free radicals which trigger apoptosis of the cell by inhibiting topoisomerase II; and methotrexate inhibits the reduction of folic acid and resulting in the inhibition of tumour proliferation (Wittig *et al.*, 2002; Bielack *et al.*, 2008; Ando *et al.*, 2013). However, around 25% of the total patients who respond to the current standard treatment will still relapse due to the chemotherapy resistance. The current standard treatment also result in low-survival rates for osteosarcoma patients with metastases at diagnosis, which furthermore decreases the efficacy for high-risk patients (Marchandet *et al.*, 2021).

Chemotherapy resistance can be divided into two categories, which are intrinsic resistance and acquired resistance (Holohan *et al.*, 2013). Intrinsic resistance is the pre-existing tumour cells that are already resistant prior to any drug treatment (Lippert, Ruoff and Volm, 2008). Sensitive tumour cells will be eliminated by the toxic effects of chemotherapeutic drug at the time of administration. However, some of the tumour cells which had become resistant before through genetic mutation or activation of specific signalling pathways will survive through the treatment and proliferate. Meanwhile, acquired resistance happens on tumours cells gradually gaining the resistance mechanism after the drug treatment. On tumour cells with acquired resistance, a gradual reduction of the efficacy of the drugs from the beginning will be seen due to the developed mechanisms such as genetic mutation, activation of proto-oncogene, increased or decreased expression of transport proteins, and changes in the tumour microenvironment

(Wang, Zhang and Chen, 2019). After multiple rounds of treatment, the drugs will eliminate sensitive tumours cells while the resistant clones with those adaptations would allow them to survive and be selected.

1.6.1 DNA repair

Endogenous and exogenous agents can damage DNA under physiological conditions, which will trigger cell death due to the genomic instability during replication. Some mechanisms will prevent or reduce this damage effect such as DNA repair, cell cycle checkpoint, and damage tolerance. However, these mechanisms in the cells are not sufficient to completely neutralise and DNA damage may persist. The main DNA repair mechanisms include base excision repair (BER), nucleotide excision repair (NER), mismatch repair (NMR), direct reversal repair, homologous recombination (HR), and non-homologous end-joining (NHEJ) (Chatterjee and Walker, 2017). Chemotherapeutic drugs, especially cisplatin is known to cause DNA damage in tumour cells and finally leading to cell death. Resistant osteosarcoma cells can then resist the drugs by increasing expression of the DNA repair pathways which frequently results in cross-resistance to other chemotherapeutic agents such as doxorubicin and ifosfamide (Siddik, 2003; Fanelli *et al.*, 2020).

The increase in BER mechanisms, especially the over-regulation of apurinic endonuclease APE-1 is found to be one of the key enzymes contributing to the resistance of osteosarcoma (PosthumaDeBoer, van Royen and Helder, 2013). Poorer overall survival rates have been shown in osteosarcoma patients with high expression of APE-1 (Wang, Luo and Kelley, 2004). Local osteosarcoma recurrence and metastasis has also been linked to the overexpression of APE-1 (Yang *et al.*, 2010). APE-1 has also been associated with MDR and poor prognosis in many other cancers (Fishel and Kelley, 2007).

Poly (ADP-ribose) polymerase 1 (PARP1), another important protein of the BER pathway may also be involved in osteosarcoma chemoresistance. The correlation between the high expression of PARP1 in osteosarcoma patients and shorter survival rate has been demonstrated (Park *et al.*, 2018). Olaparib is used as the inhibitor of PARP1, has been successfully sensitised osteosarcoma cell lines to doxorubicin. Moreover, the use of olaparib with doxorubicin has significant induction of apoptosis and inhibition of proliferation and induction of apoptosis (Park *et al.*, 2018). The NER pathway has also been shown to correlate to the response to chemotherapy in osteosarcoma patients (Nathrath *et al.*, 2002). Osteosarcoma patients with high expression of ERCC2 and ERCC4 have been shown with high tumour necrosis (Li *et al.*, 2007). Conversely, poor response to chemotherapy has been correlated with low expression of ERCC4 (Nathrath *et al.*, 2002). *In vitro* studies have been carried out which silencing ERCC1, ERCC2, ERCC3, and ERCC4 genes has been successfully increase the cisplatin sensitivity of resistant osteosarcoma cell lines (Fanelli *et al.*, 2020).

1.6.2 Disruption of cell cycle and apoptosis

Cell death by apoptosis is triggered by the induction of chemotherapy through DNA damage and the DNA damage is allowed to repair by pausing the cell cycle. Some tumour cells manage to escape apoptosis and continue cell cycle. Therefore, dysregulation of cell cycle and apoptosis related gene expression can modulate the chemotherapeutic resistance in osteosarcoma cells (Fellenberg *et al.*, 2003).

TP53 has a critical role in cell cycle arrest and apoptosis in tumour cells. High levels of p53 mutations have been found in osteosarcoma cells and these mutations can provide malignant characteristics of many cancers (Overholtzer *et al.*, 2003; Muller and Vousden,

2013). Saos-2 cells with transfected with p53 mutant exhibited decreased apoptotic enzymes such as pro-caspase 3, which indicate the loss of chemo-sensitivity is caused by the resistance to p53-dependent apoptosis (Wong *et al.*, 2007). Furthermore, sensitivity to cisplatin has been increased after the transfection of wild-type p53 into osteosarcoma cells not expressing p53 (Tsuchiya *et al.*, 2000).

The Bcl-2 family is another protein regulating cell-death signalling, which includes anti-apoptotic proteins such as Bcl-2, Bcl-XL, and proapoptotic protein Bax (Hata, Engelman and Faber, 2015). Inhibiting Bcl-2 & Bcl-XL has been found to significantly increase the chemosensitivity of osteosarcoma cells to doxorubicin and cisplatin (Zhao *et al.*, 2009). Increased chemosensitivity and apoptosis activity of osteosarcoma cells have also been shown with upregulated Bax expression (Eliseev *et al.*, 2008). Furthermore, lower expression of Bcl-2 has been associated with higher overall survival rate in osteosarcoma (Wu *et al.*, 2012).

1.6.3 Involvement of autophagy

Mechanisms of autophagy have been demonstrated to promote chemotherapy resistance and survival of tumour cells by removing proteins and organelles to provide energy under cellular stress (Degenhardt *et al.*, 2006; Maiuri *et al.*, 2007). Autophagy involves a series of complex processes including forming of phagophore, generation of the autophagosome, and the association with lysosome to generate autolysosomes which degrades and recycles the content to provide energy (Levine and Kroemer, 2008). When autophagy is activated, the elongation and closure of the phagophore requires the ATG12 and LC3 conjugation system (Ohsumi and Mizushima, 2004). ATG7 and ATG12 are involved in the ATG12 conjugation system where the formation of ATG12-ATG5/ATG16 is mediated by the action of ATG7 and ATG10 (Shpilka, Mizushima and Elazar, 2012).

LC3-II and ATG7 are involved in the LC3 conjugation system where nascent LC3 is processed by protease ATG4 which activated by ATG7 and formed LC3-II. LC3-II presents in the autophagosomes is then recognised as an integral membrane protein. After the formation, the autophagosome will sequester the cellular materials which are targeted for degradation through the action of selective autophagy receptors such as SQSTM1/p62 (Shpilka, Mizushima and Elazar, 2012).

The combination of autophagy inhibitor with chemotherapy has been suggested to be an alternative treatment for osteosarcoma patients (Kim *et al.*, 2013). Increased cell death was observed when the autophagy inhibitor 3-methyladenine (3-MA) was used in combination with paclitaxel in osteosarcoma cells (Kim *et al.*, 2013). MG-63 osteosarcoma cells were had a downregulation of autophagy activity when 3-MA was introduced which increased its chemotherapeutic sensitivity to cisplatin (Zhang *et al.*, 2009). Autophagy can be facilitated by chromatin-binding nuclear protein, such as High Mobility Group Box 1 (HMGB1), and the expression of HSP90AA1. Increased autophagy and resistance have been shown in osteosarcoma cell lines with overexpression of HMGB1 and HMGB5 (Jun Huang *et al.*, 2012; Yang *et al.*, 2014). Conversely, the sensitivity of the osteosarcoma cells to chemotherapy was restored when HMGB1 and HMGB5 were knocked-down which downregulate the autophagy activity in the cells (J. Huang *et al.*, 2012; Yang *et al.*, 2014). The expression level of HSP90AA1 was also found to induce autophagy activity and lead to cisplatin, doxorubicin, and methotrexate resistance (Xiao *et al.*, 2018). P53 is also indicated to modulate autophagy in a dual fashion, depending on its subcellular localization. Nuclear p53 stimulates the autophagy pathway thereby sustaining the attempt of cells to cope with stress, and cytoplasmic p53 inhibits autophagy and hence facilitates cell death (Maiuri *et al.,* 2010).

1.7 Epithelial to Mesenchymal Transition (EMT)

The epithelial-to-mesenchymal transition (EMT) describes a cell biology process involved in the alteration of cell phenotype, migration, and invasion which occurs in broad range of tissue types and developmental stages (Savagner, 2010). The mechanism involves the conversion of epithelial cells into a mesenchymal state. Cells enter a series of intermediate phenotype states arrayed between epithelial to mesenchymal axis when related signals are received by a cell as shown in Figure 1.9. A fully mesenchymal cell is converted from a fully epithelial cell when the cell is driven to its extreme state as described as mesenchymal-to-epithelial transition (MET). The major biological differences to distinguish between these two cell types are the epithelial cell-to-cell junctions and apical-basal polarity exhibited on epithelial cells, while intensified motility and invasiveness are demonstrated on mesenchymal cells with spindle-like morphology (Polyak and Weinberg, 2009; Nieto *et al.*, 2016)**.**

EMT was first reported by Elizabeth Hay in 1982 (Greenburg and Hay, 1982), while embryonic morphogenesis is now known to be profoundly correlated to the EMT mechanism as it plays an essential role in multiple steps of embryonic morphogenesis (Lim and Thiery, 2012). The malignancy of a cancer is determined by its ability to invade into its surrounding cell tissue, spread to other organs throughout the body and to develop secondary tumours (Gupta and Massagué, 2006). A series of progress is involved to the formation of metastasis in distant organs as shown in Figure 1.10. The process is initiated when the tumour cells lose cell-to-cell adhesion and migrate out of the primary-tumour site and invade into surrounding cell tissue. After spreading to other parts of the body, the tumour cells adhere to the target-organ endothelium and form a secondary tumour site. The EMT process is often reversible to permit the carcinoma cells to convert back to epithelial cell phenotype from mesenchymal via Mesenchymal-to-Epithelial Transition

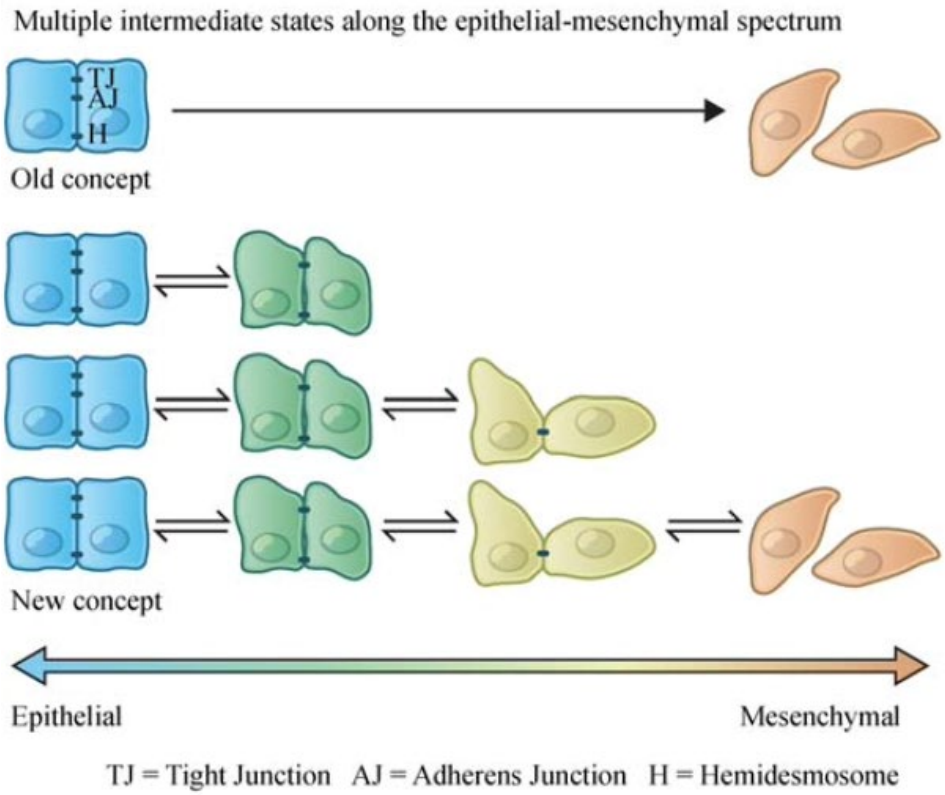

Figure 1.9: The conversion of mesenchymal cell from epithelial cell via the intermediate phenotype states arrayed from epithelial to mesenchymal axis. Instead of a unidirectional binary switch between epithelial and mesenchymal cell states, EMT mechanism involves in a spectrum of different intermediate cell states between the fully epithelial and mesenchymal endpoints. Adapted from (Zhang and Weinberg, 2018).

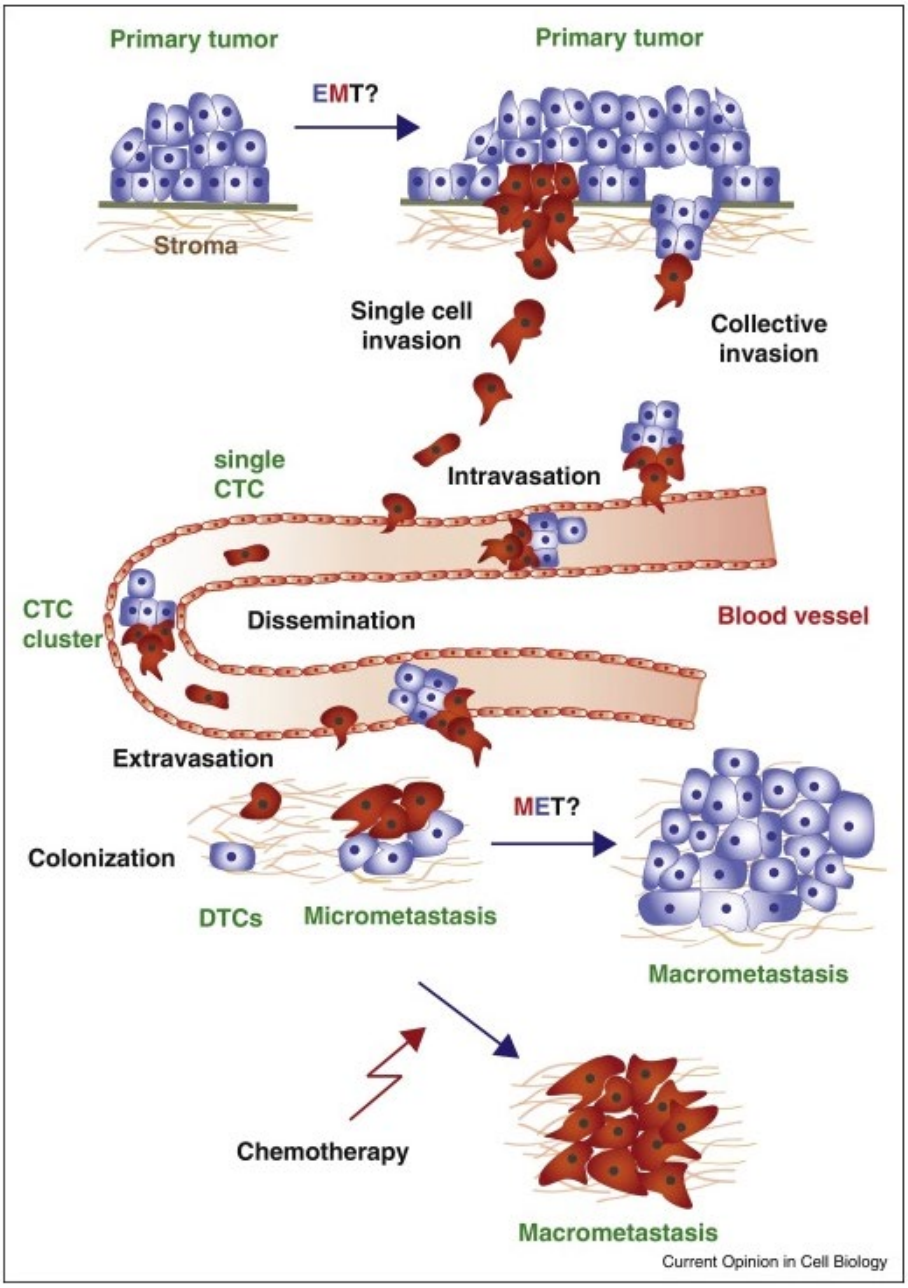

Figure 1.10: Schematic representation of series of progress involved to the formation of metastasis in distant organs. EMT is involved in the metastasis of cancer. The process is initiated by conversion of the tumour cells phenotype from epithelial to mesenchymal cell type with increased migration and invasion rate. MET is activated in the secondary tumour site when the metastatic outgrowth reverts to an epithelial phenotype. Adapted from (Diepenbruck and Christofori, 2016).

(MET) (Hah, Goldinger and Jung, 1985). The activation of MET process on carcinoma cells is often activated after the tumour cells reach the secondary site and metastatic outgrowth support is needed in distant organs (Acloque *et al.*, 2009; Thiery *et al.*, 2009; Nieto, 2013).

1.7.1 Regulation of EMT

EMT progression can be mediated by activating the signalling cascades by multiple extracellular stimuli during malignant tumour progression and tissue development or regeneration (Diepenbruck and Christofori, 2016). Classical growth factors produced by tumour cells can induce EMT progression in a context-dependent manner. Other signalling pathways such as JAK/STAT, Wnt, Hedgehog, Notch, NF-κB, AP-1 and Hippo signalling pathways are also responsible for modulating the EMT process (Acloque *et al.*, 2009; Thiery *et al.*, 2009; Nieto, 2013). EMT progression and tumour cell invasion can also be triggered by tissue hypoxia, matrix stiffness or mechanical and metabolic stresses (Lamouille, Xu and Derynck, 2014).

EMT-associated transcription factors (TFs) play a major role in these EMT-inducing pathways (Nieto and Cano, 2012). The main TF families include Zeb (Zeb1 and Zeb2), Snail (Snail and Slug), Twist (Twist1, Twist2, E12, E47 and Id) (Peinado, Olmeda and Cano, 2007). These main transcription factors are associated with the dedifferentiation process of tumour cells. EMT progression is regulated via these transcription factors by repressing or activating epithelial and mesenchymal genes, such as E-cadherin and N-cadherin (Peinado, Olmeda and Cano, 2007; Lamouille, Xu and Derynck, 2014). Other TFs such as Sox4 and Sox9, p53, members of AP-1 family also shown to be modulating and contribute to the EMT or MET progression (Chang *et al.*, 2011; Tiwari *et al.*, 2013, p. 4; Bakiri *et al.*, 2015). miRNAs such as members of miR-200 family are also associated

with the induction of EMT progression (Gregory *et al.*, 2008; Díaz-Martín *et al.*, 2014). MET in mesenchymal cells is induced by the expression of miR-200 family members via the repression of TFs Zeb1 and Zeb2 (Korpal *et al.*, 2008). The regulation of Zeb TF family by miR-200 family members also demonstrates to be involved in altering the cell migration and invasion (Burk *et al.*, 2008). Transcription factors and miRNAs are shown to act as molecular switches in modulating the reversibility of EMT and MET progression and therefore epithelial/mesenchymal cell plasticity (Brabletz and Brabletz, 2010).

1.8 Significance/ Contribution to the discipline

Two osteosarcoma cell lines (HOS-143B and MG-63) were chosen to develop into novel drug-resistant models in this study. Apart from developing resistant cell lines with one single chemotherapeutic agent, osteosarcoma cell lines MG-63 and HOS-143B were induced by combination of chemotherapeutic agents (cisplatin, doxorubicin, and methotrexate) at the same time to develop into a novel multi-drug resistant osteosarcoma model. To date, there are no studies published on developing a resistant model by using combination of drug in any osteosarcoma cell lines. Apart from inducing with combination of chemotherapeutic drugs, other sublines that were treated with single chemotherapeutic agent were also aimed to be developed into clinically relevant models. Successfully establishing multi-drug induced osteosarcoma resistant models will benefit the research area in osteosarcoma's chemoresistance. This multi-drug induced resistant model will present a more complex resistant mechanism or pathway that is associated with all three of the chemotherapeutic drugs. These multi and single drug induced resistant models will be characterised for their mechanisms of drug resistance. Studying the multi and single-drug induced osteosarcoma resistant models will allow us to understand the mechanisms of chemoresistant between cisplatin, doxorubicin, and methotrexate.

1.9 Hypothesis

Developed single- and multi-agent induced osteosarcoma resistant models of MG-63 and HOS-143B will present a molecular change based on the fold resistant acquired to each of the drugs. Due to the high degree of metastases possess by HOS-143B, we hypothesised that a higher level of resistance would be acquired earlier compared to MG-63 cell line. We also proposed that resistant models induced by multi-agents will develop a lower level of resistance compared to the single-agent induced models.

1.10 Aims and Objectives

The aim of this study was to investigate the chemoresistance mechanisms in osteosarcoma cells lines by establishing chemo-resistant osteosarcoma cell lines from MG-63 and HOS-143B.

Objective 1: To establish single- and multi-agent resistant human osteosarcoma cell lines from MG-63 and HOS-143B.

Objective 2: To assess the characteristic of the resistant models compare to the parental cell lines, including cross resistance, proliferation, migration, invasion, and apoptosis activity.

Objective 3: To characterise the expression of genes which are involved in cisplatin, doxorubicin, and methotrexate resistance in the resistant models.

Chapter 2: Materials & Methods

2.1 Supplier of commonly used reagents

Table 2.1 Supplier of commonly used reagents.

Reagent	Catalogue No.	Supplier
100 mM DTT	1120943	Invitrogen
10mM dNTP Mix	RO192	Thermo Scientific
10X Tris-Glycine SDS Buffer	28362	Thermo Scientific
2.5% Trypsin (10X)	15090-046	Gibco
2X Laemmli Sample Buffer	1610737	Bio-Rad Laboratories
2X QuantiNova SYBR Green PCR Master Mix	208054	Qiagen
5-Bromo-2'-deoxyuridine (BrDU)	B5002-500MG	Sigma-Aldrich
5X SSIV RT Buffer	1124806	Invitrogen
β–Mercaptoethanol	M6250-100	Sigma-Aldrich
Blotting-grad Blocker	170-6404	Bio-Rad Laboratories
Bovine Serum Albumin (BSA)	BP9701-100	Sigma-Aldrich
Bradford Reagent	B6916-500mL	Sigma-Aldrich
Cisplatin	WO41881AD	St. James Hospital Pharmacy
Collagen I	A1064401	Thermo Fisher
Collagen IV	234154	Sigma-Aldrich
DilC12(3) perchlorate	468495-100MG	Sigma-Aldrich
Dimethyl Sulfoxide	BP231-100	Fisher
DMEM (1X) + GlutaMAX	61965-026	Gibco
Docetaxel	PHR1883-200MG	Sigma-Aldrich
Doxorubicin	D1515-10MG	Sigma-Aldrich

EDTA	BP2482-100	Fisher Scientific
Elacridar	SML0486-10MG	Sigma-Aldrich
FastStart Essential DNA Green Master	6402712001	Roche
Fetal Bovine Serum	10270-106	Gibco
Fibronectin	10838039001	Sigma-Aldrich
Gemcitabine	G6423-10MG	Sigma-Aldrich
Halt Protease Inhibitor	1862209	Thermo Scientific
Laminin	11243217001	Sigma-Aldrich
MEM NEAA (100X)	11140-35	Gibco
Methotrexate	A6770-100MG	Sigma-Aldrich
Mini-Protean TGX Precast Gel	4561084	Bio-Rad Laboratories
Phosphatase Substrate	P4744-10G	Sigma-Aldrich
Phosphate Buffered Saline Tablets	BP2944-100	Fisher
Pierce ECL Western Blotting	32196	Thermo Scientific
Pierce RIPA Buffer	89900	Thermo Scientific
Ponceau S Solution	P7170-1L	Sigma-Aldrich
Precision Plus Protein Standards	1610374	Bio-Rad Laboratories
PureLink DNase	12185-010	Invitrogen
PureLink DNase Set	12185010	Thermo Fisher
PureLink RNA Mini Kit	12183018A	Invitrogen
QuantiNova Reverse Transcription Kit	205411	Qiagen
Qubit RNA BR Assay	Q10211	Thermo Fisher
Random Hexamer Primer	SO142	Thermo Scientific
RNase Inhibitor	N8080119	Applied Biosystem

RNeasy Plus Mini Kit	74134	Qiagen
Sodium Acetate	S8750-500G	Sigma-Aldrich
Sodium Hydroxide	S5881-500G	Sigma-Aldrich
Sodium Pyruvate (100mM)	11360-070	Gibco
SuperScript IV Reverse Transcriptase	1121053	Invitrogen
Taqman gene Expression Master Mix	4369016	Applied Biosystem
Trans-Blot Turbo Transfer Pack	1704158	Bio-Rad Laboratories
Triton X-100	T-9284	Sigma-Aldrich
Trypan Blue Stain (0.4%)	15250-061	Gibco
TWEEN 20	P1379-500	Sigma-Aldrich

Table 2.2 Cell lines.

Cell Lines	Types	Purpose
MG-63	Osteosarcoma	Developing resistant sublines
HOS-143B	Osteosarcoma	Developing resistant sublines
MCF7	Breast cancer	Negative control for migration assay
HT1080	Human fibrosarcoma	Positive control for migration assay

2.2 Cell Culture techniques

2.2.1 Cell culture conditions

All cell-culture procedures were conducted in a Class II laminar flow hood (Mars Safety Class 2, Scanlaf). Cell culture passage and expansion were maintained in CO_2 incubators (Binder), at 37°C, 5% CO_2 in a humidified environment. Centrifuge (Rotina 380R, Hettich) was used for all centrifugation of cell suspensions during cell passage. The use of cancer cell lines was approved by the Middlesex University Ethics Committee under protocol numbers 4088 (Appendix 1).

2.2.2 Culture of cancer cell lines

Osteosarcoma cell lines MG-63 and HOS-143B were sourced from the laboratory of Dr S. Robert (Institute of Musculoskeletal Science, University College London). HT1080 human fibrosarcoma cell line and MCF7 breast cancer cell lines were purchased from ATCC. All cells were grown in DMEM (Gibco 500 mL) supplemented with 10% Fetal Bovine Serum (Gibco, 500 mL), 1% sodium pyruvate (Gibco), 1% non-essential amino acids (NEAA) (Gibco), free of antibiotics. All cells were maintained in a humidified atmosphere of 5% CO_2 at 37°C. Only cells at log phase of growth were used in the experiments. Cell lines were routinely tested for mycoplasma as described in Section 2.3 and were mycoplasma-free.

Parental osteosarcoma and its corresponding resistant models were grown without the addition of antibiotic (Pen/Step) and BrDU (Bromodeoxyuridine) (Sigma-Aldrich). The HOS-143B cell line is recommended to be cultured with 10% FBS, 1% sodium pyruvate, 1% of NEAA, and 0.015 mg/mL of BrDU while MG-63 uses the same media and supplements but in the absence of BrDU (King and Attardi, 1996). As MG-63 and HOS-143B would need to be cultured for an extended period to develop their resistant models,

it was ideal to grow both cell lines in the same media and supplements (without the BrDU). Therefore, to investigate the absence of BrDU for HOS-143B, a growth assay was performed as described in Section 2.4 and the result is shown in Chapter 3 (Section 3.3.1). HOS-143B were grown in media without BrDU versus media with BrDU and the doubling time was determined and statistically analysed to validate the non-effect of the absence of BrDU. Another growth assay experiment was also performed to grow both cell lines in media with antibiotic versus without antibiotic to make sure the absence of traditional antibiotics does not affect the growth rate of both cell lines. Both cell lines were passaged once a week with 1:100 split for each passage.

2.2.3 Trypsin digestion

Trypsin (Gibco, UK) was used to detach the cells from the surface of the culture flasks when the cells were confluent. In brief, the culture media was removed from the flasks and the phosphate-buffered saline (PBS) (ThermoFisher) was added to wash the cells once to remove any remaining proteins or debris. After washing, 5 mL of 2.5% trypsin solution, no phenol red (Gibco, UK) was added to a T75 flask, or 2 mL of trypsin to a T25 flask to cover the cells. The cells were then incubated at 37°C with 5% CO_2 for 5 minutes to enable the enzymatic digestion of proteins bonding between the cultured cells to the cell culture flask.

2.2.4 Cell Counting

Cell counts were regularly carried out for all cell lines using a haemocytometer (Superior Marienfeld, Germany). After trypsinisation (as described in Section 2.2.3), 1 mL of evenly distributed cell suspension was transferred into a 1.5 mL Eppendorf tube. After that, 50 µL of the cell suspension was then transferred into a new Eppendorf tube and 50 µL of 0.4% Trypan Blue (Gibco, UK) was added and gently mixed. The haemocytometer was prepared by cleaning with 70% of ethanol and a coverslip was placed on top of the

haemocytometer. Total volume of 100 µL of cell suspension with Trypan Blue was pipetted near the edge of the chamber of the haemocytometer to gently allow the cell suspension to enter the counting chamber by capillary action. The haemocytometer was then placed under the microscope and observed with a 10X objective lens. Unstained cells indicated the live cells were counted in the central grid of both chambers of the haemocytometer and the stained cells (blue) were excluded. The average number of cells counts from each chamber were multiplied by 10,000 (10^4) and further multiplied by 2 due to the 1:2 dilution from the Trypan Blue. The final number indicates the total viable cells/mL in the cell suspension.

Some of the cell counting was carried out by using the LUNA-II™ Automated Cell Counter (Logos Biosystem, US). After trypsinised and making a cell suspension as described above, 10 µL of the cell suspension was transferred into a new Eppendorf tube, to which 10 µL 0.4% Trypan Blue Stain (Gibco, UK) was added. The total volume of 10 µL of the cell suspension with added Trypan Blue Stain mixture was then transferred into the chamber of a LUNA™ Cell Counting Slide (Logos Biosystem, US). The slide was then inserted completely into the slide port in front of the automated counter. The cells were previewed on the screen and counted automatically by the counter. The number of cells/ml was shown on the screen when the counter had done counting and the result was saved.

2.2.5 Cryopreservation of cells

When cells were confluent in a T75 flask, they were washed with 5 mL of PBS and was trypsinised with 5 mL of trypsin. The cell suspension was then centrifuged at 1,500 rpm for 5 minutes. After centrifugation, the cells pellets were resuspended in 2.7 mL of complete fresh media. Freezing medium was prepared by adding 600 µL of DMSO

(ThermoFisher) to 2.7 mL of FBS (90% of FBS with 10% of DMSO). This freezing medium was then added to the resuspended 2.7 mL of cell suspension to make up total volume of 6 mL cell suspension in freezing medium. 1 mL of the cell suspension was then aliquoted into each cryovial stored at -80°C overnight before transferring them into the liquid-nitrogen tank.

2.2.6 Thawing of cryopreserved cells

Complete media was warmed up in the water bath before thawing the frozen cells. 10 mL of warm media was transferred to a 15 mL centrifuge tube. A Pasteur pipette was used to transfer 1 mL of warm media to the cryovial containing the cells with freezing medium. The frozen cells in freezing medium was slowly thawed by mixing the warm media up and down with the Pasteur pipette. When the cells were completely thawed, the cells with the freezing medium were transferred to 10 mL of media prepared in centrifuge tube. The newly suspended cells were then centrifuged at 1,500 rpm for 5 mins. The media was discarded after centrifuged and the cells pellets were resuspended in 5 ml of media and transferred to a T25 flask, and the media was changed after 24 hours. When the cells were reached 80% confluency in T25 flask, they were then passaged to T75 flask.

2.3 Detection of mycoplasma

Mycoplasma contamination was regularly tested from the media collected from confluent flasks of all cell lines (MG-63 and HOS-143B). The mycoplasma testing protocol was adapted from (Young *et al.*, 2010). A 24 µL of PCR master mix was prepared for each sample as shown in Table 2.2. After that, 1 µL of the conditioned media collected from each cell lines were added to the PCR master mix. A confirmed positive mycoplasma sample was used for the positive control whereas DNase-free water was the negative control. After mixing the PCR master mix with the media sample, they were run in the

PCR machine (Thermocycler Techne TC-3000G) under the conditions described in Table 2.4.

Table 2.3 Mycoplasma PCR Master Mix

Reagents	Volume
Green 2X Sigma Ready Mix	12.5 µL
Forward Primer 10 µM 5'-GGGAGCAAACAGGATTAGATACCCT-3'	0.5 µL
Reverse Primer 10 µM 5'-TGCACCATCTGTCACTCTGTTAACCTC-3'	0.5 µL
DNase-free water	10.5 µL
Total volume	24 µL

Table 2.4 Mycoplasma PCR Program

No. Cycles	Temperature (°C)	Time (minutes)
1	95	5
40	94	0.5
	55	0.5
	72	1
1	72	10
1	4	Hold

A 2% agarose gel was prepared according to Table 2.5. Total volume of 150 µL of 1X Tris-acetate-EDTA (TAE) (Sigma-Aldrich) was added to the 3 g of agarose (ThermoFisher) and heated in the microwave. After that, 1.5 µL of SYBR Green nucleic gel stain (Sigma-Aldrich) was added to the solution. The gel was then poured into an

agarose gel mould when the agarose was fully dissolved, and a comb was placed into the gel to set. The gel was then submerged in 1X TAE. 12 µL of each sample and ladder (Sigma-Aldrich) was loaded into the wells of the gel. The loaded samples were prepared by adding 2 µL of DNA loading buffer (Sigma-Aldrich) to 10 µL of PCR product. The PCR ladder was prepared by mixing 5 µL of PCR ladder (Sigma-Aldrich), 5 µL sterile water, and 2 µL of loading buffer. After the samples were loaded into the wells, the samples were run at 100 Volts for an hour. The image of the gel was then taken by Licor Odyssey Infrared Imaging System at 600 nm for 30 seconds. The result was analysed using the installed instrument software. An example of the result is shown in Figure 2.1, where only the positive control was observed with a band at 219 bps. Sample MG-63 and HOS-143B showed similar result with negative control which indicate no mycoplasma contamination (Fig. 2.1).

Table 2.5 Composition of 2% Agarose gel

Compositions	Volume
Agarose	3g
1X TAE solution	150 µL
SYBR Green nucleic gel stain	1.5 µL

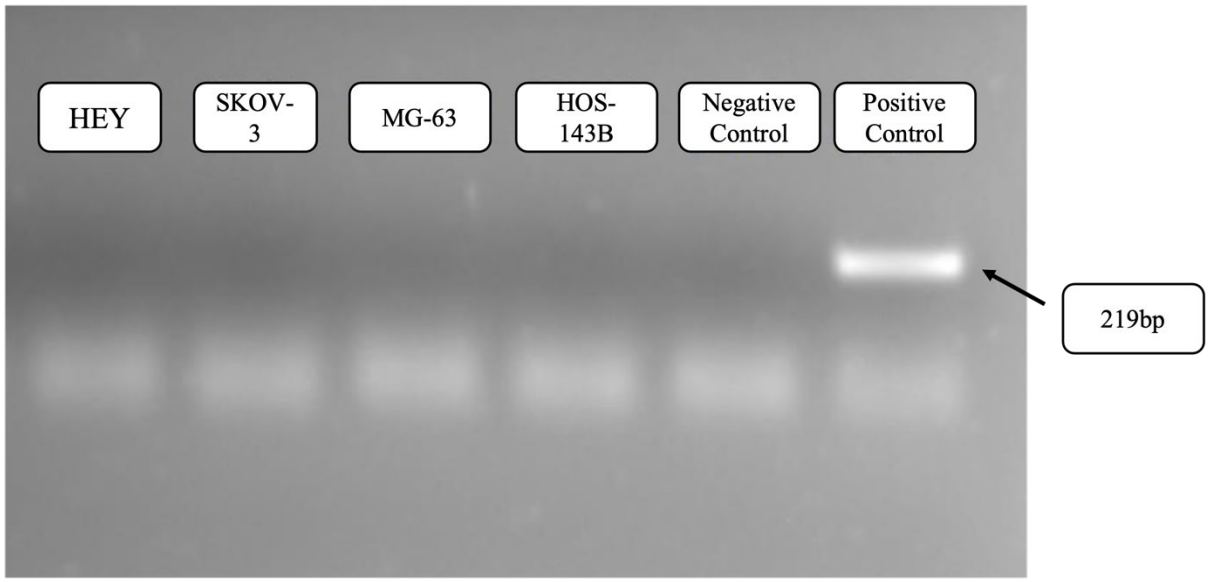

Figure 2.1: Gel image of cell lines tested for mycoplasma. Mycoplasma PCR gel image taken on Licor Odyssey Infrared Imgaing System at 600 nM for 30 seconds. Cell lines HEY, SKOV-3, MG-63 and HOS-143B were determined to be negative from mycoplasma. The positive control contains the visible band at around 219bp.

2.4 Growth Assay

2.4.1 Manual growth assay

After trypsinisation, 5 ml of cell suspension at a density of 2.6×10^4 cells/mL was transferred into a T25 flask (Sarstedt AG & Co) with 5 mL of fresh media and allowed to attach overnight. A total of 5 flasks were prepared for each cell line. After every 24 hours, one of the flasks was taken out to perform a cell count by using a haemocytometer. The media was discarded, washed with 2 mL of PBS, and 2 mL of trypsin was added. After incubation for 5 min at 37°C with 5% CO_2, 2 mL of fresh media was added to stop the reaction and the total of 4 mL of cell suspension was transferred into a 15 mL centrifuge tube and centrifuged for 5 min at 1,500 rpm. After centrifugation, the supernatant was discarded, 5 mL of fresh media was added to mix with the cell pellet and cell count was perform with haemocytometer. The same procedure of haemocytometer cell count was performed in the following days with the rest of the flasks and cell growth graph was plotted using GraphPad Prism software.

2.4.2 Area fraction output method

The area fraction output method was also used to determine the cell growth (Busschots *et al.*, 2015b). Cell density of 2.6×10^4 cells/ml was added into T25 flask (Sarstedt AG & Co) and allowed to attach overnight. After the cell was attached, images of the flask were taken by microscope at interval of 24 hours as shown in Figure 2.2. A cupboard template was cut by using a scalper in the middle as shown in Figure 2.2 and placed under the flasks. The images were then taken at the holes to ensure the same area of the flask was photographed each time. The images were then analysed by using software "ImageJ" (Collins, 2007) to determine area fraction output number and the graph of cell growth was plotted using Prism software. Area fraction output method was also used in

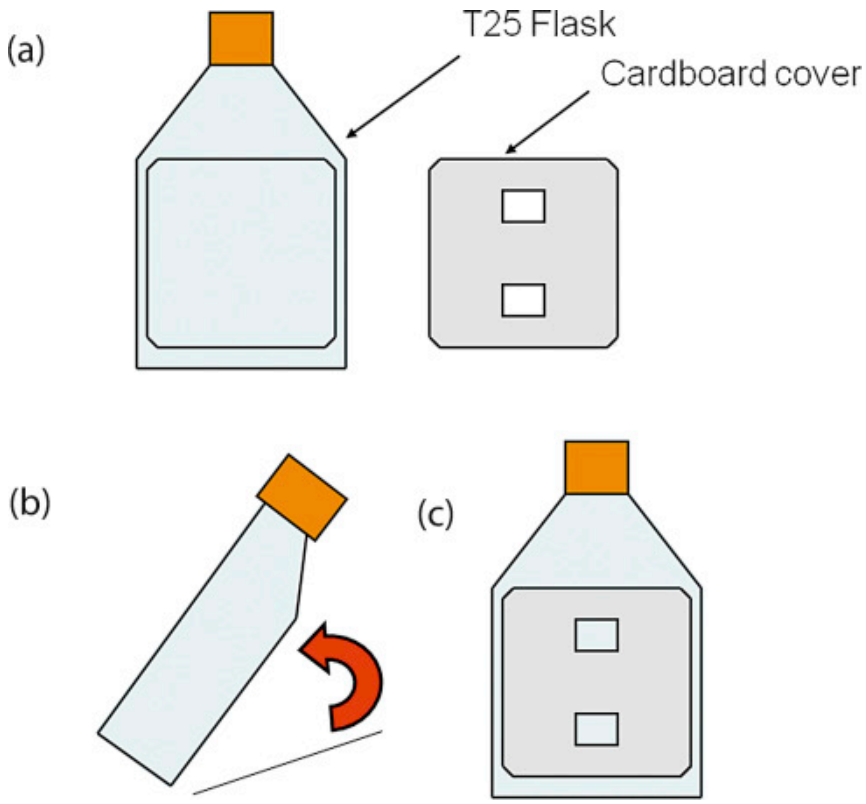

Figure 2.2: T25 cardboard cover for measuring AF output method. (A) shows the designs of a cardboard cover based on a T25 flask. (B) shows the cardboard placed under the T25 flask on a microscopy. (C) shows the empty spot at top and bottom of the cupboard where the images would be taken. Adapted from (Busschots *et al.*, 2015b).

developing drug resistant cell lines for monitoring the cell growth and recovery process after each round of drug treatment.

2.5 Cytotoxicity assay

The sensitivity of the cells to chemotherapy drugs was determined by acid phosphatase assay (Yang, Sinai and Kain, 1996). Cells were plated in 96-well plate (Sarstedt AG & Co) at the cell density of 1×10^4 cells/well in 100 μL and were allowed to attach overnight by incubating at 37°C with 5% CO_2. Drugs were prepared using a 1:2 serial dilution, making a total of 9 doses. The drugs were prepared at 2× the desired concentration, as they were diluted 1:2 in the following procedure: 100 μL were added into each wells making the total volume of 200 μL. Drug-free controls were added with 100 μL of fresh medium. The plates were then incubated for 5 days at 37°C with 5% CO_2. After incubation, drugged media was discarded, and plates were washed with PBS twice. A minimum of three biological triplicates (n=3) were set up for each drug. Cisplatin, doxorubicin, methotrexate, gemcitabine, docetaxel were used in this assay.

On day 5, sodium acetate buffer was prepared by mixing 4.012 g of 0.1M sodium acetate to 500 mL of deionised water. After the sodium acetate was dissolved, 500 uL of 0.1% Triton X 100 was added and the pH was adjusted to 5.5 using glacial acetic acid. Acid phosphatase substrate (Sigma-Aldrich) was measured at 0.00263 g/ml and mixed with sodium acetate buffer. 100 μL of acid phosphatase buffer was added into each well and incubated at 37°C with 5% CO_2 for 2 hours. After that, 50 μL of sodium hydroxide (NaOH) was added into each well to stop the reaction. The absorbance was measured at 405 nm wavelength on the Plate Reader (Omega FLOUStar, BMG Labtech).

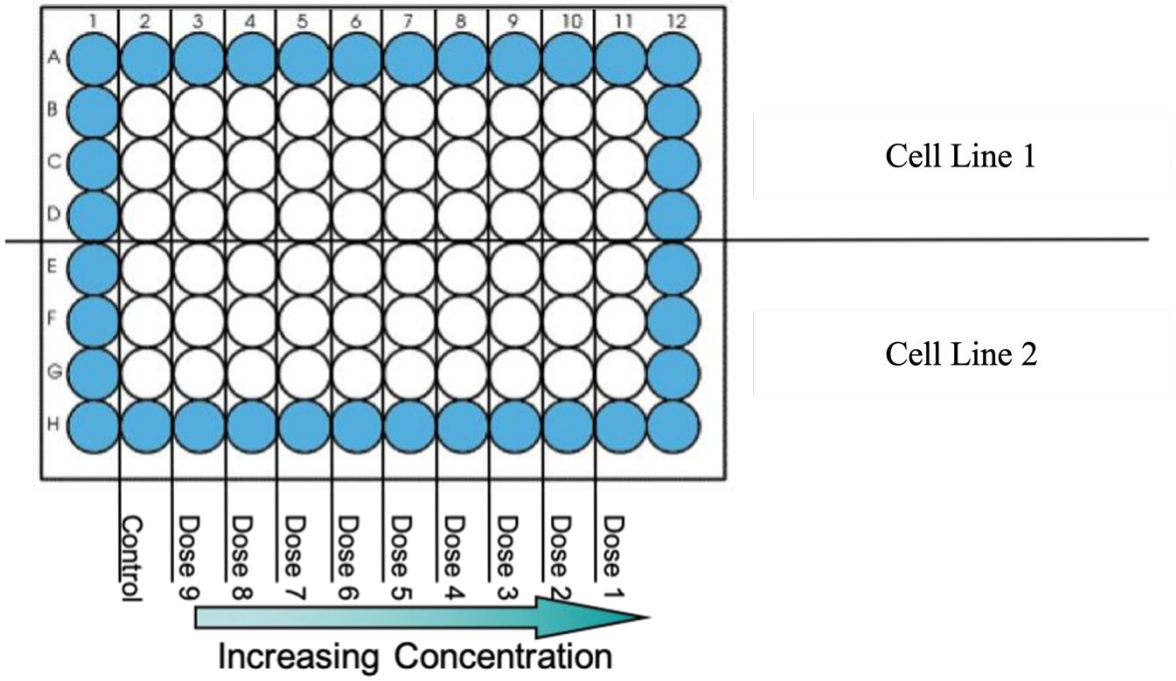

Figure 2.3: Cytotoxicity assay in 96 well plates. The serial dilution of drugs with concentration increasing from left to the right of the plate. Dose 1 as the highest concentration and dose 9 as the lowest concentration of the drugs. Sterile deionised water was placed in blue wells around the plate to reduce dehydration.

The data was then collected and exported to Microsoft Excel using the complimentary Omega data analysis software (BMG Labtech). The mean and standard deviation of the absorbance for each drug dose was calculated before exporting to GraphPad Prism. The data was then normalised to the absorbance values of those wells with no drug treatment as 100% cell viability, which controls wells containing no cells as 0%. The IC_{50} value of each drug was then determined by further analysis using a nonlinear regression fit (four parameter) on GraphPad Prism software. The relative resistance of sublines developed was determined by using Equation 2.1.

Equation 2.1 Relative resistance

$$\frac{IC50\ of\ resistant\ subline}{IC50\ of\ parental\ cell\ line}$$

2.6 Cytotoxicity assay with inhibitors

The effect of inhibitors was determined by using acid phosphatase assay, as described in Section 2.5. After cells were plated into 96-well plates at the cell density of 1×10^4 cells/well and incubated overnight to allow attachment of the cells, an inhibitor was prepared in complete fresh media according to the desired concentration corresponding to each cell line. The concentration of inhibitor was prepared 4× the desired concentration, as it will be diluted in the following procedure. 50 µL of the 4× concentrated inhibitor was added into each well including controls making the total volume of 150 µL and allowed to incubate overnight at 37°C with 5% CO_2. Serial dilutions of drugs were prepared at 4× the original concentration and added 50 µL into each wells making the total volume of 200 µL. Drug-free controls were added with 50 µL of fresh medium. The plates were then incubated for 5 days at 37°C with 5% CO_2. After incubation, the drugged media was discarded, and plates were washed with PBS twice. Different drugs and inhibitors were used on each cell line and a minimum of three biological triplicates (n=3)

were set up for each drug. P-glycoprotein inhibitor elacridar (Sigma-Aldrich) was used in this assay, 2.5 μM for HOS-143B cell lines and 5 μM for MG-63 cell lines. On day 5, the plates were taken down and absorbance was measured as described in Section 2.2.9. The concentration of elacridar were optimised on MG-63 and HOS-143B starting from 20 μM. The concentrations were chosen for each cell lines when the concentrations did not affect the cell growth compared to non-treated cells.

2.7 Wound-healing assay

The migration rate of the parental cell lines and developed sublines were determined by performing a wound-healing assay (Rodriguez, Wu and Guan, 2004). Cells were first seeded in 24-well plate (Sarstedt AG & Co) at cell density of 3×10^4 to create a confluent monolayer of cells. The cells were incubated overnight at 37°C with 5% of CO_2. When the cells were confluent, the cell monolayer was scraped in a straight line to create a "scratch" with a sterile P200 pipette tip. Debris was removed and the edge was smoothed by washing the cells with 1 mL of fresh media. After removing the debris from the wells, 5 mL of fresh medium was added. Markings were made on the cover of the plates to ensure same position was photographed during image acquisition. The marking was made close to the scratch as a reference point. The reference points were made by using an ultrafine tip marker.

After the reference points were made, the plates were placed under a microscope and manoeuvred the plate to ensure the reference mark was not within the capture image but within the eyepiece filed for view. The first image of the scratch was acquired at T0 (0 hours). After the first image was taken, the plates were placed in a tissue culture incubator at 37°C with 5% of CO_2 for 16 hours. After the incubation, the plate was placed again under a microscope at the matched reference point, the photographed region was aligned

as described in previous step and second image was acquired T16 (16 hours). The acquired images were then further analysed quantitatively by using computer software "ImageJ" to determine the percentage of area the cells had migration to the centre point following to Equation 2.2.

Equation 2.2 Migration rate

$$\frac{Area\ of\ scratch\ at\ 0\ h}{Area\ of\ scratch\ at\ 16\ h}$$

2.8 Invasion assay

Cell lines were first grown in complete medium until they were confluent in T75 flasks. When the cells were reaching confluency, the complete media was removed, and 10 mL of serum-free media (SFM) was added. The SFM prepared for MG-63 and HOS-143B cell lines and its sublines was DMEM (Gibco, UK) with 1% of sodium pyruvate (Gibco, UK) and non-essential amino acids (NEAA) (Gibco, UK). The cells were then incubated in SFM at 37°C with 5% of CO_2 for 5 hours to starve the cells. After 5 hours of incubation, the cells were pre-labelled by 10 μg/mL of DilC12 dye (Sigma-Aldrich) and incubated further for 2 hours at 37°C with 5% of CO_2. DilC12 dye was prepared by dissolving 10 mg of DilC12(3) perchlorate dye in 1 mL of DMSO. DilC12 dye will fluoresce intensely when it is incorporated into the cells.

During the incubation time, the extracellular matrix (ECM) was prepared according to the Table 2.6. Solution A and solution B were then mixed by vortexing before adding 45 μL of Collagen I (3 mg/mL) (ThermoFisher) and pipetting up and down as the last component of ECM. 96-well Transwell inserts (Corning, 8 μm pore size) were used for the invasion assay. After preparing the ECM, the plate was then coated with 25 μL of the above ECM mixture and incubated at 37°C with 5% of CO_2 for 2 hours. The ECM

mixture was added into the insert vertically to the bottom of the wells to avoid ECM contacted to the side of the well. After the incubation, 100 µL of serum-free DMEM was added to the inserts and followed by removing 80 µL of the serum-free DMEM. Several inserts were setup without the coating of ECM for technical control purposes.

Table 2.6 Component of collagen based extracellular matrix (ECM) for coating Transwell inserts for invasion assay.

Component	Volume (µL)	Concentration
Solution A		
Serum-free DMEM	1,036	
Collagen IV	135	1 mg/mL
Fibronectin	15.4	1 mg/mL
Laminin	15.4	1 mg/mL
Solution B		
Sterile deionised water	87.1	
10× PBS	14.7	
NaOH	2.25	0.5M
Reagent added in the mixture of Solution A & B		
Collagen I	45	3 mg/mL

After coating the plates with ECM, the pre-labelled cells were then washed and trypsinised to measure the concentration by using haemocytometer and a 4×10^5 cells/mL concentration was prepared in serum-free DMEM. 50 µL of the cell suspension in serum-free DMEM was seeded to each insert coated with ECM. After that, 170 µL of complete fresh medium containing serum which act as the chemoattractant was added to the receiver wells, located at the bottom of the Transwell 96-well plate (Corning, US). Three

wells were not seeded with any cells and used as blank control. The cell lines HT1080 was used as a positive control while MCF7 was used as a negative control in this invasion assay (Gayan, Teli and Dey, 2017). The fluorescence was measured before proceeding to 24 hours incubation at 549/565 nm in the plate reader (Omega FLUOStar, BMG Labtech) by using the top optic option. After completed seeding the cells into the wells and taking first fluorescence reading, the plates were incubated at 37°C with 5% of CO_2 for 24 hours.

After 24 hours incubation, the uninvaded cells were removed from the plate inserts by removing the ECM with a cotton swab. A fresh cotton swab was used for each well. After removing the ECM from the insert, the top chamber was placed back into the receiver plate and the fluorescence of invaded cell was measured again at 549/565 nm in the plate reader using the top optic. The fluorescence readings of the invaded cells were then exported into Excel for analysis and the graph was plotted by using GraphPad Prism software.

2.9 Molecular Biology Techniques

2.9.1 RNA extraction

2.9.1.1 Harvesting cells for gene expression analysis

Cell lines were first grown in T75 flasks (Sarstedt AG & Co) during cell passaging and expansion. When the cells reached 70% – 80% confluency, the media was discarded and washed with PBS once before adding trypsin to detach the cells from the flasks. After incubation for 5 minutes 37°C, the same volume of fresh media was added to the trypsin and the cell suspensions were transferred into a 15 mL tube to centrifuge at 1,500 rpm for 5 minutes. Supernatants were discarded and 10 mL of cold PBS was added to re-suspend the cell pellets and centrifuged at 1,500 rpm for 5 minutes. This step was repeated once again to wash the cell pellets with cold PBS twice. After done washing twice with cold

PBS, the cell pellets were re-suspended with 1 mL of PBS and transferred to 1.5 mL of Eppendorf tube. The cell suspensions were then further centrifuged again at 10,000 × g for 10 minutes. The supernatants were once again discarded, and the cell pellets were stored in -20°C for short term or -80°C for long-term storage.

2.9.1.2 Lyse and homogenise cells

RNA extraction was performed using a PureLink RNA Mini Kit (ThermoFisher) as per the manufacturer's protocol described in this section. Frozen cell pellets prepared earlier were thawed on ice. RNase-free pipette tips were using during RNA extraction. When the frozen cell pellets were completely thawed, 600 µL of lysis buffer containing 1% of 2-mercaptoethanol were added to re-suspend the cell pellets. The cell suspensions were then vortexed at high speed until the cell pellet was completely dispersed and cells appeared lysed. The lysates were passed through 18-gauge needle attached to RNase-free syringe 10 times for homogenisation steps to break down the cells. An equal volume (600 µL) of 70% ethanol was added to each volume of cell homogenate following by vortexing to mix thoroughly to disperse any visible precipitate that formed after adding the ethanol.

2.9.1.3 Bind and wash RNA

Seven hundred microlitres of the sample was transferred to the Spin Cartridge placed in the Collection Tube (provided by PureLink RNA Mini Kit, ThermoFisher). The Spin Cartridge was centrifuged at 12,000 × g for 15 seconds at room temperature. The flow-through in the Collection Tube was discarded after centrifugation, and the same Spin Cartridge was reinserted to the same Collection Tube. These steps were repeated by transferring the remaining 700 µL sample including any remaining precipitate to the same Spin Cartridge and centrifuge at 12,000 × g for 15 seconds at room temperature. The flow-through was discarded the Spin Cartridge reinserted to the same Collection Tube.

2.9.1.4 On-column PureLink DNase treatment and wash RNA

This step was required to remove DNA from the samples that bound on the Spin Cartridge and to purify DNA-free total RNA by using PureLink DNase (ThermoFisher). PureLink DNase was first re-suspended by dissolving the lyophilised DNase in 550 µL of RNase-free water (provided with PureLink DNase). The resuspended DNase was stored at 4°C for short-term storage and aliquots were stored at -20°C for long-term storage. The PureLink DNase for mixture was prepared by mixing 8 µL of 10X DNase I Reaction Buffer, 10 µL of resuspended DNase (~3U / µL), and 62 µL of RNase-free water to make up a total volume of 80 µL for one sample as shown in Table 2.7.

Table 2.7 Components of PureLink DNase mixture for on-column treatment.

Component	Volume
10X DNase I Reaction Buffer	8 µL
Resuspended DNase (~3U / µL)	10 µL
RNase-free water	62 µL
Final volume	80 µL

Before adding the PureLink DNase mixture, 350 µL of Wash Buffer I was added to the Spin Cartridge containing the bound RNA and centrifuged at 12,000 × g for 15 seconds at room temperature. The flow-through and the Collection Tube was discarded. The Spin Cartridge was inserted into a new Collection Tube. After the first wash, 80 µL of PureLink DNase mixture (prepared as described above) was added directly onto the surface of the Spin Cartridge membrane, avoiding contact to the side of the tube. The Spin Cartridge was then incubated at room temperature for 15 minutes. After 15 minutes of incubation,

350 µL of Wash Buffer I was added to the Spin Cartridge to wash the cartridge membrane again by centrifuged at 12,000 × g for 15 seconds at room temperature. The flow-through and Collection Tube was discarded, and the Spin Cartridge was inserted into a new Collection Tube. After that, 500 µL of Wash Buffer II with ethanol was added to the Spin Cartridge and centrifuged at 12,000 × g for 15 seconds at room temperature. Flow-through was discarded and the Spin Cartridge was reinserted not the same Collection Tube. This step was repeated once again by adding 500 µL of Wash Buffer II and centrifuged at the same speed. Lastly, the Spin Cartridge was centrifuged at 12,000 × g for 1 minute to dry the membrane with bound RNA. After centrifugation, the Collection Tube was discarded, and Spin Cartridge was inserted into a labelled Recovery Tube.

2.9.1.5 Elution of RNA

A volume of 40 µL of RNase-free water was added to the centre of the Spin Cartridge and incubated at room temperature for 1 minute. After incubation, the Spin Cartridge and Recovery Tube were centrifuged for 1 minute at 12,000 × g at room temperature. The purified RNA was then stored at -20°C for short-term storage or -80°C for long-term storage.

2.9.2 Evaluation of RNA yield and quality

UV-VIS spectrophotometry and Qubit RNA assay were used in this study to determine the concentration of RNA. UV-VIS spectrophotometry was mainly used to determine the ratio of A260/A280 for the purity of the sample (Wilfinger, Mackey and Chomczynski, 1997) and Qubit RNA assay was used to determine for higher range of concentration of RNA.

2.9.2.1 UV-VIS spectrophotometry

The RNA concentration and purity was measured by using the NanoDrop 2000/2000c spectrophotometer for reverse transcription performed in Section 2.9.3. The concentration of the RNA was calculated using the Beer-Lambert law (Swinehart, 1962), which based on the absorbance at 260 nm and the default defined extinction coefficient. The quality of the RNA was determined by using the ratio of sample absorbance at 260 and 280 nm. A ratio of ~2.0 (>1.9) is generally accepted as "pure" for RNA, without contaminates by the presence or protein, phenol, or other contaminates that strongly absorb at or near 280 nm (Desjardins and Conklin, 2010).

After the completion of RNA extraction from cell pellets, the RNA samples were either stored in the freezer or proceeded to analyse the RNA yield and its quality. Determining the concentration of RNA is essential for the cDNA conversion step prior the qPCR. The sampling arm of NanoDrop 2000/2000c was raised and cleaned by wiping the surface of the lower and upper measurement pedestal before pipetting any solution onto the instrument. After cleaning the instrument, 1 μL of RNase-free water was pipetted onto the lower measurement pedestal. The sampling arm was then lowered and initiated a blank measurement using the NanoDrop 2000 software on the computer. RNase-free water was used as the blanking solution to match the elution solution used in the RNA elution step as described in Section 2.3.1.5 to minimise any signal disturbance. After the blank was established, the sampling arm was raised and cleaned again by using a dry laboratory wipe. A volume of 1 μL of RNA sample was then pipetted onto the lower measurement pedestal. The sampling arm was lowered, and a spectral measurement was initiated using the NanoDrop2000 software. The concentration of RNA and ratio of A260/280 was determined and exported to Excel for further analysis and calculation for cDNA conversion step.

2.9.2.2 Qubit RNA assay

Qubit RNA assay was performed by using Qubit 4 Fluorometer (Invitrogen, ThermoFisher) to determine precise RNA concentration for QuantiNova Reverse Transctiption Kit (Qiagen) in Section 2.9.5.2. Qubit Protein BR assay (Invitrogen, ThermoFisher) was used to determine the precise concentration of RNA. The Qubit working solution was first prepared by diluting the Qubit reagent 1:200 in Qubit buffer. Two standard assay tubes were then prepared for Standard #1 and Standard #2. Volume of 10 µL of Standard #1 and #2 (provided from kit) was added to 190 µL of Qubit working solution. After preparing for the standard assay tubes, RNA sample assay tubes were prepared by adding 5 µL of RNA sample to 195 µL of Qubit working solution making up total volume of 200 µL as shown in Table 2.8. All tubes were vortexed at high speed for 2 to 3 seconds. The tubes were then incubated at room temperature for 2 minutes. After incubation, the standard assay tubes were inserted in the Qubit Fluorometer, and readings were taken. Standard #1 was read first before Standard #2. After the calibration was completed by reading standard assay tubes, RNA assay tube was inserted into the instrument and measured. This step was repeated until all samples' readings were taken.

Table 2.8 Component of Standard and RNA sample assay tubes

	Standard assay tubes	**RNA sample assay tubes**
Qubit working solution	190 µL	185 µL
Standard #1 & #2	10 µL	-
RNA sample	-	5 µL
Total volume	200 µL	200 µL

2.9.3 Reverse transcription

The RNA extracted from the cell pellets were reverse transcribed to cDNA using the SuperScript IV Reverse Transcriptase (Invitrogen, ThermoFisher) as per the manufacturer's instructions. After the measurement of RNA yield and quality tests were performed as described in Section 2.3.2. The volume of 1 µg of the RNA sample was calculated and diluted in RNase-free water to make up total volume of 11 µL RNA template. A volume of 1 µL of 50 µM Random Hexamers (Invitrogen) and 1 µL pf 10 mM dNTP mix (Thermo Scientific) was added to the template RNA to make up a final volume of 13 µL of RNA-primer mixture as shown in Table 2.9.

Table 2.9 Component of RNA-primer mixture for cDNA conversion.

Component	Volume
50 µM random hexamers	1 µL
10 mM dNTP mix (10 mM each)	1 µL
Template RNA (1 µg total RNA)	11 µL
Total Volume	13 µL

The RNA-primer mixture was mixed, and the components were briefly centrifuged. The RNA-primer mixture was then heated at 65°C by using a thermocycler (Techne TC-3000G) for 5 minutes. After incubation, the RNA-primer mixture was then incubated on ice for at least 1 minute. 5X SuperScript IV RT buffer (Invitrogen, Thermo Fischer) was briefly centrifuged and vortexed and rest of the components were added to make up the Reverse Transcription (RT) reaction mix according to Table 2.10.

Table 2.10 Components of the Reverse Transcription (RT) reaction mix

Component	Volume
5× SuperScript IV RT buffer	4 µL
100 mM DTT	1 µL
RNaseOUT RNase Inhibitor (40 U/ µL)	1 µL
SuperScript IV Reverse Transcriptase (200 U/ µL)	1 µL
Final volume	7 µL

After preparing the RT reaction mix, it was briefly centrifuged. A total volume of 7 µL of RT reaction mix was then added to the RNA-primer mixture to make up final volume of 20 µL. The reaction tube was placed in thermocycler (Techne TC-3000G) at the setting described in Table 2.11.

Table 2.11. cDNA conversion thermocycler setting

	Step 1	Step 2	Step 3	Step 4
Temperature (°C)	23	55	80	4
Time (minutes)	10	120	5	Hold

After running the program on the thermocycler, the cDNA conversion was then completed, and cDNA template was generated. The cDNA template was either used directly for qPCR or stored in -20°C freezer for short-term storage.

2.9.4 Real Time – Polymerase Chain Reaction (RT-PCR)

2.9.4.1 SYBR Green PCR gene-expression assay

SYBR™ Green PCR was carried out to assess the expression level of the genes (Table 2.12) in the cDNA samples reverse transcripted as described from Section 2.9.3. cDNA mix and primer mix were prepared separately. cDNA mix was prepared based on the concentration of cDNA conversion. Total of 10 ng of total cDNA was calculated and transferred into a RNase-free tube. The cDNA was then further diluted with RNase-free water to make up final volume of 2.5 µL. The SYBR™ Green primer mix was prepared by adding 1 µL of forward primer, 1 µL reverse primer, 0.5 of RNase-free water, and 5 µL of FastStart Essential DNA Green Master Mix (Roche) as shown in Table 2.13.

Table 2.12 Primers used in SYBR™ Green gene expression assay

Primer	Forward (F) & Reverse (R) Primer
SQSTM1 (P62)	F: 5'-GACAATGGCCATGTCCTACG-3'
	R: 5'-GCACTTGTAGCGGGTTCCTA-3'
LC3-II	F: 5'-GATGTCCGACTTATTCGAGAGC-3'
	R: 5'-TTGAGCTGTAAGCGCCTTCTA-3'
ATG7	F: 5'-GGCGGAGGCACCAAATGAT-3'
	R: 5'-CCACATCCAAGGCACTGCTA-3'
ATG12	F: 5'-AGTAGAGCGAACACGAACCA-3'
	R: 5'-GGGAAGGAGCAAAGGACTGA-3'
GAPDH	F: 5'-AATCCCATCACCATCTTCCA-3'
	R: 5'-TGGACTCCACGACGTACTCA-3'

Table 2.13 SYBR™ Green PCR reaction mix

	Component	Per reaction (µL)
cDNA Mix	cDNA template (10 ng)	1
	RNase-free water	1.5
Primer Mix	Forward primer (200 nM)	1
	Reverse primer (200 nM)	1
	RNase-free water	0.5
	2× SYBR™ Green PCR Master Mix	5
	Final volume	10

A non-template control (NTC) was prepared by adding 2.5 µL of RNase-free water to the primer mix. After preparing the SYBR™ Green qPCR reaction mix, 7.5 µL of the primer mix was first pipetted onto the LightCycler® 480 Multiwell Plate 96 (Roche), followed by 2.5 µL of cDNA mix to make up final volume of 10 µL. All samples were plated in technical triplicate and experiments performed in biological triplicate. The plate was sealed and loaded into the LightCycler 96 PCR machine (Roche) and run-on program conditions shown in Table 2.14.

Table 2.14 PCR cycling conditions for SYBR™ Green gene expression assays

Step		Number of cycles	Temperature (°C)	Time (Seconds)
Pre-incubation		1	95	600
3-step amplification	Denaturation	40	95	10
	Annealing		60	10
	Extension		72	10
Melting curve analysis		1	95	10
			65	60
			97	1

After the PCR cycling had completed, the data was exported to an Microsoft Excel file and the comparative cycle threshold (C_t) method was used to analyse relative gene expression of the genes to their respective controls (Livak and Schmittgen, 2001). GAPDH was used as the housekeeping gene in this assay and the C_t value of GAPDH was used to normalise the target genes C_t values. Fold change in expression levels of genes and statistical significance was determined using GraphPad Prism software.

2.9.4.2 Taqman® PCR gene-expression assay

Taqman® PCR was carried out to assess the expression level of the genes (Table 2.15) in the cDNA samples reverse transcribed as described in Section 2.9.3. The cDNA mix and primer mix were prepared separately, similar to Section 2.9.4.1. A total volume of 4 µL of cDNA template was transferred into a RNase-free tube. The cDNA was then further diluted with 5 µL of RNase-free water to make up final volume of 9 µL. The Taqman® primer mix was prepared by adding 1 µL of 20× Taqman Gene Expression Assay and 10

μL of 2× Taqman Gene Expression Master Mix to make up the total volume of 11 μL as shown in Table 2.16.

Table 2.15 Primers used in Taqman® PCR gene-expression assay

Primer	Assay ID
ABCB1	Hs01067802_m1
ZEB1	Hs00232783_m1
VIM	Hs00185584_m1
CDH1 (E-CAD)	Hs01023895_m1
CDH2 (N-CAD)	Hs00983056_m1
GAPDH	Hs02758991_g1

Table 2.16 Taqman® PCR reaction mix

	Component	Per reaction
cDNA Mix	cDNA template (10 ng)	4 μL
	RNase-free water	5 μL
Primer Mix	20× Taqman Gene Expression Assay	1 μL
	2× Taqman Gene Expression Master Mix	10 μL
	Final volume	20 μL

An NTC was prepared by adding 4 μL of RNase-free water to the Taqman primer mix. After preparing the Taqman® qPCR reaction mix, 11 μL of the primer mix was first pipetted onto the LightCycler® 480 Multiwell Plate 96 (Roche), followed by 9 μL of cDNA mix to make up final volume of 20 μL. All samples were plated in technical triplicate and performed biological triplicate. The plate was sealed and loaded into the

Roche LightCycler 96 PCR machine (Roche) and run according to the setting shown in Table 2.17.

Table 2.17 PCR cycling conditions for Taqman® gene-expression assays

Step		Number of cycles	Temperature (°C)	Time (Seconds)
Pre-incubation		1	95	600
2-step amplification	Denaturation	40	95	15
	Annealing/Extension		60	60
Melting curve analysis		1	95	10
			65	60
			97	1

After the PCR cycling had completed, the data was exported to a Microsoft Excel file and the C_t method was used to analyse relative gene expression level similar as described in section 2.9.4.1.

2.9.5 PCR Arrays

2.9.5.1 RNeasy® Plus Mini Kit

Cell lines were seeded in a T75 flask and cell pellets were harvested as described in Section 2.9.1.1. RNA extraction was performed using a RNeasy® Plus Mini Kit (Qiagen) as per manufacturer's protocol described in this section. Six hundred microlitres of Buffer RLT Plus (provided form the kit) with 1% of 2-mercaptoethanol was added to the pelleted cells and vortexed to mix. The lysate was homogenised by passing 5 times through a 20-gauge needle (0.9 mm diameter) fitted to an RNase-free syringe. The homogenised lysate was then transferred to a gDNA Eliminator spin column (provided form the kit) and

placed in a 2 mL collection tube (supplied). The column and tube were then centrifuged for 30 seconds at 10,000 rpm at room temperature. After centrifugation, the column was discarded while the flow through was saved. Six hundred microlitres of 70% ethanol was added to the flow through and mixed well by pipetting. Seven hundred microlitres of the total sample including any precipitate was transferred to a RNeasy-spin column (provided from the kit) and placed in a 2 mL collection tube (supplied). The lid of the column was closed gently and centrifuged for 15 seconds at 10,000 rpm. The flow through was discarded and the collection tube was reused. This step was repeated until all the volume of the sample were completely processed. Seven hundred microlitres of Buffer RW1 (provided from the kit) was added to the RNeasy-spin column and centrifuged for 15 seconds at 10,000 rpm to wash the spin-column membrane. The flow through was discarded and the collection tube was reused. After centrifugation, the RNeasy-spin column was carefully removed from the collection tube to avoid contact with the flow through. After that, 500 µL of Buffer RPE with ethanol was added to the RNeasy spin column and centrifuged at 10,000 rpm for 15 seconds. The flow through was discarded and the collection tube reused. Another 500 µL of Buffer RPE was added to the RNeasy-spin column again and centrifuged for 2 minutes at 10,000 rpm to wash the spin-column membrane. The spin-column membrane was dried by a long centrifugation step ensuring that no ethanol was carried over during RNA elution. After centrifugation, the RNeasy spin column was placed in a new 2 mL collection tube and centrifuged at full speed for 1 minute to eliminate any possible carryover of Buffer RPE. The RNeasy-spin column was then placed in a new 1.5 mL collection tube and 40 µL of RNase-free water was added to the spin column membrane. The tubes were centrifuged for 1 minute at 10,000 rpm to elute the RNA. The concentration and quality were measured by using Nanodrop as described in section 2.9.2.

2.9.5.2 QuantiNova™ Reverse Transcription Kit

The cDNA conversion of the extracted RNA was carried out by using QuantiNova™ Reverse Transcription Kit (Qiagen) as per manufacturer's protocol described in this section. The genomic DNA removal reaction was prepared on ice according to Table 2.18. After adding the RNA template with total volume of 1 µg, the reaction was incubated for 2 minutes at 45°C using a thermocycler (Techne TC-3000G).

Table 2.18 Genomic DNA removal reaction components

Component	Volume / reaction
gDNA Removal Mix*	2 µL
Template RNA (1 µg)	Variable
Internal Control RNA	1 µL
RNase-free water	Variable
Total reaction volume	15 µL

* Contains RNase inhibitor.

The reverse transcription master mix was prepared on ice according to Table 2.19. All the components were mixed and stored on ice. The reverse transcription master mix contained all the components required for first-strand cDNA synthesis except template RNA.

Table 2.19 Reverse transcription reaction components

Component	Volume / reaction
Reverse Transcriptase Enzyme	1 µL
Reverse Transcription Mix*	4 µL
Template RNA	15 µL
(Entire genomic DNA elimination reaction)	
Total reaction volume	20 µL

*Includes Mg^{2+} and dNTPs.

The freshly prepared reverse transcription master mix was added to each tube containing template RNA from the previous genomic DNA elimination step. The reaction was well mixed and stored on ice. The samples were first incubated for 3 minutes at 25°C, then 10 minutes at 45°C, and 5 minutes at 85°C to inactivate the Reverse Transcriptase Enzyme. After that, the cDNA samples were placed on ice and further diluted by adding 90 µL of RNase-free water to make up the final volume of 110 µL of cDNA.

Table 2.20 gDNA elimination and RT temperature protocol

Step	Time	Temperature	
gDNA elimination reaction	2 min	45°C	
	Paused cycler	25°C	Samples removed, placed on ice, added RT components
Reverse transcription reaction:			After adding RT components, samples placed in the cycler again and continued
Annealing step	3 min	25°C	
Reverse transcription step	10 min	45°C	
Inactivation of reaction	5 min	85°C	

2.9.5.3 PCR Arrays

2.9.5.3.1 QuantiNova LNA PCR Flexible Panels

The PCR Arrays was carried out by using QuantiNova® LNA® PCR Assay (Qiagen) and QuantiNova LNA PCR Flexible Panels (Qiagen) with configured genes list. 16 assays × 6 samples were designed in one single 96-well plate. The list of the genes is shown in Table 2.21. The controls in this assay include 4 reference genes, which are QIC, PPC, HGDC, and GAPDH. The layout of the plate is shown in Figure 2.4.

Table 2.21 List of assays for PCR array

Assay ID	Name
QIC	QuantiNova Internal Control RNA
PPC	Positive PCR Control
HGDC	Human Genomic DNA Control
GAPDH	Housekeeping Control
RB1	Retinoblastoma Protein
RFC1	Reduced Folate Carrier 1
SKP2	S-phase Kinase Associated Protein 2
GSTP1	Glutathione S-transferase P
TGM2	Transglutaminase-2 Promoter
MARK2	Microtublue Affinity Regulating Kinase 2
ATM	Ataxia Telangiectasia Mutated
CCN2	Cellular Communication Network Factor 2
BCL2L1	Bcl-2 like Protein 1
HIF1A	Hypoxia Inducible Factor 1 Subunit Alpha
SPHK1	Sphingosine Kinase 1
MSH2	MutS Homolog 2/6

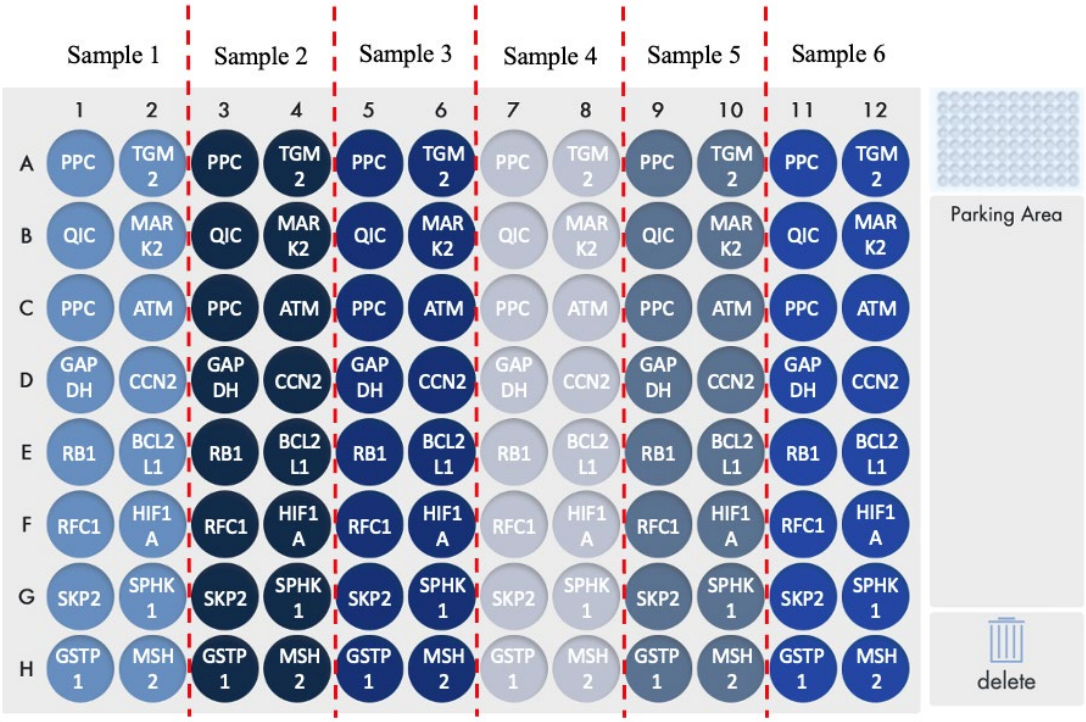

Figure 2.4: QuantiNova LAN PCR Flexible Panel. Six samples were loaded into one 96-well PCR array plate. Controls include positive PCR control (PPC), internal control RNA assay (QIC), human genomic DNA control (HGDC). GAPDH was used as the reference gene to normalise the target genes.

2.9.5.3.2 QuantiNova® LNA® PCR Assay

QuantiNova SYBR® Green PCR Master Mix, template cDNA, and RNase-free water were thawed on ice. As mentioned in section 2.12.2, 90 µL of RNase-free water was added to each 20 µL of reverse transcription reaction to dilute the cDNA. The Master Mix was then prepared according to Table 2.22 for 6 samples for one single 96-well plate.

Table 2.22 Master Mix setup for QuantiNova LNA PCR Flexible Panels for 6 samples per 96-well plate

Component	6 sample per 96-well plate
2× QuantiNova SYBR® Green PCR Master Mix	200 µL
Diluted cDNA template	100 µL
RNase-free water	100 µL
Total Master Mix volume	400 µL

The reaction mix was mixed thoroughly and 20 µL was dispensed per well into the PCR plates. The plates were sealed and vortexed carefully to dissolve the primers. The plates were also briefly centrifuged at room temperature. After that, the plates were incubated at room temperature for 5 minutes while the primers dissolved in the reaction mix. The plates were placed into the Roche LightCycler 96 PCR machine (Roche) and started the cycling program as stated in Table 2.22. Melting curve analysis was also performed in this assay.

Table 2.23 PCR cycling conditions for QuantiNova LNA PCR Flexible Panels

Step	Time	Temperature	Ramp rate	Additional comments
PCR initial heat activation	2 min	95°C	Maximal / fast mode	QuantiNova DNA Polymerase was activated by this heating step
2-step cycling				
Denaturation	5 sec	95°C	Maximal / fast mode	
Combined annealing/ extension	10 sec	60°C	Maximal / fast mode	Perform fluorescence data collection
Number of cycles	45			
Melting curve analysis		95°C 65°C 97°C		

Initial data analysis was performed by using the software supplied by Roche. The data was also analysed by using GeneGlobe software (https://geneglobe.qiagen.com/gb/) provided by Qiagen.

2.10 Protein analysis

2.10.1 Harvesting cell lines for protein analysis

Cells were first cultured in T75 flask and trypsinised when they were reaching 70% – 80% confluence as described in Section 2.2.2 and 2.2.3. The cell suspension was transferred

to 15 mL centrifuge tube and washed with cold PBS twice. The cell pellets were then re-suspended in 1 mL of cold PBS and transferred into a new 1.5 mL Eppendorf tube. The cell suspension was then centrifuged again at 10,000 × g at 4°C for 10 minutes. The supernatant was discarded after centrifugation. RIPA – PI buffer was prepared by adding 10 µL of Halt™ Protease Inhibitor (Thermo Scientific) to 990 µL of Pierce™ RIPA Buffer (Thermo Scientific). According to the cell density, 350 µL of RIPA – PI buffer was added to re-suspend the cell pellet and incubated on ice for 15 minutes. The lysate was then sonicated at 50% amplitude 3 times for 2 seconds each and further incubated on ice for 15 minutes. After incubation, the lysate was centrifuged at 13,000 × g at 4°C for 5 minutes. The supernatant (cell lysate) was collected and transferred to a new labelled tube. It was then stored in -20°C for short-term storage or used immediately for protein analysis.

2.10.2 Quantification of total protein

The protein concentration of the cell lysate was determined by performing the Bradford assays. To perform a Bradford assay, a known concentration of protein standards ranging from 0 – 2,000 µg/mL was first prepared using Bovine Serum Albumin (BSA) (Sigma-Aldrich). A total weight of 0.02 g of BSA was measured and dissolved in 10 mL of 1× PBS. After that, a dilution scheme of BSA standards was prepared according to Table 2.24.

Table 2.24 Preparation of diluted albumin (BSA) standards

Vial	Volume of diluent	Volume and source of BSA	Final BSA concentration
A	0	300 µL of Stock	2,000 µg/mL
B	125 µL	375 µL of Stock	1,500 µg/mL
C	325 µL	325 µL of Stock	1,000 µg/mL
D	175 µL	175 µL of vial B dilution	750 µg/mL
E	325 µL	325 µL of vial C diliton	500 µg/mL
F	325 µL	325 µL of vial E dilution	250 µg/mL
G	325 µL	325 µL of vial F dilution	125 µg/mL
H	400 µL	100 µL of vial G dilution	25 µg/mL
I	400 µL	0	0 µg/mL = Blank

A total volume of 5 µL of known BSA concentration standard was pipetted into a 96-well plate (Sarstedt AG & Co) in triplicates. After that, 1 µL of unknown sample (cell lysate) was diluted with 4 µL of PBS (1:5 dilution) and transferred into the same 96-well plate. 250 µL of Bradford Reagent (Sigma) was added to each well and the plate was incubated in dark for 10 minutes. After incubation, the plate was read at 595 nm using a microplate reader (Omega FLUOStar, BMG Labtech). Linear regression and interpolation of protein concentrations from the standard curve was performed using Microsoft Excel software as shown in Figure 2.4. The absorbance determined from unknown sample (cell lysate) was then calculated based on the equation of the line generated from the standard curve (Figure 2.5).

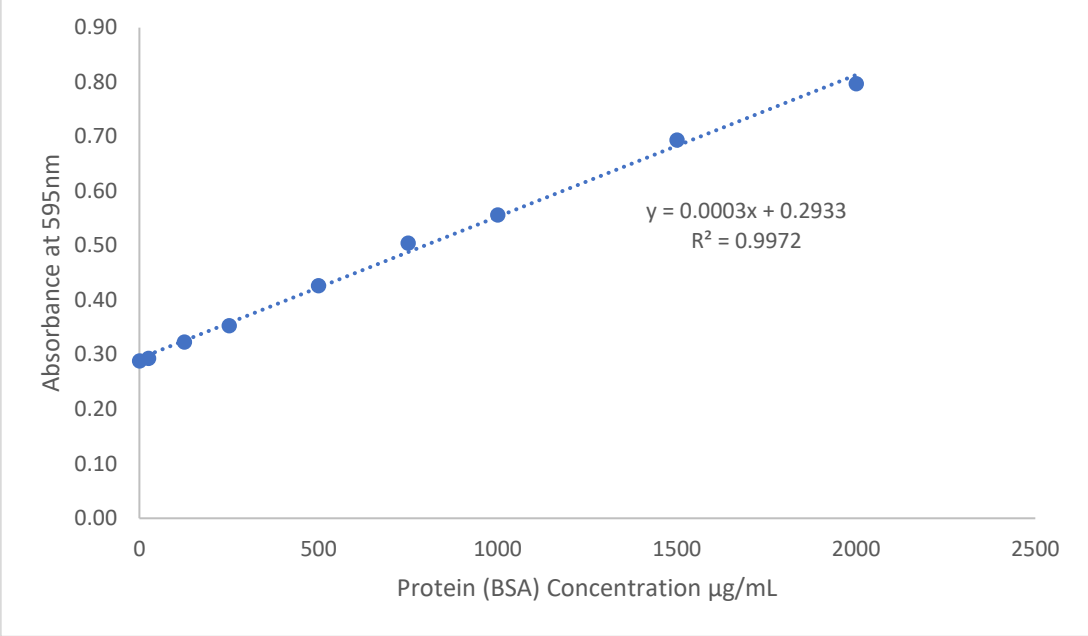

Figure 2.5: Standard curve generated by dilution scheme of diluted albumin (BSA) standards. BSA standard ranging from 0 - 2,000 µg/mL, prepared according to the Table 2.23. The equation generated was used for protein concentration calculation for unknown sample (cell lysates).

2.10.3 Sodium dodecysulphate-polyacrylamide gel electrophoresis (SDS-PAGE)

After determining the protein concentration of the cell lysate, the required concentration was then calculated and transferred to a new Eppendorf tube. An equal volume of loading buffer, made up of 2× Laemmli (Biorad) with 5% of 2-mercaptoethanol (Sigma) was added to the protein lysate and heated at 95°C for 5 minutes to denature the proteins. The protein lysate was then cooled on ice.

The Biorad Mini-Protean® Tetra System (Bio-Rad Laboratories) was used as per system protocol. Firstly, Mini-Protean® TGX™ Precast Gels (4% – 15%, 10-well comb, 50 µL/well) (Bio-Rad Laboratories) were loaded into gel tanks. Running buffer was prepared by adding 100 µL of 10× Tris-Glycine SDS Buffer (Thermo Scientific) to 900 µL of deionised water. Running buffer was poured into the tank and ensuring the bottom of gels containing slits were fully covered. 5 µL of pre-stained molecular ladder, Precision Plus Protein™ Standards (Bio-Rad Laboratories) was loaded onto the first well of the gel. Protein samples were then loaded onto the remaining and desired wells. The gels were electrophoresis-ed at 100 volts, 0.02A (2 gels) for approximately 75 minutes.

2.10.4 Western blotting – Membrane transfer

The Trans-Blot® Turbo™ Transfer System (Bio-Rad Laboratories) was used as per system protocol. After electrophoresis, the cassettes were removed from the tank and the used running buffer was discarded. The gels were carefully removed from the cassette and transferred onto the Trans-Blot Turbo™ Transfer Pack (Mini format, 0.2 µm Nitrocellulose) (Bio-Rad Laboratories) in the ascending order as shown in Figure 2.6. A clean roller was used to gently press the layers to remove bubbles. The membrane was then placed in the Trans-Blot®

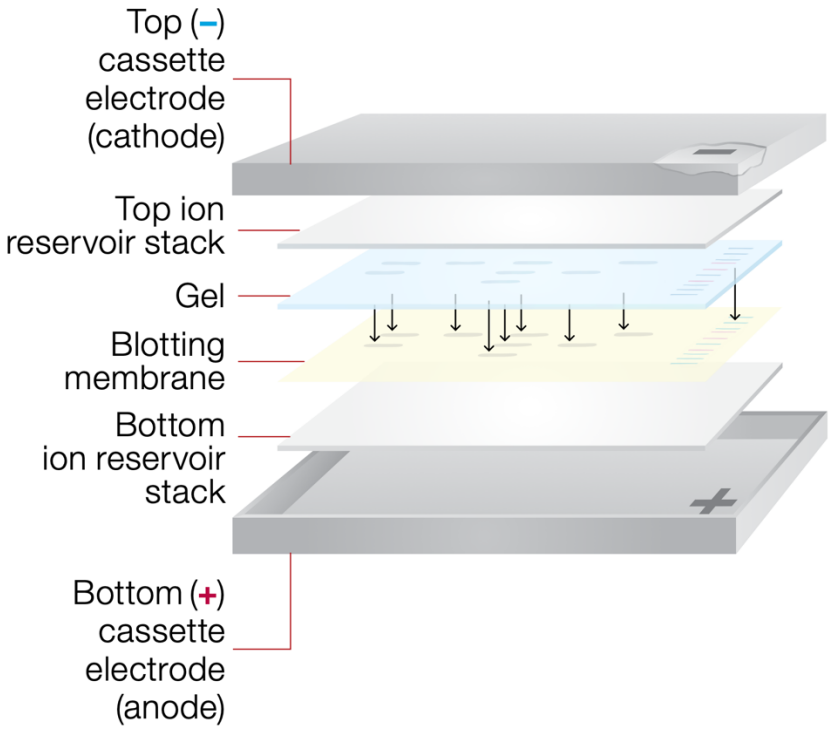

Figure 2.6: Western blot membrane transfer assemble. Membrane transfer direction from top (- cathode) to bottom (+ anode). The membrane transfer was done by using Trans-Blot® Turbo™ Transfer System and Trans-Blot Turbo™ Transfer Pack from Bio-Rad Laboratories. Adapted from (Abraham-Juárez, 2019).

Turbo™ to transfer the gels to the membrane according to the pre-programme setting as tabulated in Table 2.25.

Table 2.25 Bio-Rad pre-programmed protocol

Protocol Name	MW (kD)	Time (min)	2 Mini Gels	1 Mini Gel
Standard SD	Any	30	Up to 1.0 A; 25 V constant	
1.5 MM Gel	Any	10	2.5 A constant; up to 25 V	1.3 A constant; up to 25 V
High MW	>150	10		
Low MW	<30	5		
Mixed MW	5 – 150	7		
1 Mini TGX	5 - 150	3	N/A	2.5 A constant; up to 25 V

2.10.5 Western blot development – Immunoblotting

During gel electrophoresis, blocking and washing buffer were prepared. Washing buffer was prepared by 0.1% of TWEEN® 20 (Sigma) to 1 L of 1× PBS to make up 0.1% PBST. Blocking buffer was prepared by dissolving 5% Blotting-Grad Blocker (Non-fat dry milk) (Bio-Rad Laboratories) in 0.1% PBST to make up 5% Non-fat dry milk / 0.1% PBST.

After the protein was transferred to the membrane, the cellulose membrane was placed in a flat container. The membrane was rinsed twice in a small volume of washing buffer (0.1% PBST). A small volume of Ponceau S solution (Sigma) was poured onto the container to cover the membrane and agitated for 2 minutes at room temperate until the total protein bands were appeared on the membrane. Ponceau S solution was discarded

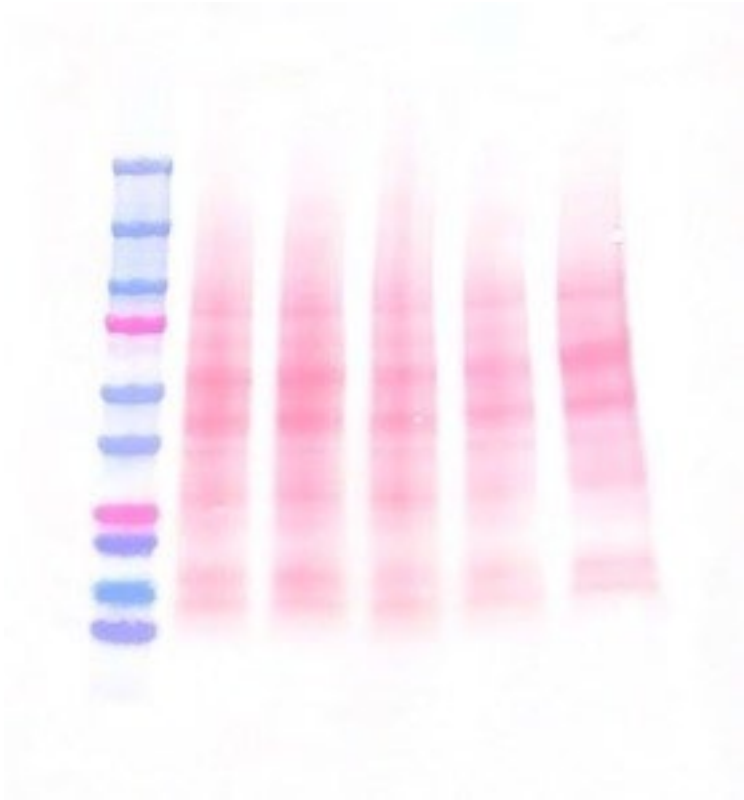

Figure 2.7 Nitrocellulose membrane after incubation with Ponceau S staining before immunoblotting

Ponceau S staining was incubated on the membrane to visualise the protein bands after gel electrophoresis. This method was used to determine the efficiency of gel electrophoresis and cellulose membrane transfer before immunoblotting. First lane with blue and purple colour bands indicating the molecular ladder and the rest of the lanes with pink bands across the membrane were the separated proteins according to their respective molecular weight.

and the image of the membrane with the protein bands were captured and saved. Figure 2.7 shows an example of the membrane after incubation with Ponceau S solution.

25 mL of 0.1% PBST was poured into the container and agitated for 5 minutes at room temperature. After that, the washing buffer was discarded, and 25 mL of blocking buffer (0.5% Non-fat dry milk / 0.1% PBST) was added and incubated for 1 hour at room temperature with slight agitation. After blocking the membrane for an hour, the blocking buffer was decanted, and the membrane was washed with 0.1% PBST three times for 5 minutes each.

The antibody solution was prepared by adding specific concentration of primary antibody in 10 mL of 5% BSA / 0.1% PBST. The membrane with primary antibody solution were incubated at 4°C overnight with slight agitation on rocking platform. A table of antibodies and specific dilutions used are shown in Table 2.26. On the following day, the primary antibody solution was discarded followed by washing with 0.1% PBST for three times 5 minutes each. The secondary antibody solution was prepared by adding specific concentration of secondary antibody in 10 mL of 5% BSA / 0.1% PBST. The secondary antibody solution was added and incubated at room temperature for 1 hour with slight agitation. After incubation, the secondary antibody solution was discarded followed by washing with 0.1% PBST for three times 5 minutes each.

Table 2.26 Table of antibodies used for Western blotting.

Protein	kDa	Host	Supplier	Catalogue #	Dilution
P-glycoprotein	141	Rabbit	Abcam	Ab170904	1:1,000
E-cadherin	135	Rabbit	Cell Signalling Technology	24E10	1:1,000
N-cadherin	140	Rabbit	Cell Signalling Technology	D4R1H	1:1,000
HIF-1A	120	Rabbit	Cell Signalling Technology	D1S7W	1:1,000
SPHK1	45 – 60	Rabbit	Cell Signalling Technology	D1H1L	1:1,000
GAPDH	36	Mouse	Abcam	Ab8245	1:1,000
Anti-Mouse HRP	N/A	Goat	Bio-Rad Laboratories	1706516	1:2,000
Anti-Rabbit HRP	N/A	Goat	Bio-Rad Laboratories	1706515	1:2,000

HIF-1A = Hypoxia-inducible factor 1 – alpha, SPHK1 = Sphingosine kinase 1, GAPDH = Glyceraldehyde 3 – phosphate dehydrogenase, HRP = Horseradish peroxidise

2.10.6 Signal development by electrochemiluminescence (ECL)

The Pierce™ ECL Western Blotting Substrate (Thermo Scientific) was used to develop the signal on the membrane and detected by using Licor Odyssey Infrared Imaging System (LI-COR). Equal volume of ECL reagents (Luminol Enchancer and Peroxide

Solution) were mixed in a 1:1 ratio. 3 mL of the mixed ECL solution was then poured on the cellulose membrane and incubated for 2 minutes in the dark. After 2 minutes, the ECL solution was removed from the membrane and placed on a clean membrane tray and made sure to avoid bubbles generated in-between the membrane and the tray. The membrane was immediately loaded into the Li-Cor instrument to visualise the protein bands by using Image Studio 4.0 Programme. The result analysed on the software was then exported to Microsoft Excel to calculate relative fold change and graph was plotted by using GraphPad Prism.

2.11 Fluorescence-activated cell sorting (FACS) analysis

2.11.1. Preparation and harvesting cell lines

Fluorescenin Isothiocyanate (FITC) Annexin V Apoptosis Detection Kit I (BD Bioscience) was used to determine the percentage of cells undergoing apoptosis according to the manufacturer's protocol. A total concentration of 1×10^6 cells / mL of cells were re-suspended in 2 mL and media transferred into the wells of a 6-wells plate (Sarstedt AG & Co). The plates were then incubated at 37°C with 5% of CO_2 for 24 hours. On the second day, drug concentrations were prepared based on the IC_{50} value determined from the cytotoxicity assay as described in Section 2.5 and cells were further incubated for 3 days under the same condition as the previous step.

2.11.2 FITC annexin V / PI apoptosis assay

After the incubation for 3 days, the media from the 6-well plate was discarded and the cells were washed with 2 mL of PBS once before adding trypsin. The cells were then detached by trypsin and transferred to a 15 mL centrifugation tube. The cells were centrifuged at 1,500 rpm for 5 minutes. Trypsin was removed and the cell pellets were re-suspended in cold PBS and centrifuged at the same condition. This step was repeated

twice to completely wash the cell with cold PBS twice. After washing, the cells were re-suspended in 1 mL of 1× Annexin V Binding Buffer (provided from the kit). 1× Annexin V Binding Buffer was prepared by mixing 10 µL of 10× Annexin V Binding Buffer (BD Bioscience) to 90 µL of deionised water. 100 µL of the cell suspension with binding buffer was transferred to a 5 mL Falcon tube. Five microliters of the FITC Annexin V (BD Bioscience) and 5 µL of Propidium Iodine (PI) Staining solution (BD Bioscience) were added and incubated at room temperature in the dark for 15 minutes. After the incubation, 400 µL of the 1× Annexin V Binding Buffer was added to each tub and analysed by flow cytometry (BD FACSCalibur, BS Bioscience) within 1 hour. The data was analysed by using the software (CellQuest Pro) and producing the quadrant statistical result. Quadrant statistical result would then show the percentage of cells at different stages including live cells, cells undergoing early apoptosis, cells undergoing late apoptosis, and necrotic cells. The percentage of the cells undergoing apoptosis was then plotted in graphs using GraphPad Prism software.

2.12 Systematic review

2.12.1 Identification of relevant studies

Searching for relevant literature was conducted up to May 2022. Electronic searches were performed using Pubmed (http://www.ncbi.nlm.nih.gov/pubmed). The search terms in the search strategy included as follows: “Osteosarcoma OR osteogenic sarcoma OR bone cancer OR bone sarcoma”, “Second-line OR refractory OR recurrent OR resistant OR relapsed”, “Gemcitabine”, “Docetaxel OR Taxotere OR DTX”. Overlapping data from the same authors were excluded from our meta-analysis. Due to the limited number of Phase II trials for osteosarcoma patients, retrospective reviews were included, and the search was not restricted to a specific time.

Table 2.27 Search terms used to identify studies for inclusion in the review.

PubMed Category	Search Terms	Number of Hits
Title / Abstract	Osteosarcoma OR osteogenic sarcoma OR bone sarcoma OR bone cancer	26,196
Title / Abstract	Refractory OR second line OR resistant OR relapsed	849,838
Title / Abstract	Gemcitabine	15,742
Title / Abstract	Docetaxel OR Taxotere OR DTX	15,979
Combine these 4 with AND		**114**

2.12.2 Inclusion criteria

Studies were included according to the following criteria: 1) patients had to have been diagnosed with osteosarcoma (papers that studied other sarcomas were acceptable only if the outcome data for osteosarcoma patients was extractable); 2) patient's osteosarcoma had to be relapsed or refractory; 3) patients had to have undergone a previous standard chemotherapy regimen for their disease; 4) any prior chemotherapy regimen had not included gemcitabine or docetaxel; 5) patients had to be receiving gemcitabine and docetaxel as combination therapy, not either as a single-agent therapy. Studies were excluded if they met the following criteria: 1) the trial had not been conducted; 2) osteosarcoma patient data could not be extracted; and 3) frontline treatment history of patients were not described.

2.12.3 Data collection and analysis

The review site Covidence was used to collate the data extracted from each paper. Data was extracted according to a purpose-built extraction template in Covidence (https://app.covidence.org). All data was extracted by two independent researchers (Kaan Low, Paola Foulkes) and any disagreements were resolved by a third party (Britta Stordal). Data collected from the papers included the primary author, author contact details and the institution where the research was carried out. Patient characteristics included age, sex, and previous treatments. Intervention details included the dose of docetaxel and gemcitabine patients received, the administration schedule, the number of cycles and any additional medications that were given alongside treatment.

The primary treatment outcome measurements that were extracted from the studies include overall survival (OS), progression free survival (PFS) and overall response rate (ORR). Other measurements collected include the number of patients who experienced a complete response (CR), partial response (PR), stable disease (SD), or progressive disease (PD). These measures were defined by Response Evaluation Criteria in Solid Tumour (RECIST) for all papers (Eisenhauer *et al.*, 2009). A complete response is defined as the "disappearance of all target lesions", whilst a partial response is characterised by a minimum 30% decrease in the overall diameter of all target lesions (Eisenhauer *et al.*, 2009). Progressive disease is defined as a minimum 20% increase in the sum of the diameters of the target lesions, as well as the appearance of 1 or more new lesions (Eisenhauer *et al.*, 2009). Finally, stable disease refers to incidence where the shrinkage or increase in lesion diameter is insufficient to classify as partial response or progressive disease (Eisenhauer *et al.*, 2009).

Grade 3 or 4 haematological and neuropathological toxicities including neutropenia, thrombocytopenia, anaemia, and neuropathy were recorded, along with any instances where treatment was discontinued due to toxicity. Any pre-treatment medications that patients received to ameliorate or prevent toxicity were also recorded. All studies included in this review used the common terminology criteria for adverse events (CTCAE) to assess toxicities (National Cancer Institute, 2017). Grade 3 toxicities are "severe or medically significant" and require hospitalisation, whilst grade 4 toxicities have "life-threatening consequences" and require urgent treatment (National Cancer Institute, 2017). The data collected were summarised according to patient characteristics, response data, toxicity data, dose data and survival data, with availability of each data set indicated for each study. Any data that was unavailable due to a lack of reporting or unextractable from the wider data set was indicated by colour coding.

2.13 Statistical Analysis

2.13.1 *In vitro* study

Data analysis was carried out using GraphPad Prism 9 (GraphPad Software, LA Jolla, CA, http://www.graphpad.com/) and Minitab 17 (Minitab, LLC, https://www.minitab.com/). GraphPad Prism 9 was used for the generation of graphs and Minitab 17 was used for statistical significance analysis. Statistical differences (*) of $p<0.05$ between samples were shown based on Two-sample *t*-test as indicated. $r > 0.5$ represents moderate correlation and $r > 0.7$ represents strong correlation based on Pearson correlation test.

2.13.2 Systematic review

A weighted average of median participant age was produced in SPSS; median age was weighted by the number of participants to account for the different patient numbers in each study. Subgroups of studies were created according to the following characteristics: the median age of the participants (<18 or ≥18 years), the dose of gemcitabine that patients received (675 mg/m^2 or 1000 mg/m^2) and their sex (studies that contained approximately equal numbers of males and females, and studies that contained approximately double the number of males than females). A Chi-square test of association was used to compare the frequencies of categorical variables, including response data and toxicity data. Comparisons were performed between the two subsets of studies in the subgroups of age, dose of gemcitabine and sex. Statistical significance was defined as a p value ≤ 0.05.

Chapter 3: Developing chemoresistant osteosarcoma cell lines

3.1 Introduction

The main purpose of developing drug resistant model of cancer cells is to investigate the mechanisms of response and resistance to chemotherapy agents. The first drug resistant *in vitro* model was developed in 1970, where Chinese hamster cells were used to develop into resistant models with stepwise increasing dose of actinomycin D (Biedler and Riehm, 1970). The resistant models were 2500-fold more resistant to the actinomycin D compared to their respective parental cell lines. Cross resistance to other chemotherapy drugs was also observed in these resistant cells lines such as mithramycin, vinblastine, puromycin, daunomycin, vincristine, demecolcine, and mitomycin C (Biedler and Riehm, 1970). These drug resistant cell lines served as useful models to explore for the mechanisms of anticancer drug resistance. Before the development of the first *in vitro* drug resistant cell lines in laboratory in 1970, drug resistant cell lines were also developed using *in vivo* mouse models in the 1950 and 1960s. These *in vivo* resistant cell lines include models resistant to vinblastine, terephthalanilide (Kessel, Botterill and Wodinsky, 1968), methotrexate (Burchenal and Robinson, 1950), and 8-azaguanine (Law, 1951).

In general, developing drug resistant models of cancer cells is accomplished by repeatedly exposing the cancer cells to chemotherapeutic drugs. Different strategies used in exposing the drugs to the cancer cells will result in different characteristics of the drug resistant cancer models. Clinically relevant level of resistance was examined in a review study published by McDermott *et al*. in 2014. Cancer cell lines established from patients after the chemotherapy treatment were 2 to 12-fold more resistant compared to cancer cell lines developed from patients before the treatment (parental cell lines). However, most of the cell lines were in the range between 2 to 5-fold increase and only three cell lines had a 8 to 12-fold increase compared to their respective parental cells (McDermott *et al.*, 2014). Hence, a clinically relevant resistance could define as a 2 to 5-fold increase from the IC_{50}

value of the parental cell line; while models with more than 5-fold resistance level are categorised as high-level laboratory models (McDermott *et al.*, 2014). The IC_{50} value, which is the drug concentration to inhibit half population of the cell growth, is determined through cell cytotoxicity assay such as acid phosphatase (Martin and Clynes, 1993, p. 5), MTT (Martin and Clynes, 1993), or clonogenic assays (Franken *et al.*, 2006). The higher the IC_{50} value indicates the higher resistance level of the cancer cells to a drug. The fold resistance of the resistant cell lines is determined using the following the equation:

$$Fold\ Resistance = \frac{\text{IC50 value of Resistant Cell Line}}{\text{IC50 value of Parental Cell Line}}$$

3.1.1 Selection strategy planning

3.1.1.1 Parental cell line

The choice of parental cell line is crucial as the following experiment in developing the resistant models will be influenced by the fundamental characteristic of the parental cell lines. The ideal parental cell line should be easy and convenient to maintain in cell culture lab as the developing process progresses, it will increase its difficulty in growing the resistant sublines (McDermott *et al.*, 2014). The researcher should select the parental cell line that they are familiar and have experience with, such as the doubling time so that the researcher will have more of an idea on the timing of performing sub-culture. The timing of performing sub-culture is critical in developing resistant models during the recovering stage after the drug treatment (McDermott *et al.*, 2014).

The choice of the parental cell lines is also another critical element to consider carefully to develop the resistant models. For developing chemoresistant model, the parental cell line is better to be radiation and chemotherapy naïve cell line. Chemotherapy or radiation treated tumour cells may have already altered the expression of the genes related to

resistance pathway. Identifying the changes of the gene expression is one the major objective in developing the resistance model, and therefore a chemotherapy naïve parental cell line is important in the selection progress. A chemotherapy naïve tumour will also increase the chances in observing small changes of gene expression especially for clinically relevant resistant models. If a naïve parental cell line is not possible to acquire, a lower baseline IC_{50} value for interested chemotherapy agent is preferred when selecting amongst other cell lines. An IC_{50} value within the clinical range is recommended, to allow for a 2 to 5-fold increase in resistance (McDermott *et al.*, 2014).

3.1.1.2 Clinically relevant and high-level laboratory drug-resistant models

Two categories of drug-resistant cell models were proposed by McDermott *et al*., and they are clinically relevant and high-level laboratory drug-resistant models. These two types of drug-resistant models have their own advantages and disadvantages for research purposes. Different type of drug-resistant models may require specific strategy plan to accomplish, which would demand specific optimised conditions such as concentration of the drug used and the exposure period of the drug.

The main purpose of clinically relevant drug-resistant models is trying to simulate the conditions a cancer patient experiences in the laboratory. These resistant models usually require a lower dose of drug to develop, which fall within the range the drug concentration found in patients' blood after intravenous infusion. A pulsed selection strategy is normally used for these models, where the drug is exposed to the cancer cells for a short period and the cancer cells are allowed to recover in drug-free media. This is to mimic the cycles of chemotherapy that the patients received in hospital. Nevertheless, some disadvantages of this type of drug-resistant models includes low-level resistance fold acquired, of the resistance may be unstable, and the molecular changes may be lower and

difficult to detect and analyse (McDermott *et al.*, 2014). Some of the studies had developed osteosarcoma resistant models using pulsed selection strategy (Yin *et al.*, 2007; Li *et al.*, 2009), however the doses of the drugs used were not fall within the range of concentration found in patients' blood. Moreover, their method also includes increasing doses overtime which does not mimic the cycles of chemotherapy that the patients received in hospital.

High-level laboratory models are developed mainly to study and investigate the resistance to chemotherapy drugs and potential mechanisms of drug toxicity. These models often require high doses of drug treatment with escalated concentration over time to induce the cancer cells to develop resistance (Niu *et al.*, 2010; Ding *et al.*, 2018; Zhao, Zhang and Zhang, 2021). Continuous and stepwise increasing selection strategies are normally used to develop high-level laboratory models, where the drug is exposed to the cells continuously and gradually increased in dose (Yin *et al.*, 2007; Han *et al.*, 2014; Buondonno *et al.*, 2019). The advantage of these models includes that high-level resistance is more easily acquired, a more stable level of resistance, and a higher of molecular changes which is easier to identify and recognise (McDermott *et al.*, 2014). However, one of the main disadvantages of these models is it becomes less relevant to the clinic when the higher the level of resistance occurs (McDermott *et al.*, 2014). To date, most of the established osteosarcoma resistant cell lines were developed as a high-level laboratory resistant models (Perego *et al.*, 1999; Oda *et al.*, 2000; Serra, 2004; Niu *et al.*, 2010; Han *et al.*, 2014; Roncuzzi, Pancotti and Baldini, 2014; Wang and Li, 2014; Jiang *et al.*, 2017; Song *et al.*, 2017; Ding *et al.*, 2018; Buondonno *et al.*, 2019; Zhao, Zhang and Zhang, 2021), where high dose treatment with escalated concentration overtime was used to induce the cancer cells to develop resistance.

3.1.1.3 Drug dose used for clinically relevant models

The drug dose used to treat the parental cell lines in developing the resistant model depends on the type of models of interest. A clinically-relevant model requires a more specific and sensitive considerate dose compared to high-level laboratory model. The drug dose used for clinically relevant models is optimised to remain constant throughout the development process and the resistant subline is recovering quicker after each round of treatment.

The unit of drug dose administered via intravenous injection (I.V.) in the clinical treatment of cancer is expressed in mg / m^2. This unit is determined by the milligram of drug based on the surface area of the body of the patient (Pinkel, 1958). In contrast, the drug concentration prepared and used in a research laboratory is normally expressed in µg/ml or µM. The difference in units between the clinical setting and research laboratory can be overcome by consulting pharmacokinetic studies of the drug of interest, which show a range of drug concentration present in the bloodstream of the patient over time after intravenous injection (Himmelstein *et al.*, 1981; Vermorken *et al.*, 1984). The highest concentration is normally observed right after the injection and gradually decreases over several hours or days due to the metabolism that breaks down the drugs molecule. Therefore, the broad range of drug doses observed in a pharmacokinetic study can be used as starting point for the development of clinically-relevant drug resistant models (McDermott *et al.*, 2014).

3.1.1.4 Risk reduction strategies

Developing resistant cancer cell models is a lengthy and uncertain process where it is common to fail to acquire significant resistance compared to the parental cell line. A risk reduction strategy is implemented to overcome the uncertainty in the process of

developing resistant models. The risk reduction strategy includes a comparative-selection strategy where multiple cell lines are used, and more than one chemotherapeutic agent are used in developing the resistant models. This comparative selection strategy reduces the chance of complete failure of the project where multiple cell lines are developing in parallel and some of the sublines should produce significant resistance (McDermott *et al.*, 2014).

Examples of successful comparative selection strategies include: H69 SCLC cells treated with cisplatin or oxaliplatin for 2 hours and 4 days and the 4-day pulse selection treated showed a more stable resistance compared to the 2-h pulse (Stordal, Davey and Davey, 2006). A study by Tegza *et al.* aimed to develop large number of drug-resistant models from breast cancer cell lines MCF-7 and MDA-MB-231 using paclitaxel and doxorubicin. Instead of 40 resistant models which they aimed at the beginning of the study, they managed to developed total of 29 drug-resistant models, 14 resistant models from MCF-7 cell lines, and 15 from MDA-MB-231 cell lines (Tegze *et al.*, 2012). A study Busschot *et al.* aimed to develop resistant ovarian cancer cell from OVCAR8 and UPN251 cell lines to investigate the resistant mechanism by treating carboplatin and taxol with a prolonged pulse and recover in drug-free media for 4 – 5 weeks. After 6 rounds of selection, all OVCAR8 sublines developed much less resistance with less than 2 fold to carboplatin and less than 2.5 fold to taxol; whereas the UPN251 resistant sublines all had significant resistance to taxol with 4 to 8 fold (Busschots *et al.*, 2015a).

3.1.1.5 The influence of cell selection strategies on resistance development

There are different selection strategies to develop resistant cancer cell models. Different method of selection strategies used will have different impact on the mechanisms of drug resistance during the development progress. The most common methods can be

categorised into two types, low-dose intermittent incremental inducement (Takeda *et al.*, 2007; Machioka *et al.*, 2018; Varamo *et al.*, 2019; Yu *et al.*, 2019; Liu *et al.*, 2020) and increasing continuous administration (Losada *et al.*, 2004; Y.-K. Zhang *et al.*, 2017; Wen *et al.*, 2019; Lei *et al.*, 2020).

The major difference between these two methods is the duration of drug exposure to the cancer cell lines. Low-dose intermittent incremental inducement method is exposing the drugs to the cancer cell lines only for a certain period and the drugs will be removed. The cancer cell will only receive the next higher dose drug exposure treatment after subsequent rounds of subculture. In contrast, for increasing continuous administration method, the chemotherapeutic drugs will continuously expose to cancer cell starting with a minimal acceptable dose. The different method used in developing the resistant models will also determine the type of resistant models discussed in Section 3.1.1.2.

3.1.1.5.1 Increasing continuous administration

Developing resistant cell models is a lengthy process which normally requires months of culturing work. A human carcinoma cell line resistant to aplidin was developed using the increasing continuous dose method (Losada *et al.*, 2004). The initial aplidin concentration was 0.5 nM and was increased step wisely to 450 nM over a year in culture. Hela-APL appeared to have delayed growth in the presence of 450 nM of aplidin compared to parental cells, but no significant difference in growth was found without the presence of aplidin. HeLa-APL acquired high-level stable resistance to aplidin, 1,000-fold compared to parental HeLa cells (Losada *et al.*, 2004)

A leukaemia cell line resistant to decitabine was also developed using continuous treatment from K562 parental cells (Wen *et al.*, 2019). The starting concentrations of

decitabine was 2.5 μmol/L and increased up to 320 μmol/L. K562/DAC showed 12-fold increased resistance to decitabine compared to the parental cell line. Moreover, after the treatment of decitabine, a significant increased proliferation and survival rates and decreased apoptosis level was observed in K562/DAC compared to K562 (Wen *et al.*, 2019). Continuous treatment was also used to develop resistant non-small cell lung cancer cells (Lei *et al.*, 2020). NCI-H460 was continuously exposed to topotecan with a gradually increased concentration from 0.1 μM topotecan up to 10 μM for a total of 5 months of culturing. NCI-H460/TPT10 showed a 394.7-fold increased resistance to topotecan compared to the parental cell line (Lei *et al.*, 2020).

3.1.1.5.2 Intermittent incremental inducement

Intermittent incremental inducement is a selection strategy method where the selected drug is exposed to the cancer cells sporadically with increasing dose over time. Two cabazitaxel-resistant, one docetaxel-resistant and one paclitaxel-resistant human prostate cancer cell lines were developed by this method from PC-3 and DU145 cell lines (Takeda *et al.*, 2007; Machioka *et al.*, 2018; Liu *et al.*, 2020). PC-3 and DU145 cell lines were exposed to stepwise increased concentration of paclitaxel up to 10 nM (48 hours) for a total duration of 9 and 15 months. DU145/TxR and PC-3/TxR demonstrated 34-fold and 43.4-fold increased resistance to paclitaxel respectively (Takeda *et al.*, 2007). PC-3/DTX was exposed to docetaxel for 12 months at an intermittently increasing concentration starting from 0.1 nM to 30 nM docetaxel. PC-3/DTX was 10.9-fold resistant to docetaxel compared to PC-3 (Liu *et al.*, 2020). Another example of resistant cancer cell lines established by this method is MT-CHC01R1.5 (Varamo *et al.*, 2019). MT-CH01R1.5 was developed from cholangiocarcinoma (CCA) cell line by exposing to intermittently increasing doses of gemcitabine from 10 nM to 1.5 μM for total 9 months and it showed significant resistance with 18.9-fold to gemcitabine (Varamo *et al.*, 2019).

The example of above drug-resistant cell lines from different cancer cells developed by both these selection methods led to a high fold resistance compared to their parental cell line and may be classified as high-level laboratory models as discussed in Section 3.1.1.2. Even though this type of resistant models may produce a stable and high resistance across long periods of cell culture, the resistant mechanisms in these models might not emulate the mechanism acquired in the clinic where low level of drug concentration was administered.

3.1.1.5.3 Pulsed-selection strategy

Pulsed-selection strategy is another method used by number of studies in their development of resistant cancer cell lines. This strategy is used to develop clinically relevant resistant models and attempts to simulate the clinical setting for certain drugs (Ying *et al.*, 2012; Lv *et al.*, 2014; Wen *et al.*, 2015; Panayotopoulou *et al.*, 2017; Viscarra *et al.*, 2019). Pulsed-selection strategies usually expose the selected drugs for a short period over long intervals mostly every week. This method is not often to develop resistant cancer models due to the application of low concentration of chemotherapeutic drugs which normally results in low and unstable resistance compared to other methods. One of the ovarian cancer cell line examples was A2780 exposed to 100 μM of carboplatin for 2 hours and replaced with drug-free culture media to allow for recovery until reaching 70% confluence for one cycle. The study took 20 cycles and total of 18 months to successfully generate the CBDCA-resistant A2780 (carboplatin resistant). CBDCA-resistant A2780 showed a 3.2-fold higher resistance to carboplatin compared to parental A2780 cell (Viscarra *et al.*, 2019). Another example of resistant breast cancer cell lines developed by this method is paclitaxel-resistant MDA-MB-231-P cell by exposed to 10 cycles of paclitaxel treatment of 25 nM. MDA-MD-231-P cell showed six times higher of IC_{50} value compared to its parental cell line (Wen *et al.*, 2015). Another

study also using pulsed-selection method to develop paclitaxel-resistant breast cancer cell lines from MCF-7 and MDA-MB-231. MCF-7 and MDA-MB-231 were exposed to 200 nM and 100 nM of paclitaxel respectively for 4 hours, once a week. MCF-7 TIM10 and 231 TIM10 resistant models were developed after 10 pulses of treatment, a total of 6 months in culture. The fold resistance for both resistant models were 11.9 for 231 TIM10 and 5.5 for MCF-7 TIM10 compared to their respective parental cell line (Ying *et al.*, 2012).

A very interesting study done by Yan *et al.* had investigated the different impact of cell and molecular changes on resistant epithelial ovarian cancer cells by using low-dose intermittent incremental inducement and a pulsed-selection strategy. Cisplatin-resistant models SKOV3/CDDP-P were developed by exposing to 100 μM of cisplatin for a 2-hour for pulse selection and the next treatment was administered only when the cells were in exponential growth. A total of 20 pulsed cycles were given to SKOV3/CDDP-P (SD-P). SKOV3/CDDP-80 (SD-80) was another cisplatin resistant developed in their study by exposing intermittently by different dosage of CDDP starting from 10 μM to 80 μM. Each dosage was given to the cells for 10 times for 48 hours each. Similar methods were used again to establish taxol resistant ovarian cancer cell lines. SKOV3/Taxol-P (ST-P) was developed by exposing to 2.5 μM of Taxol for 1 hour each cycle and 20 pulse cycles were given in total. SKOV3/Taxol-25 (ST-25) was also established by exposing to various concentrations of taxol starting from 10 nM to 25 nM for 24 hours each and 10 times each dosage. These four resistant models were developed over a total of 16 months (Yan *et al.*, 2007). Fold resistance developed in resistant models established by the intermittent method was higher compared to pulsed-selection method. SD-80 showed a 2.8-fold higher resistant cisplatin compared to SD-P and ST25 showed 2.4-fold higher resistant to taxol compared to ST-P. Even though the intermittent strategy produced a more stable

and higher-fold resistance cancer model, the pulsed-selection method's models showed a more similar level of resistance to clinical chemoresistance (McDermott *et al.*, 2014). Despite the same origin parental cell line and same chemotherapeutic drugs used, the cellular and molecular changes of these resistant models generated by different methods were also different (Yan *et al.*, 2007). This study had shown the different selections used for developing resistant models in cancer cells would lead to different distinct resistant molecular profile and the gene expression related to the drugs mechanisms. Therefore, the decision on which selection method to deploy in a study is important in generating a resistant model that could provide a resistant profile which is clinically relevant.

Our study where the resistant models were produced under the pulsed-selection strategy which could potentially mirror the clinical chemoresistant mechanism for osteosarcoma. One prolonged pulse of treatment was given to the parental cells over 72 hours and the cells were allowed to recover under drug-free media for 3 to 4 weeks. A long period of recovery phase and prolonged time of the pulse given was to represent a more accurate clinical setting for osteosarcoma patients (Whelan *et al.*, 2015).

3.1.2 Pharmacokinetic studies

3.1.2.1 Cisplatin

According to the EURAMOS-1 protocol, cisplatin doses at 120 mg / m^2 were used as the standard treatment for osteosarcoma patient with the combination of doxorubicin and high-dose methotrexate (Whelan *et al.*, 2015).Cisplatin can be administered intra-arterially or intravenously. Single-agent cisplatin or in combination with doxorubicin was used and administered to patient with metastatic or un-retrievable osteosarcoma in the earlier studies and resulted in 30 to 50% of responses (Ochs *et al.*, 1978; Jaffe, 2009). However, single agent cisplatin used for primary osteosarcoma treatment had increased

response rate up to 60% to 90% when administered intra-arterially (Jaffe *et al.*, 1983; Jaffe, 2009). Studies suggested that intra-arterial injection improved tumour penetration via increasing local cytotoxic concentrations in osteosarcoma patient (Jaffe *et al.*, 1983; Pan *et al.*, 1990). The regimen for osteosarcoma used by studies at the University of Texas MD Anderson Cancer Centre consist of 120 mg /m^2 of cisplatin intra-arterially over 4 hours with 95 mg /m^2 doxorubicin over 24 hours in a series of 4 courses at 40 week intervals (Lamplot *et al.*, 2013).

One study investigated the platinum level in plasma samples from osteosarcoma patients who had administered cisplatin at 150 mg / m^2 intra-arterially and intravenously. The plasma samples were obtained at three different time points, which are before, at the midpoint, and at the end of each 1 hour infusion (Bielack *et al.*, 1989). Their result showed the platinum level in the plasma was reaching the peak at the end of 1 hour infusion at 5.5 µg / mL for intra-arterially administered and 5.8 µg /mL intravenously administered. The platinum was also detected 3 weeks after the first cisplatin infusion at concentration around 10% of the maximum level (~0.55 µg /mL) detected at the end of 1 hour infusion (Bielack *et al.*, 1989). Another study detected a similar range of platinum concentration in the plasma of osteosarcoma patients with the peak at 6.2 µg /mL, and the concentration dropped to 1.6 µg /mL after 360 minutes (Table 3.1) (Himmelstein *et al.*, 1981). Considering that most of the drug will be broken down and excreted out from the body, it is reasonable to indicate that a range of approximately 1.6 to 6 µg /mL is clinically relevant.

Table 3.1 Plasma concentrations of cisplatin.

Agents	Dosage	Time (min)	Cisplatin Concentration (µg/ml)
Cisplatin (Himmelstein *et al.*, 1981)	100 mg/m^2	5	6.2 ± 1.9
		10	4.4 ± 1.3
		15	3.9 ± 0.74
		30	3.3 ± 0.75
		45	2.9 ± 0.57
		60	2.5 ± 0.62
		90	2.2 ± 0.48
		120	1.9 ± 0.47
		240	1.7 ± 0.50
		360	1.6 ± 0.55
Cisplatin (Bielack *et al.*, 1989)	150 mg/m^2	5	5.80
		90	3.85
		240	3.10

3.1.2.2 Doxorubicin

Doxorubicin doses at 75 mg / m^2 for 48 hours of infusion had been used in the EURAMOS-1 protocol for osteosarcoma with the combination of cisplatin and high-dose methotrexate for pre-operative treatment (Whelan *et al.*, 2015). The peak concentration of doxorubicin determined was determined to reduce from 638.7 ng / mL to 27.5 ng /mL after 24 hours when breast-cancer patients were administered with 60 mg / m^2 of doxorubicin intravenous infusion for 40 minutes (Barpe, Rosa and Froehlich, 2010) (Table 3.2). Another study from Greene *et al*. investigated the plasma concentration of doxorubicin using HPLC from blood samples of breast-cancer patients after they were administered with 75 mg / m^2 through intravenous infusion over 15 minutes. The plasma concentration of doxorubicin reached its peak concentration at 2.72 µg / ml after 15

minutes of infusion and rapidly declined to approximately 0.05 μg / ml within an hour (Greene *et al.*, 1983) (Table 3.2). Therefore, it is reasonable to indicate that a range of approximately 0.05 to 2.7 μg /mL is clinically relevant.

Table 3.2 Plasma concentration of doxorubicin.

Agent	Dosage	Time (min)	Doxorubicin Concentration (μg/mL)
Doxorubicin (Greene *et al.*, 1983)	75 mg/m^2	1 15	2.72 0.05
Doxorubicin (Barpe, Rosa and Froehlich, 2010)	60 mg/m^2	1 1440	0.64 0.28

3.1.2.3 Methotrexate

According to EURAMOS-1 protocol, methotrexate doses at 12 g / m^2 was used as the standard high-dose methotrexate treatment for osteosarcoma patient with the combination of cisplatin and doxorubicin (Whelan *et al.*, 2015). High-dose methotrexate was first designed by Delepine *et al*. and was reported to improve the histologic response of osteosarcoma patients by achieving more than 454.44 μg / ml of serum methotrexate concentration at the end of 6 hours infusion (Delepine *et al.*, 1988). A study from Crews *et al*. had investigated the plasma concentration of methotrexate from osteosarcoma patients who had received high-dose methotrexate at a dose of 12 g /m^2 intravenously over 4 hours with leucovorin rescue. They found that 96% of the total patients had a peak plasma methotrexate concentration of more than 454.44 μg /mL after the infusion. The overall mean of the peak concentration of 140 patients was 729.38 μg /mL and it

decreased to only 5.36 µg / ml after 24 hours (Crews *et al.*, 2004). A similar result also found in Ferrari *et al.* investigation as the plasma concentration from osteosarcoma patients was approximately 437.17 µg / ml and declined to only 7.73 µg / ml after 24 hours as shown in Table 3.6 (Ferrari *et al.*, 2005). Thus, it is reasonable to indicate that a range of approximately 5 to 729.38 µg /mL is clinically relevant.

Table 3.3 Plasma concentration of methotrexate.

Agent	Dosage	Time (hours)	Methotrexate Concentration (µg/ml)
Methotrexate (Ferrari *et al.*, 2005)	12 g/m^2	6	437.16 ± 90.59
		12	114.65 ± 45.89
		24	7.49 ± 6.59
		48	0.17 ± 0.19
Methotrexate (Crews *et al.*, 2004)	12 g/m^2	6	729.38
		24	5.36

3.1.3 Established osteosarcoma cell lines

3.1.3.1 Cisplatin-resistant osteosarcoma cell lines

Han *et al*. developed cisplatin-resistant osteosarcoma cell line SOSP-9607/CDDP from SOSP-9607 by stepwise incremental strategy for 12 months. SOSP-9607/CDDP exhibited 6.24-fold resistant to cisplatin compared to its parental cell lines and also cross resistant to methotrexate and doxorubicin. Altered morphology was observed in SOSP-9607/CDDP compared to its parental cell lines as it became larger in size, triangular or

irregular in shape, and notably enlarged nucleus and cytoplasm. Moreover, the growth rate and doubling time of SOSP-9607/CDDP was increased and higher compared to parental cell lines and lost most of the proliferative ability. A contrasting result was obtained from Perego *et al*. as their developed cisplatin-resistant osteosarcoma model U2-OS/Pt was not associated with significant change in the proliferation rate (Perego *et al.*, 1999).

All these established cisplatin resistant osteosarcoma models are in the range of 3 to 14-fold resistance to cisplatin compared to their according parental cell lines. Most of these cisplatin resistant models were developed by continuous stepwise selection strategy (Table 3.4) except for MG-63-R12 and U2OS-R5 from Song *et al*. study, which was developed by using constant drug concentration. Moreover, the drug concentration used to establish cisplatin-resistant cell lines in Zhao et al. study was above the clinically relevant range of drug treatment determined in Table 3.1 (Zhao, Zhang and Zhang, 2021). According to McDermott *et al*. review study, MG-63-R12 and U2OS-R5 were represented as clinically relevant resistant models with resistance level acquired below 5-fold, while others were categorised as high-level laboratory resistant models (Jiang *et al.*, 2017). MG63-R12 and U2OS-R5 developed from Jiang *et al.* successfully acquired up to 14-fold resistance with 10 μM of cisplatin without increasing over time, which is higher than MG-63/CDDP and U2OS/CDDP developed by Zhao *et al.* with increasing concentration strategy. These data could suggest that the level of resistance to cisplatin acquired by osteosarcoma cells was not associated with the drug concentration used but might influence by the exposure period of the drug.

Table 3.4 Established cisplatin-resistant osteosarcoma sublines.

Cell Lines	Sublines	Method	Concentration	Fold Resistance
SOSP-9607 **(Han *et al.*, 2014)**	SOSP-9607/CDDP	Continuous incremental exposure	0.1 to 2 μg /mL	6.24-fold
MG-63 **U2OS** **(Zhao, Zhang and Zhang, 2021)**	MG-63/CDDP U2OS/CDDP	Continuous incremental exposure	0.3 to 9.6 μg/mL	6.07-fold 6.04-fold
MG-63 **U2OS** **(Jiang *et al.*, 2017)**	MG63-R12 U2OS-R5	Continuous constant exposure	3 μg/mL	14.49-fold 14.13-fold
MG-63 **Saos-2** **(Song *et al.*, 2017)**	MG-63-CR Saos2-CR	Stepwise incremental exposure	0.45 to 4.8 μg/mL	3-fold 3-fold
U2OS **(Perego *et al.*, 1999)**	U2-OS/Pt	Continuous incremental exposure	Up to 1 μg/mL	6-fold

Clinically relevant dose range of cisplatin is 1.6 to 6 μg/mL (Himmelstein *et al.*, 1981; Bielack *et al.*, 1989).

3.1.3.2 Doxorubicin-resistant osteosarcoma cell lines

Saos-2/ADM1 and Saso-2/ADM4 were established by a pulsed dose of 24 hours of doxorubicin concentration of 1mg/l and 4mg/l respectively (Niu *et al.*, 2010). The fold resistance of methotrexate for Saos-2/ADM1 and Saos-2/ADM4 cell lines to ADM were 49.8 and 75.6 times higher than that of SaoS-2. The two cell lines had cross-resistance to methotrexate, ifosfamide, epirubicin, taxotere, and paclitaxel, while the cells were found to remain sensitive to cisplatin (Niu *et al.*, 2010). MNNG/HOS/DXR1000 and MG63/DXR1000 were also established by stepwise selection to increasing doses of doxorubicin. MNNG/HOS/DXR1000 and MG63/DXR1000 showed 96-fold and 121-fold higher resistance to doxorubicin than their parental cell lines (Oda *et al.*, 2000).

All these established doxorubicin resistant osteosarcoma models were developed by exposing increasing concentration of doxorubicin over time as shown in Table 3.5. The lowest concentration was from 2.5 ng/mL in Oda *et al*.'s study up to 4 μg/mL in Niu *et al*'s development process. The clinically relevant dose range of doxorubicin established from pharmacokinetic study is 0.05 to 2.7 μg/mL as shown in 3.2. The highest doxorubicin fold resistance acquired by osteosarcoma cell lines is U-2OS/DX580 and Saos-2/DX580 developed by Boundunno *et al.* in 1993 by exposing up to 580 ng/mL doxorubicin continuously, which reported to exhibit more than 300-fold resistant compared to their parental controls. A similar cell line Saos-2 used by Niu *et al*., the highest resistant acquired was only 74.6-fold after exposing up to 4 μg/mL of doxorubicin in a stepwise manner. This suggests that the drug exposure duration plays an important role for osteosarcoma to obtain high levels of doxorubicin fold resistance rather than the concentration.

Table 3.5 Established doxorubicin-resistant osteosarcoma sublines.

Cell Lines	Sublines	Method	Concentration	Fold Resistance
U-2OS **Saos-2** **(Buondonno *et al.*, 2019)**	U-2OS/DX580 Saos-2/DX580	Continuous incremental exposure	30 to 580 ng/mL	>300-fold
MG-63 **(Roncuzzi, Pancotti and Baldini, 2014)**	MG-63DXR30 MG-63DXR100	Continuous incremental exposure	30 to 100 ng/mL	10-fold 28-fold
Saos-2 **(Niu *et al.*, 2010)**	Saos-2/ADM1 Saos-2/ADM4	Stepwise incremental exposure	100 to 4,000 ng/mL	49.8-fold 74.6-fold
MNNG/HOS **MG-63** **(Oda *et al.*, 2000)**	MNNG/HOS/DXR1000 MG63/DXR1000	Continuous incremental exposure	2.5 to 1,000 ng/mL	96-fold 121-fold

Clinically relevant dose range of doxorubicin is 0.05 to 2.7 µg/mL (Greene *et al.*, 1983; Barpe, Rosa and Froehlich, 2010).

3.1.3.3 Methotrexate-resistant osteosarcoma cell lines

Serra *et al*. had established methotrexate resistant osteosarcoma models of U-2OS and Saos-2. The resistant models were developed by continuous exposure of increasing concentration of methotrexate up to 300 ng/mL for U-2OS and 1 μg/mL for Saos-2. The final fold resistance acquired was 135- and 281-fold as shown in Table 3.6, which is the highest amongst among the other methotrexate resistant models (Serra, 2004; Yin *et al.*, 2007). Due to high-dose methotrexate usually used in the combination chemotherapy treatment, the clinically relevant dose of methotrexate established is 5 to 729.38 μg /mL determined pharmacokinetic studies on osteosarcoma patients (Whelan *et al.*, 2015).

As all the developed methotrexate-resistant osteosarcoma cell lines shown in Table 3.6, the highest methotrexate fold resistant acquired is Saos-2/MTX1μg by Serra and lowest is Saos-2/MTX2.2 by Wang and Li. The main difference between both of their methods is the methotrexate concentration and period of drug exposure. The second main factor that determined the fold resistant acquired by osteosarcoma cell lines is the drug concentration. However, an interesting comparison could be discussed between the resistant models Saos-2/MTX1μg (281-fold) and Saos-2/R (13.34-fold) as shown in Table 3.6. Even though Saos-2/R was induced by up to 2 μg/mL of methotrexate in a stepwise manner, compared to Saos-2/MTX1μg up to 1 μg/mL continuously, Saos-2/R only has 13.34-fold resistant to methotrexate. This again suggests that the time duration of drug exposure plays an important role in determining the levels of fold resistance acquired by the cell lines. A different selection strategy method will develop diverse characteristic of resistant models, and a careful selection of methods is important based on the ideal resistant models that fit into the experiments.

Table 3.6 Established methotrexate-resistant osteosarcoma sublines.

Cell Lines	Sublines	Method	Concentration	Fold Resistance
U-2OS **(Yin *et al.*, 2007)**	U-2OS/MTX300	Stepwise increasing exposure	Up to 300 μg/L	119.3-fold
U2OS **MG63** **(Ding *et al.*, 2018)**	MTX resistant variant	Continuous incremental exposure	4.54 to 18 μg/L	N/A
U-2OS **Saos-2** **(Serra, 2004)**	U-2OS/MTX300 Saos-2/MTX1μg	Continuous incremental exposure	Up to 0.3 μg/L Up to 1 μg/mL	135-fold 281-fold
Saos-2 **(Wang and Li, 2014)**	Saos-2/MTX4.4 Saos-2/MTX2.2	Stepwise incremental exposure	0.5 to 2 μg/mL	12.73-fold 4.87-fold
Saos-2 **(Li *et al.*, 2009)**	Saos-2/R	Stepwise incremental exposure	0.05 to 2 μg/mL	13.34-fold

Clinically relevant dose of methotrexate is 5 to 729.38 μg /mL (Crews *et al.*, 2004; Ferrari *et al.*, 2005).

3.1.4 Significance / Contribution to the discipline

Two osteosarcoma cell lines (HOS-143B and MG-63) were chosen to develop into a novel drug-resistant models in this research. Table 3.4 – 3.6 have shown the previously established osteosarcoma resistant models from the literature. Different osteosarcoma cell lines were used in their studies and all the established resistant models were induced by single chemotherapeutic agents. In this study, apart from developing resistance cell lines with one single chemotherapeutic agent, osteosarcoma cell lines MG-63 and HOS-143B were induced by combination of chemotherapeutic agents (cisplatin, doxorubicin, and methotrexate) at the same time to develop into a novel multi-drug resistant osteosarcoma model. Other sublines that were treated with single chemotherapeutic agent were also aimed to be developed into clinically relevant models. Successfully establishing multi-drug induced osteosarcoma resistant models will benefit the research area in osteosarcoma's chemoresistance. This multi-drug induced resistant model will present a more complex resistant mechanism or pathway that associated with all three of the chemotherapeutic drugs.

Escalated drug doses and continuous selection strategy was used in most of the studies from Table 1 – 3. To mimic the clinical situation of an osteosarcoma patient in hospital to laboratory, constant drug concentration and pulse selection strategy was used in this study. This selection strategy also matches with the condition of a patient when receiving chemotherapeutic drugs intravenously. These multi and single drug induced resistant models were characterised for their mechanisms of drug resistance. Studying the multi and single-drug induced osteosarcoma resistant models will allow us to understand the mechanisms of chemoresistance between cisplatin, doxorubicin, and methotrexate.

3.1.5 Aims and objectives

The aim of this chapter was to establish clinically relevant single-agent and multi-agent chemoresistant osteosarcoma cell lines from MG-63 and HOS-143B.

Objective 1: To determine the sensitivity profile of parental MG-63 and HOS-143B on cisplatin, doxorubicin, methotrexate, and the combination of three.

Objective 2: To optimise drug dose of cisplatin, doxorubicin, and methotrexate to inhibit 80% of the cells for the resistant model's selection process.

3.1.6 Hypothesis

Due to the complex mechanism and toxicity of the triple combination of drugs treatment, osteosarcoma cells treated with the combination drugs of cisplatin, doxorubicin, and methotrexate will acquire slower and a lower-level fold of resistant compared to single-agent treated sublines.

The osteosarcoma cell line with the higher metastatic potential (HOS-143B) was also hypothesised to develop drug resistance faster and at a higher level compared to the osteosarcoma cell line with lower metastatic potential (MG-63).

3.2 Design and methods of cell selection strategy

3.2.1 Selection strategy design

MG-63 cells were derived from a 14-year-old Caucasian boy who had treatments including disarticulation of coxal joint followed by chemotherapy; metastases occurred in the lungs and right femur after 8 months (Heremans *et al.*, 1978). HOS-143B was derived from the HOS cell line via a KRAS oncogene transformation and HOS was

derived from a 13-year-old Caucasian female (Mohseny *et al.*, 2011). The patient received treatment with amputation following by radiation therapy and chemotherapy 3 months before she passed away with extensive pulmonary metastases (McAllister *et al.*, 1971). HOS-143B is found to be highly tumorigenic and metastatic and to the lungs of the animals after xenotransplantation. The metastases HOS-143B expresses high level of mutated p53 protein similar to the originating HOS-143B cell line (Ottaviano *et al.*, 2010). These osteosarcoma cell lines MG-63 and HOS-143B are not chemo-naïve as they had been exposed to chemotherapy prior to their establishment (Heremans *et al.*, 1978; Mohseny *et al.*, 2011). However, the exposed chemotherapeutic drugs are the same drugs used in our study, therefore any possible resistance pathways aroused by the chemotherapeutic drugs would be relevant for our study. Cisplatin, doxorubicin, and methotrexate were used as selecting agents throughout the selection process because these three agents are the standard combination of drugs used for osteosarcoma patients in the clinical setting. The standard chemotherapy regimen for high-grade osteosarcoma includes the combination of cisplatin, doxorubicin, and high-dose methotrexate in the total duration of 6 to 12 months (Carrle and Bielack, 2006).

Clinically relevant models were chosen to be developed in our study instead of high-level laboratory models. We wished to develop a model which could represent a similar situation in clinical setting as accurate as possible. A risk reduction strategy was implemented in this study by developing two different osteosarcoma cell lines in parallel with different chemotherapeutic agents individually and in combination form. The details and outline of the selection planning will be shown in Section 3.2.3. In brief, osteosarcoma cells were exposed to either individual agents or combination of agents for 3 days and were allowed to recover in complete drug-free media. When they were fully confluent is when they were indicated as fully recovered following by initiating the next

treatment selection. A pulsed treatment strategy was used in this study and each round of selection took approximately 4 to 5 weeks.

3.2.2 Dose optimisation

The starting doses of cisplatin, doxorubicin and methotrexate is crucial for the selection strategy. The doses use for the selection process should lie in a clinically relevant range to develop clinically relevant models. Therefore, clinical trial publications were studied and used as references to validate clinical relevance and pharmacokinetic studies were used to translate the doses from clinical into usable doses in laboratory (Table 3.1 – 3.3).

3.2.2.1 Dose finding method

The doses of cisplatin, doxorubicin, and methotrexate used in the selection strategy were evaluated separately on both cell lines MG-63 and HOS-143B. A range of doses of drugs were determined by performing a cytotoxicity assay to generate a sensitivity profile of each drug on both cell lines. The doses range were selected from the result of cytotoxicity assay on parental cell lines initially encompassing inhibitory concentration (IC) values ranging from IC_{60} – IC_{90} (Table 3.7).

The drugs doses chosen within this range was also validated as clinically relevant by referring to the pharmacokinetic studies shown in Table 3.1 – 3.3. The ranges of the drug doses were flexible and could be altered depending on the outcome during the optimisation round prior the first treatment.

3.2.2.2 Cell selection strategy method

Cell lines were treated with single-agent cisplatin, doxorubicin, methotrexate, or triple combination as shown in Figure 3.1. Sublines were named in the format of "(Parental cell

lines)/ (Treatment) (Round)". The parental cell line parameter can either be MG-63 or HOS-143B. The treatment parameter can be single agent cisplatin (CIS), single agent doxorubicin (DOX), single agent methotrexate (MTX), or the triplet combination of cisplatin, doxorubicin, and methotrexate (TRI). The round parameter can take the values 1 – 8 describing which round of selection the subline originates from. For example, MG-63/DOXR6 refers to "(MG-63)/ (single agent doxorubicin) (Round 6)".

On the first day, a cell density of 2.6×10^4 cells/mL was seeded in a T25 flask with 5 mL of complete fresh media and incubated at 37°C with 5% CO_2 overnight to allow the cells to attach. The drug dose was prepared on the day 2 and were added into the flasks at 37 °C with 5% CO_2. After 72 hours, the drugged media was removed and replaced with drug-free media. Over the subsequent days, the T25 flasks were examined using a measure of confluence, the area fraction output method (Busschots *et al.*, 2015). In brief, 2 images of the flasks were taken from the T25 flasks, one from the top and one from the bottom spot of the cardboard cover slip (Fig. 2.2). The images were taken twice a week. The images were then analysed by using ImageJ software to determine the area fraction (AF) output number. If the AF output number is ≥ 30, the cells are determined to be confluent.

Upon reaching confluence, the cells were reseeded and transferred into a T75 flask. Some of the leftover cells were then frozen and stored at -80°C to use as a freeze stock. Cytotoxicity assays were performed by using acid phosphatase assay at 1-week intervals for continuous 3 weeks (Yang, Sinai and Kain, 1996). The fold resistance of the sublines was determined by comparing to the subline's parental cell line according to the equation 3.1. After 3 weeks of recovery and cytotoxicity assay, the next round of treatment commenced following the same format a above.

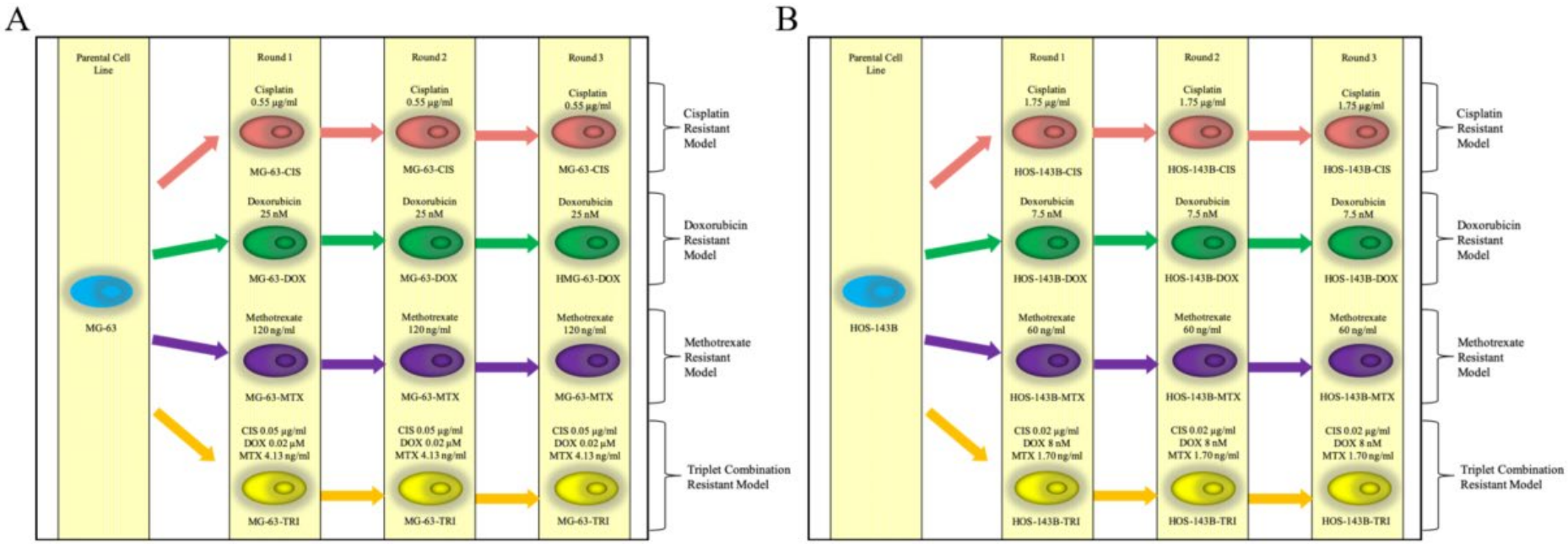

Figure 3.1: Selection strategy outline of (A) MG-63 and (B) HOS-143B. Parental cell lines were treated with various drugs concentration as indicated according to their sensitivity profile. The next round of treatment was continued when the cells were fully recovered.

Equation 3.1 Relative fold resistance

$$\frac{IC50\ of\ resistant\ subline}{IC50\ of\ parental\ cell\ line}$$

3.3 Results

3.3.1 Growth rate of parental cell lines

A growth curve assay was performed to determine the doubling time of parental cell lines MG-63 and HOS-143B prior to the cell selection for resistance models. In a standard cell culture condition, antibiotic such as streptomycin and penicillin are recommended to add into the cell culture medium to prevent contamination. In addition for HOS-143B it is recommended to add bromodeoxyuridine as it is thymidine kinase negative (King and Attardi, 1996). Due to the complex mechanisms of chemoresistance in cancer cells and to prevent unnecessary triggers of any chemoresistance pathway by irrelevant substances, it is ideal to remove excessive chemical element added into the daily culture media. Therefore, the growth curve assay was also used to determine the effect of withdrawal of culture supplements such as antibiotic and bromodeoxyuridine in cell culture medium on the doubling time of parental cell lines.

HOS-143B displayed a higher growth rate compared to MG-63 with doubling time of 11.80 ± 4.21 hours and 33.57 ± 6.06 hours, respectively as shown in Fig. 3.2A. It was a 3.02 ± 0.42-significant fold ($p=0.003$) shorter doubling time in HOS-143B compared to MG-63. Growth curve of HOS-143B in Fig. 3.2B had shown no difference on the doubling time with or without the additional supplements of antibiotics (streptomycin and penicillin) and bromodeoxyuridine (BrDU) to the cell line with $p=0.5939$. Fig. 3.2C showed a similar result as no significant difference with or without the additional supplement of antibiotics to MG-63 with $p=0.5203$. Another growth curve assay was

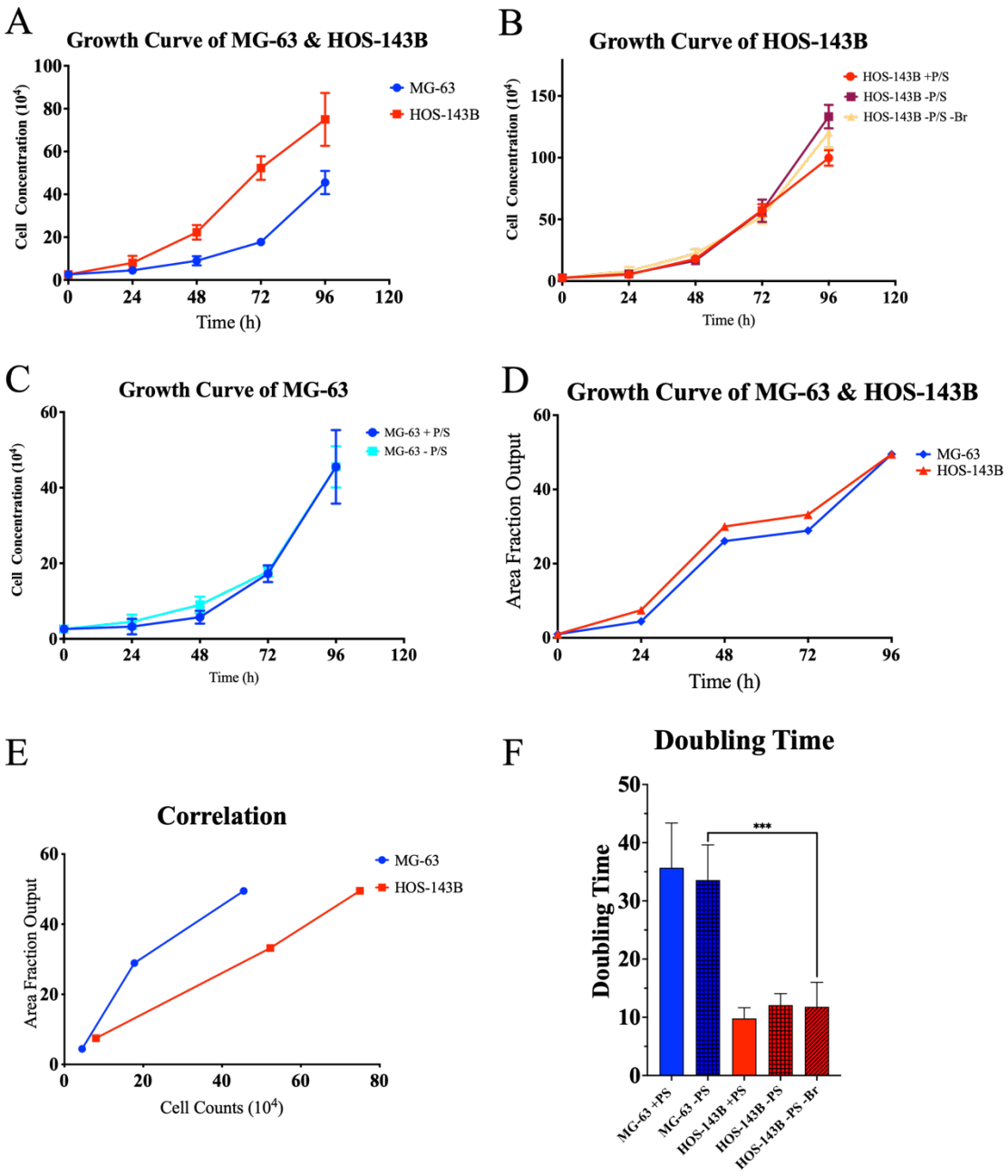

Figure 3.2: Growth curve of MG-63 and HOS-143B analysis by two different methods. (A) Growth curve of parental cell line MG-63 and HOS-143B by manual cell count method. (B) Growth curve of HOS-143B with and without the addition of supplements. (C) Growth curve of MG-63 with and without the addition of supplement. (D) Growth curve of parental cell line MG-63 and HOS-143B by area fraction output method. (E) The correlation was determined between two different methods. (F) Bar chart of doubling time of MG-63 and HOS-143B with and without supplements. (n=3) Data presented in Mean ± SD, ***= $p<0.001$, Two sample *t*-test.

performed for both parental cell lines by using AF output with the ImageJ software analysis a shown in Fig. 3.2D. A strong correlation (r = 0.813) was determined between the growth curve by AF output method and manual cell count method as shown in Fig. 3.2E. The correlation of AF output method and manual cell count method for MG-63 is 0.9823, p = 0.0005. For HOS-143B, the correlation is r = 0.9823, p = 0.0234. The summary of the doubling time of MG-63 and HOS-143B with and without supplements is show in Figure 3.2F.

3.3.2 Drugs sensitivity profile of parental cell lines

The drugs sensitivity profile of both parental cell lines MG-63 and HOS-143B was determined by performing cytotoxicity assay with chemotherapeutic drugs cisplatin, doxorubicin, and methotrexate, and the triple combination of drugs prior the selection process. The sensitivity profile was then used to determine the ranges of doses of drugs to select the final doses of drugs for developing the resistant models. The highest drug concentrations used for single-agent cisplatin was 2.5 µg / mL, doxorubicin was 0.5µg / mL, and methotrexate was 200 ng / mL. The triple combination was optimised from the highest drug concentration used in single-agent cytotoxicity assay. The final highest concentrations used for triple-drug combination was cisplatin at 0.25 µg / mL, doxorubicin 0.05 µg / mL, and methotrexate 20 ng / mL. The baseline resistance (IC_{50}) value of HOS-143B is significantly higher when treated with single-agent cisplatin (p=0.0002) and methotrexate (p=0.012) compared to MG-63. In contrast, MG-63 displayed a significantly higher baseline resistance to single-agent doxorubicin (p=0.001). HOS-143B has a higher baseline IC_{50} values compared to MG-63 when treated with the triplet combination of drugs (CIS, DOX and MTX) but not with statistically significant difference as shown in Table 3.7 and Figure 3.3. The sensitivity profile of MG-63 and HOS-143B for combination of drugs was also determined by performing the cytotoxicity

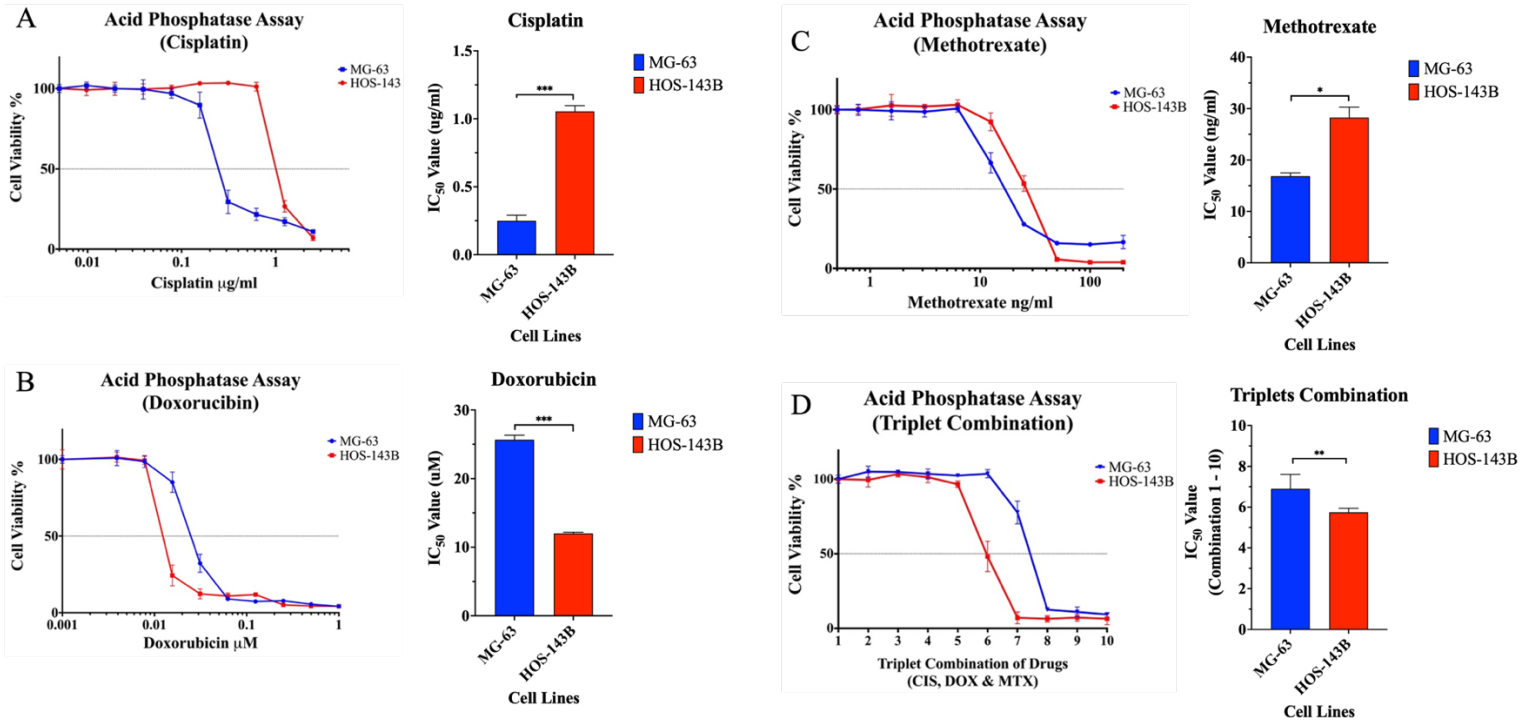

Figure 3.3: Cytotoxicity assay of MG-63 and HOS-143B, n=3. The cytotoxicity assay graphs were plotted with drug concentration on the x-axis and the percentage of cell viability on the y-axis. Baseline IC_{50} values were indicated at the 50% cell viability at the y-axis. The graphs are showing the sensitivity profile for (A) cisplatin (p=0.0002), (B) doxorubicin (p=0.001), (C) methotrexate (p=0.012), and (D) triplet combination of drugs (p=0.004) for both parental cell lines. Y-axis represents the IC_{50} value in A – C, and 10 different combinations of drugs from the highest (10) to lowest (1) in D. * = $p<0.05$, ** = $p<0.01$, *** = $p<0.001$, Two-sample t-test.

assay with the mixture of CIS, DOX and MTX. The baseline resistance of each drug for combination of drugs is included in Table 3.7 for MG-63 (TRI) and HOS-143B (TRI). All drugs were combined in the cytotoxicity assay, and the values are the IC_{50} of the individual agents in the combination.

Table 3.7 IC_{50} values of parental cell lines treated with single-agent and triplet combination (n=3).

Cell Lines	Cisplatin (μg/ml)	Doxorubicin (ng/ml)	Methotrexate (ng/ml)
MG-63	0.25 ± 0.04	13.93 ± 0.37	16.85 ± 0.64
HOS-143B	1.03 ± 0.08	6.53 ± 0.09	28.23 ± 2.05
MG-63 (TRI)	0.0181 ± 0.001	3.98 ± 0.34	1.45 ± 0.13
HOS-143 (TRI)	0.0108 ± 0.001	5.89 ± 0.53	0.85 ± 0.07

3.3.3 Dose optimisation

Based on the sensitivity profile determined in Section 3.3.2, the IC_{60} – IC_{90} value of each drugs including the triplet combination on both cell lines were used as a range for dose optimisation (Table 3.8). For example, the IC_{60} – IC_{90} of cisplatin determined on MG-63 was 0.29 to 1.75 μg / mL. Therefore, the starting dose used for optimisation was fallen within this range to ensure the cells were inhibited up to 60% – 90% to select the resistant sublines.

Table 3.8 Range of doses selected on parental cell lines encompassing IC_{60} to IC_{90} values.

Cell Lines	Cisplatin (μg/ml)	Doxorubicin (ng/ml)	Methotrexate (ng/ml)
MG-63	0.29 – 1.75	15.91 – 32.53	20.11 – 69.64
HOS-143B	1.17 – 2.45	7.03 – 8.30	32.47 – 48.88
MG-63 (TRI)	0.023 – 0.050	4.984 – 13.083	1.828 – 4.789
HOS-143B (TRI)	0.012 – 0.020	2.560 – 4.446	0.947 – 1.585

Cells were subjected to 3-day drug exposure and the time taken for the cells to recover was recorded by using AF method as described in Section 3.2.2.5. The recovery time was then compared to the drug-free control. Drugs doses used for first round of optimisation started from the lowest doses within the range (Table 3.8) and was then optimised by either increasing or decreasing the concentration based on the response of the cells. The most ideal doses for the selection strategy must display an initial large amount of cell death (>90% of cell population) during the drug exposure incubation time, then followed by recovery growth gradually reaching to cell confluence again in drug-free media. This could ensure only the resistant clone in the flask manage to survive, while the sensitive clone would be eliminated.

After a couple rounds of optimisation with different concentrations within the established clinically relevant ranges, the final concentrations used for single-agent treatment are as follow: MG-63 (0.55 μg / mL for cisplatin, 13.59 ng / mL for doxorubicin, and 120 ng / mL for methotrexate), HOS-143B (1.75 μg / mL for cisplatin, 4.08 ng / mL for doxorubicin, and 60 ng / mL for methotrexate) as shown in Table 3.9. Final concentrations for multi-agent triplet combination used in the selection strategy are as follow: MG-63 (0.05 μg / mL for cisplatin, 4.08 ng / mL for doxorubicin, and 4.16 ng /

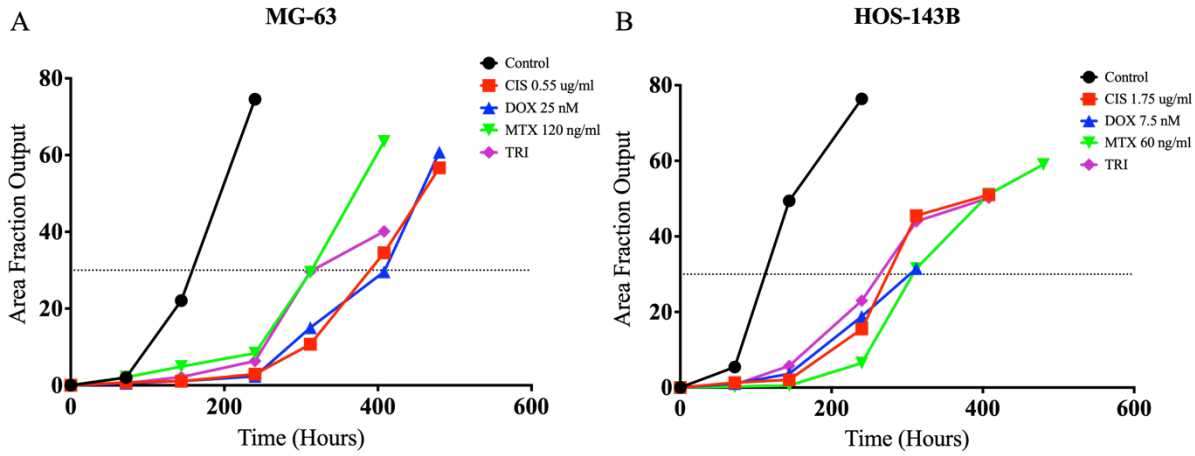

Figure 3.4: Recovery plots for dose finding evaluation in cell selection strategy optimisations. Each graph is a representative of 1 of at least 3 biological repeats and shows cell number graphed over time (hours). (A) Selected doses for MG-63. (B) Selected doses for HOS-143B. (n=1)

mL for methotrexate), HOS-143B (0.02 μg / mL for cisplatin, 4.35 ng / mL for doxorubicin, and 1.70 ng / mL for methotrexate) as shown in Table 3.9. Cells recovery for single and multi-agent treatment on both cell lines were recorded and compared to drug-free controls as shown in Fig. 3.4.

Table 3.9 Final drug doses selected for single-agent and multi-agents triplet combination strategy.

Cell Lines	Cisplatin (μg/ml)	Doxorubicin (ng/ml)	Methotrexate (ng/ml)
MG-63	0.55	13.59	120.00
HOS-143B	1.75	4.08	60.00
MG-63 (TRI)	0.05	4.08	4.16
HOS-143B (TRI)	0.02	4.35	1.70

3.3.4 Recovery

Generally, all sublines required lesser time to recover as the rounds of selection progressed. The recovery plots are shown in Fig. 3.5 grouped per ascending rounds of selection for MG-63 and HOS-143B. Recovery rate was also the first indication we used in the selection progress to estimate when the sublines had acquired drug resistance. When the sublines required a lesser time to recover after the same doses of treatment, it indirectly indicated the cells were mainly becoming more resistant to the drug. A decreasing in recovery time required was shown as a trend in all the sublines as more rounds of treatment was given (Fig. 3.5).

The recovery rate of HOS-143B subline treated with cisplatin had shown greater difference between rounds of selection compared to MG-63 subline. MG-63 subline

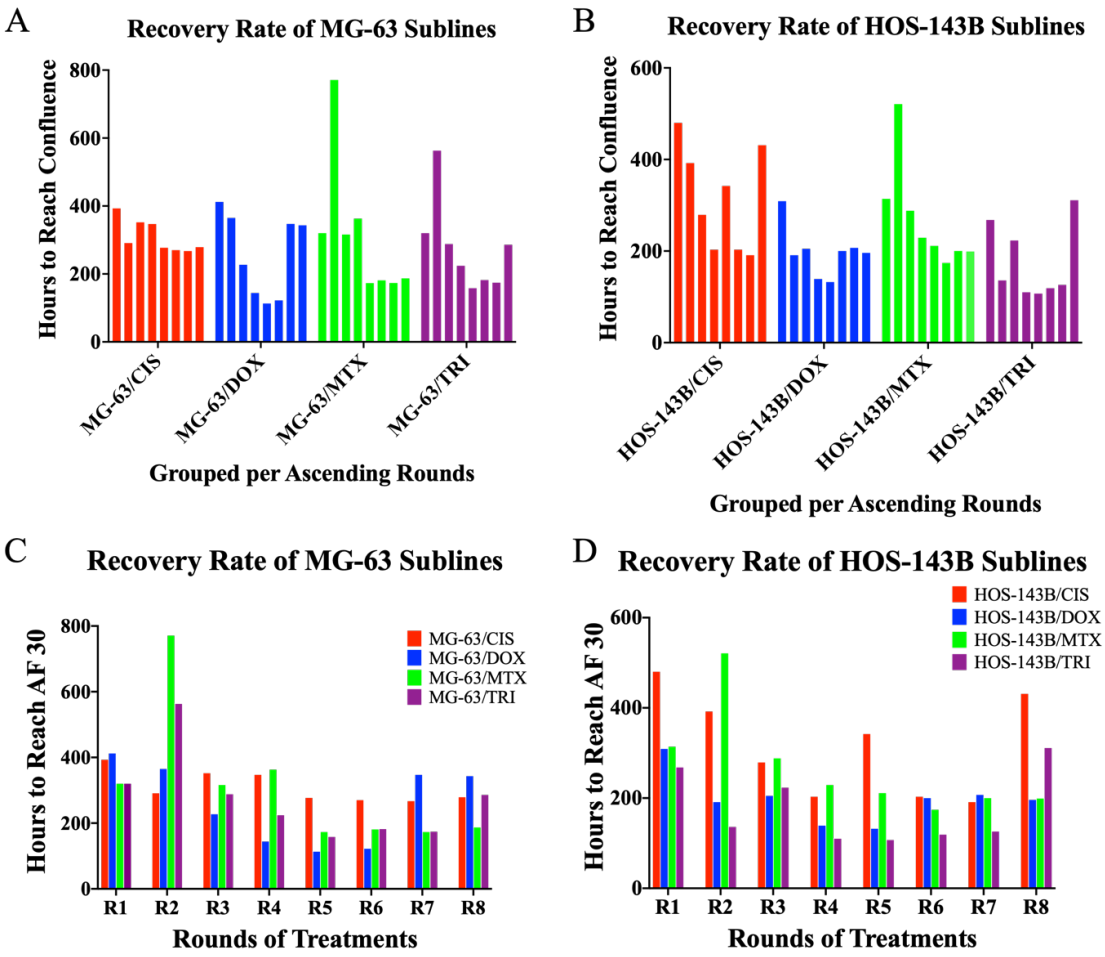

Figure 3.5: Recovery was indicated by the hours to reach AF output number 30 shown on y-axis. (A) Recovery plot for MG-63 sublines grouped per ascending round of selection (1-8). (B) Recovery plot for HOS-143B sublines grouped per ascending round of selection (1-8). (C) Recovery of MG-63 sublines in each round. (D) Recovery of HOS-143B sublines in each round.

treated with cisplatin took a longer time in average to recover than the other sublines treated with other agents. HOS-143B subline treated with triplet combination of drugs recovered quicker in overall compared to other sublines treated with single agent. In Round 7, HOS-143B sublines treated with single agent cisplatin, doxorubicin, and methotrexate shows a similar recovery rate, but they all took a longer to recover than the subline treated with triplet combination of drugs.

3.3.5 Fold Resistance

The fold resistance of each subline was determined at weekly intervals for 3-weeks in each round of selection for single-agent cisplatin, doxorubicin, methotrexate, and multi-agent triplet combination of drugs are shown in Fig. 3.6. After 8 rounds of selection, the MG-63/CISR8 treated solely with single-agent cisplatin also had the highest fold resistance, with 3.56 ± 0.43 fold ($p=0.002$) compared to parental cell line. MG-63/MTXR8 treated with single-agent methotrexate displayed a fold resistance at 2.11 ± 0.39 fold ($p=0.015$). MG-63/TRIR8 exhibited 2.28 ± 0.63 fold resistance ($p=0.047$) to the drugs in combination. Most of the sublines retained their resistance with fold resistance increasing from round to round except for MG-63 subline treated solely with doxorubicin. Moreover, MG-63 sublines receiving single-agent methotrexate treatment developed a very high degree of resistance in round 2, up to 23.75 fold ($p=0.002$). However, the level of resistance dropped over and started to regain stable resistance in round 8.

Similarly, HOS-143B/MTXR8 treated with single-agent methotrexate displayed the highest level of resistance to methotrexate with 3.77 ± 0.90 fold resistance ($p=0.046$). HOS-143B/CISR8 treated with single-agent cisplatin also exhibited 3.51 ± 0.5 fold resistance ($p=0.04$) compared to parental cell line. HOS-143B/DOXR8 showed the lowest fold resistance obtained in the single-agent treatment, with 1.99 ± 0.20 fold

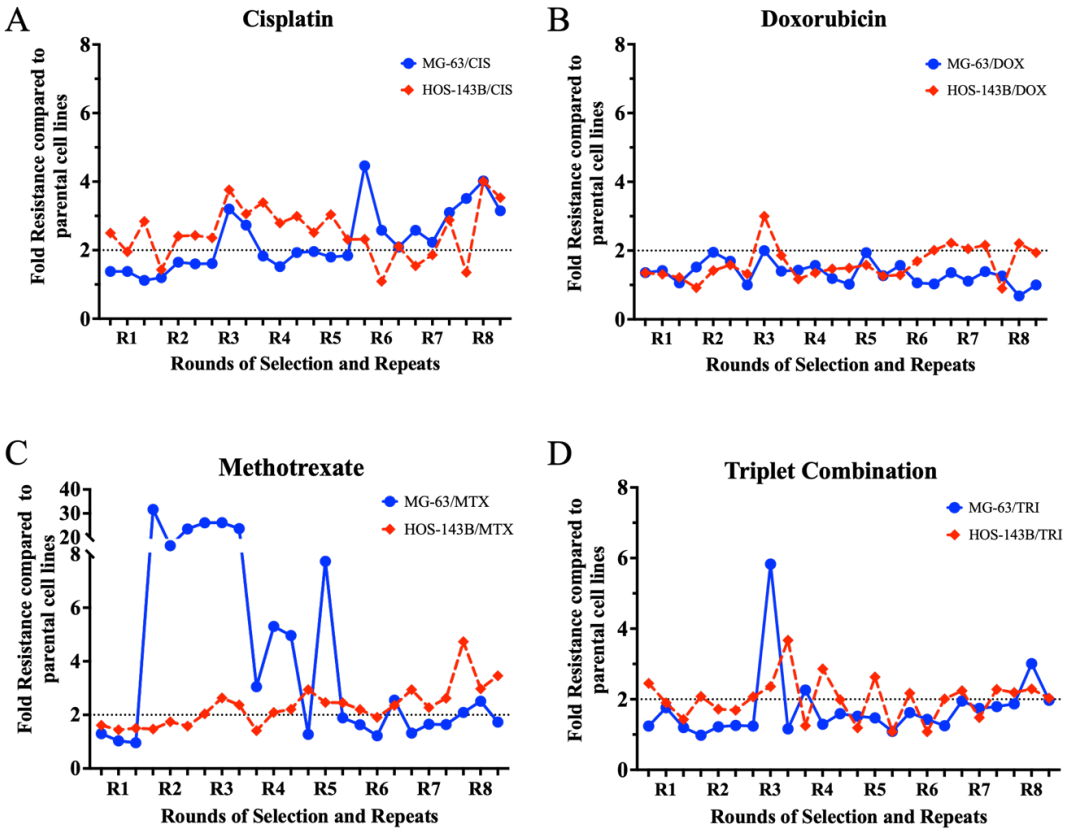

Figure 3.6: Fold resistance to single-agent and multi-agents from round 1 to 8. Single-agent (A) cisplatin, (B) doxorubicin, (C) methotrexate and multi-agent (D) triplet combination of drugs given from round 1 to 8. The x-axis gives a time progression for 3 weekly cytotoxicity assays in 8 rounds of selection. The y-axis indicates fold resistance compared to parental cell lines. Indication line at x-axis is the threshold of 2 fold that determines for clinical resistance.

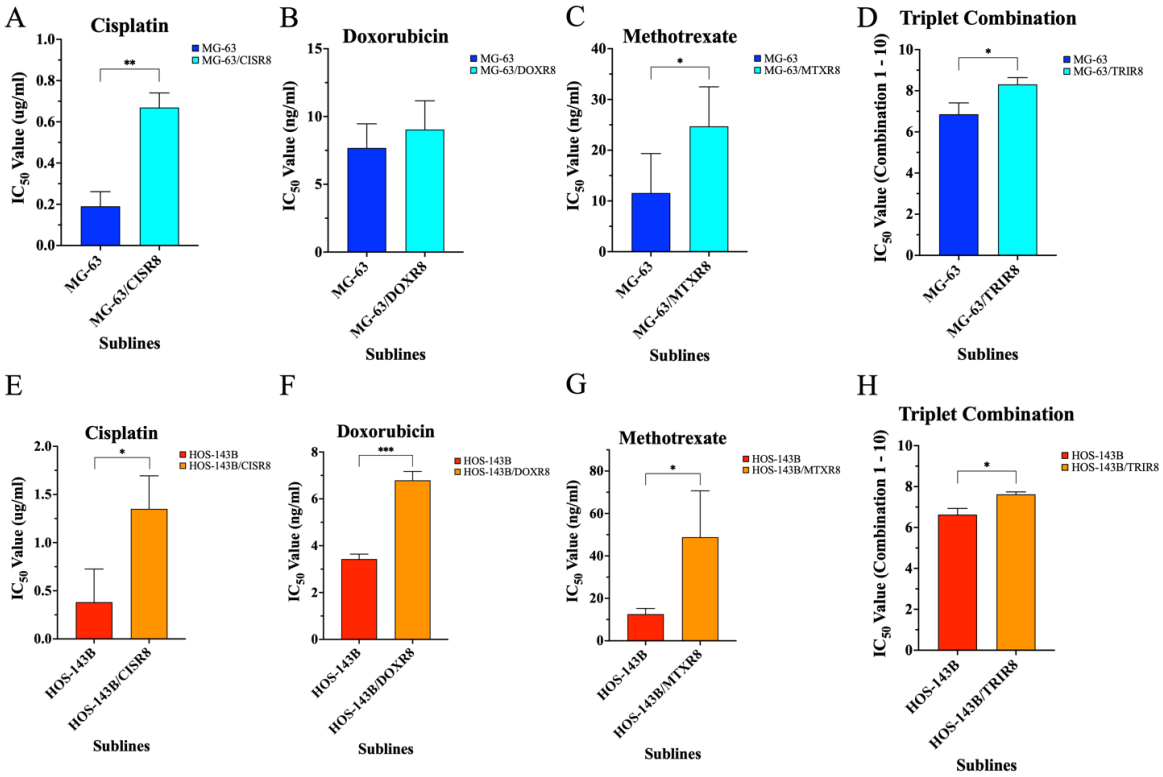

Figure 3.7: IC_{50} value of each subline compared to their parental cell lines (n=3). IC_{50} value of MG-63 resistant subline treated with (A) cisplatin (p=0.002), (B) doxorubicin (p=0.456), (C) methotrexate (p=0.015), and (D) combination of drugs (p=0.047). IC_{50} value of HOS-143B resistance subline treated with (E) cisplatin (p=0.04), (F) doxorubicin (p=0.001), (G) methotrexate (p=0.046), (H) combination of drugs (p=0.033). Y-axis represents the IC_{50} value in A – C and E – G, and 10 different combinations of drugs from the highest (10) to lowest (1) in D & H. * = $p<0.05$, ** = $p<0.01$, *** = $p<0.001$, Two-sample *t*-test.

(p=0.0001). HOS-143B/TRIR8 treated with multi-agent triplet combination displayed a level of resistance at 2.17 ± 0.13 fold resistance (p=0.033) to the drugs in combination.

Fig. 3.6 show the extent of resistance development after 8 rounds of selection for single-agent cisplatin, doxorubicin, and methotrexate treatments in MG-63 and HOS-143B sublines. This was examined to investigate whether cells with higher level metastases (HOS-143B) would develop resistance to drugs faster than cells with lower level of metastases (MG-63). We found that both cells with different degree of metastases behaved similarly in developing drug resistance as the highest and the most stable degree of resistance retained in both cell lines was cisplatin and no significant resistance retained in both sublines treated with doxorubicin. Although, MG-63 sublines treated with single-agent methotrexate developed the highest fold resistance in round 2, however, there was no consistency in holding that high degree of resistance as it dropped over time.

Fig. 3.6D shows the results of fold resistance after 8 rounds of selection for triplet combination of drugs. This was to investigate as we hypothesised that cells receiving combination treatment of cisplatin, doxorubicin and methotrexate should develop resistance slower or not at all compared to single-agent treatments. From this result, we can see that single-agent treatments with cisplatin and methotrexate have higher fold resistance than the triplets' combination treatments expect for single-agent doxorubicin treatment.

3.4 Discussion

Different methods of selection used can vary the mechanism of resistance that develops in a drug resistance model. The most common methods of selection used to develop resistance model are increasing continuous dose selection method (Asada, Tsuchiya and

Tomita, 1999; Oda *et al.*, 2000; Yin *et al.*, 2007; Han *et al.*, 2014) and intermittent incremental inducement method (Niu *et al.*, 2010) where cells are exposed sporadically to increasing doses of drug over time. The only difference between the two selection methods is the time duration of the drug exposure in the complete medium. Niu *et al*. used a pulsed strategy of a 24-hours drug exposure to osteosarcoma cells with increasing doses over time for total of 6 months producing sublines at different concentrations of drug (Niu *et al.*, 2010). Our model had one prolonged pulse over 3 days then was allowed to recover in a drug-free media for 4 to 5 weeks. This selection strategy was designed because it is a more accurate representation of the clinical setting in osteosarcoma, where patients received a drug infusion every 3 to 4 weeks (Carrle and Bielack, 2006). Yan *et al.* studied the biological difference between the two methods in the same ovarian cancer cell lines and they found great differences in the resistance mechanisms from both strategies. A higher level of fold resistance was developed by the continuous incremental strategy, however the pulsed-selection strategy produced a model in which the resistance mechanisms were closer to the mechanisms seen in clinic (Yan *et al.*, 2007). Therefore, models developed by pulsed-selection strategy serve as a better model in studying the drug resistance mechanisms in cancer cells.

Before we started to develop our resistance models, some experiments were done to limit the excess of chemical substance used in the cell culture. We have excluded the antibiotic (penicillin and streptomycin) used for all the parental cell lines and sublines to prevent any possible trigger of additional resistance factor by unrelated substances. From Figure 3.2, the result has shown that there was no difference on the doubling time of the cell lines with or without the supplement of antibiotic. Bromodeoxyuridine (BrdU) is a synthetic nucleoside that is an analogue of thymidine, and it was instructed to add into the complete medium for HOS-143B due to the characteristic of HOS-143B is thymidine

kinase negative (TK-). Exclusion of BrdU was also examined on HOS-143B with growth assay and it had shown no influence on the doubling time of cell. Therefore, to prevent and minimise any additional resistance mechanism develop by any other factors, we have excluded the supplement of BrdU for HOS-143B and antibiotic for both cell lines during cell culture.

We hypothesised that osteosarcoma cancer cells with higher metastatic potential (HOS-143B) would develop resistance easier and quicker than osteosarcoma with lower potential of metastasis (MG-63). Fig. 3.6 shows the extent of resistance development after 8 rounds of selection for single-agent and multi-agent treatments. Both cell lines MG-63 and HOS-143B showed a similar behaviour in retaining the fold resistance despite their different degree of metastasis. Except for single-agent methotrexate treated MG-63 subline, it acquired resistance quicker and at a higher fold than HOS-143B, irrespective to the level of metastasis. The highest fold resistance of MG-63 subline treated with methotrexate determined was 23.75-fold, $p=0.002$ in round 2. However, the level of resistance was not sustained in the subsequent rounds with the treatments given to the subline and the final level of resistance was interestingly lower than HOS-143B/MTXR8 in round 8. After 8 rounds of methotrexate treatment, the final level of resistance for MG-63/MTXR8 was 2.11 ± 0.39 fold, $p=0.021$ compared to MG-63. When the subline was reaching the highest level of resistance to methotrexate, the subline had increased in doubling time of the cell in the recovery phase after the treatments without changing the morphology of the cell. Alterations of doubling time was not discovered in other sublines with increased level of resistance in MG-63. However, when the resistant level decreased in the following rounds of selection, the doubling time was back to normal. This might suggest that the mechanism of methotrexate resistance was developed and was extremely effective in between round 2 and 3, but the efficacy of the methotrexate resistant was

reduced in the following rounds, and this might be due to the selection strategy used in this study.

We also hypothesised that cells receiving triplet combination treatment would develop resistance slower and at a lower fold compared to single-agent treatments. On the first inspection this seems to hold true. Fig 3.6D shows the results of fold resistance after 8 rounds of selection for combination treatments, and we can see that the HOS-143B resistance sublines treated with single-agent treatment of cisplatin and methotrexate have a higher significant fold resistance compared to triplet combination treatment. After 8 rounds of selection, the fold resistance acquired in multi agent osteosarcoma resistant models (MG-63/TRIR8 and HOS-143B/TRIR8) were lower compared to single agent resistant models of which received cisplatin and methotrexate treatments. MG-63/TRIRR8 and HOS-143B/TRIR8 were 2.28 fold and 2.17 fold increased resistant to combination of drugs compared to MG-63/CISR8, HOS-143B/CISR8, and HOS-143B/MTXR8 with 3.56 fold, 3.51 fold, and 3.77 fold respectively. This indicated that even though drug resistance could be acquired in osteosarcoma cell lines by using multi-agent treatment, however the level of resistance was lower compared to single-agent treatment. The lower level of resistance acquired could be due to the multiple drug mechanism pathways occurred in the cancer cells at the same time when the multi-agent treatment was given. If one of the resistant pathways for a certain drug was established, the other drugs could still compensate the efficacy of the treatment with a different pathway and therefore, maintaining the sensitivity of the cancer cells to the combination treatment.

3.5 Conclusion

In this chapter, clinically relevant osteosarcoma resistant models were successfully developed by single-agent and multi-agents induced strategy. These resistant models could serve as an invaluable tool for investigating the resistant mechanisms in osteosarcoma cell lines. Based on the different metastatic potential of the two osteosarcoma cell lines used to develop the resistant models, it was concluded that the metastatic potential was not associated with the chemoresistance acquired in osteosarcoma cells. Resistant models developed by using single-agent treatment showed a higher fold of resistance than resistant models developed by multi-agent treatment. This suggested that the current standard clinical treatment practice for osteosarcoma patients where combination of drugs was normally used is better for the patients as lower level of resistance will be developed after the chemotherapy treatment.

Chapter 4: Characterisation of osteosarcoma resistant cell lines

4.1 Introduction

This chapter discusses the characterisation of the developed resistant osteosarcoma models established by single and multi-agents. The known resistance mechanisms of each agent were discussed in Chapter 1 (Section 1.3, 1.4 & 1.5, respectively). These mechanisms will now be investigated which are likely to be the major contributing factors in our developed resistance models.

4.1.1 Models of cisplatin resistance and related mechanisms

Cisplatin-resistant osteosarcoma cell lines have been previously established to understand drug resistant mechanism (Perego *et al.*, 1999; Han *et al.*, 2014; Jiang *et al.*, 2017; Song *et al.*, 2017; Zhao, Zhang and Zhang, 2021). Most of these cisplatin-resistant osteosarcoma models were developed by continuous incremental strategy as shown in Table 3.4, which acquire a stable and higher level of resistance compared to the pulsed-selection strategy discussed in Section 3.1.3. The highest level of cisplatin resistance was shown in resistant models developed by Jiang *et al*. in 2017 by continuous selection method where the MG63-R12 and U2OS-R5 showed 14.49-fold and 14.13-fold compared to their respective parental cell lines (Jiang *et al.*, 2017). In contrast, the lowest level of resistant was from the models developed by Song *et al*. 2017 by stepwise incremental method, MG-63-CR and Saos2-CR were both showed 3-fold cisplatin resistant (Song *et al.*, 2017). MG-63-R12 and U2OS-R5 were treated with 10 μM continuously throughout the process of development, whereas MG-63-CR and Saos2-CR received up to 16 μM of cisplatin. This has emphasised again that the characteristic and resistant profile of the resistant cell lines would be influenced by the different selection method used.

Apart from acquiring resistance to cisplatin, some of the osteosarcoma also shown cross resistance to others chemotherapeutic drugs, such as carboplatin from U2-OS/Pt (Perego *et al.*, 1999) and methotrexate and doxorubicin from SOSP-9607/CDDP (Han *et al.*, 2014). SOSP-9607/CDDP also demonstrated a decreased growth rate compared to its parental cell line (Han *et al.*, 2014). Molecular characteristic of these cisplatin-resistant models had been widely investigated with the aim of understanding the resistant pathway in osteosarcoma. Glutathione S-Transferase Pi 1 (GSTP1) has been observed at an elevated level in cisplatin-resistant cells both *in vitro* and *ex vivo*, which believed in contributing to the cisplatin resistance by acting on ATP-binding cassette (ABC) transporter to mediate cisplatin transportation. GSTP1 is also involved in detoxifying cisplatin via the redox-regulating capacity of glutathione. The uptake of cisplatin in resistant cells also shown to be affected by regulation of the intracellular copper pool (Chen and Kuo, 2010).

The mRNA expression level of GSTP1, MRP1, MRP2 were upregulated in SOSP-9607/CDDP compared to parental cell line SOSP-9607 (Han *et al.*, 2014). MG-63/CDDP and U2OS/CDDP were also showed to have increased expression level of MDR1, MRP1 and BCRP compared to their respective parental cell lines (Zhao, Zhang and Zhang, 2021). Cisplatin-resistant osteosarcoma cell lines from Song *et al*., MG-63-CR and SaOS-2-CR were also showed elevated expression level of P-gp, MRP1, GST and Bcl-2 in both mRNA and protein levels (Song *et al.*, 2017). Another investigated autophagy mechanisms in cisplatin-resistant osteosarcoma MG63-R12 and U2OS-R5 by investigating the expression level of autophagy genes LC3-II/LC-I, ATG5, and ATG7. The expression level of these genes and proteins were increased in the cisplatin-resistant cells and the conclusion suggested the elevated activity of autophagy was the reason behind the cisplatin resistance (Jiang *et al.*, 2017). These cellular and molecular

characteristics were examined in our clinically-relevant resistant models to determine the major mechanisms of cisplatin resistance present in our resistant cell line panel.

4.1.2 Models of doxorubicin resistance and related mechanisms

Several osteosarcoma cells line such as MG-63, U2OS, MNNH/HOS, and Saos-2 have been used to generate doxorubicin-resistant cell lines as doxorubicin is one of the most effective chemotherapeutic drugs for first-line treatment of high-grade osteosarcoma (Oda *et al.*, 2000; Niu *et al.*, 2010; Roncuzzi, Pancotti and Baldini, 2014; Buondonno *et al.*, 2019). Table 3.4 shows the list of studies and resistant cell lines established by inducing doxorubicin with either continuous or stepwise incremental selection strategy. The highest level of doxorubicin resistance was acquired by U-2OS/DX580 and Saos-2/DX580, which showed a level of resistant more than 300-fold compared to their parental cell lines (Buondonno *et al.*, 2019). Conversely, MG-63DXR30 generated by Niu *et al.* was the lowest amongst the list but still with significant 10-fold resistance compared to the parental cell line.

Morphological changes were observed for resistant cell lines developed from Saos-2 with an irregular shape and enlarged nucleus and cytoplasm. The growth rate of Saos-2/ADM1 and Saos-2/AMD4 were both decreased compared to Saos-2 (Niu *et al.*, 2010). This was further investigated by flow cytometry and the result showed more cells were presented in phase G_1 and G_2 than in S phase, while the parental cell line Saos-2 showed a contrast result (Niu *et al.*, 2010). A similar finding was shown on cisplatin-resistant models SOSP-9607/CDDP mentioned in Section 4.1.2. The percentage of cells in the G_0/G_1 phases of the cell cycle was significantly increased in SOSP-9607/CDDP compared to its parental SOSP-9607 (Han *et al.*, 2014).

P-glycoprotein (P-gp) or known as ATP-binding cassette sub-family B member 1 (ABCB1) and multidrug resistance mutation 1 (MDR1) is an important protein presents at the cell membrane that facilitates transport of foreign substances out from the cells (Thomas and Coley, 2003). P-gp has been widely studied and demonstrated the increased expression of P-gp (ABCB1/MDR1) is one of the major causes of doxorubicin resistance mechanisms in osteosarcoma, which effluxes doxorubicin and therefore reducing its efficacy (Gottesman, Fojo and Bates, 2002; Fanelli *et al.*, 2016). Most of the doxorubicin resistant variants from Table 3.5 had demonstrated an increased mRNA expression level compared to their respective parental cell lines (Oda *et al.*, 2000; Niu *et al.*, 2010; Roncuzzi, Pancotti and Baldini, 2014). Interestingly, Niu *et al*. and Oda *et al*. discovered the gene expression level P-gp is proportional to the fold resistance of doxorubicin (Oda *et al.*, 2000; Niu *et al.*, 2010). Furthermore, a study from Roncuzzi *et al*. indicated a significant induction of HIF-1α gene expression in doxorubicin-resistant MG-63 under normaxic condition, which may be caused by the response mechanisms of the cells to hypoxic stress induced by doxorubicin (Roncuzzi, Pancotti and Baldini, 2014). The activation of HIF-1α may lead to the induction of the P-gp gene transcription due to the presence of functional HIF-1α binding site within the MDR1 gene promoter, and therefore responsible for the doxorubicin resistance (Comerford *et al.*, 2002; Li *et al.*, 2006; Chen *et al.*, 2009).

P-gp gene and protein expression level was investigated in all our resistant panel as this is one of the major resistance mechanisms developed in response to doxorubicin. Moreover, a P-gp inhibitor, elacridar, will be used to assess if P-gp-mediated resistance can be reversed. One of the features of elacridar compared to previous generation inhibitors is that it is specific non-competitive inhibitor of P-gp (Thomas and Coley, 2003). The mechanism of elacridar's inhibition of P-gp is through the regulation of

ATPase activity resulting in inhibiting the ATP hydrolysis for P-gp activity (Fox and Bates, 2007). Elacridar has been shown to reduce the IC_{50} level of doxorubicin on hepatoblastoma cell line HepT1 by 1.7-fold when treated as combination compared to native doxorubicin (Warmann *et al.*, 2002). The cellular uptake of doxorubicin had been indicated to be increased by 1.5-fold in combination of elacridar and doxorubicin compared to native doxorubicin alone (Wong *et al.*, 2006).

4.1.3 Models of methotrexate resistance and related mechanisms

Several example of methotrexate-resistant osteosarcoma cell lines are listed in Table 3.6, and they were developed by either continuous or stepwise-incremental selection strategy. These models have a fold resistance to methotrexate ranging from 4.87- to 283-fold compared to their corresponding parental cell lines (Serra, 2004; Yin *et al.*, 2007; Li *et al.*, 2009; Wang and Li, 2014; Ding *et al.*, 2018; Han and Shi, 2018).

U-2OS MTX-resistant variants developed from Serra *et al.* observed a significant longer doubling time compared to parental cell line U-2OS (Serra, 2004), showing a similar decreased growth rate from some of the cisplatin and doxorubicin-resistant variants discussed in Section 4.1.2 & 4.1.3. Morphological changes were also observed in U2OS and MG63 MTX-resistant cell lines with elongated and more spindle-like shape (Ding *et al.*, 2018). Dihydrofolate reductase (DHFR) is one of the key enzymes in intracellular folate metabolism and is crucial for the cell growth and DNA synthesis (Slansky *et al.*, 1993; Bertino *et al.*, 1996). The overexpression of the DHFR gene and downregulation of reduced folate carrier (RFC), resulting in the impaired intracellular transport of methotrexate is one of the methotrexate resistance mechanisms in osteosarcoma cells (Guo *et al.*, 1999). Overexpression of the DHFR gene occurred in U-2OS MTX-resistant variants which ranged from 3.5- to 50.9-fold resistant. However, there was no significant

amplification of DHFR gene observed in Saos-2 MTX-resistant variants, which possessed resistant level ranges from 15- to 281-fold compared to parental cell line (Serra, 2004).

Ding *et al.* also observed an epithelial-to-mesenchymal transition (EMT) phenotype in both of their U2OS and MG63 MTX-resistant cell lines. Their resistant cell lines demonstrated a significant increase in invasion and migration ability compared to their corresponding parental cell lines. They had also confirmed the EMT phenotype on the resistant variants by investigating the mesenchymal (Vimentin, Slug, and N-cadherin) and epithelial (ZO-1 and E-cadherin) biomarkers by qRT-PCR. Their results showed the classic EMT switch, a significant increase in the mRNA expression level of mesenchymal biomarkers and decrease in epithelial biomarkers. Their result had suggested that their MTX-resistant osteosarcoma cells acquired the EMT-like characteristics and may be attributed to drug-resistant capabilities (Ding *et al.*, 2018). Increased invasion and migration rate of cancer cells is one of the characteristics when the tumour cells undergo transition to mesenchymal from epithelial cell. EMT is also believed to be associated with drug resistance in cancer cells (De Las Rivas *et al.*, 2021) and thus, migration and invasion rate will be investigated in all our osteosarcoma resistant models, followed by the EMT biomarkers expression level to examine the phenotype of the resistant cells.

4.1.4 Aims and objectives

The aim for this chapter is to characterise the major mechanisms of osteosarcoma resistant developed in our MG-63 and HOS-143B derived cisplatin, doxorubicin, methotrexate, and triplet combination resistant osteosarcoma sublines (developed in Chapter 3).

Objective 1: To determine the cross-resistance profile of the resistant models by using cytotoxicity assay.

Objective 2: Investigate the migration and invasion of the resistant models using Transwell assay

Objective 3: Determine the activity of drug resistant mechanisms such as P-gp, autophagy, EMT, and apoptosis.

4.1.4.1 Hypothesis

Several cisplatin, doxorubicin, and methotrexate resistant mechanisms have developed in our osteosarcoma MG-63 and HOS-143B resistant sublines, which could mirror the osteosarcoma patients in the clinic due to the clinically relevant selection strategy used in the development progress.

4.1.4.2 Objectives

The objective of this chapter is to identify the resistant characteristic that have been established in our MG-63 and HOS-143B derived cisplatin, doxorubicin, methotrexate, and triplet combination sublines. Mechanisms that will be examined include P-gp overexpression, apoptosis level, autophagy and EMT. This will be achieved by examining the cross resistance to other drugs, migration and invasion assays, mRNA and protein expression level, and suppression of P-gp activity by an inhibitor.

4.2 Methods

The characteristic of MG-63 and HOS-143B resistant osteosarcoma cell lines (MG-63/CISR8, MG-63/DOXR8, MG-63/MTXR8, MG-63/TRIR8, HOS-143B/CISR8. HOS-143B/DOXR8, HOS-143B/MTXR8, and HOS-143B/TRIR8) were examined by several techniques.

The cross resistance of the resistant sublines was examined by performing several cytotoxic drugs by using acid phosphatase cytotoxicity assays (Section 2.5). The IC_{50} value of the resistant sublines were compared to the parental cell lines and fold resistance was calculated on several cytotoxic drugs. The sensitivity of resistant sublines to cisplatin and doxorubicin was also examined following by incubating with elacridar for P-gp inhibition (Section 2.6).

The migration rate was assessed by wound healing assay (Secttion 2.7) and invasion rate by Transwell assay (Section 2.8). The migration rate was determined by the percentage of the cells migrated to the centre point horizontally, while the invasion rate was determined by the percentage of cells invade through a matrix gel vertically. This allows the comparison between the resistant sublines to MG-63 and HOS-143B.

The mRNA expression level of P-gp, autophagy and EMT biomarkers was examined by carrying out RNA extraction (Section 2.9.1), reverse transcription (Section 2.9.3), and RT-PCR (Section 2.9.4). Protein expression levels was assessed by performing Western blotting (Section 2.10).

Apoptosis assays was performed using fluorescence-activated cell sorting (FACS). A FITC annexin V / PI (Propidium iodide) was carried out on the MG-63 and HOS-143B parental, and the resistant sublines to see the effect of drug exposure on initiation of apoptosis (Section 2.11).

4.3 Results

4.3.1 Cell morphology

Morphology of the resistant cells was investigated by light microscopy as shown in Figure 4.1 for MG-63 resistant sublines and Figure 4.2 for HOS-143B resistant sublines. As shown in Figure 4.1A, the cell morphology of parental cells MG-63 presented in spindle cell shape compared to HOS-143B (Fig. 4.2A) with an irregular rectangular shape. HOS-143B cells showed to grow more aggregated together compared to MG-63 which the cells were more widely separated (Fig. 4.1A & 4.2A).

Cell morphology of the cisplatin-treated resistant model MG-63/CISR8 showed the largest morphology difference compared to MG-63 (Figure 4.1B). MG-63/CISR8 was showed an elongated and thinner spindle cell shape with enlarged nuclear compared to MG-63 as shown in Figure 4.1B. For MG-63/DOXR8, the spindle cell shape and the nuclear were enlarged (Figure 4.1C). Enlarged nuclear of the cells was also found on resistant models MG-63/TRIR8 without alteration of the shape of the cell (Fig. 4.1E). MG-63/MTXR8, which was developed by using methotrexate had no difference in the cell morphology compared to MG-63 (Fig. 4.1D).

The cisplatin-induced resistant model HOS-143B/CISR8 has the same cell morphology as the parental control HOS-143B (Fig. 4.2B). An enlarged nucleus of the cells was mainly seen in resistant models HOS-143B/DOXR8 (Fig. 4.2C) and HOS-143B/MTXR8 (Fig. 4.2D). An irregular shape was also seen on both of these resistant models HOS-143B/DOXR8 and HOS-143B/MTXR8 (Fig. 4.2C & D) compared to HOS-143B. The largest alteration of morphology was demonstrated on resistant model HOS-143B/TRIR8, where some of the cells had an elongated and thinner spindle cell shape and

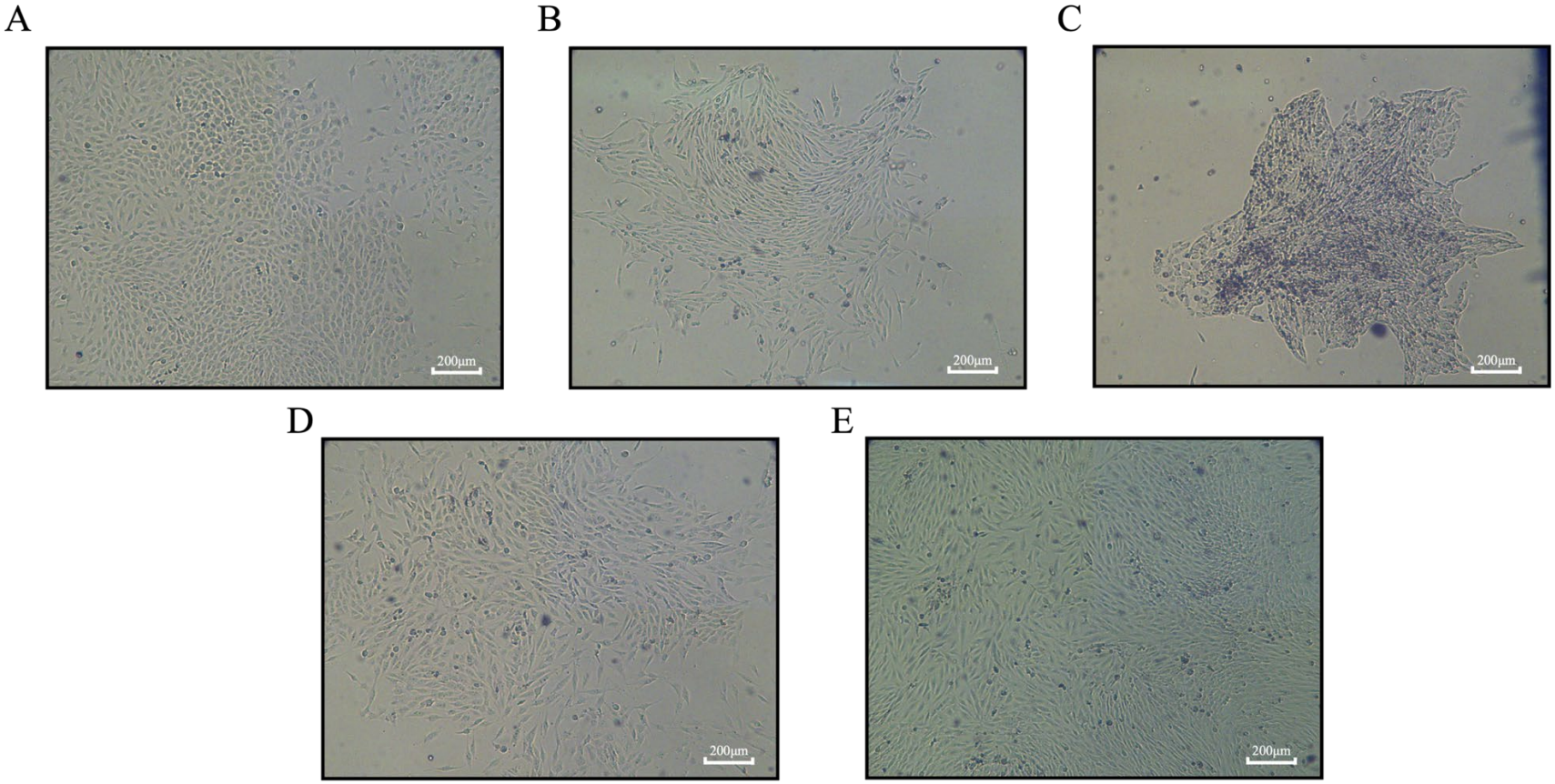

Figure 4.1: Cell morphology of MG-63 resistant models captured under light microscopy at 20× magnification. Cell morphology image of (A) MG-63 parental control, (B) MG-63/CISR8, (C) MG-63/DOXR8, (D) MG-63/MTXR8, and (E) MG-63/TRIR8. (Scale bar = 200µm)

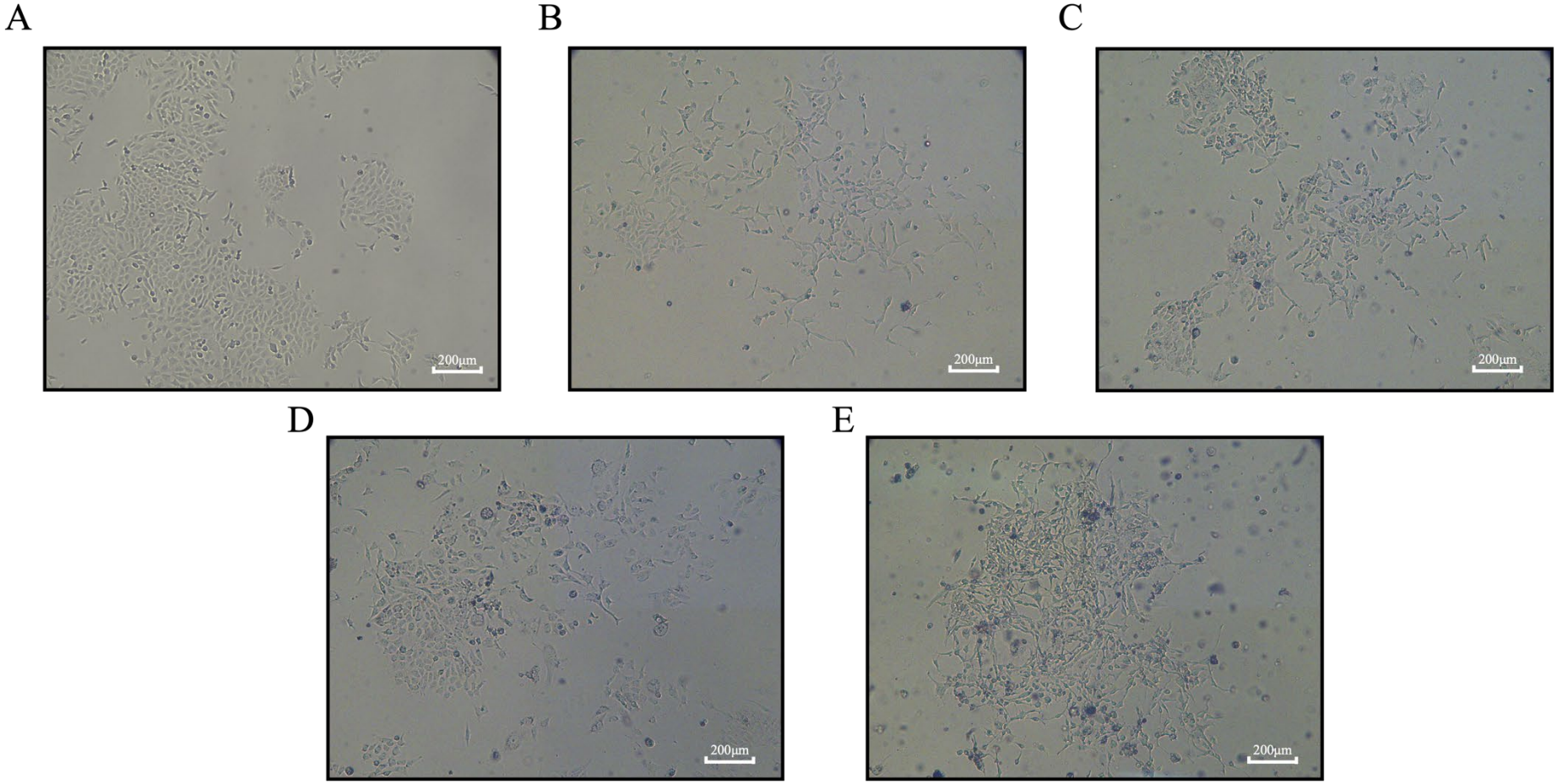

Figure 4.2: Cell morphology of HOS-143B resistant models captured by light microscopy at 20× magnification. Cell morphology image of (A) HOS-143B, (B) HOS-143B/CISR8, (C) HOS-143B/DOXR8, (D) HOS-143B/MTXR8, and (E) HOS-143B/TRIR8. (Scale bar = 200µm)

some showing irregular enlarged cytoplasm and nuclear as shown in Figure 4.1E compared to HOS-143B.

4.3.2 Cross resistance

A drug screen was performed to evaluate the cross resistance to other drugs and to help elucidate resistance mechanisms that have developed in the cells. It would be interesting to investigate and compare between single and multi-agent treated resistant sublines. Cytotoxic drugs cisplatin, doxorubicin, and methotrexate were used to performed cytotoxicity assay on all the resistant sublines. Table 4.1 gives a summary of all cytotoxicity data collected and presented diagrammatically in Figure 4.3 and Figure 4.4.

Fig 4.3 is the bar chart that shows the developed resistance sublines from MG-63 carrying out cytotoxicity assay with cisplatin, doxorubicin, and methotrexate to investigate if cross resistance was acquired between different cytotoxic drugs. Fold resistance was calculated by dividing the IC_{50} value of resistant sublines to the IC_{50} value of parental cell line and plotted in the bar charts. MG-63/CISR8 (Fig. 4.3A) and MG-63/MTXR8 (Fig. 4.3C) did not show significant resistance to other chemotherapeutic agents excepts from the drugs that used in their selection progress. Conversely, resistant subline MG-63/DOXR8 (Fig. 4.1B) which had not retained significant resistance to doxorubicin after 8 rounds of selection, was showed significant cross resistant to cisplatin at 1.88 ± 0.14-fold, $p=0.047$.

Fig. 4.3D – F is the result of fold resistance of each drug on HOS-143B resistant sublines compared to their parental cell lines. All the resistant sublines of HOS-143B did not show significant cross resistance to other chemotherapeutic agents. Despite the higher level of resistance acquired in HOS-143B sublines in overall compared to MG-63 sublines, the resistant sublines only acquired the resistance to the drugs they had been

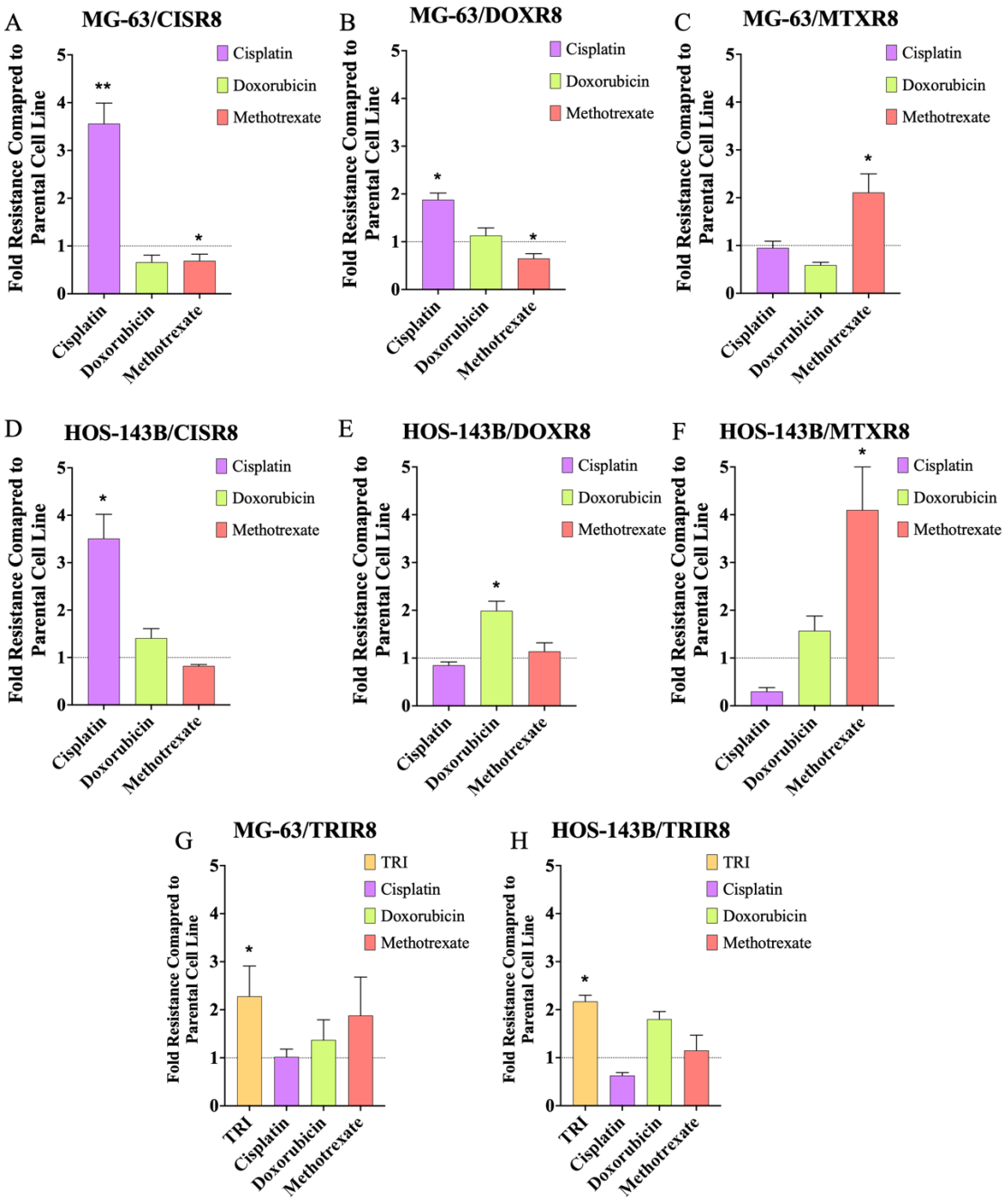

Figure 4.3: Drug screen on MG-63 and HOS-143B resistant models. In each graph the y-axis shows fold resistance compared to the parental cell line and x-axis shows the chemotherapeutic agents. Error bars represent SEM. Fold resistance of each chemotherapeutic agents are shown in (A) for MG-63/CISR8, (B) for MG-63/DOXR8, (C) MG-63/MTXR8, (D) HOS-143B/CISR8, (E) HOS-143B/DOXR8, (F) HOS-143B/MTXR8, (G) MG-63/TRIR8, and (H) HOS-143B/TRIR8. (n=3) * = $p<0.05$, ** = $p<0.01$, Two-sample t-test compared to MG-63 and HOS-143B parental cell line.

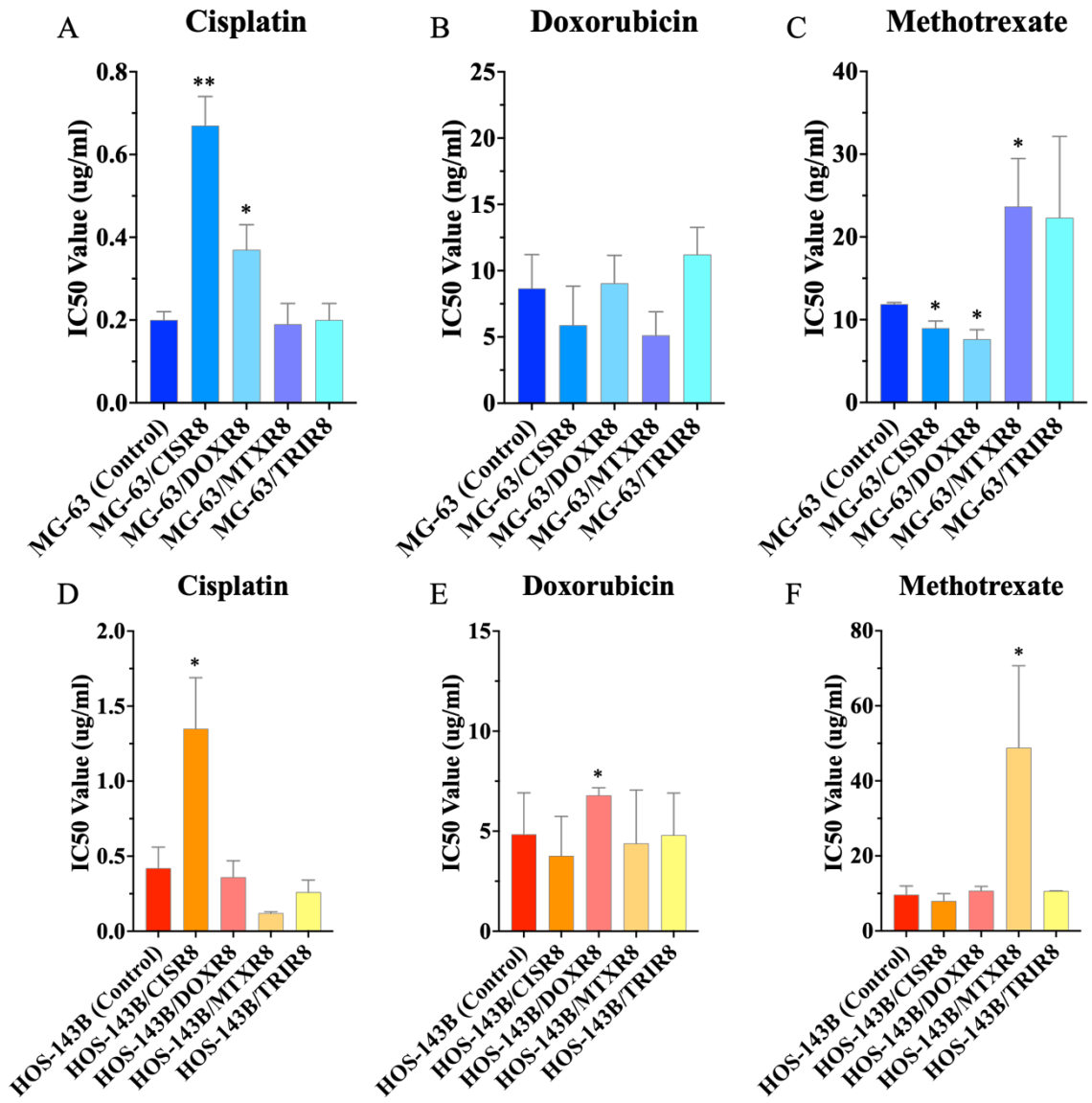

Figure 4.4: IC_{50} value of MG-63 and HOS-143B resistant sublines. In each graph the y-axis represents IC_{50} value compared to the parental cell line. The x-axis represents cell lines. Error bars represent SD. MG-63 and its resistant sublines treated with (A) cisplatin, (B) doxorubicin, and (C) methotrexate. HOS-143B and its resistant sublines treated with (D) cisplatin, (E) doxorubicin, and (F) methotrexate. (n=3) * = $p<0.05$, ** = $p<0.01$, Two-sample *t*-test compared to MG-63 and HOS-143B parental cell line.

given as treatment during the selection progress and not showing any significant cross resistance to other drugs.

MG-63/TRIR8 and HOS-143B/TRIR8 are resistant subline developed by the combination of cisplatin, doxorubicin, and methotrexate. The cytotoxicity assay used to determine the sensitivity of this subline was carried out by a serial dilution of combination of these drugs. Fig. 4.3G & H shows the fold resistant of MG-63/TRIR8 to combination of drugs (yellow), cisplatin (red), doxorubicin (blue), methotrexate (green). Interestingly, when MG-63/TRIR8 was performed cytotoxicity assay with combination drugs, the result show a significant fold resistance increased compared to MG-63. However, when the cytotoxic assay was carried by using the drugs separately as a single individual cytotoxic drug using the drugs separately as a single individual cytotoxic drug, no significant level of resistant was observed to any of the drugs.

Some of the resistant sublines from MG-63 showed increasing sensitivity level of fold resistance to other chemotherapeutic drugs. For example, MG-63/CISR8 showed a reduced IC_{50} value compared to MG-63 to methotrexate with 0.69 ± 0.14-fold ($p=0.03$). MG-63/DOXR8 also showed a lower IC_{50} value to methotrexate with 0.65 ± 0.10-fold ($p=0.024$). A decreased in IC_{50} value from the resistant sublines also indicated the sublines had increased sensitivity (decreased level of resistance) to the chemotherapeutic drug.

Table 4.1 IC_{50} values and fold resistance of drug resistant sublines comparing to parental cell.

Cell Lines	Cisplatin (μg/ml) (± SD)	Fold Resistance (± SEM)	Doxorubicin (ng/ml) (± SD)	Fold Resistance (± SEM)	Methotrexate (ng/ml) (± SD)	Fold Resistance (± SEM)
MG-63/CISR8	0.67 ± 0.07 **	3.56 ± 0.43	5.88 ± 2.95	0.66 ± 0.15	8.98 ± 0.87 *	0.69 ± 0.14
MG-63/DOXR8	0.37 ± 0.06 *	1.88 ± 0.14	9.04 ± 2.12	1.19 ± 0.16	7.65 ± 1.15 *	0.65 ± 0.10
MG-63/MTXR8	0.19 ± 0.05	0.95 ± 0.14	5.11 ± 1.78	0.59 ± 0.06	23.68 ± 5.78 *	2.11 ± 0.39
MG-63/TRIR8	0.20 ± 0.04	1.02 ± 0.16	11.22 ± 2.05	1.37 ± 0.42	22.32 ± 9.82	1.88 ± 0.80
HOS-143B/CISR8	1.35 ± 0.34 *	3.51 ± 0.51	3.77 ± 1.97	1.41 ± 0.20	7.96 ± 1.96	0.82 ± 0.03
HOS-143B/DOXR8	0.36 ± 0.11	0.85 ± 0.07	6.79 ± 0.38 *	1.99 ± 0.20	10.73 ± 1.13	1.14 ± 0.18
HOS-143B/MTXR8	0.12 ± 0.01	0.30 ± 0.08	4.39 ± 2.67	1.57 ± 0.31	48.84 ± 21.82 *	3.77 ± 0.90
HOS-143B/TRIR8	0.26 ± 0.08	0.63 ± 0.06	4.80 ± 2.10	1.80 ± 0.16	10.65 ± 0.05	1.15 ± 0.32

SEM = Standard error of mean, n=3. * = $p<0.05$, ** = $p<0.01$, Two-sample *t*-test compared to MG-63 and HOS-143B parental cell line.

4.3.3 Migration assay

The migration rate of MG-63 and HOS-143B derived cisplatin, doxorubicin, methotrexate, and triplet combination sublines were assessed by wound-healing assay. The migration rate was determined by measuring the percentage of area where the cells have migrated toward the centre after 16 hours as described in Section 2.7. The fold change was calculated by dividing the area migrated from resistant subline to parental cell line.

Figure 4.5A&B shows the percentage of area MG-63 cells and HOS-143B cells and its resistant sublines migrated after 16 hours, respectively. The percentage of area that MG-63 had migrated was 22 ± 0.82% and HOS-143B was 91.05 ± 5.64%. Comparison between the parental cell lines shown that HOS-143B was having a higher migration rate compared to MG-63 with 4.22 ± 0.22-fold higher (p=0.0052). This could be explained by HOS-143B was originally a highly metastatic osteosarcoma cell line and has a higher growth rate, therefore a higher migration rate was determined compared to MG-63 with only marginal metastatic potential.

The resistant sublines MG-63/CISR8, MG-63/MTXR8, and MG-63/TRIR8 were determined to have a significantly increased migration rate compared to parental cell line MG-63 as shown in Figure 4.5A. The wound healing assay determined the area percentage for MG-63/CISR8 was 49.68 ± 5.86% (p=0.015), MG-63/MTXR8 was 57.41± 5.77% (p=0.009), and MG-63/TRIR8 was 56.11 ± 2.53% (p=0.002) (Fig. 4.3A). The highest migration rate increased amongst them comparing to parental cell line was MG-63/MTXR8 with 2.55 ± 0.42- fold (p=009), followed by MG-63/TRIR8 with 2.46 ± 0.16-fold (p=0.002), and MG-63/CISR8 with 2.12 ± 0.33- fold (p=0.015) as shown Figure

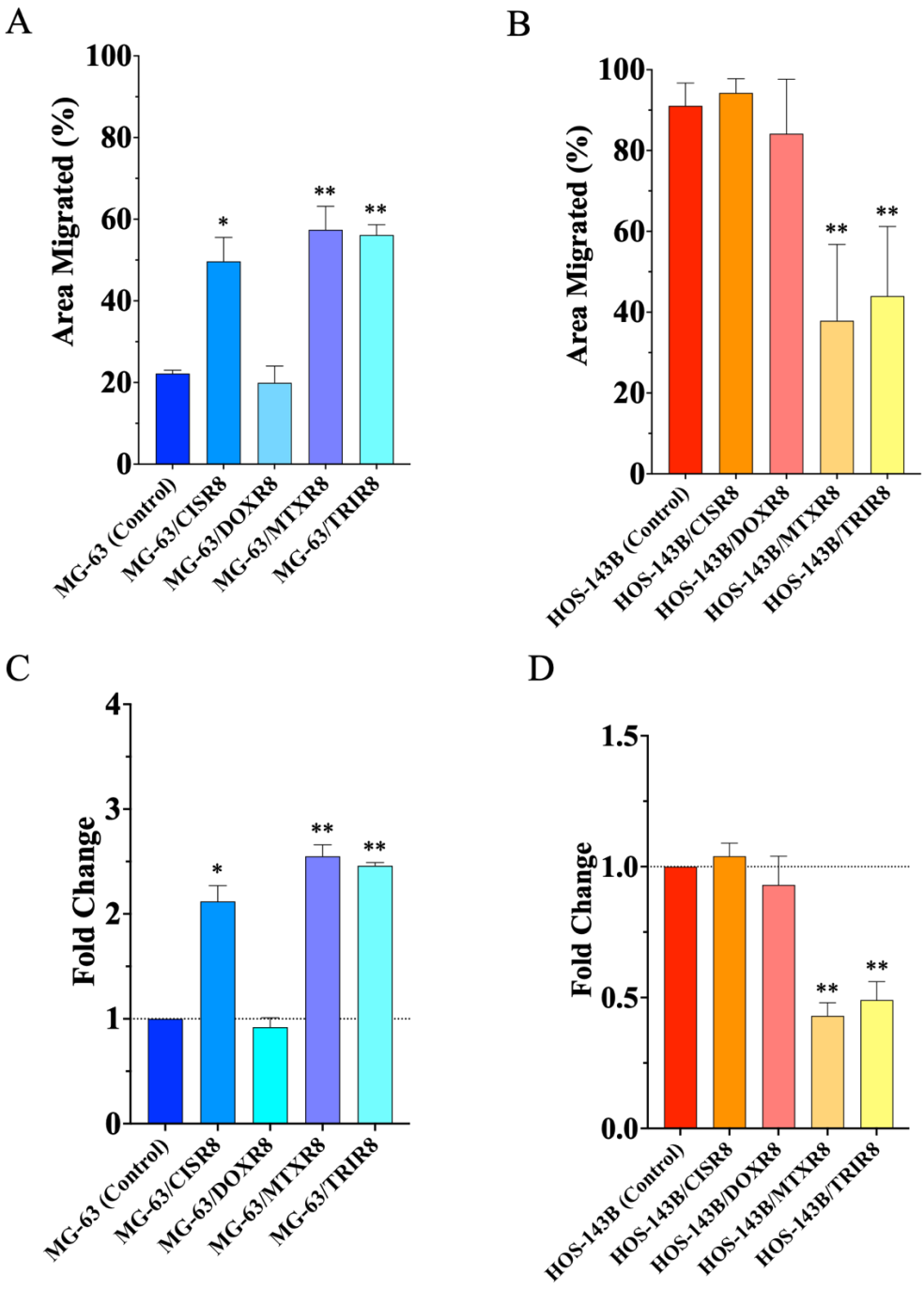

Figure 4.5: Wound healing assay of MG-63 and HOS-143B resistant sublines. Wound healing assay was determined by measuring the area migrated to the centre after 16 hours (n=3). Percentage of area migrated shown in (A) for MG-63 resistant sublines and (B) for HOS-143B resistant sublines. Fold change is calculated and shown in (C) for MG-63 resistant sublines and (D) for HOS-143B resistant sublines. Error bars representing SD in (A) & (B) and representing SEM in (A) & (D). * = $p < 0.05$, ** = $p<0.01$, Two-sample *t*-test.

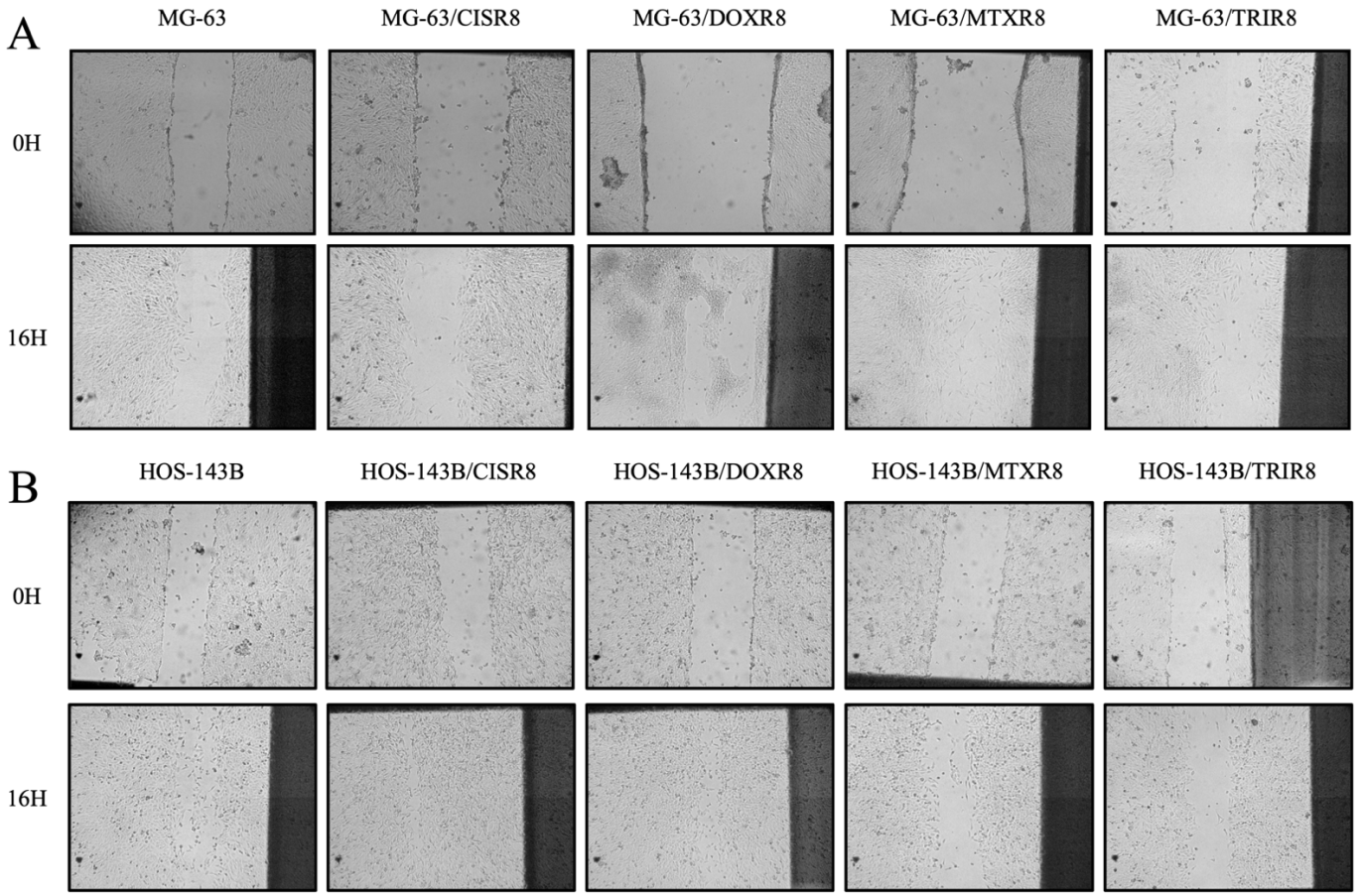

Figure 4.6: Images of wound healing assays taken to investigate the migration rate of the resistant sublines compared to their parental cell lines.

(A) Images of MG-63 resistant sublines and parental control taken at 0H and 16H. (B) Images of HOS-143B resistant sublines and parental control taken at 0H and 16H.

4.5B. While resistant subline MG-63/DOXR8, which did not acquire significant increase of resistance, had a similar migration rate with MG-63.

The migration rate of HOS-143B and its resistant sublines is shown in Figure 4.5C. In contrast to the MG-63, some resistant sublines derived from HOS-143B had a significantly decreased migration rate compared to their parental cell line. The area percentage for HOS-143B/MTXR8 and HOS-143B/TRIR8 was 37.86% ± 18.89% (p=0.003), and 43.99% ± 17.21% (p=0.004) respectively. While HOS-143B/CISR8 and HOS-143B/DOXR8 were 94.27% ± 3.49% and 84.16 %± 13.47%, similar to the parental cell line HOS-143B (Fig. 4.5C). The highest fold in migration rate of HOS-143B resistant sublines was HOS-143B/MTXR8 with 0.33% ± 0.05-fold decreased (p=0.003), followed by HOS-143B/TRIR8 with 0.41 ± 0.07-fold decreased (p=0.004) (Fig. 4.5D).

4.3.4 Invasion assay

The invasion rate of MG-63 and HOS-143Bresistant sublines were assessed by Transwell assay. Extracellular matrix gel was freshly prepared in 96-well Transwell insert as described in Section 2.8. The fold change was calculated by dividing the percentage of resistant cells with the percentage of parental cells invaded through the extracellular matrix (ECM) after 24 hours. HT1080 cells was used as positive control and MCF7 as negative control (Gayan, Teli and Dey, 2017). Figure 4.7A & B show the percentage of cell MG-63 and HOS-143B and its resistant sublines invaded through the extracellular matrix gel after 24 hours, respectively. The percentage of cells for MG-63 invaded through the gel was 16.02 ± 1.12% and HOS-143B was 70.34 ± 8.7%. Therefore, HOS-143B has a significantly higher invasion rate compared to MG-63 with 5.01 ± 0.42-fold (p=0.022).

Again, the comparison between the parental cell lines had shown HOS-143B had a higher invasion rate compared to MG-63 with 5.01 ± 0.42-fold (p=0.022). This could be explained with the highly metastatic characteristic of HOS-143B. A slight increase of invasion rate was determined in some of the MG-63 resistant cell lines after 8 rounds of selection. A significant increased invasion rate was determined in MG-63/DOXR8 with 26.45% ± 1.77% (p=0.012), 1.65-fold (p=0.012) comparing to MG-63 (Fig. 4.7A & C). The rest of the MG-63 resistant models showed an increasing trend with 19.91% ± 2.3% (p=0.202) in MG-63/MTXR8 and 21.88% ± 6.78% (p=0.431) in MG-63/TRIR8 compared to MG-63 (Fig. 4.7A). The invasion rate determined for MG-63/CISR8 was 16.72% ± 1.7% (p=0.495), which was almost similar with MG-63. Conversely, a significant decrease in rate was seen in HOS-143B/DOXR8 with 27.6% ± 4.31%, 0.35 ± 0.03-fold (p=0.032) compared to HOS-143B (Fig. 4.7B & D).

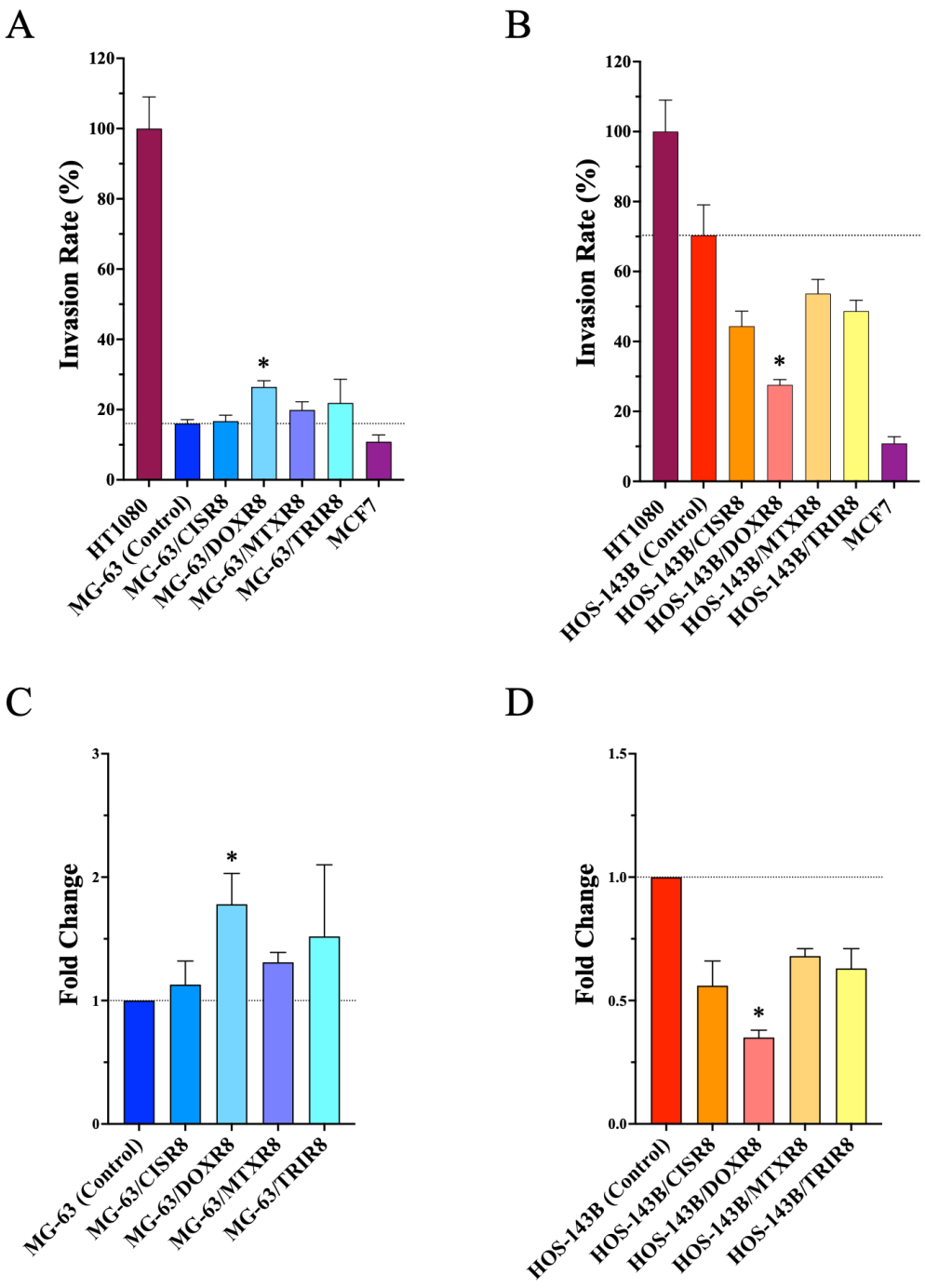

Figure 4.7: Transwell assay of MG-63 and HOS-143B resistant sublines. Invasion rate was determined by measuring the percentage cells invaded through the extracellular matrix after 24 hours. Percentage of cells invaded shown in (A) for MG-63 resistant sublines and (B) for HOS-143B resistant sublines. Fold change was calculated and shown the HOS-143B resistant models were also show a decreasing in (C) for MG-63 resistant sublines and (D) for HOS-143B resistant sublines. * = $p < 0.05$, Two-sample *t*-test.

4.3.5 Expression of P-glycoprotein

P-glycoprotein is an ABC transporter present in the cell membrane and responsible for facilitating transport of foreign substances from cells (Jiang, Yan and Wu, 2019). P-gp is suggested as one of the contributing factors in chemoresistance, therefore the expression of P-gp in mRNA and protein levels was investigated. The mRNA expression level was assessed by RT-PCR and the protein expression level by Western blotting.

The ABCB1 gene was investigated in the parental and resistant sublines as it encodes for P-gp. Figure 4.8A & B are the ABCB1 mRNA expression level for MG-63 and HOS-143B parental and resistant sublines. Figure 4.8 shows gene expression level of resistant subline compared to parental control (MG-63 and HOS-143B). The gene expression data was analysed by using $\Delta\Delta C_q$ method to normalise the gene expression to housekeeping gene GAPDH and plotted in fold change on the y-axis. ΔC_q value of the parental control MG-63 and HOS-143B was 17.37 ± 0.51 and 10.97 ± 0.25 respectively. By comparing the ΔC_q value of the parental control, the expression level of ABCB1 was higher in HOS-143B than MG-63 with 87.89 ± 15.86-fold (p=0.002).

Most of the MG-63 resistant sublines showed a significant upregulated expression level of ABCB1 gene except for MG-63/MTXR8 (Fig. 4.8A). The highest upregulated fold change was determined on MG-63/CISR8 with 23.24 ± 5.07-fold (p=0. 005), following by MG-63/TRIR8 with 11.84 ± 2.60-fold (p=0. 026), and MG-63/DOXR8 with 6.26 ± 1.16-fold (p=0. 024), comparing to parental control MG-63.

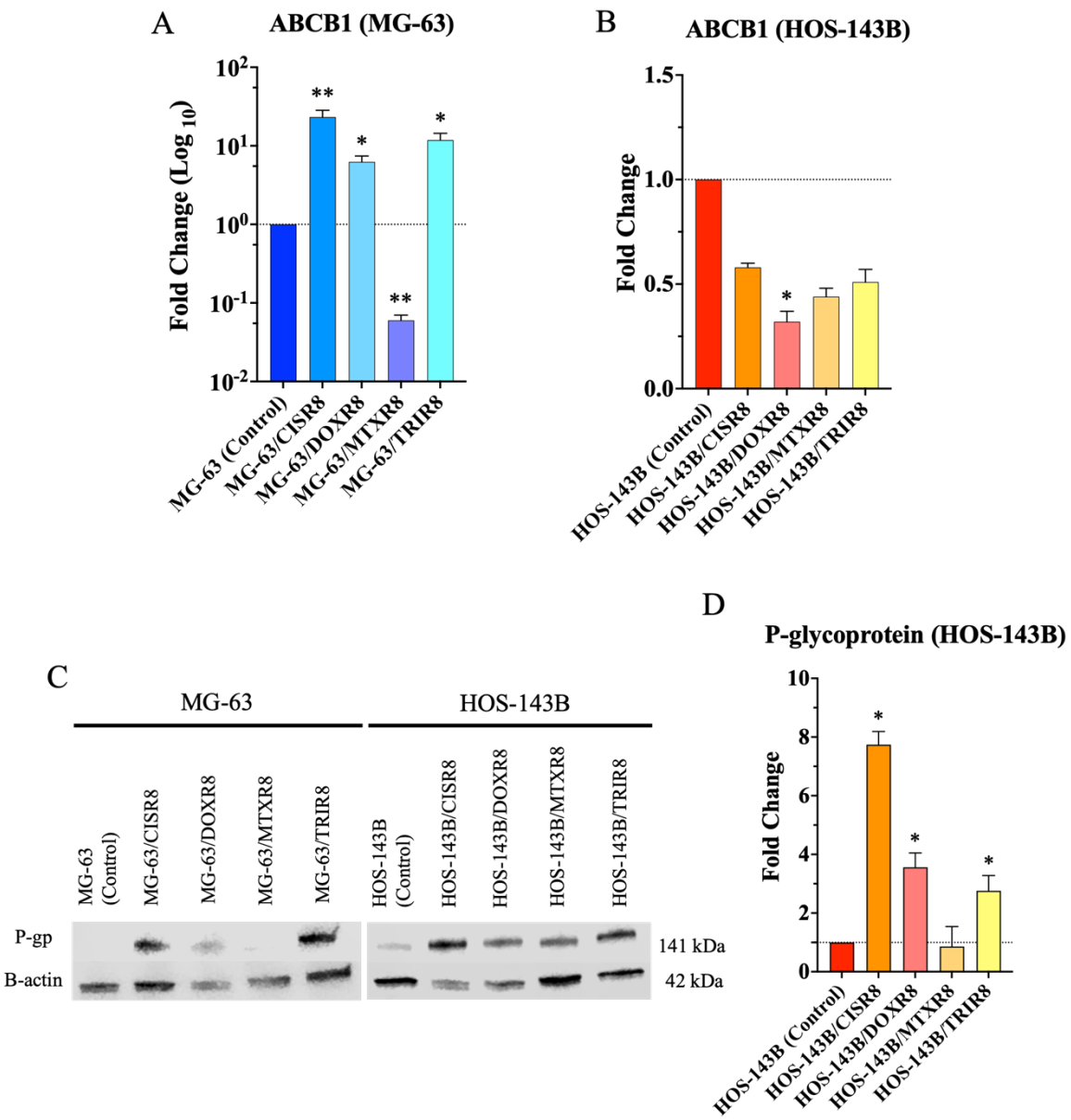

Figure 4.8: mRNA and protein expression level of P-gp in MG-63 and HOS-143B resistant sublines. mRNA expression level of ABCB1 for (A) MG-63 resistant cell lines and (B) HOS-143B resistant cell lines analysed by RT-PCR (n=3). (C) P-glycoprotein protein expression level for MG-63 and HOS-143B resistant cell lines analysed by Western Blot by using ECL quantification method. (D) Fold change level of P-gp expression level compared to parental HOS-143B. (n=3). Error bars represent SEM. * = $p < 0.05$, ** = $p<0.01$, Two-sample *t*-test.

Conversely, MG-63/MTXR8 showed a significant downregulation in the ABCB1 mRNA expression level with 0.06 ± 0.01-fold (p=0. 007).

For HOS-143B resistant sublines, the fold change of the expression level of ABCB1 gene is shown in Figure 4.8B. All HOS-143B resistant sublines showed an opposite result to most of the MG-63 resistant sublines. Instead of increasing the mRNA expression level of ABCB1, HOS-143B resistant sublines show a decreased compared to parental control HOS-143B (Fig. 4.6B). The largest downregulated fold change was determined on HOS-143B/DOXR8 with 0.32 ± 0.05-fold (p=0. 0.01) compared to HOS-143B.

The rest of the HOS-143B resistant models were also showed a decreasing trend with 0.44 ± 0.04-fold in HOS-143B/MTXR8, 0.51 ± 0.06-fold in HOS-143B/TRIR8, and 0.58 ± 0.02-fold in HOS-143B/CISR8 comparing to parental control HOS-143B. After determining the mRNA expression level of ABCB1 which encodes for P-gp, the protein level of P-gp was investigated by Western blot. Figure 4.8C shows the P-gp expression in protein level including parental control and resistant sublines of MG-63 and HOS-143B. The protein expression level of P-gp was normalised to beta-Actin to measure the fold change comparing to parental control. From the result showing in Figure 4.8C, there was no band determined on parental control MG-63 and a light band shown on the parental control HOS-143B. This has suggested that P-gp was not expressed in parental control MG-63 and only expressing in parental control HOS-143B. This corresponded to the result determined on mRNA expression level of ABCB1 discussed above, as the expression level of ABCB1 was significantly lower in MG-63 compared to HOS-143B (Figure 4.8A & B).

Since the parental control MG-63 did not express P-gp protein, the expression level of P-gp was unable to be measured in fold change manner for MG-63 resistant sublines. However, bands were observed for resistant sublines as shown in Figure 4.8C. This suggests that the expression level of P-gp was drastically upregulated in MG-63/CISR8, MG-63/DOXR8, and MG-63/TRI. The highest level of P-gp expression increased was resistant subline MG-63/TRIR8 as it showed the darkest bands compared to others, followed by MG-63/CISR8 and MG-63/DOXR8. This showed a similar result to the expression level of ABCB1, as the gene was upregulated in MG-63/CSIR8, MG-63/DOXR8 and MG-63/TRIR8 (Figure 4.8A & C).

The P-gp protein expression level for HOS-143B and its resistant subline is shown in Figure 4.8C. Most of the resistant sublines showed significant upregulated expression of P-gp comparing to parental control HOS-143B, except for HOS-143B/MTXR8. Fold change of expression level was measured and shown in Figure 4.8D. The most significant increase of P-gp expression level was determined in HOS-143B/CISR8 with 7.74 ± 0.45-fold (p=0. 02), followed by HOS-143B/DOXR8 with 3.56 ± 0.49-fold (p=0. 011), and HOS-143B/TRIR8 with 2.76 ± 0.52-fold (p=0.033), comparing to parental control HOS-143B. Conversely, HOS-143B/MTXR8 showed a trend for downregulated expression of P-gp with 0.86 ± 0.68-fold (p=0.647). The expression level of P-gp in HOS-143B resistant sublines showed a contrasting result with the expression level of ABCB1 gene. Despite the ABCB1 mRNA expression level was downregulated in all the resistant models compared to HOS-143B, the P-gp protein expression level was upregulated in some of the resistant models as shown in Figure 4.8. Furthermore, A strong correlation (r=0.941) was determined between the IC_{50} value of doxorubicin and ΔCq of P-gp in HOS-143B resistant sublines.

4.3.6 Effect of elacridar (P-gp inhibitor)

Elacridar was used as a P-gp inhibitor to investigate the chemoresistant mechanism in MG-63 and HOS-143B derived resistant sublines. Elacridar was incubated with the cells for 24 hours prior the addition of chemotherapeutic agents as described in Section 2.6. The cell cytotoxicity of cisplatin and doxorubicin was investigated with elacridar due to the reported possible resistant mechanisms involved with P-gp as described in Section 4.1.2 and 4.1.3. Elacridar as a P-gp inhibitor was used to investigate the reversal of P-gp mediated resistant efflux to enhance the cytotoxicity of cisplatin and doxorubicin.

Figure 4.9 shows the effect of elacridar on all resistant sublines derived from MG-63 and HOS-143B. IC_{50} value of cisplatin and doxorubicin was determined by acid phosphatase assay with and without the combination of elacridar. Figure 4.9A & B shows the IC_{50} value of cisplatin determined on both MG-63 and HOS-143B resistant sublines and Figure 4.9C & D are displaying the IC_{50} value of doxorubicin. There was no significant increase or decrease of IC_{50} value of cisplatin and doxorubicin on parental cell lines HOS-143B with the combination of elacridar, but the IC_{50} value of cisplatin with the combination of elacridar on MG-63 was significantly increased with 2.71 ± 0.13-fold ($p=0.002$). This indicated that elacridar had no effect on parental cell line HOS-143B despite the expression of P-gp was determined by RT-PCR and Western blotting. Moreover, elacridar was increasing the resistance of cisplatin on parental cell line MG-63 instead.

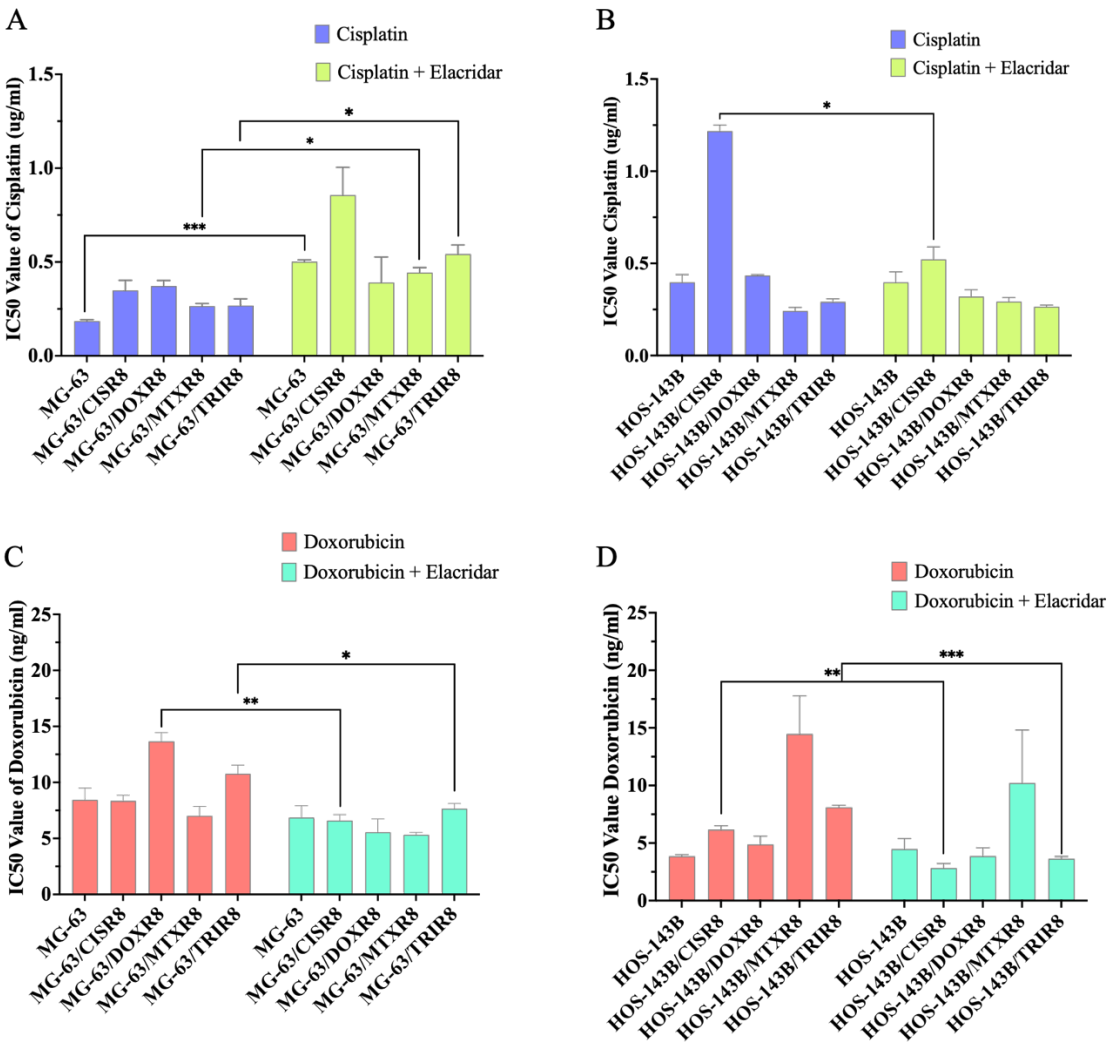

Figure 4.9: Sensitivity profile of resistant models - cisplatin and doxorubicin with and without the inhibitor of elacridar. IC_{50} value of cisplatin with and without elacridar for parental and resistant sublines of (A) MG-63 and (B) HOS-143B. IC_{50} value of doxorubicin with and without elacridar for parental and resistant sublines of (C) MG-63 and (D) HOS-143B. (n=3) Error bars represent SEM. * = $p < 0.05$, ** = $p < 0.01$, *** = $p < 0.00$, Two sample *t*-test.

Elacridar also determined to increase the IC_{50} value of some MG-63 resistant sublines and therefore increasing their resistance to cisplatin. MG-63, MG-63/MTXR8 and MG-63/TRIR8 showed a significant increase in their IC_{50} value to cisplatin with the combination of elacridar with 2.71 ± 0.13-fold (p=0.0001), 1.67 ± 0.06-fold (p=0. 028) and 2.1 ± 0.31-fold (p=0.02), respectively (Fig. 4.9A). Thus, the effect of elacridar increased the resistance of cisplatin on the parental cell lines, MG-63, MG-63/MTXR8, and MG-63/TRIR8. However, when the combination of doxorubicin and elacridar was administered to MG-63 resistant sublines, some of the sublines had a significant decrease in the IC_{50} value of doxorubicin.

MG-63/DOXR8 and MG-63/TRIR8 showed a significantly decreased of IC_{50} value of doxorubicin with 0.36 ± 0.06-fold (p=0.003) and 0.72 ± 0.07-fold (p=0.04) respectively compared to the IC_{50} value without the combination of elacridar (Fig. 4.9C). This indicated that the combination of elacridar was effectively increasing the sensitivity of doxorubicin on MG-63/DOXR8 and MG-63/TRIR8 with 2.96 ± 0.52-fold (p=0.0.003) and 1.42 ± 0.14-fold (p=0.0.04), respectively.

For HOS-143B derived resistant sublines, HOS-143B/CISR8 was determined to have a significant decreased IC_{50} value of cisplatin when combination of cisplatin and elacridar was given as shown in Figure 4.9B. HOS-143B/CISR8 showed a significant decrease of IC_{50} value of cisplatin with 0.43 ± 0.07-fold (p=0.021) compared to without elacridar (Fig. 4.9B). HOS-143B/CISR8 and HOS-143B/TRIR8 were also determined to have a significant reduction of IC_{50} value of doxorubicin when in combination with elacridar as shown in Figure 4.9D. HOS-143B/CISR8 and HOS-143B/TRIR8 showed a significant decrease of IC_{50} value of doxorubicin with 0.47 ± 0.09-fold (p=0.009) and 0.45 ± 0.03-fold (p=0. 0005) respectively, compared to without elacridar (Fig. 4.9D). Thus, this

indicated that elacridar was able to increase the sensitivity of HOS-143B/CISR8 to cisplatin with 2.43 ± 0.39-fold (p=0.0.021), HOS-143B/CISR8 and HOS-143B/TRIR8 to doxorubicin with 2.33 ± 0.52-fold (p=0.0.009) and 2.25 ±0.17-fold (p=0.0.0005), respectively.

4.3.7 Expression of EMT biomarkers

Due to the alteration in migration and invasion rate of some of the MG-63 and HOS-143B resistant sublines, the EMT mechanism was further investigated. EMT biomarkers ZEB1, Vimentin, E-cadherin (E-CAD), and N-cadherin (N-CAD) were examined by performing RT-PCR as described in Section 2.9.

The result indicates that the parental control HOS-143B itself initially expressed higher level of mesenchymal biomarkers (N-CAD) than MG-63. This also explains the higher migration and invasion rate and the high degree metastatic characteristic on HOS-143B. The expression level of EMT biomarkers were identified on parental cell lines MG-63 and HOS-143B as shown in Figure 4.10A. Expression level of ZEB1 showed an upregulated trend in HOS-143B compared to MG-63 but with non-statistical significance. While the expression of VIM was found to be similar between those two parental control MG-63 and HOS-143B. E-CAD which is one of the epithelial biomarkers showed a slightly lower expression level in HOS-143B compared to MG-63, and the N-CAD which is one of the mesenchymal biomarkers had a significantly higher expression level in HOS-143B with 11.21 ± 2.33-fold (p=0.007), compared to MG-63 (Fig. 4.10A).

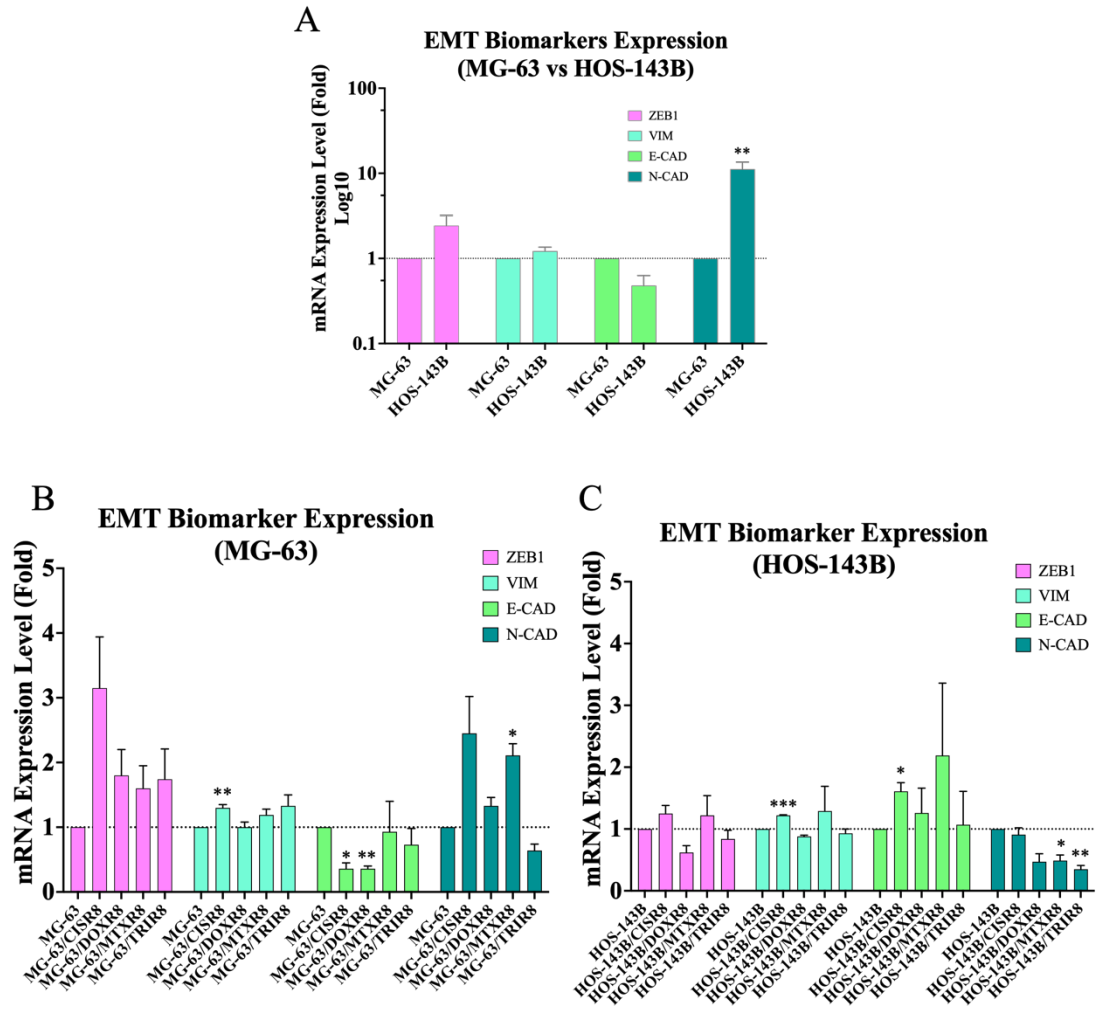

Figure 4.10: EMT biomarkers gene expression level on parental and resistant sublines of MG-63 and HOS-143B. (A) The EMT biomarkers expression of HOS-143B compared to MG-63. The EMT biomarkers expression of (B) parental and MG-63 derived resistant sublines, (C) parental and HOS-143B derived resistant sublines in fold change compared to parental controls using RT-PCR (n=3). Error bars = SEM. * = $p < 0.05$, ** = $p < 0.01$, *** = $p < 0.0001$. One-sample *t*-test with hypothesised mean = 1.

Figure 4.10B shows the fold change of EMT biomarkers expression level on MG-63 resistant sublines compared to parental control MG-63. The expression level of ZEB1 tend to be upregulated trend in all the resistant sublines and the most significant increase was determined on resistant subline MG-63/CISR8 as shown in Figure 4.10B. The expression of epithelial biomarker (E-CAD) was decreased in all the resistant sublines of MG-63 at different level. MG-63/CISR8 and MG-63/DOXR8 were determined to significantly downregulate on the expression level of E-CAD compared to MG-63 with 0.36 ± 0.15-fold (p=0.018) and 0.36 ± 0.07-fold (p=0.005). The corresponding mesenchymal biomarker (N-CAD) was increased in most of the MG-63 resistant sublines except for MG-63/TRIR8 as shown in Figure 4.10B. MG-63/MTXR8 was found to be significantly upregulated with 2.11 ± 0.18-fold (p=0.026) on the gene expression of N-CAD.

Figure 4.10C demonstrated the overall expression level of EMT biomarkers for HOS-143B derived resistant sublines. There were no significant changes of on the expression of ZEB1 and VIM on the resistant sublines compared to parental control HOS-143B except for HOS-143B/CIS. HOS-143B/CISR8 was determined with significant upregulated of VIM with 1.22 ± 0.01-fold (p=0.0004). Furthermore, the expression of E-CAD (epithelial biomarker) was increased in all HOS-143B resistant sublines and decreased in the expression of mesenchymal biomarker (N-CAD) as shown in Figure 4.7C. HOS-143B/CISR8 was significantly upregulated on the expression of E-CAD with 1.61 ± 0.14-fold (p=0.047). While the expression level of N-CAD was significantly downregulated in HOS-143B/MTXR8 and HOS-143B/TRIR8 with 0.49 ± 0.09-fold (p=0.03) and 0.35 ± 0.06-fold (p=0.007), respectively, compared to parental control HOS-143B.

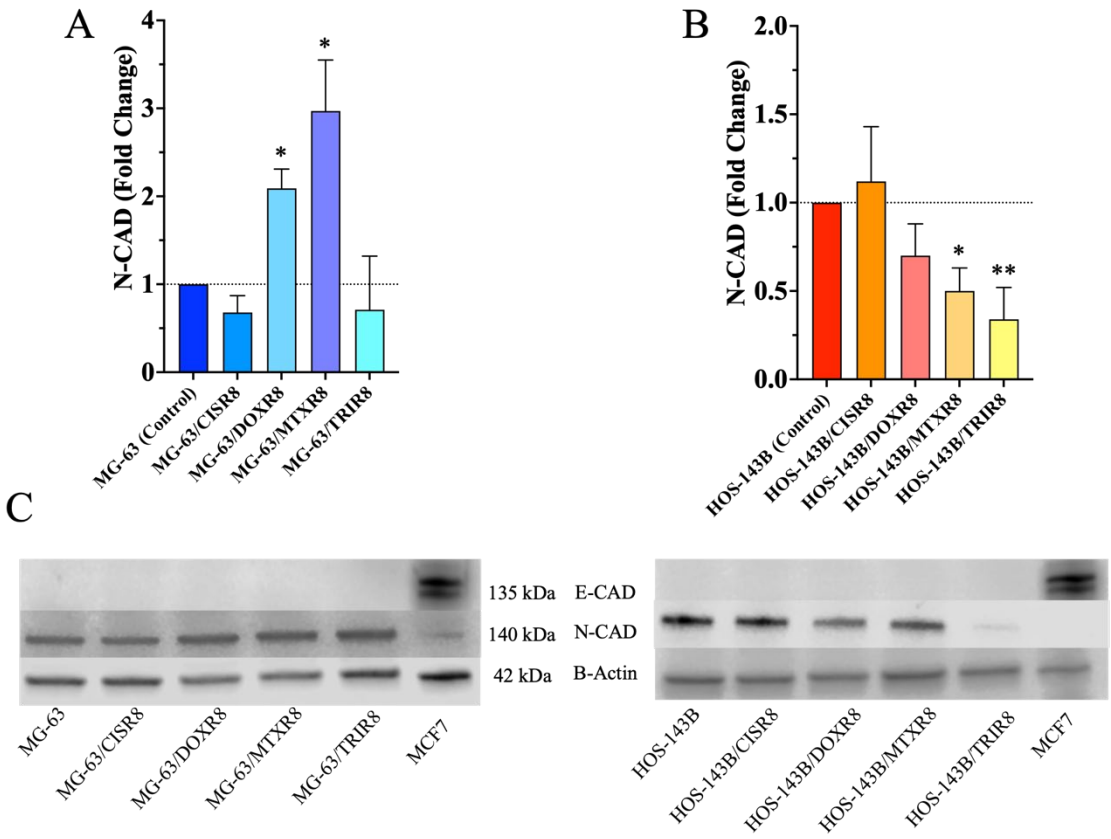

Figure 4.11: EMT biomarkers protein expression level on parental and resistant sublines of MG-63 and HOS-143B. The E-CAD protein expression of (A) parental and MG-63 derived resistant sublines, (B) parental and HOS-143B derived resistant sublines in fold change compared to parental controls. (C) Protein expression level of E-CAD and N-CAD on parental and resistant sublines of MG-63 and HOS-143B. MCF7 was used as the positive control for E-CAD (n=3). Error bars = SEM. * = $p < 0.05$, ** = $p < 0.01$, One-sample *t*-test with hypothesised mean = 1.

This upregulation and downregulation of the EMT biomarkers especially the epithelial and mesenchymal biomarkers could be used to determine the indication of the epithelial to mesenchymal transition (EMT) or mesenchymal to epithelial transition (MET). Based on the expression of E-CAD and N-CAD of our resistant sublines, we determined that most of the resistant sublines of MG-63 includes MG-63/CISR8, MG-63/DOXR8 and MG-63/MTXR8 underwent EMT due to the upregulated expression of N-CAD and downregulated expression of N-CAD. In contrast, HOS-143B resistant sublines including HOS-143B/CISR8, HOS-143B/DOXR8, HOS-143B/MTXR8, and HOS-143B/TRIR8 underwent MET due to the downregulated expression of N-CAD and upregulated expression of E-CAD.

Figure 4.11 shows the protein expression of E-CAD and N-CAD of parental and resistant sublines of MG-63 and HOS-143B by Western blot. No band was determined on E-CAD for both parental and resistant sublines of MG-63 and HOS-143B. MCF7 was used as the positive control for E-CAD, which showed the protein bands as in Figure 4.11C. However, a similar result was obtained on the expression level of N-CAD in protein level with the mRNA expression level. After normalised to beta-Actin, MG-63/MTXR8 was determined to have the highest increased of protein expression N-CAD with 2.97 ± 0.58-fold ($p=0.038$) compared to parental control, followed by MG-63/DOXR8 with 2.09 ± 0.22-fold ($p=0.04$). MG-63/CISR8 and MG-63/TRIR8 showed a decreasing trend with 0.68 ± 0.19-fold ($p=0.815$) and 0.71 ± 0.61-fold ($p=0.858$), respectively.

In contrast, HOS-143B/CISR8 showed a similar protein expression level of N-CAD compared to HOS-143B with only 1.12 ± 0.31-fold ($p=0.986$) increase, while the rest of the HOS-143B resistant sublines showed a decreased expression of N-CAD. The highest decreased protein expression of N-CAD compared to HOS-143B was HOS-143B/TRIR8

with 0.34 ± 0.18-fold (p=0.007), followed by HOS-143B/MTXR8 with 0.50 ± 0.13-fold (p=0.023), and HOS-143B/DOXR8 with 0.70 ± 0.18-fold (p=0.719). This has again showed a similar result with the mRNA expression level of N-CAD obtained from RT-PCR.

4.3.8 Expression of autophagy-related genes

The expression of autophagy related genes ATG7, ATG12, LC3-II and p62 were investigated by using RT-PCR as shown in Figure 4.12. Figure 4.12A demonstrated the expression level of autophagy related genes on MG-63 resistant sublines. Upregulated expression level of p62, LC3-II, ATG7, and ATG12 were determined on MG-63/CISR8. Significant increased expression of p62 was determined on MG-63/CSIR8 with 1.68 ± 0.10-fold compared to parental control MG-63. Expression of LC3-II, ATG7, and ATG12 was increased with 1.52 ± 0.22-fold, 1.90 ± 0.34-fold and 1.31 ± 0.10-fold, respectively. However, for resistant sublines MG-63/DOXR8, MG-63/MTXR8, and MG-63/TRIR8, the expression level of autophagy-related genes was either decreased or similar with the parental control as shown on Figure 4.12A.

Figure 4.12B shows the expression level of autophagy related genes on HOS-143B resistant sublines. A slight increase of p62 and ATG12 expression determined on HOS-143B/CISR8 and HOS-143B/DOXR8 but were statistically insignificant. However, the expression level of p62, LC3-II, ATG7 and ATG12 were downregulated on HOS-143B/MTXR8 and HOS-143B/TRIR8. Significant decreased of p62 and ATG7 was determined on HOS-143B/TRIR8 with 0.18 ± 0.05-fold and 0.28 ± 0.08-fold, respectively. The expression level of LC3-II and ATG7 were also decreased on HOS-143B/CISR8 and HOS-143B/DOXR8 as shown in Figure 4.12B.

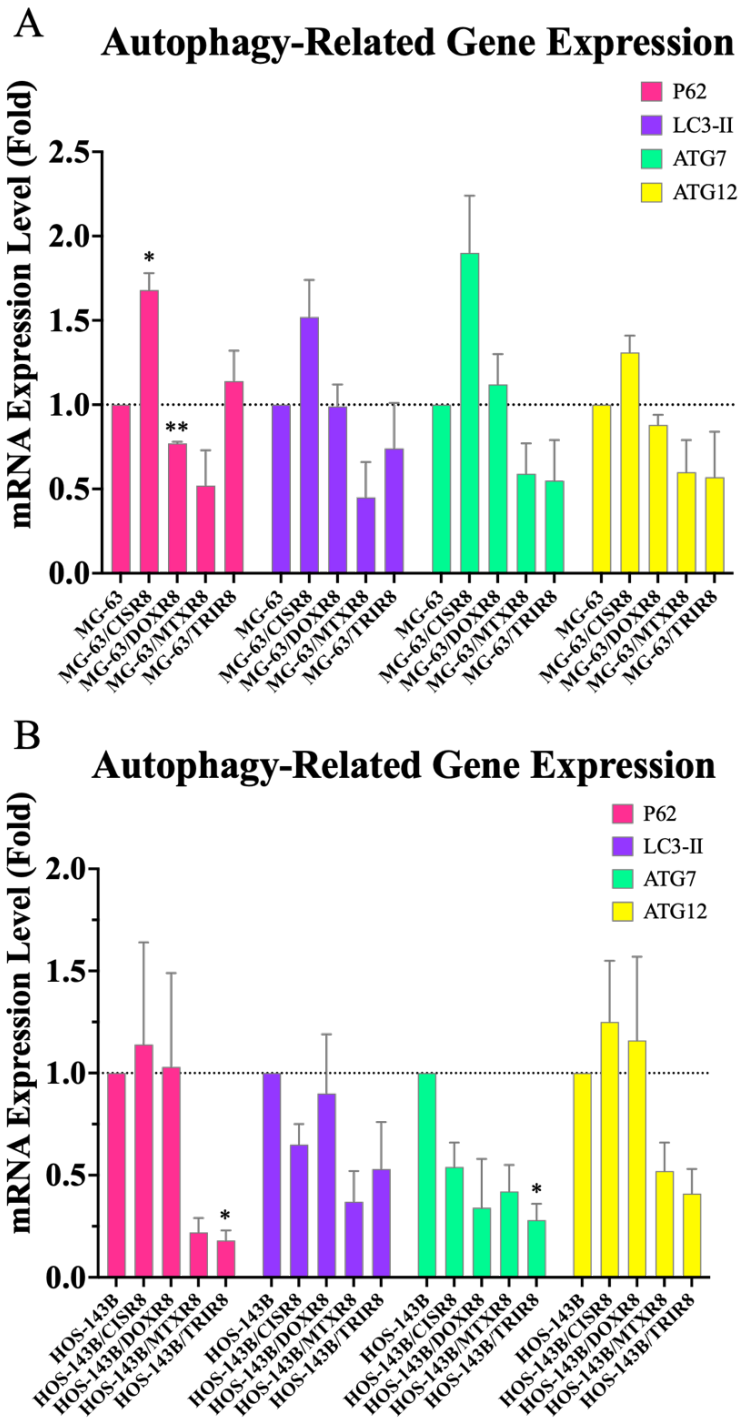

Figure 4.12: The expression level of autophagy related genes. The expression level of p62, LC3-II, ATG7, and ATG12 were determined by RT-PCR and fold change was measured corresponding to their respective parental control as shown in (A) MG-63 resistant sublines and (B) HOS-143B sublines. (n=3) Error bars = SEM. * = $p < 0.05$, ** = $p < 0.01$, Two sample *t*-test.

4.3.9 Apoptosis assay

FITC annexin V / PI was carried out on parental and resistant sublines of MG-63 and HOS-143B to investigate the apoptosis activity after 24 hours of exposure to chemotherapeutic drugs. Doses of the drugs used in this apoptosis assay were selected from the IC_{50} value of the single agent derived resistant subline. For example, the IC_{50} value of cisplatin on HOS-143B/CISR8 was 380 ng/mL, this drug dose of cisplatin was then used for the treatment for HOS-143B, HOS-143B/CISR8, and HOS-143B/TRIR8. The doses of doxorubicin and methotrexate used for HOS-143B, and its resistant sublines were 10.87 ng/mL and 12.56 ng/mL accordingly. For MG-63 and its resistant sublines, the doses of cisplatin, doxorubicin, and methotrexate was 190 ng/mL, 5.44 ng/mL, and 11.16 ng/mL, respectively. Figures 4.13 and 4.14 show the FITC annexin V / PI apoptosis assay result by FACS analysis for parental and resistant sublines of MG-63 and HOS-143B accordingly. Figure 4.15 demonstrates the percentage of apoptotic cells includes early and late apoptosis of parental and resistant sublines of MG-63 and HOS-143B after 24 hours exposure to chemotherapeutic drugs.

FACS analysis diagrams of MG-63, MG-63/CISR8, and MG-63/TRIR8 treated with cisplatin (190 ng/mL) are shown in Figure 4.13A. Each of the diagrams are separated into four quadrants. The upper left quadrant represents the necrotic cells, upper right quadrant represents the late apoptotic cells, lower right quadrant represents the early apoptotic cells, and the lower left represents the live cells. The percentage of early and late apoptotic cells of MG-63, MG-63/CISR8, and MG-63/TRIR8 were show in Figure 4.15A. There was only a minor change in the percentage of early and late apoptotic cells determined in between MG-63, MG-63/CISR8, and MG-63/TRIR8. MG-63 treated with cisplatin shown the highest percentage of early (EA) and late apoptotic (LA) cells (EA=1.84 ±

0.45%, LA=14.42 ± 0.67%), followed by MG-63/TRIR8 (EA=1.38 ± 0.26%, LA=13.29 ± 1.63%), and MG-63/CISR8 (EA=0.94 ± 0.08%, LA=10.92 ± 0.46%).

HOS-143B, HOS-143B/CISR8, and HOS-143B/TRIR8 were treated with 380 ng/ml of cisplatin for 24 hours before analysing by FACS. The FACS analysis results are shown in Figure 4.14A. A significant difference was determined between the percentage of early and late apoptotic cells between HOS-143B with HOS-143B/CISR8 and HOS-143B/TRIR8 as shown in Figure 4.14A. The percentage of apoptotic cells of HOS-143B was EA=4.04 ± 0.52% and LA=16.23 ± 1.01%. A significant decrease of apoptotic cells was determined in HOS-143B/CISR8 with EA=1.39 ± 0.03% (p=0. 037) and LA=7.68 ± 0.22% (p=0.014) comparing to HOS-143B. However, HOS-143B/TRIR8 had a significant increase in percentage of apoptotic cells with EA=11.08 ± 1.57% (p=0.049) and LA=27.01 ± 1.42% (p=0.014) comparing to HOS-143B.

The FACS analysis result of MG-63, MG-63/DOXR8, and MG-63/TRIR8 treated with 5.44 ng/mL of doxorubicin was shown in Figure 4.13B. For MG-63 resistant sublines treated with doxorubicin, no significant changes were determined compared to parental MG-63 as shown in Figure 4.15B. The highest percentage of apoptotic cells was determined on MG-63/TRIR8 (EA=1.08 ± 0.23%, LA=12.05 ± 1.92%), followed by MG-63/DOXR8 (EA=0.94 ± 0.07%, LA=10.11 ± 1.10%), and MG-63 (EA=1.03 ± 0.21%, LA=9.64 ± 1.58).

HOS-143B, HOS-143B/DOXR8, HOS-143B/TRIR8 treated with 10.87 ng/ml of doxorubicin and the FACS analysis results were shown in Figure 4.14B. Significant difference of the percentage of apoptotic cells was determined between HOS-143B with HOS-143B/DOXR8 and HOS-143B/TRIR8 as shown in Figure 4.15B. HOS-143B

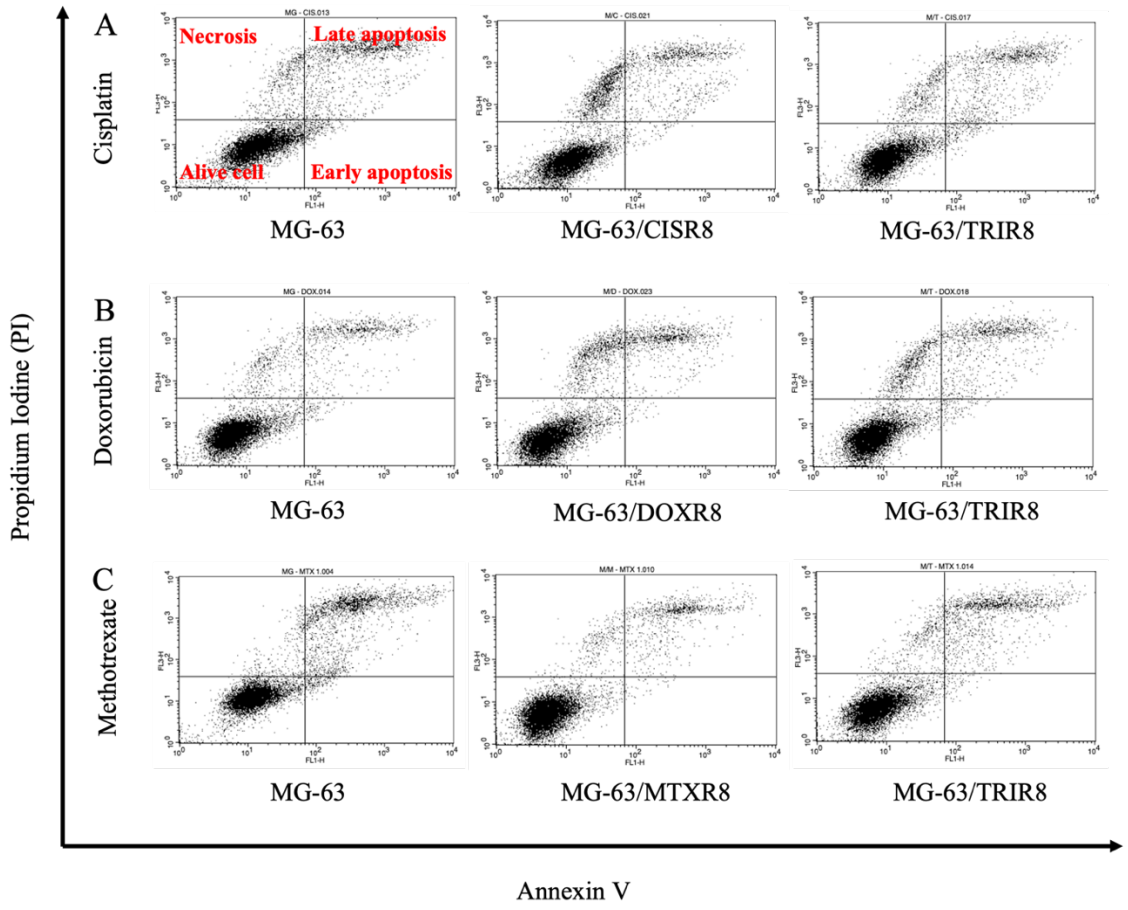

Figure 4.13: FITC Annexin V / PI apoptosis assay by FACS (MG-63 resistant sublines). (A) MG-63, MG-63/CISR8, and MG-63/TRI8 treated with cisplatin (190 ng/mL) for 24 hours. (B) MG-63, MG-63/DOXR8, and MG-63/TRIR8 treated with doxorubicin (5.44 ng/mL) for 24 hours, and (C) MG-63, MG-63/MTXR8, and MG-63/TRIR8 treated with methotrexate (11.16 ng/mL) for 24 hours. Figure is shown for 1 representative replicate of n=3 biological replicates. The diagrams' y-axis represents Log of PI and x-axis represents Log of Annexin V-FITC.

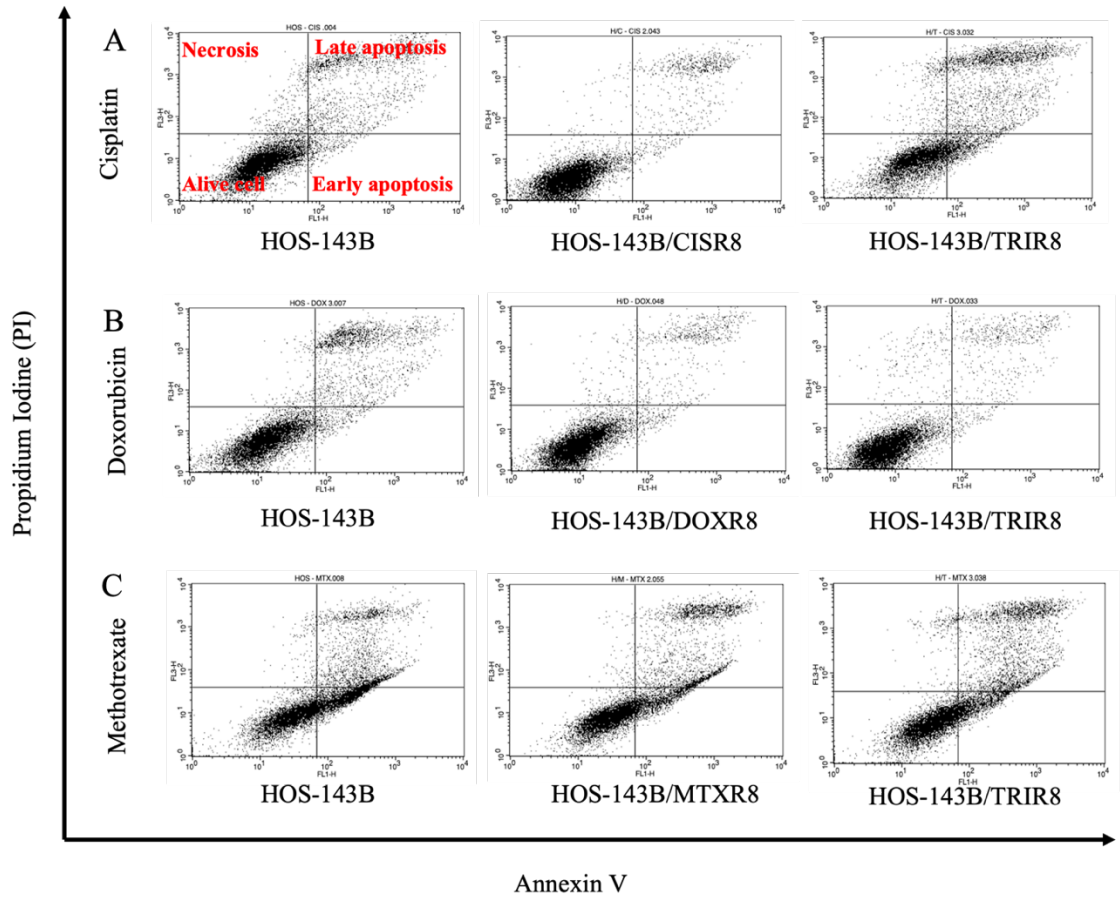

Figure 4.14: FITC Annexin V / PI apoptosis assay by FACS (HOS-143B resistant sublines). (A) HOS-143B, HOS-143B /CISR8, and HOS-143B /TRI8 treated with cisplatin (380 ng/mL) for 24 hours. (B) HOS-143B, HOS-143B, and HOS-143B treated with doxorubicin (10.87 ng/mL) for 24 hours, and (C) HOS-143B, HOS-143B /MTXR8, and HOS-143B /TRIR8 treated with methotrexate (12.56 ng/mL) for 24 hours. Figure is shown for 1 representative replicate of n=3 biological replicates. The diagrams' y-axis represents Log of PI and x-axis represents Log of Annexin V-FITC.

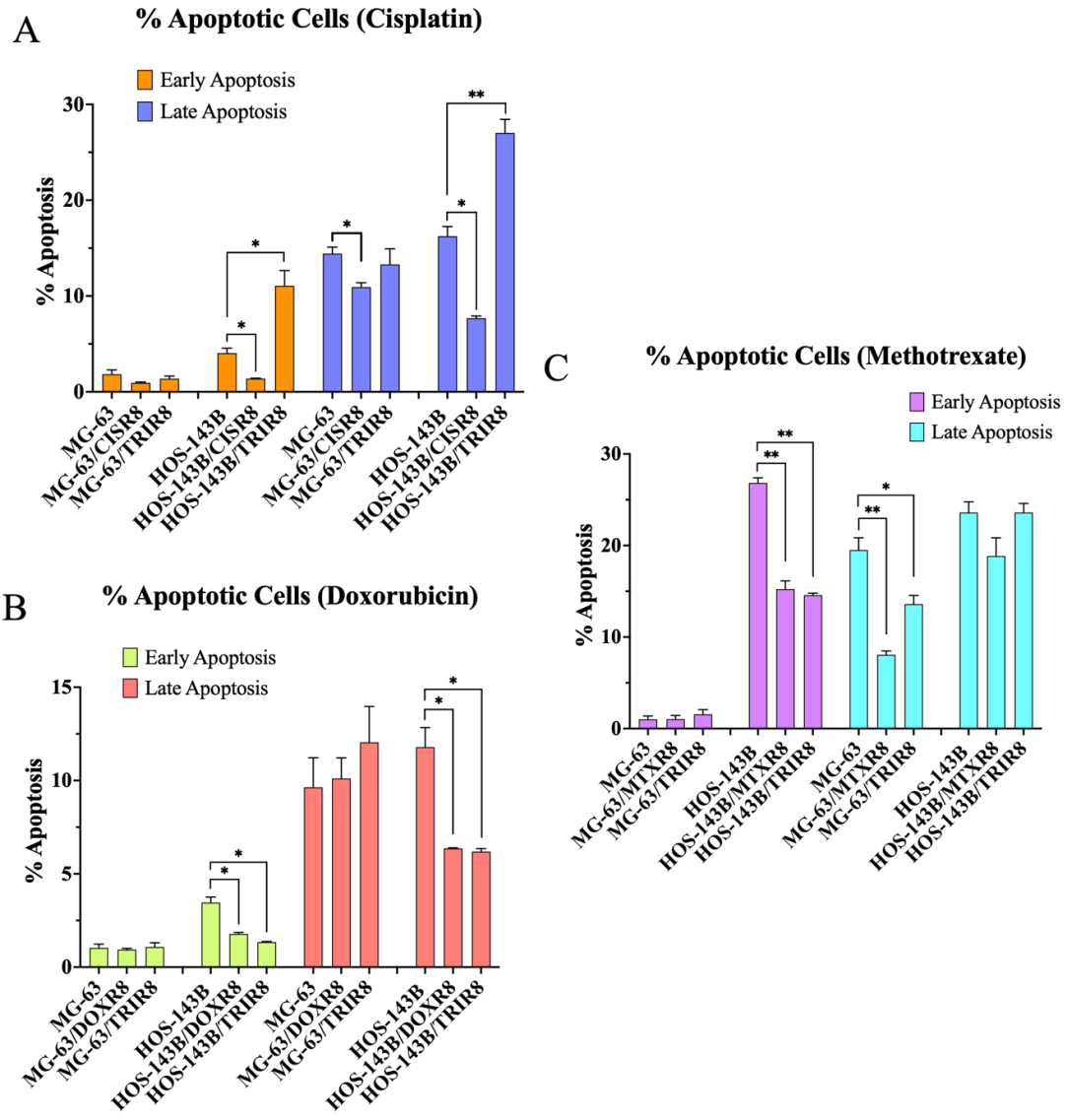

Figure 4.15: Percentage of apoptotic cells including early and late apoptosis. (A) Percentage of apoptotic cells treated with cisplatin in MG-63, MG-63/CISR8, MG-63/TRIR8 (190 ng/mL) and HOS-143B, HOS-143B/CISR8, HOS-143B/TRIR8 (380 ng/ml). (B) Percentage of apoptotic cells treated with doxorubicin in MG-63, MG-63/DOXR8, MG-63/TRIR8 (5.44 ng/mL) and HOS-143B, HOS-143B/DOXR8, HOS-143B/TRIR8 (10.87 ng/ml). (C) Percentage of apoptotic cells treated with methotrexate in MG-63, MG-63/MTXR8, MG-63/TRIR8 (11.16 ng/mL) and HOS-143B, HOS-143B/MTXR8, HOS-143B/TRIR8 (12.56 ng/ml). (n=3) Error bars = SEM. * = $p < 0.05$, ** = $p < 0.01$, Two sample t-test.

showed the highest percentage of apoptotic cells with EA=3.46 ± 0.30% and LA=11.79 ± 1.05%. Significant decrease of percentage of apoptotic cells was found in HOS-143B/DOXR8 with EA=1.78 ± 0.08% (p=0.032) and LA=6.36 ± 0.04% (p=0.036), and HOS-143B/TRI with EA=1.34 ± 0.04% (p=0.02) and LA=6.19 ± 0.16 (p=0.034), comparing to HOS-143B.

Figure 4.13C demonstrates the FACS analysis result of MG-63, MG-63/MTXR8, and MG-63/TRIR8 treated with methotrexate (11.16 ng/mL). No significant difference found on the early apoptosis between MG-63 with MG-63/MTXR8 and MG-63/TRIR8 but percentage of late apoptotic cells was significantly decreased in MG-63/MTXR8 and MG/TRIR8 compared to MG-63 as shown in Figure 4.15C. The highest percentage of apoptotic cells was indicated in MG-63 with EA=1.01 ± 0.36% and LA=19.51 ± 1.34%. MG-63/MTXR8 was significantly decreased in the percentage of late apoptotic cells with 8.07 ± 0.41% (p=0.015) (EA=1.04 ± 0.39) compared to MG-63. MG-63/TRIR8 also determined with a significant decreased in the percentage of late apoptotic cells compared to MG-63 with 13.60 ± 0.95% (p=0.037) (EA=1.56 ± 0.52%).

HOS-143B, HOS-143B/MTXR8, and HOS-143B/TRIR8 were treated with methotrexate (12.56 ng/ml) and the FACS analysis results are shown in Figure 4.14C. The highest percentage of apoptotic cells was determined on HOS-143B with EA=26.83 ± 0.57% and LA=23.61 ±1.17%. A significant decreased was found on the percentage of early apoptotic cells of HOS-143B/MTX and HOS-143B/TRIR8 with EA=15.24 ± 0.90% (p=0.002) and EA=14.58 ± 0.21% (p=0.002), respectively, compared to HOS-143B. However, no significant difference was determined on the percentage of late apoptotic cells comparing HOS-143B to HOS-143B/MTXR8 (LA=18.85 ± 2.00%) and HOS-143B/TRIR8 (LA=23.60 ± 1.00%) as shown in Figure 4.15C.

4.4 Discussion

4.4.1 Chemoresistance mechanisms in single and multi-agent induced osteosarcoma resistant models

Our established resistant cell lines using the pulsed strategy and triplet combination of drugs provides a novel strategy in osteosarcoma with drug resistant mechanism that would have the potential to mimic the clinical setting. Amongst MG-63 single agent resistant model, only MG-63/DOXR8 displayed cross resistant to cisplatin with 1.88-fold increased. However, contrary result was shown on Oda *et. al* study while their doxorubicin resistant variants were cross resistant to vincristine but not to cisplatin or methotrexate (Oda *et al.*, 2000). Moreover, Han *et. al* also found their cisplatin-resistant variant exhibiting cross resistance to methotrexate and doxorubicin (Han *et al.*, 2014). Both studies were conducted by employing incremental continuous strategy to develop their resistant models, which demonstrated different mechanisms could be produced based on the different selection strategies used.

The resistant sublines MG-63/TRIR8 and HOS-143B/TRIR8 were established using the combination of drugs cisplatin, doxorubicin, and methotrexate as a single treatment throughout the development progress. From the result shown in Chapter 3, these triplet combination resistant models acquired a significant level of resistance toward the combination of drugs compared to parental cell lines MG-63 and HOS-143B. When these triplet combination resistant sublines acquired the resistant, we hypothesised that the resistant sublines acquired the resistance either from cisplatin, doxorubicin, or methotrexate. However, when a drug screen was performed with individual drug separately, MG-63/TRIR8 and HOS-143B/TRIR8 did not show any significant fold resistant to either of the drugs as shown in Table 4.1. This interesting result indicated that a different resistant mechanism was developed within these triplet-combination resistant

cells, and this specific resistant mechanism might share a similar pathway among three of the drugs and therefore decrease the sensitivity toward the combination of the drugs. However, when a single individual drug was given to these resistant cells, the original resistant pathway of the single drug was not fully established yet due to lower concentration administrated during the development process, and thus the sensitivity of these resistant cells toward single drug remained.

P-glycoprotein (P-gp), the product of ATP Binding Cassette Subfamily B Member 1 (ABCB1), is responsible for one of the well-established causes of drug resistant in tumour cells (Chan *et al.*, 1997; Jiang, Yan and Wu, 2019). Figure 4.8B shows that the P-gp gene-expression level was decreased in HOS-143B resistant models compared to their parental control, however, the P-gp protein expression level was increased (Figure 4.8D). This suggested that the parental control HOS-143B itself was exhibiting a high expression level of ABCB1 gene and the P-gp protein would only be expressed when experiencing certain stress from the drugs. This was confirmed by comparing the ΔΔCq value of HOS-143B to MG-63 and HOS-143B was found to be 87.89 ± 15.86-fold ($p=0.002$) higher in the ABCB1 gene expression compared to MG-63. Besides, even though the resistant sublines of HOS-143B showed a decreased expression of ABCB1 compared to HOS-143B, however their expression level was still higher than MG-63 resistant sublines by comparing to their ΔΔCq. In our investigation, P-gp was overexpressed in all the resistant models developed from MG-63 and HOS-143B except from the resistant models established by methotrexate solely (MG-63/MTXR8 & HOS-143B/MTXR8). This suggested that the P-gp could be one of the contributing factors to the resistance of cisplatin and doxorubicin. Overexpression of P-gp was well studied in cancer cells, and it had demonstrated to be contributed to the doxorubicin-resistance mechanism in various type of cancers as doxorubicin is one of the substrates of P-gp. However for cisplatin,

Stordal *et al.* had found that the overexpression of P-gp in cisplatin-treated cancer cells was only a representation of a generalised stress response because cisplatin is not a substrates of P-gp (Stordal *et al.*, 2012).

A meta-analysis study from Liu *et al*., involved 11 osteosarcoma studies conducted between 1995 and 2016 with a total of 723 participants from different territories showed that the higher expression of P-gp may predict poorer survival. Sensitivity of the KHOSR2 osteosarcoma cell line to doxorubicin was also restored with the knockout of ABCB1 by CRIPSR-Cas9 (Fanelli *et al.*, 2016). Our study also demonstrated a similar result as the sensitivity of MG-63/CISR8, MG-63/DOXR8, HOS-143B/CISR8 and HOS-143B/TRIR8 to doxorubicin was restored when the P-gp was inhibited by elacridar (Fig. 4.9). The inhibition of P-gp had not increased the sensitivity of MG-63 resistant sublines to cisplatin but increases resistance instead. This again has suggested cisplatin was not a substrate of P-gp and therefore sensitivity of cisplatin was not restored. However, the sensitivity of HOS-143B/CISR8 to cisplatin was restored by the inhibition of P-gp as shown in Figure 4.9B. Another study from Ali *et al*., also obtained a similar result as their lung cancer resistant variants H23/CPR and H2126/CPR had significantly increased sensitivity to cisplatin when exposed to elacridar (Ali *et al.*, 2019). Though, the effect of P-gp inhibitor on cisplatin resistance models was not immediate relevant stress response. Inhibiting the P-gp transporter had a sensitisation effect on the cisplatin-resistance models, however it was not directly associated to the P-gp as cisplatin is not a P-gp substrate (Stordal *et al.*, 2012).

The apoptosis assay results shown in Figure 4.15 demonstrate that the percentage of early and late apoptosis of single-agent induce resistant models of MG-63 and HOS-143B were significant lower compared to parental controls except for MG-63/DOXR8. This was

expected as MG-63/DOXR8 had not acquired any significant resistant fold compared to parental cell line. This result also indicated that the established resistant sublines derived by the single-agent induced method had a lesser percentage of cell undergone apoptosis caused by the respective chemotherapeutic drug and thus, again verifying that they were more resistant to the drugs compared to parental cell lines.

However, for multi-agent induced sublines, a different trend of percentage of apoptosis was seen for different chemotherapeutic drugs. Multi-agent induced resistant sublines MG-63/TRIR8 demonstrated a higher percentage of early and late apoptosis of cells compared to single-agent induce models (MG-63/CISR8) after 24 hours of cisplatin exposure, but lower than parental control MG-63. Similar results were also seen for on methotrexate as shown in Figure 4.14C. However, the percentage of apoptosis cells on doxorubicin was the highest on MG-63/TRIR8 compared to MG-63 and MG-63/DOXR8. This suggests that the multi-agent induced resistant subline MG-63/TRIR8 was more sensitive to cisplatin and methotrexate compared to MG-63/CISR8 and MG-63/MTXR8 but was more resistant compared to parental control MG-63. However, it was more sensitive to doxorubicin compared to both MG-63/DOXR8 and parental control MG-63. This indicated that the resistance acquired in MG-63/TRIR8 might be contributed mainly from the resistant mechanism of cisplatin and methotrexate instead of doxorubicin even though MG-63/TRIR8 had not exhibited a significant fold resistant on both drugs from the drug screen result on Table 4.1.

For HOS-143B/TRIR8, the percentage of early and late apoptosis of cells were significantly higher than HOS-143B/CISR8 and parental HOS-143B. However, the percentage of early and late apoptosis cells were significantly lower than HOS-143B after exposure of doxorubicin for 24 hours, which also showed a similar percentage to HOS-

143B/DOXR8. Besides, a comparable result was also shown on drug methotrexate, where the early apoptosis cell percentage was significantly lower than HOS-143B but similar to HOS-143B/MTXR8. This has suggested the acquired resistance in HOS-143B/TRIR8 on the combination of drugs was largely contributed from the resistant pathway of doxorubicin and methotrexate instead of cisplatin. This finding could also be validated by the protein expression level of HOS-143B (Fig. 4.8D) and the effect of P-gp inhibitor on HOS-143B/TRIR8 (Figure 4.9D). The increased expression of P-gp and the reduced IC_{50} value of doxorubicin with the combination of elacridar validated that HOS-143B/TRIR8 acquired resistance was partly contributed by the doxorubicin resistance mechanism.

4.4.2 Autophagy mechanisms in clinically-relevant osteosarcoma cell lines

Autophagy is an intracellular degradation mechanism that eliminates and recycles damaged proteins and organelles to sustain cell survival (Mizushima, 2007). It involves a series of complex processes including forming of phagophore, generation of autophagosome, and the association with lysosome to generate autolysosomes which degraded and recycles the content (Levine and Kroemer, 2008). These complex processes are found to be regulated by more than 30 autophagy-related proteins (ATG) (Camuzard *et al.*, 2019).

To study the autophagy mechanisms in osteosarcoma sublines, ATG7, ATG12, LC3-II, p62 was examined by RT-PCR. ATG7 and ATG12 are responsible in the biogenesis of autophagosome. In brief, when autophagy is activated in the cells, the formation of autophagosome is initiated by Class III PI3K Complex I to exhibit the elongation and closure of phagophore. The elongation and closure of phagophore required two complexes conjugation machineries (Ohsumi and Mizushima, 2004), which are ATG12

and LC3 conjugation system. ATG7 and ATG12 are involved in the ATG12 conjugation system where the formation of ATG12-ATG5/ATG16 was mediated by the action of ATG7 and ATG10. LC3-II and ATG7 are involved in the LC3 conjugation system where nascent LC3 is processed by protease ATG4 which activated by ATG7 and formed LC3-II. LC3-II is used as an autophagosome marker as it is present in the autophagosomes as an integral membrane protein (Shpilka, Mizushima and Elazar, 2012). After the formation, the autophagosome will sequester the cellular materials which are targeted for degradation through the action of selective autophagy receptors such as SQSTM1/p62.

Figure 4.12 demonstrated the expression of p62, LC3-II, ATG7, and ATG12 for parental and resistant sublines of MG-63 and HOS-143B. From the result only MG-63/CISR8 was determined a significant upregulation of p62 compared to MG-63. However, the expression of LC3-II, ATG7, and ATG12 also increased but not significant. In theory, the combination of increased LC3-II and ATG7 expression with the decreased p62 and ATG12 expression are the indication of increase autophagy activity as explained above. The exhibition of MG-63/CSIR8 with increased expression of four of these autophagy-related gene might be caused by the resistant development process. The cells had been exposed to multiple rounds of cisplatin treatment which might initiate the autophagy pathway for cell survival and therefore increased the expression level of autophagy-related gene. However, autophagy mechanism would only be initiated when the cells were under certain stress or responding to cytotoxic insult. In our study, the resistant cells were extracted without prior exposure to drugs, and this might not cause any initiation of the autophagy pathway. Therefore, the overall expression of the autophagy-related genes was increased but no autophagy was induced.

Autophagy and apoptosis are both cellular degradation pathways essential for organismal homeostasis (Su *et al.,* 2013). The crosstalk between autophagy and apoptosis includes the Beclin 1-BCL-2 interaction (Liang *et al.,* 1998); caspase-mediated Beclin 1 cleavage (Wirawan *et al.,* 2010); UVRAG-BAX interaction (Yin *et al.,* 2011); ATG12-ATC3 conjugation (Radoshevich *et al.,* 2010); ATG12-Mcl-1 interaction (Rubinstein *et al.,* 2011); ATG5-FADD interaction (Pyo *et al.,* 2005); Calcium-dependent, nonlysosomal, cysteine protease-mediated ATG5 cleavage (Yousefi *et al.,* 2006); tumour protein 53-mediated cross-regulation (Feng *et al.,* 2006). As inhibition of both autophagy and apoptosis has been shown to cause cancer, it is likely that proteins involved in the crosstalk between these pathways may have particularly important roles in this disease.

4.4.3 Relationship between migration and invasion rate and EMT progression in resistant osteosarcoma

Migration and invasion rate of MG-63 and HOS-143B derived resistant sublines were investigated in this study. Results shows that the migration and invasion rate was dramatically increased in MG-63/CISR8, MG-63/MTXR8, and MG-63/TRIR8 except for MG-63/DOXR8 (Fig. 4.5 & 4.7). This was first indicated that the increased migration rate might correlated to the progression of drug resistant in MG-63 as MG-63/DOXR8 was the only subline with no significant increase fold resistant detected and no significant increase of migration rate. However, despite significant increase of fold resistant displayed in HOS-143B resistant sublines, the migration and invasion were significantly decreased. Therefore, the expression of EMT biomarkers were examined on both MG-63 and HOS-143B resistant sublines to study the relation between migration and invasion rate and the EMT progression in osteosarcoma cells.

The expression of ZEB1, VIM, E-CAD, and N-CAD was examined by RT-PCR as shown in Figure 4.10. Based on the result, we determined that MG-63/CISR8, MG-63/DOXR8 and MG-63/MTXR8 undergone EMT progression as the expression of E-CAD (epithelial biomarker) was downregulated and N-CAD (mesenchymal biomarker) was upregulated. This had been confirmed with the upregulation of protein expression of N-CAD by Western blot as shown in Figure 4.10D. Decreasing level of E-CAD in carcinoma cells could lead to activation of several EMT transcription factors and resulting in increasing invasion and metastasis (Onder *et al.*, 2008), therefore, promoting the migration and invasion rate of MG-63 resistant models. ZEB1 is one of the transcription factor that could induce EMT progression in cancer cells which result in promoting tumour invasion and metastasis (Zhang, Sun and Ma, 2015). The expression of ZEB1 was also shown in an increasing trend among the MG-63 resistant sublines. This could explain the increased migration and invasion rate determined in MG-63 resistant sublines as they undergone EMT progression.

HOS-143B resistant sublines exhibited upregulated expression level of E-CAD (epithelial biomarker) and downregulated expression of N-CAD (mesenchymal biomarker) compared to parental HOS-143B. This is again confirmed by the protein expression level of N-CAD shown in Figure 4.10D. HOS-143B resistant sublines showed a contrasting and opposite result in the trend of the regulation of EMT genes compared to MG-63 resistant sublines. This had suggested that they undergone mesenchymal to epithelial transition (MET) instead of EMT. This was confirmed by the increasing trend observed in the expression of E-CAD and decreasing in the expression of N-CAD (Figure 4.10C). E-CAD and N-CAD are also knowing as the "cadherin switch" to expressing in the opposite trend to each other to regulate the progression of EMT or MET (Loh *et al.*, 2019). Thus, the decreasing migration and invasion could be clarified by the MET progression

in HOS-143B resistant sublines. However, the reason behind the induction on MET in HOS-143B resistant sublines remained unknown.

4.5 Conclusion

The overexpression of P-gp was the dominant mechanism in doxorubicin induced resistant subline including HOS-143B/TRIR8. The elevated expression of P-gp on cisplatin-induced resistant sublines might be due to generic stress as elacridar could not increase the sensitivity of cisplatin. Autophagy mechanisms was also found to be not participating in most of the resistant models derived from MG-63 and HOS-143B.

The multi-agent resistant models MG-63/TRIR8 and HOS-143B/TRIR8 did not show any significant fold resistance to any of the drugs individually. However, the resistance of MG-63/TRIR8 were determined to be compensated more from cisplatin and methotrexate resistant mechanisms, while HOS-143B/TRIR8 were complimented largely from doxorubicin and methotrexate.

Resistance of osteosarcoma cells appears to induce an EMT switch in the osteosarcoma cells with a lower metastatic potential (MG-63) but reverse (MET) in the higher metastatic potential osteosarcoma cells (HOS-143B). This also shows that drug resistance in osteosarcoma cells is not always associated to increased migration and invasion rate of the cells.

Chapter 5: PCR Array gene expression profiling

5.1 Introduction

This chapter cover the analysis of deregulated genes which are related to chemoresistance in osteosarcoma. A panel of genes were carefully selected from the literature associated with cisplatin, doxorubicin, and methotrexate resistance. The gene-expression levels were examined using PCR array in the cisplatin, doxorubicin, methotrexate, and triplet-combination resistant models developed in Chapter 3.

5.1.1 PCR array technology

PCR array is a technique that has been used in high-throughput gene profiling, which provide an attractive alternative to next-generation sequencing (NGS) or microarray. PCR arrays are available for mRNA and microRNAs profiling in either 96-well or 386-well plate formats. These arrays provide a more cost-effective method for screening large numbers of gene in a species by the ease of use of RT-PCR (Fassbinder-Orth, 2014). The benefit of using PCR arrays for profiling is that each array plate can either screen the entire specific panel or sub-panel of mRNA depending on the researcher's needs, which produce a certain flexibility in designing the panel (Qiagen, 2021).

QuantiNova LNA PCR Flexible Panels were used in this study to design a unique chemoresistant panel which contains genes related to cisplatin, doxorubicin, and methotrexate resistant in osteosarcoma. Total of 16 genes including 3 controls and 1 housekeeping gene were analysed for each parental and resistant osteosarcoma model. These PCR arrays are quick and provide reliable result for gene expression profiling by using SYBR Green-based qPCR. The locked nucleic acid technology used in this PCR array assay enable a shorter primer with optimal T_m and also increase the sensitivity and analysis of short RNA targets compared with traditional DNA or RNA oligonucleotides (Tolstrup *et al.*, 2003).

Locked nucleic acids are a novel nucleic acid analog that can be incorporated into any RNA or DNA oligonucleotide and induce a conformational change in the local helix (Kaur *et al.*, 2006). This modified state provides the locked nucleic acid bases with greater mismatch discrimination, stronger binding strength for complementary sequences, and enhanced duplex formation (Jensen *et al.*, 2001; Levin *et al.*, 2006; You *et al.*, 2006). Therefore, these features from incorporating locked nucleic acid increase the amplification success and also increase duplex melting temperature, which could shorten the probes and primers and give greater specificity (Braasch and Corey, 2001).

5.1.2 Genes associated with cisplatin resistance

Four genes were selected to be examined by PCR array associated with cisplatin resistance in osteosarcoma, which are glutathione S-Transferase Pi 1 (GSTP1), Transglutaminase 2 (TGM2), Microtubule affinity regulating kinase 2 (MARK2), and ATM serine/threonine kinase (ATM).

5.1.2.1 Glutathione S-Transferase Pi 1

The overexpression of GSTP1 in tumour cells had been linked to chemoresistance in several different type of cancers due to its roles in cancer cell survival and pathogenesis via drug detoxification (Tew, 1994; Townsend and Tew, 2003). Several studies have been conducted on GSTP1 in osteosarcoma cell lines and osteosarcoma patients. GSTP1 gene expression was studied by Pasello *et al.* in their established cisplatin-resistant models from osteosarcoma cell lines U-2OS, Saos-2, MG-63, and HOS. They found that the GSTP1 gene expression level was increased in drug-resistant models U-2OS/CDDP 4μg, U-2OS/DX580, Saos-2/DX580, U-2OS/MTX300, and Saos-2/MTX 1μg (Pasello *et al.*, 2008). They also found that the GSTP1-specific enzymatic activity was increased in all cisplatin-resistant variants compared to their parental cell line. Nevertheless, they found

that the higher GSTP-1 enzymatic activity was correlated with the increased GSTP1 gene and protein expression level in U-2OS/CDDP-resistant variant but not in the Saos-2/CDDP-resistant variant (Pasello *et al.*, 2008). Another study by Huang *et al*. also showed that the overexpression of GSTP1 gene and protein was associated with the cisplatin and doxorubicin resistance in osteosarcoma cell lines via the initiation of phospho-ERK1/2 pathway (Huang, Mills and Worth, 2007).

5.1.2.2 Transglutaminase 2

Transglutaminase 2 (TGM2) is a multifunctional protein from the transglutaminase family, which is involved in extracellular degradation and apoptosis (Lauzier *et al.*, 2012; Hsieh *et al.*, 2013). TGM2 is suggested to be associated with poor patient survival and drug response as overexpression of TGM2 was observed in multiple cancer cells type such as ovarian cancer and non-small cell lung cancer (Singer *et al.*, 2006; Park *et al.*, 2010). TGM2 has been found to be inhibit apoptosis in osteosarcoma cells via regulating the BCL2-associated X protein and releasing the cytochrome C under hypoxic conditions (Wang *et al.*, 2015). TGM2 has also been suggested to be a potential therapeutic target in taxane-resistant ovarian cancer from *in vitro* and *in vivo* experiments (Hwang *et al.*, 2008).

One of the most important mechanisms of chemoresistance in cancer is the deregulation of apoptosis-related protein expression such as the caspase family and the Bcl-2 family of proteins (Letai, 2008). A study from Li *et al*. demonstrated the role of TGM2 was associated with cisplatin resistance in osteosarcoma by increasing chemosensitivity of osteosarcoma cells after the TGM2 expression was knocked down. They also found TGM2 was involved in the activation of MAPK and Akt pathways, which affects the chemosensitivity of osteosarcoma (Li *et al.*, 2018). Moreover, TGM2 was indicated in

promoting metastatic phenotypes in osteosarcoma which enhanced the invasive potential of the cells (Fuja *et al.*, 2018).

5.1.2.3 Microtubule affinity regulated kinase 2

Microtubule affinity regulated kinase 2 (MARK2) is a serine/threonine protein kinase from the MARK family. MARK2 is also reported to play a crucial role in neurodegeneration, neurodifferentiation, cell migration, and intracellular transport (Matenia and Mandelkow, 2009). The association of MARK2 with drug resistance and malignant biological behaviour was also demonstrated in recent studies as overexpression of MARK2 was observed in a cisplatin-resistant lung cancer cell line (Xu, Mei and Tan, 2017). Cervical cancer cells have also been sensitised to cisplatin was observed after knocked down of MARK2 expression (Wu, Lu and Chao, 2010).

MARK2 was also found to play a role in cell cycle activation and DNA damage repair in non-small cell lung cancer (Hubaux *et al.*, 2015). Another recent study from Xu *et al.* also found that cisplatin resistance in lung cancer was associated with the downregulation of MARK2 expression and p-Akt (Xu, Mei and Tan, 2017). MARK2 expression was also studied in osteosarcoma stem cells by Xu *et al.* and they found the expression of DNA-PKcs was inhibited by the downregulation of MARK2 via the inhibition of PI3K/Akt/mTOR pathway in osteosarcoma stem cells (CD133+ MG-63 and MNNG/HOS). Thus, inhibition of MARK2 suppresses cisplatin resistance and plays an important role in chemoresistance of osteosarcoma stem cells (Xu *et al.*, 2020). Furthermore, another study also suggested the regulation of MARK2 was associated with the expression of P-gp and cell apoptosis via activating the PI3K/AKT/NF- κB pathway and therefore promoting cisplatin resistance in osteosarcoma cells (Wei *et al.*, 2020).

5.1.2.4 Ataxia telangiectasia mutated

Ataxia telangiectasia mutated (ATM) is a member of the phosphatidylinositol 3-kinase-related kinase family of Ser/Thr protein kinase. ATM was found to be involved in the cisplatin resistance in osteosarcoma cells, whereas the cisplatin-resistant osteosarcoma cells showed an increased sensitivity of cisplatin after the knocked down of ATM in MG-63/CDDP cells (Wang *et al.*, 2019). The overexpression of ATM was also found in cisplatin resistant non-small cell lung carcinoma (NSCLC) (Weber and Ryan, 2015). ATM mediates the prevention of anti-apoptosis, cell cycle arrest, and enable DNA repair via the activation of p53 and checkpoint 2 protein (Shiloh and Ziv, 2013). 5-azacytidine-resistant myeloid leukaemia cell lines were also found to have constitutive activation of the ATM pathway and increased sensitivity of radioresistant breast cancer was also demonstrated by inhibiting ATM activation in radioresistant breast cancer (Imanishi *et al.*, 2014; Zhang *et al.*, 2015). Several studies also investigated the role of ATM in NSCLC and demonstrated a correlation between ATM and cisplatin resistance. One study from Zhang *et al.* found that the *in vitro* and *in vivo* supported the evidence that the inhibition and knocking down of ATM and Mcl-1 increased the cisplatin sensitivity in NSCLC (Zhang *et al.*, 2017). Another study from Shen *et al.* also found high expression of ATM in cisplatin-resistant NSCLC and the overexpression of ATM was involved in the contribution of mediating EMT via $JAK_{1,2}/STAT_3$-PD-L1 pathway (Shen *et al.*, 2019).

5.1.3 Genes associated with doxorubicin resistance

Four genes were selected in this study to be examined by PCR arrays related to doxorubicin resistance in osteosarcoma, which are CCN family 2 (CCN2), Bcl-2-like protein 1 (BCL2L1), Hypoxia-inducible factor 1-alph (HIF1A), and Sphingosine kinase 1 (SPHK1).

5.1.3.1 CCN family member 2

CCN family member 2 (CCN2) is a multifunctional signalling modulator in various biological processes, also known as connective tissue growth factor (CTGF) (Luft, 2008). The CCN family consists of 6 members, including CCN1 (cysteine-rich protein 61, Cyr61), CCN2 (connective tissue growth factor, CTGF), CCN3 (nephroblastoma overexpressed gene, Nov), CCN4 (Wnt-1-induced secreted protein 1, WISP-1), CCN5 (WISP-2), and CCN6 (WISP-3) (Brigstock *et al.*, 2003). The various biological properties of CCN proteins include regulation of tumorigenesis, formation of extracellular matrix (ECM), cellular adhesion, migration, and proliferation (Perbal, 2004).

The expression of CCN2 has been extensively studied in different cancer cell types and overexpression was determined in cancers including breast cancer, pancreatic cancer, lung cancer, chondrosarcoma, and melanoma (Kubo *et al.*, 1998; Wenger *et al.*, 1999; Xie *et al.*, 2001; Chen *et al.*, 2007; Hou *et al.*, 2009). Increasing tumour size and lymph node metastasis was also proven to be associated with the overexpression of CCN2 in malignant melanoma (Braig *et al.*, 2011). A study from Tsai *et al.* indicated that the enhanced expression of CCN2 in osteosarcoma cells increased the expression of ABCG2 and therefore promoted drug resistance by downregulating miRNA-519d (Tsai *et al.*, 2019). ABCG2 is one of the ABC transporter genes which have the potential to transport a range of anticancer agents including doxorubicin and resulting in drug resistance (Ejendal and Hrycyna, 2002; Mlejnek *et al.*, 2017). Another study from Tsai *et al.* also found a correlation between the overexpression of CCN2 with increased tumour cell survival in their *in vitro* and *in vivo* osteosarcoma study. An increased cisplatin sensitivity was observed after the suppression of CCN2 expression *in vitro* (Tsai *et al.*, 2014).

5.1.3.2 Bcl-2-like protein 1

The Bcl-2 family of proteins play an essential role in the regulation of the intrinsic apoptosis pathway. Apoptosis is a regulated cell death mechanism that is triggered in response to cellular stresses such as DNA damage. Intrinsic apoptosis is activated by a member of the Bcl-2 family, Bax. The activated Bax will promote the release of cytochrome c and mitochondrial fission, which results in caspoae-3 activation and promoting apoptosis (Youle and Strasser, 2008). A study from Zhang *et al.* found that the expression of BCL2L1 was supressed by the upregulation of let-7c, which results in the inhibition of apoptosis in colorectal cancer cells (Zhang *et al.*, 2018). Genomic alteration in BCL2L1 was also reported to contribute to doxorubicin sensitivity in gastric cancer (Park *et al.*, 2015).

5.1.3.3 Hypoxia-inducible factor 1-alpha

In recent studies, the theory of the condition of tumour microenvironment could play a crucial role in contributing significantly to drug resistance or chemotherapy failure is widely accepted (Morin, 2003; Westhoff and Fulda, 2009). The tumour responsiveness to chemotherapy can be influenced by the characteristic of tumour microenvironment such as the region of hypoxia and acidity and also the marked gradients in the rate of cell proliferation (Trédan *et al.*, 2007). Hypoxia-inducible factor 1-alpha (HIF1A) is one of the transcription factors from hypoxia-inducible factor family and they are the major regulator of cellular adaptation to hypoxia (Weidemann and Johnson, 2008).

The first molecular mechanism on HIF1 contributes to the drug resistance in cancer cells was reported to acticate the multidrug resistance 1 (MDR1) gene in response to hypoxia (Comerford *et al.*, 2002). The activation of MDR1 leads to the expression of P-gp on the membrane of the cancer cells which decreased the intracellular concentration of range of

chemotherapeutic drugs (Gottesman, Fojo and Bates, 2002). The contribution to drug resistance from this HIF1-mediated P-gp expression was observed in various tumour cells such as breast carcinoma, colon cancer cells, gastric cancer, and glioma (Mizobuchi *et al.*, 2008; Gupta and Wish, 2017; Comerford *et al.*, 2002; Zhu *et al.*, 2005; Li *et al.*, 2006; Liu *et al.*, 2008; Nardinocchi *et al.*, 2009). Furthermore, the expression level of HIF1A was also indicated to be significantly associated with the P-gp human colon cancer tissues in recent study (Ding *et al.*, 2010). A study from Zhu *et al.* also showed the gene expression of HIF1A was upregulated in doxorubicin-resistant osteosarcoma cell line MG-63/DXR (Zhu *et al.*, 2015).

5.1.3.4 Sphingosine kinase 1

The process of the production of sphingosine-1-phosphate (S1P) via the phosphorylation of sphingosine is catalysed by a type of lipid kinases, named sphingosine kinases 1 (SPHK1). This process is reported to be responsible for cell differentiation, proliferation, motility, angiogenesis and apoptosis (Heffernan-Stroud and Obeid, 2013). The expression of SPHK1 in tumour cells were reported by several studies to play a role in tumour progression (Schiefler *et al.*, 2014; Hatoum *et al.*, 2017; Chen *et al.*, 2018; Wang *et al.*, 2018). The overexpression of SPHK1 was reported to be correlated with poor patient prognosis in prostate cancer and NSCLC patients (Malavaud *et al.*, 2010; Gachechiladze *et al.*, 2019). Malignant progression was also reported to be contributed by SPHK1/S1P signalling through manipulating the proliferation rate and metastatic potential of cancer cells (Cuvillier *et al.*, 2010). The correlation between the overexpression of SPHK1 and doxorubicin resistance was also demonstrated in multiple cancer cell lines including leukemia cell lines and prostate cancer cell lines (Gault and Obeid, 2011). A study from Yao *et al.* had shown that inhibiting the expression of SPHK1

was successfully reversed the SPHK1-induced doxorubicin resistance in osteosarcoma in both *in vitro* and *in vivo* (Yao *et al.*, 2012).

5.1.4 Genes associated with methotrexate resistance

Three genes were selected in this study to be examined by PCR array related to methotrexate resistance in osteosarcoma, which are Retinoblastoma protein (RB1), Reduced folate carrier 1 (RFC1), and S-phase kinase associated protein 2 (SKP2).

5.1.4.1 Reduced folate carrier 1

Reduced folate carrier 1 (RFC1) is one of the members from reduced folate family, which is located at the cell membrane and is one of the major transporters for methotrexate into the cells (Patiño-García *et al.*, 2009). The expression of RFC1 was studied and investigated in (Serra, 2004; Wang and Li, 2014; Jabeen *et al.*, 2015). The mechanism of methotrexate involves the interaction with various enzyme of folate metabolic pathway that results in inhibiting DNA synthesis (Genestier *et al.*, 2000). Depletion in RFC1 protein expression will affect the uptake of methotrexate into the cells due to the less efficient intracellular transport and consequently a reduction of the drugs cytotoxicity (van der Heijden *et al.*, 2007). Serra *et al.* had found the expression of the RFC1 gene was remarkedly downregulated in methotrexate-resistant variants derived from Saos-2 and U-2OS (Serra *et al.*, 2004). Poor response to pre-operative chemotherapy was found to be associated with the reduced RFC1 expression in osteosarcoma patients receiving high-dose methotrexate treatment (Guo *et al.*, 1999). Another study by Jabeen *et al.* concluded that different genetic variants of RFC1 in osteosarcoma patients will lead to different clinical outcome, for example patients with RFC1 rs1051266 GG genotype had a better clinical outcome compared to patients with AA genotype (Jabeen *et al.*, 2015).

5.1.4.2 Retinoblastoma protein

Retinoblastoma protein (RB1) is a tumour-suppressor gene that is reported to be dysfunctional in several different cancer types including osteosarcoma (Murphree and Benedict, 1984). One of the major methotrexate resistant mechanisms is the overexpression of dihydrofolate reductase (DHFR) protein level (Guo *et al.*, 1999). Studies also found that the RB1 gene negatively regulates the expression of DHFR, therefore the drugs sensitivity targeting to DHFR may be subjective to the expression of RB1 (Johnson *et al.*, 1993; Almasan *et al.*, 1995; Qin *et al.*, 1995). Cell proliferation is regulated by the RB1 gene and the mutation or deletion of RB1 has been identified in osteosarcoma tumour cells was demonstrated with significant loss of growth regulation (Almasan *et al.*, 1995). The RB1 gene was reported to regulate the expression of DHFR gene via the interaction with E2F family of transcriptional factors (Wadayama *et al.*, 1994). RB1-positive osteosarcoma cells such as U-2OS cells with upregulated expression level of RB1 showed an increase of DHFR gene expression level which contributed to methotrexate resistance *in vitro* (Serra *et al.*, 2004). Conversely, RB1-negative osteosarcoma cells such as Saos-2 cells with decreased gene expression of RB1 showed a significant downregulation of reduced folate carrier (RFC) gene expression instead of significant involvement of DHFR to establish the methotrexate resistance *in vitro* (Serra, 2004). Therefore, the RB1 gene expression is indirectly influences the osteosarcoma cell lines in acquiring methotrexate-resistance mechanisms in the cells.

5.1.4.3 S-phase kinase associated protein 2

S-phase kinase associated protein 2 (SKP2), also known as p45, is an oncoprotein involved in cell proliferation, migration, invasion, apoptosis, angiogenesis, and metastasis of several tumour cells including breast cancer, prostate cancer, and lung cancer (Wang *et al.*, 2012; Cai *et al.*, 2020). Overexpression of SKP2 was reported in

various cancer cell types including breast cancer, gastric cancer, prostate cancer, and osteosarcoma (Wu, Gu and Cui, 2021). Several molecular mechanisms of SKp2 involved in cancer drug resistance was reported including promoting DNA damage response and repair, modulating substrate p27 and contribute to autophagy, and inducing EMT (Cai *et al.*, 2020). The overexpression of SKP2 in osteosarcoma cells was showed to promote cell growth and inhibit cell apoptosis, whereas inhibition of SKP2 showed an opposite result on osteosarcoma cells (Ding, Li, Han, *et al.*, 2017; Ding, Li, Sun, *et al.*, 2017). A recent study from Ding *et al.* also indicated that the overexpression of SKP2 was observed in their methotrexate-resistant osteosarcoma variants. Inhibition of SKP2 expression in their resistant variants demonstrated a decreased migration, cell proliferation and also enhanced the sensitivity of resistant cells to methotrexate. Therefore, their study concluded that the methotrexate resistance and EMT progression properties were largely associated with the overexpression of SKP2 in osteosarcoma cells (Ding *et al.*, 2018).

5.1.5 Aims and objectives

This chapter examines the gene expression profile of our cisplatin, doxorubicin, methotrexate, and triplet-combination resistant osteosarcoma sublines. Potential deregulated genes identified from the PCR arrays were validated using Western blots.

Objective 1: To determine the gene candidates from recent publication which are related to the resistant mechanisms of cisplatin, doxorubicin, and methotrexate.

Objective 2: To identify the regulation of these genes on resistant models compared to parental cell lines by PCR arrays.

5.1.5.1 Hypothesis

The identified deregulated genes in single agent resistant sublines and triplet combination resistant sublines from MG-63 and HOS-143B can be used to distinguish chemo-resistant and chemo-sensitive osteosarcoma cells. The identified deregulated genes could also be used in the development of novel targeted therapies for osteosarcoma patients.

5.2 Methods

PCR arrays were performed on all resistant models of MG-63 and HOS-143B developed from Chapter 3 by using QuntiNova LNA PCR Flexible Panels as described in section 2.9.5. A total of 16 qPCR assays was performed on each sample. One array was performed for all samples and then Western blot analysis was also carried out as described in section 2.10 for validation purposes.

Controls included in the PCR arrays were Positive PCR Control (PPC), QuantiNova Internal Control RNA (QIC), Human Genomic DNA Control (HGDC), and GAPDH for the reference gene. The PPC control contained pre-dispensed artificial DNA sequence that served the purpose to test the efficiency of the polymerase chain reaction. The efficiency of reverse transcription performed with QuantiNova Reverse Transcription Kit was tested by the QIC control by detecting the template synthesised from the built-in external RNA control. Human genomic contamination was tested by HGDC control where the non-transcribed genomic DNA would be detected by this assay (Qiagen, 2021)

Data analysis was carried out by using GeneGlobe software provided by Qiagen (https://geneglobe.qiagen.com/gb/). Its analysis was based on the fold change and regulation calculated by using $2^{-\Delta\Delta CT}$ method (Livak and Schmittgen, 2001).

5.3 Results

5.3.1 PCR array quality control

The PCR arrays quality control results are shown in Table 5.1 for MG-63 parental and resistant models and Table 5.2 for HOS-143B parental and resistant models. According to the QuantiNova LNA Flexible Panel handbook, Quality control assessment for Positive PCR Control was determined as "Pass" when the sample Positive PCR Control Cq value was less than 25 and less than 2 away from the average Positive PCR Control Cq value of all samples, otherwise "Inquire" was reported. QuantiNova Internal Control RNA control was determined as "Pass" when the sample's Delta Cq (average QIC Cq – average PPC Cq) was less than 6, otherwise "Inquire" was reported. Human Genomic DNA Control was reported as "Pass" when the Cq value was greater than 35, otherwise "Inquire" was reported.

Table 5.1 Data quality control (QC) for MG-63 parental and resistant models (n=1)

Samples	**Positive PCR Control**		**QuantiNova Internal RNA Control**		**Human Genomic DNA Control**	
	Cq	**Result**	**Delta Cq**	**Result**	**Cq**	**Result**
MG-63	20.04	Pass	5.14	Pass	35.00	Pass
MG-63 /CISR8	19.96	Pass	5.12	Pass	35.00	Pass
MG-63 /DOXR8	20.69	Pass	4.49	Pass	35.00	Pass
MG-63 /MTXR8	20.16	Pass	5.49	Pass	35.00	Pass
MG-63 /TRIR8	19.77	Pass	3.75	Pass	35.00	Pass

Quality control data analysis showed that the Human Genomic DNA Contamination Control was passed on all samples in MG-63 and HOS-143B parental and resistant models as the Cq value was greater than 35 (Table 5.1 & 5.2). This indicated no human genomic DNA contamination determined in all samples. Positive PCR Control showed "Pass" in all samples. This indicated low efficiency of polymerase chain reaction detected in these samples. QuantiNova Internal Control also showed "Pass" in all samples. This indicated high efficiency of cDNA synthesis from the reverse transcription.

Table 5.2 Data quality control (QC) for HOS-143B parental and resistant models (n=1)

Samples	Positive PCR Control		QuantiNova Internal RNA Control		Human Genomic DNA Control	
	Cq	Result	Delta Cq	Result	Cq	Result
HOS-143B	19.80	Pass	4.82	Pass	35.00	Pass
HOS-143B/CISR8	20.33	Pass	5.52	Pass	35.00	Pass
HOS-143B/DOXR8	19.68	Pass	4.98	Pass	35.00	Pass
HOS-143B/MTXR8	21.14	Pass	4.79	Pass	35.00	Pass
HOS-143B/TRIR8	22.09	Pass	3.70	Pass	35.00	Pass

Table 5.3 and Table 5.4 show the fold change determined for each gene in the MG-63 and HOS-143B resistant models compared to the parental control. The comment was provided based on several criteria met on the Cq values determined in each of the samples. Comment "A" was given when the Cq of the gene was relatively high (>30) in either the control or the test sample and was reasonably low in the other sample (<30). Comment "B" was given when the Cq of the gene was relatively high (>30) in both control and test

samples. Comment “C” was given when the Cq of the gene was either not determined or greater than the defined cut-off value (Cq value at 35), in both test and control sample. The comments were provided for the analysis, therefore genes with fold changes with comment “A” and “B” were used for discussion and further analysis.

5.3.2 mRNA gene-expression profile of MG-63 resistant models

The gene-expression profile of MG-63/CISR8, MG-63/DOXR8, MG-63/MTXR8, and MG-63/TRIR8 is shown in Table 5.3. GAPDH was used as the reference gene for normalisation and fold change was calculated by using the $2^{-\Delta\Delta CT}$ method (Livak and Schmittgen, 2001). Table 5.3 includes the fold change determined for each gene on MG-63 resistant models and the comment provided from the GeneGlobe analysis. The comment provided in Table 5.3 was based on several criteria met on the Cq values as previously described in Section 5.3.1.

In Table 5.3, MG-63/CISR8 shows an upregulation of gene expression SPHK1 (11.16 fold), HIF1A (2.25 fold), and a downregulation of ATM (-4.99 fold) and CCN2 (-2.68 fold) compared to MG-63. MG-63/DOXR8 shows an upregulation of MSH2 (5.74 fold), SPHK1 (2.77 fold), CCN2 (2.41 fold), and a downregulation of BCL2L1 (-2.17 fold). MG-63/MTXR8 shows a downregulation of ATM (-2.27 fold) and BCL2L1 (-2.25 fold) comparing to parental control. MG-63/TRIR8 shows an upregulation of RFC1 (2.89 fold), SKP2 (2.89 fold), TGM2 (7.01 fold), HIF1A (4.86 fold), and a downregulation of ATM (-2.95 fold) and BCL2L1 (-2.06 fold) comapred to MG-63. The gene-expression results in Table 5.3 with comment “C” was not included in the analysis as the Cq of the gene was either not determined or greater than the defined cut-off value (Cq value at 35), in both test and control sample. Therefore, the most deregulated gene in MG-63 resistant

sublines was SPHK1 with 11.16 fold in MG-63/CISR8 and HIF1A with 2.25 fold and 4.86 fold in MG-63/CISR8 and MG-63/TRIR8, respectively.

Table 5.3 Fold change of MG-63 resistant models comparing to parental control. (n=1)

Gene Symbol	MG-63/CISR8		MG-63/DOXR8		MG-63/MTXR8		MG-63/TRIR8	
	Fold	Comment	Fold	Comment	Fold	Comment	Fold	Comment
GAPDH	1.00		1.00		1.00		1.00	
RB1	1.23	C	9.92	C	1.09	C	1.99	C
RFC1	1.93		1.27	A	-1.04		2.89	
SKP2	1.35		1.55	A	1.42		2.89	
GSTP1	1.23	C	9.92	C	1.09	C	1.99	C
TGM2	1.23	C	9.92	C	1.09	C	7.01	
MARK2	1.23	C	9.92	C	1.09	C	1.99	C
ATM	-4.99	A	-1.77	A	-2.27		-2.95	A
CCN2	-2.68		2.41		-1.71		1.15	
BCL2L1	-1.49		-2.17		-2.25		-2.06	
HIF1A	2.25		-1.01		1.28		4.86	
SPHK1	11.16	A	2.77		-1.57		1.44	
MSH2	1.02		5.74		-1.56		-2.06	

Fold regulation in red colour indicates for upregulation and blue colour indicates for downregulation. Comment “A” was given when the Cq of the gene was relatively high (>30) in either the control or the test sample and was reasonably low in the other sample (<30). Comment “B” was given when the Cq of the gene was relatively high (>30) in both control and test samples. Comment “C” was given when the Cq of the gene was either not determined or greater than the defined cut-off value (Cq value at 35), in both test and control sample.

5.3.3 mRNA gene expression profile of HOS-143B resistant models

The gene expression profile of HOS-143B/CISR8, HOS-143B/DOXR8, HOS-143B/MTXR8 and HOS-143B/TRIR8 is shown in Table 5.4. GAPDH was used as the reference gene for normalisation and fold regulation was calculated by using $2^{-\Delta\Delta CT}$ method (Livak and Schmittgen, 2001). The comment provided in Table was based on several criteria met on the Cq values as previously described in section 5.3.1.

In Table 5.4, HOS-143B/CISR8 was showed an upregulation of HIF1A (35.51 fold), SPHK1 (4.56 fold), MSH2 (2.55 fold), BCL2L1 (3.41 fold), RFC1 (5.46 fold), SKP2 (5.70 fold), and a downregulation of ATM (-3.07 fold) compared to parental control HOS-143B. HOS-143B/DOXR8 showed an upregulation of SKP2 (10.34 fold), RFC1 (6.36 fold), HIF1A (3.36 fold), and downregulation of SPHK1 (-5.24 fold) compared to parental control. HOS-143B/MTXR8 showed an upregulation of RFC1 (2.55 fold), SKP2 (5.39 fold), ATM (3.03 fold), BCL2L1 (8.06 fold), MSH2 (3.76 fold), and downregulation of SPHK1 (-7.01 fold). HOS-143B/TRIR8 showed upregulation of RFC1 (2.16 fold), SKP2 (5.06 fold), MSH2 (4.82 fold), and downregulation of HIF1A (-3.61 fold) and SPHK1 (-4.92 fold).

The gene-expression result in Table 5.4 with comment “C” was not included in the analysis as the Cq of the gene was either not determined or greater than the defined cut-off value (Cq value at 35), in both test and control sample. Therefore, the most deregulated gene across the HOS- 143B resistant sublines was HIF1A with 35.51 fold, 3.36 fold, and -3.61 fold in HOS-143B/CISR8, HOS-143B/DOXR8, and HOS-143B/TRIR8, respectively.

Table 5.4 Fold change of HOS-143B resistant models comparing to parental control. (n=1)

Gene Symbol	HOS-143B/CISR8		HOS-143B/DOXR8		HOS-143B/MTXR8		HOS-143B/TRIR8	
	Fold	Comment	Fold	Comment	Fold	Comment	Fold	Comment
GAPDH	1.00		1.00		1.00		1.00	
RB1	1.04	C	-1.53	C	12.21	C	11.47	C
RFC1	5.46	A	6.36	A	2.55		2.16	
SKP2	5.70		10.34	A	5.39		5.06	
GSTP1	1.04	C	-1.53	C	12.21	C	11.47	C
TGM2	1.04	C	-1.53	C	12.21	C	11.47	C
MARK2	1.04	C	-1.53	C	12.21	C	11.47	C
ATM	-3.07		1.72	A	3.03		-1.46	
CCN2	1.04	C	-1.53	C	12.21	C	11.47	C
BCL2L1	3.41		1.22		8.06		-1.77	A
HIF1A	35.51		3.36		1.41	A	-3.61	A
SPHK1	4.56		-5.24	A	-7.01	A	-4.92	A
MSH2	2.55		-1.30		3.76		4.82	

Fold regulation in red colour indicates for upregulation and blue colour indicates for downregulation. Comment “A” was given when the Cq of the gene was relatively high (>30) in either the control or the test sample and was reasonably low in the other sample (<30). Comment “B” was given when the Cq of the gene was relatively high (>30) in both control and test samples. Comment “C” was given when the Cq of the gene was either not determined or greater than the defined cut-off value (Cq value at 35), in both test and control sample.

5.3.4 Clustergram

A clustergram of all samples are shown in Figure 5.1 with hierarchical clustering to visualise the relationship between the different samples and gene expression. The clustergram shows a high similarity in the expression level of HIF1A and SPHK1 across all the samples include resistant and parental cell lines of MG-63 and HOS-143B. Hihgest expression level of HIF1A and SPHK1 was determined in HOS-143B/CISR8 and the lowest in the HOS-143B/MTXR8. Another pair of genes, RFC1 and SKP2 which related to the methotrexate-resistant mechanism was also showed a high similarity expression level amongst the samples. The highest expression level of RFC1 and SKP2 was seen in MG-63/TRIR8. While the rest of genes were expressed in similar pattern under the same cluster with the higher similarity between ATM and BCL2L1 (Fig. 5.3).

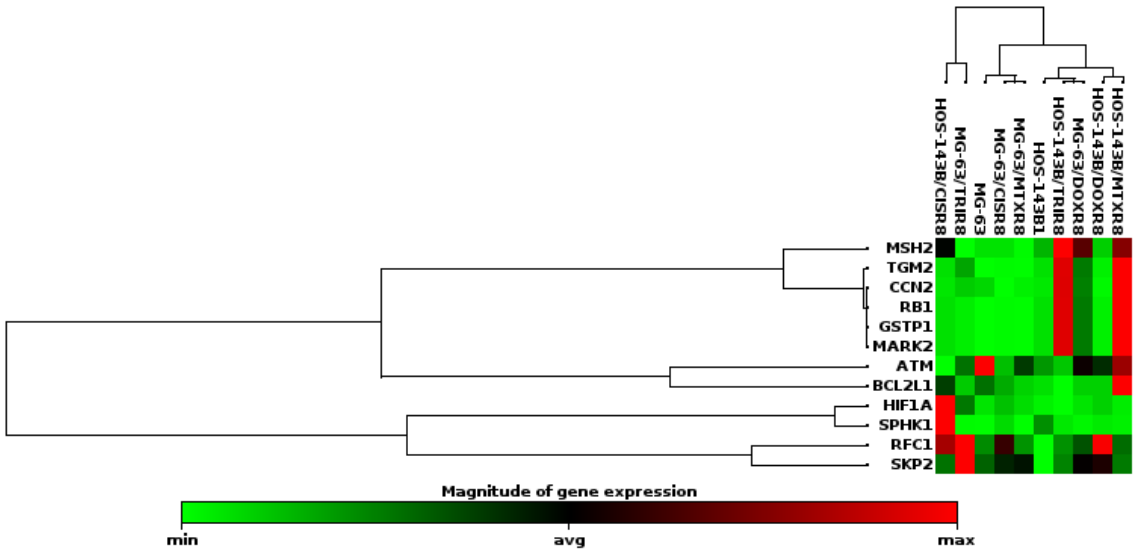

Figure 5.1: Clustergram of all samples run on PCR array. The different genes and resistant models clustered together have a high similarity in their gene expression profile. Intensity of red colour indicates maximum expression level and green colour indicates minimum expression level.

5.3.5 Validation of selected deregulated genes

Based on the result obtained from the PCR arrays in Section 5.3.2 & 5.3.3, the most deregulated genes were selected for further validation by using Western blotting to study the protein expression level. HIF1A and SPHK1 were selected to perform protein analysis based on their highest upregulated expression level determined in both MG-63 and HOS-143B resistant models.

Figure 5.2A and 5.2B show the fold change of SPHK1 protein expression determined in the MG-63 resistant sublines and HOS-143B resistant sublines, respectively. A significant increase of SPHK1 protein expression was seen in MG-63/CISR8 with 2.03 ± 0.08-fold ($p=0.034$) compared to parental control. Significant expression of SPHK1 was also seen in MG-63/DOXR8 (1.77 ± 0.24-fold, $p=0.02$) and decreased in MG-63/MTXR8 (0.85 ± 0.10-fold) and MG-63/TRIR8 (0.37 ± 0.14-fold) compared to MG-63 (Figure 5.2A). This validated the PCR arrays result in Table 5.4 where SPHK1 gene expression level was upregulated in MG-63/CISR8 and MG-63/DOXR8.

A similar result was also shown in HOS-143B resistant sublines, where SPHK1 protein expression level was significantly increased in HOS-143B/CISR8 with 3.55 ± 0.84-fold ($p=0.0459$) comparing to parental control. HOS-143B/DOXR8 and HOS-143B/TRIR8 were having a similar protein expression level of SPHK1 with HOS-143B, and a decreased protein level was found in HOS-143B/MTXR8 with 0.36 ± 0.12-fold (Figure 5.4B). This also validates the result seen in the PCR arrays where an upregulation of SPHK1 gene expression level was shown in HOS-143B/CISR8 (Table 5.4).

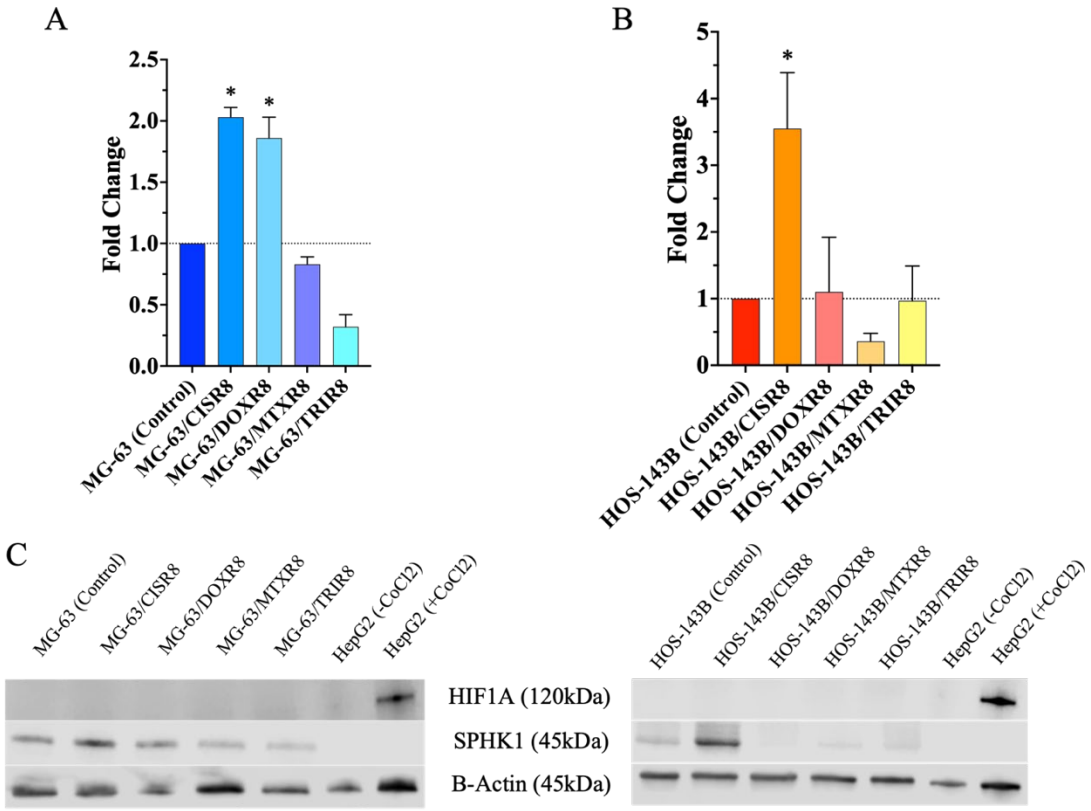

Figure 5.2: Protein analysis of SPHK1 and HIF1A by Western blots for the validation of PCR arrays. Fold change of SPHK1 protein expression level determined on (A) MG-63 resistant models comparing to parental cell line MG-63 and (B) HOS-143B resistant models comparing to parental cell line HOS-143B, using ECL for signal development. (C) HIF1A and SPHK1 protein expression of both MG-63 and HOS-143B parental and resistant cell lines analysed by Western blot. Error bars represent SEM. * = $p < 0.05$, Two sample *t*-test. (n=3)

Figure 5.4C shows the result of protein analysis by Western blot. HepG2 lysate with cobalt chloride ($CoCl_2$) treatment was used as a positive control and HepG2 lysate without cobalt chloride treatment was used as a negative control for HIF1A protein analysis. As the result has shown in Figure 5.4C, no HIF1A protein expression was determined on both MG-63 and HOS-143B parental and resistant sublines except for the positive control which was a HepG2 lysate with cobalt chloride treatment.

5.4.6 Correlation between SPHK1 and HIF1A, and SPHK1 and P-gp

The correlation analysis was shown in Figure 5.3 for SPHK1 and HIF1A, and Figure 5.4 for SPHK1 and P-gp. The correlation analysis was performed by Pearson correlation (Nahler, 2009).

Figure 5.3A is the correlation between SPHK1 gene expression and HIF1A gene expression in MG-63 resistant sublines and Figure 5.3B in HOS-143B resistant sublines. The result has shown the r value is 0.216 in MG-63 resistant sublines indicating a weak correlation between SPHK1 and HIF1A. A strong correlation between gene expression between SPHK1 and HIF1A in HOS-143B resistant sublines (r=0.716).

Figure 5.4A is the correlation between SPHK1 gene expression and P-gp (ABCB1) gene expression in MG-63 resistant sublines and Figure 5.5B in HOS-143B sublines. The result has shown the r value is 0.798 (Fig. 5.4A) in MG-63 resistant sublines and 0.573 in HOS-143B resistant sublines. This indicates a strong correlation between gene expression between SPHK1 and P-gp (ABCB1) in MG-63 resistant sublines and a moderate correlation in HOS-143B resistant sublines.

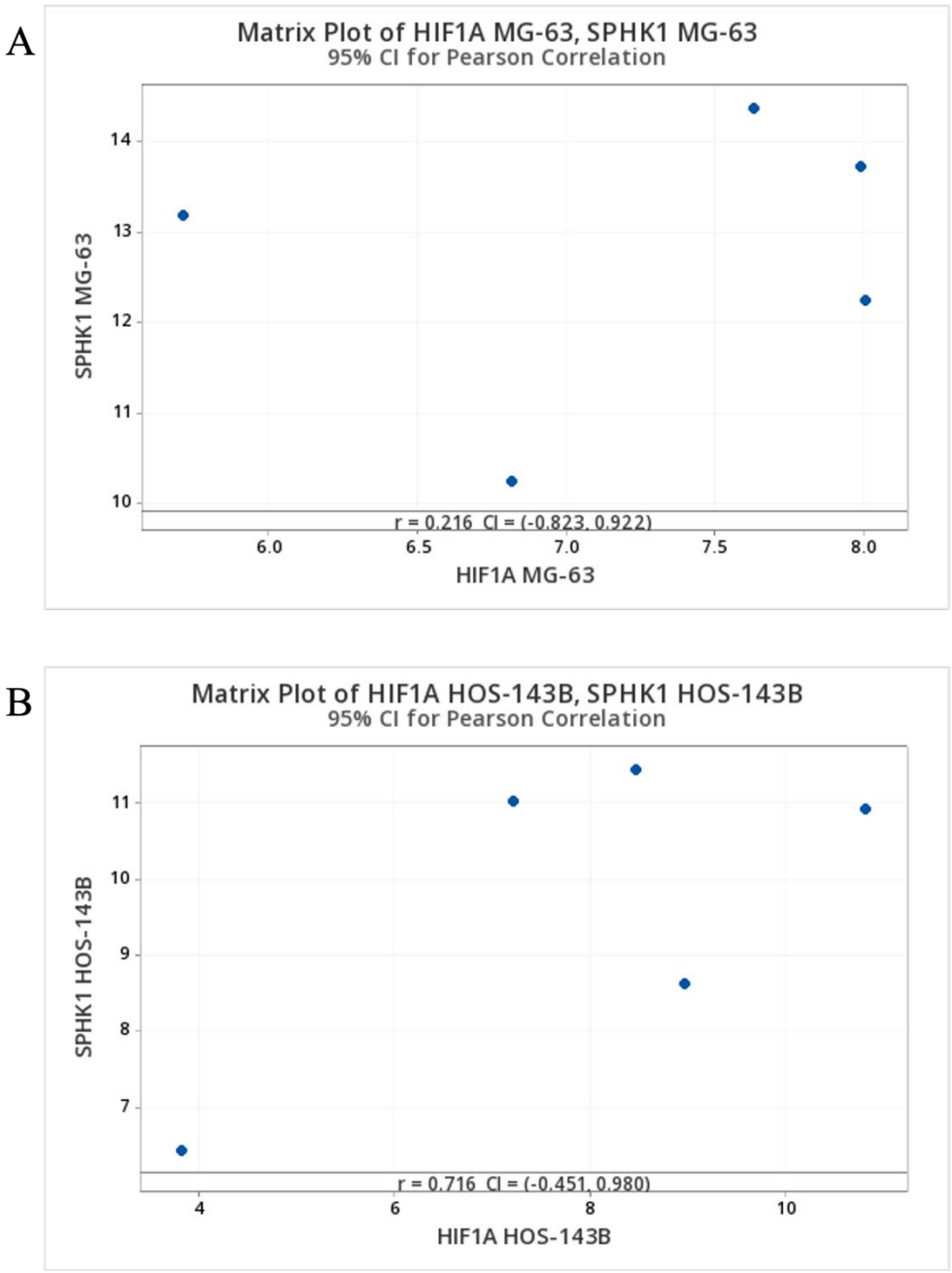

Figure 5.3: Correlation analysis between gene expression SPHK1 and HIF1A. Result of the correlation analysis of (A) MG-63 resistant sublines and (B) HOS-143B resistant sublines. r > 0.1 weak correlation, r > 0.4 moderate correlation, r > 0.7 strong correlation, r > 0.9 very strong correlation.

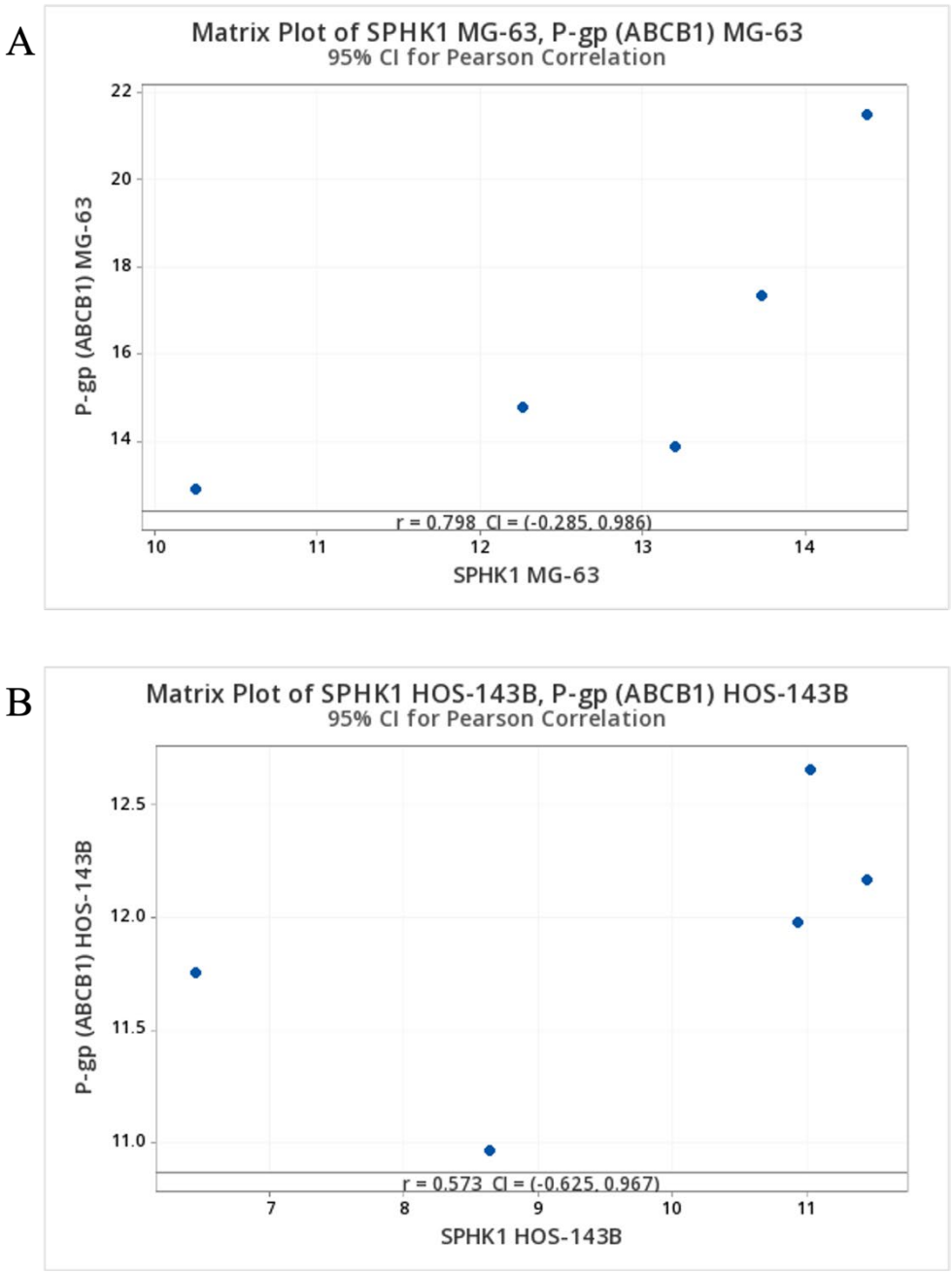

Figure 5.4: Correlation analysis between gene expression SPHK1 and P-gp (ABCB1). Result of the correlation analysis of (A) MG-63 resistant sublines and (B) HOS-143B resistant sublines. r > 0.1 weak correlation, r > 0.4 moderate correlation, r > 0.7 strong correlation, r > 0.9 very strong correlation.

5.4 Discussion

Based on the PCR array results in Table 5.3 & 5.4, the top five deregulated genes identified in the MG-63 resistant sublines are HIF1A, SPHK1, RFC1, SKP2; and CCN2 and on HOS-143B resistant sublines are HIF1A, SPHK1, RFC1, SKP2, and BCL2L1. Amongst the top 5 deregulated genes from both of the different types of resistant cell lines, HIF1A and SPHK1 showed the most deregulated expression in both of the resistant cell lines. Therefore, HIF1A and SPHK1 were selected to further investigate their protein expression level to validate the result.

A study from Serra *et al.* has shown that the major methotrexate-resistance mechanisms are the upregulation of DHFR and the reduction of RFC1. They conducted the DHFR and RFC1 analysis on methotrexate-resistant osteosarcoma cells in the relation of RB1 expression of the cells and they found out RB1 expression was influencing the type of resistant mechanism to be developed in the cells (Serra *et al.*, 2004). Increased expression level of RB1 was associated to the upregulation of DHFR and the decreased expression level of RB1 was associated to the downregulation of RFC1 to establish the methotrexate resistant in osteosarcoma cells (Serra *et al.*, 2004). In contrast, in our study (Table 5.3 & 5.4), the expression of RFC1 was upregulated in all the resistant sublines of HOS-143B and MG-63/TRIR8 and minor downregulation in MG-63/MTXR8 by -1.07 fold. This result indicates that the methotrexate-resistance mechanism acquired in HOS-143B/MTXR8 and MG-63/MTXR8 is not mainly through the reduction of RFC1. Furthermore, the expression of RB1 in both resistant osteosarcoma cell lines showed a trend for upregulation (Table 5.3 & 5.4), which could be associated with the increased expression of DHFR as the main methotrexate resistance mechanisms in these methotrexate-resistant cell lines.

GSTP1, TGM2, and MARK2 are the genes that were associated to cisplatin-resistance mechanisms. Table 5.3 & 5.4 show the result of these 3 genes were not included in the analysis for this chapter due to the Cq value of the gene was either undetermined or greater than the defined cut-off value at 35 in both of the control and resistant subline samples. When the expression level of these genes was undetermined or determined at a high Cq value, which indicates these genes were not being expressed in these cell lines or at a minimum level. Therefore, it is unlikely that these genes contributes to the cisplatin-resistance mechanisms in MG-63/CISR8 or HOS-143B/CISR8.

The SPHK1 gene-expression level was upregulated in MG-63/CISR8 (16.83-fold), MG-63/DOXR8 (2.00-fold), HOS-143B/CISR8 (2.75-fold) and downregulated in HOS-143B/DOXR8 (-2.56-fold) and HOS-143B (-3.97-fold) compared to their respective parental controls. This result was validated from the protein analysis by Western blot (Figure 5.4), where the SPHK1 protein level was significantly increased in MG-63/CISR8 with 2.06 ± 0.13-fold ($p=0.0497$) and HOS-143B/CISR8 with 3.55 ± 0.84-fold ($p=0.0459$) compared to their respective parental controls. A slight increase of SPHK1 protein level was also determined on MG-63/DOXR8 with 1.77 ± 0.24-fold compared to MG-63 (Figure 5.4A). This indicates that SPHK1 might play a significant role in the drug resistance in osteosarcoma cell lines, especially in the cisplatin and doxorubicin resistance mechanism but is not involved in contributing to the methotrexate-resistance mechanism.

Sphingosine is phosphorylated by sphingosine kinases (SPHK), including SPHK1 and SPHK2 to Sphingosine-1-phosphate (S1P), which play a role as a signalling lipid messenger to promote cell proliferation and survival (Spiegel and Milstien, 2003; Maceyka *et al.*, 2012). Cancer initiation and progression can thereby promotes by the

increase cellular S1P which caused by the overexpression and activation of SPHK1 (Pyne and Pyne, 2010). However, if SPHK1 is inhibited or silenced which caused the reduction of cellular S1P, cell death and apoptosis will occur (Shida *et al.*, 2008). A similar result was also obtained in the study of Ren and Su, where they found the expression of SPHK1 both in gene and protein level were higher in osteosarcoma cells exhibited greater resistance to doxorubicin. Furthermore, they also determined the inhibition of SPHK1 by siRNA transfection successfully increased the sensitivity of doxorubicin in osteosarcoma cells with higher extent of doxorubicin resistant (Ren and Su, 2020). Another study by Yao *et al*. determined the regulation of microRNA-3677 targets SPHK1 in osteosarcoma cells, where the inhibition of microRNA-3677 led to an enhanced expression of SPHK1 and caused cancer progression. In contrast, the overexpression of microRNA-3677 inhibited osteosarcoma cell progression by inhibiting SPHK1 (Yao *et al.*, 2020).

However, both of these studies investigated the effect of SPHK1 on primary osteosarcoma cell lines with different amount of intrinsic drug resistance, which might not present a clear idea on the effect of SPHK1 on acquired drug resistance in osteosarcoma cells that is more related to a subset of patient with secondary or relapsed osteosarcoma. In this study, the developed cisplatin and doxorubicin resistant sublines show an upregulation in gene and protein level of SPHK1 compared to the parental controls. This has supported the concept of increasing expression of SPHK1 confers drug resistance in osteosarcoma cells with acquired resistance, where the increased expression was indicated in the developed resistant sublines compared to parental cell line which share the same primary cell line of osteosarcoma. This finding has suggested a new therapeutic target for primary and secondary osteosarcoma patient by targeting SPHK1.

Some studies had been conducted to explore the therapeutic strategy targeting SPHK1 in osteosarcoma cells. Sphingosine kinase 1 inhibitor (SKI-V) is a non-competitive SPHK1 small molecule inhibitor which inhibits SPHK1 activity by preventing the formation of cellular S1P and increase accumulation level of ceramide that causes apoptosis (French *et al.*, 2006). A study conducted by Sun *et al*. demonstrated SKI-V provided significant anti-tumour activity in osteosarcoma cells by inhibiting cancer progression and inducing cell death and apoptosis. They also found that osteosarcoma xenograft tumour growth was suppressed *in vivo* by daily injection of SKI-V (Sun *et al.*, 2022). Recent study by Ji *et al*. shows the sensitivity of doxorubicin in cancer cells could be also increased by the enhanced level of cellular ceramide which could be triggered by one of the effects of sphingosine kinase inhibitor (Ji *et al.*, 2010). A study by Yao *et al.* determined the co-administration of phenoxodiol and doxorubicin resulted in significant inhibition of osteosarcoma cell growth both *in vitro* and *in vivo* via the increased sphingosine and ceramide level due the inhibition of SPHK1 activity by phenoxodiol (Yao *et al.*, 2012). These studies have again suggested SPHK1 as a potential therapeutic target for osteosarcoma patients. Moreover, a correlation between the expression of SPHK1 and Pgp was also determined on leukaemia cancer cells (Bonhoure *et al.*, 2006). A similar result was also shown in this study where a strong correlation was determined between the gene expression of SPHK1 and P-gp (ABCB1) on MG-63 cell lines (r=0.798) and a moderate correlation on HOS-143B cell lines (r=0.573) (Fig. 5.6).

Development of hypoxic microenvironment normally resulted from the growth of solid tumours has a significant consequence on the prognosis of the tumour and biological processes (Philip *et al.*, 2013). This hypoxic environment could induce hypoxia-inducible factor (HIF), which is a transcription factor comprises of two sub-units, HIF1A and HIF1B that are related to tumour metastasis, angiogenesis and progression (Ke and Costa,

2006). Several studies have indicated the overexpression of HIF1A in different types of tumours including osteosarcoma and is correlated with metastasis (Ding *et al.*, 2010). Moreover, HIF1A also found to be involved in hypoxia-induce migration in human osteosarcoma cells (Guo *et al.*, 2014).

Based on the PCR arrays result in this study, gene expression level of HIF1A was upregulated in all the resistant sublines derived from both osteosarcoma cell lines MG-63 and HOS-143B compared to parental control ranging from 2.04 – 9.27-fold except for HOS-143B/TRIR8. However, when the protein expression level of HIF1A was further investigated a by Western blot, no protein band was determined in all of the samples including parental and resistant sublines. To further validate this result, control samples HepG2 with and without cobalt chloride ($CoCl_2$) treatment were used as positive and negative controls respectively (Figure 5.4C) and HIF1A protein was successfully detected in positive control HepG2 with cobalt chloride treatment. One of the explanations for undetected HIF1A protein in the gene upregulated samples could be due to the nature of this protein is activated under the hypoxia condition and the protein would rapidly degraded under normoxic conditions (Mizobuchi *et al.*, 2008). Stressing the cell samples under hypoxia condition or treating with a hydroxylase inhibitor such as cobalt chloride could induce the expression of the HIF1A protein (Gupta and Wish, 2017).

Nevertheless, the upregulated gene expression of HIF1A in the resistant sublines suggested HIF1A plays an important role in drug resistance in osteosarcoma. Study by Adamski *et al.* has reported chemotherapeutic drug such as doxorubicin increases the synthesis of free radical in the cancer cells to cause cytotoxicity could also induce hypoxia (Adamski *et al.*, 2013). This also explained the upregulation of HIF1A gene expression in the resistant sublines might be triggered by the chemotherapeutic drug treatment during

the developing process and the HIF1A proteins which is responsible for the regulation of cancer progression is only expressed when the cells are under the hypoxia condition. A study by Keremu *et al.* also demonstrated a reversal of cisplatin resistance on osteosarcoma cell lines both *in vitro* and *in vivo* by inhibiting the HIF1A expression via overexpression of miR-199a. These finding has again indicated HIF1A as a potential therapeutic target for osteosarcoma.

Correlation between SPHK1 and HIF1A has also been investigated in the literature and SPHK1/S1P signalling was identified as a new modulator of HIF1A in different types of cancer cell including breast, lung, prostate, glioma, and renal cell carcinoma both *in vitro* and *in vivo* (Ader *et al.*, 2008, 2015; Bouquerel *et al.*, 2016). The correlation analysis in our study also shows a strong correlation between the gene expression of SPHK1 and HIF1A in HOS-143B resistant sublines (r=0.716) (Fig. 5.5B). Ren and Su also suggested that glycolysis was promoted in osteosarcoma cells by the increased expression level of SPHK1 and this SPHK1-mediated effects on glycolysis required HIF1A expression for the doxorubicin resistance in osteosarcoma cell lines (Ren and Su, 2020).

5.5 Conclusion

Overall, upregulation of SPHK1 and HIF1A from the PCR array analysis determined that these two genes play an important role in the drug resistant mechanism in osteosarcoma. The strong correlation determined between these two genes in this study indicates a new promising potential therapeutic target for osteosarcoma which could be further investigated. The increased gene expression of SPHK1 in resistant sublines derived by cisplatin and doxorubicin was also validated by increased protein expression. This has demonstrated the significant role of SPHK1 in contributing to cisplatin and doxorubicin resistance mechanisms in osteosarcoma cell lines.

Chapter 6: Efficacy of gemcitabine and docetaxel treatment on relapsed osteosarcoma: A systematic review and *in vitro* primary studies

6.1 Introduction

6.1.1 Current treatment of relapsed osteosarcoma

Currently, the expected 5-year survival rate of patients under the age of 40 with non-metastatic osteosarcoma is around 70% when treating with surgery and chemotherapy with the combination of cisplatin, doxorubicin, methotrexate, and ifosfamide (Bielack *et al.*, 2002; Ferrari and Palmerini, 2007). Since the development of multi-agent chemotherapy in combination with surgery, the outcome of patients with localised osteosarcoma has been improved (Bielack *et al.*, 2002; Ferrari and Palmerini, 2007). However, the survival rate for patients with relapsed disease of osteosarcoma is poor with 5-year post relapse survival rate below 30% and the treatment option for this cohort of patients are limited (Ferrari *et al.*, 2003).

There is currently no accepted standard regimen for recurrent osteosarcoma patients as second-line chemotherapy. Some active chemotherapeutic drugs such as carboplatin, etoposide or ifosfamide have been used as the treatment for relapsed osteosarcoma based on the prior disease-free interval of the patients (Casali *et al.*, 2018). The efficacy of high-dose ifosfamide (HDIFO) has also been widely studied on patient with metastatic osteosarcoma (Rosen *et al.*, 1994; Patel *et al.*, 1997), but no new drugs were synthesised and have been approved by Food and Drug Administration (FDA) or European Medicines Agency (EMA) to improve the survival of osteosarcoma in the last 30 years. Clinical trials of different chemotherapy drug and kinase inhibitor such as pemetrexed, sorafenib, and everolimus have been performed on patients with metastatic and relapsed osteosarcoma as second-line chemotherapy treatment, but unfortunately no positive results were seen in these clinical trials that warrant further development (Duffaud *et al.*, 2012; Grignani *et al.*, 2012, 2015).

Table 6.1 Gemcitabine and docetaxel doses used in relapsed osteosarcoma

Drugs	Patient Number	Response Rate	Complete Response/ Partial Response
Gemcitabine 1,000 mg/m^2 (Merimsky *et al.*, 2000)	7	0%	0/ 0
Gemcitabine 675 mg/m^2, Docetaxel 75 – 100 mg/m^2 (Navid *et al.*, 2008)	10	30%	0/ 3
Gemcitabine 900 mg/m^2, Docetaxel 80 – 100 mg/m^2 (Fox *et al.*, 2012)	14	7%	0/ 1
Gemcitabine 675 mg/m2, Docetaxel 75 – 100 mg/m^2 (Gosiengfiao *et al.*, 2012)	4	25%	0/ 1
Gemcitabine 675 mg/m^2, Docetaxel 75 – 100 mg/m^2 (Qi *et al.*, 2012)	18	5%	0/ 1
Gemcitabine 675 mg/m^2, Docetaxel 100 mg/m^2 (Song *et al.*, 2014)	17	24%	3/1

The combination of gemcitabine and docetaxel has shown high efficacy on soft-tissue sarcomas patients in phase II studies compared to the treatment by gemcitabine alone (Hensley *et al.*, 2002; Maki *et al.*, 2007; Pautier *et al.*, 2012). Therefore, the study of efficacy of gemcitabine and docetaxel has also been performed on patients with relapsed osteosarcoma and conflicting results have been seen between different studies with different combination of doses used as shown in Table 6.1. (Merimsky *et al.*, 2000; Navid *et al.*, 2008; Fox *et al.*, 2012; Gosiengfiao *et al.*, 2012; Qi *et al.*, 2012; Song *et al.*, 2014).

6.1.2 Mechanisms of action of gemcitabine

Gemcitabine (2',2'-difluoro-2'-deoxycytidine; dFdC) is a deoxycytidine analogue used as a chemotherapeutic drug to treat variety of solid tumours with the combination of platinum-based drugs such as cisplatin and carboplatin for ovarian, breast, and non-small cell lung cancer (Pfisterer *et al.*, 2006; Nagourney *et al.*, 2008; Reck *et al.*, 2009). Gemcitabine is activated upon administration when it is metabolised to the active diphosphate (dFdCDP) and triphosphate (dFdCTP) form of gemcitabine (Mackey *et al.*, 1998). These active forms of gemcitabine are involved in the inhibition of DNA synthesis in the cells via two main pathways. In the first pathway, ribonucleotide reductase, a key enzymes responsible in the synthesis of deoxynucleotides, is inhibited by the diphosphate form of gemcitabine (Plunkett, Huang and Gandhi, 1995). The inhibition of ribonucleotide reductase results in the depletion the number of free deoxynucleotides and therefore restrain the DNA synthesis. The second pathway of inhibiting the DNA synthesis involves the triphosphate form of active gemcitabine by competing with deoxynucleotides and incorporated into the DNA strand which results in "masked termination" during the DNA replication (de Sousa Cavalcante and Monteiro, 2014). Gemcitabine is also found to induce apoptosis in cancer cells by activating p38 mitogen-activated protein kinase (de Sousa Cavalcante and Monteiro, 2014).

6.1.3 Mechanism of action of docetaxel

Docetaxel as an anti-microtubule agent is a semisynthetic analogue of paclitaxel, and a member of the taxoid class of antineoplastic agents derived from the needle extracts of the European Yew tree (Figgitt and Wiseman, 2000). Cell proliferation is inhibited by docetaxel by preventing cell division and cell cycle arrest at the G2/M phase, which caused by the inhibition of microtubule depolymerisation (Clarke and Rivory, 1999; Figgitt and Wiseman, 2000). Furthermore, docetaxel also promotes apoptosis in cancer by the phosphorylation and inhibition of the anti-apoptotic protein Bcl-2 (Haldar, Basu and Croce, 1997; Herbst and Khuri, 2003). Docetaxel has also been demonstrated a greater cytotoxic activity than paclitaxel against tumour cell lines (Ringel and Horwitz, 1991).

6.1.4 Combination therapy of gemcitabine and docetaxel

The combination therapy of gemcitabine and docetaxel has been widely studied and investigated to demonstrate as an effective treatment for other sarcoma patients, such as leiomyosarcomas (Hensley *et al.*, 2002; Maki *et al.*, 2007). A review study by Leu *at el.* has determined a response rate of 43% with the combination therapy of gemcitabine and docetaxel on sarcomas and bone sarcoma patients, compared to a response rate of 30% with the standard doxorubicin and ifosfamide combination therapy. Moreover, reduced incidence of toxicities has also been demonstrated in gemcitabine and docetaxel treatment (Leu *et al.*, 2004). The use of the combination of these two drugs was found to result in the synergism between gemcitabine and docetaxel, which increased the sensitivity of the sarcoma cells to gemcitabine (Leu *et al.*, 2004). This has demonstrated the benefit of multi-agent therapy over single-agent treatment. Some severe side effects associated with gemcitabine includes myelosuppression, oedema, and skin reaction (Barton-Burke, 1999). The common side effects reported to be associated with docetaxel treatment include

hypersensitivity, neutropenia, oedema, and peripheral neuropathy (Baker *et al.*, 2009). The most common side effects reported on the combination therapy of gemcitabine and docetaxel is haematological, as a result of myelosuppression (Qi *et al.*, 2012).

6.1.5 Systematic review

As osteosarcoma is a rare cancer with relatively small population of cancer patients, conducting clinical trials on osteosarcoma patients has been challenging. To date, only one phase II clinical trial had been performed on osteosarcoma patients with to investigate the efficacy of combination therapy of gemcitabine and docetaxel (GEMDOX) as the second-line treatment for osteosarcoma (Fox *et al.*, 2012). However, some retrospective reviews have been performed from several institutions to study the outcome of the combination of these drugs on osteosarcoma patients with relapsed disease due to the limited number of osteosarcoma patients. The disease recurrence rate also highlights the need for a new and effective regimen for a second-line therapy for osteosarcoma patients. Some promising outcomes from sarcoma patients receiving GEMDOX therapy, along with the abundance of retrospective patient data, suggests a systematic review on GEMDOX therapy for osteosarcoma will be beneficial for the cohort of osteosarcoma patients.

6.1.6 Aims

The aim of this chapter was to establish the efficacy and toxicity of gemcitabine and docetaxel combination chemotherapy as a second-line treatment for relapsed osteosarcoma.

Objective 1: To perform a meta-analysis in identifying the efficacy of GEMDOX therapy on relapsed or refractory osteosarcoma patients.

Objective 2: To determine the effectiveness of gemcitabine and docetaxel treatment on chemoresistant osteosarcoma cells *in vitro*.

6.2 Methods

A systematic review on GEMDOX therapy on relapsed osteosarcoma patients was carried by identifying relevant published literature on PubMed search (http://www.ncbi.nlm.nih.gov/pubmed) as described in Section 2.12.1. The meta-analysis was then performed according to Section 2.12.2 & 2.12.3.

In vitro studies were also carried out by performing cell culture and cytotoxicity assays to investigate the sensitivity of the developed resistant sublines of MG-63 and HOS-143B to the individual drugs of gemcitabine and docetaxel, and also the combination of both. Cell culture was performed as described on Section 2.2 and cytotoxicity assays were performed as described in Section 2.5.

6.3 Results

6.3.1 Systematic review

6.3.1.1 Eligible studies

The total number of results produced by the PubMed search strategy was 114 up to May 2022. After screening the abstracts for suitability, 98 papers were excluded. Next, the remaining 16 full texts were assessed. Thirteen papers were retained for data extraction (Fig. 6.1). Following data extraction, two pairs of studies (Qi *et al.*, 2012; Song *et al.*, 2014; Yu *et al.*, 2014; Lee *et al.*, 2016) were determined to have been carried out at the same institutions with overlapping patient enrolment periods. The papers were reviewed

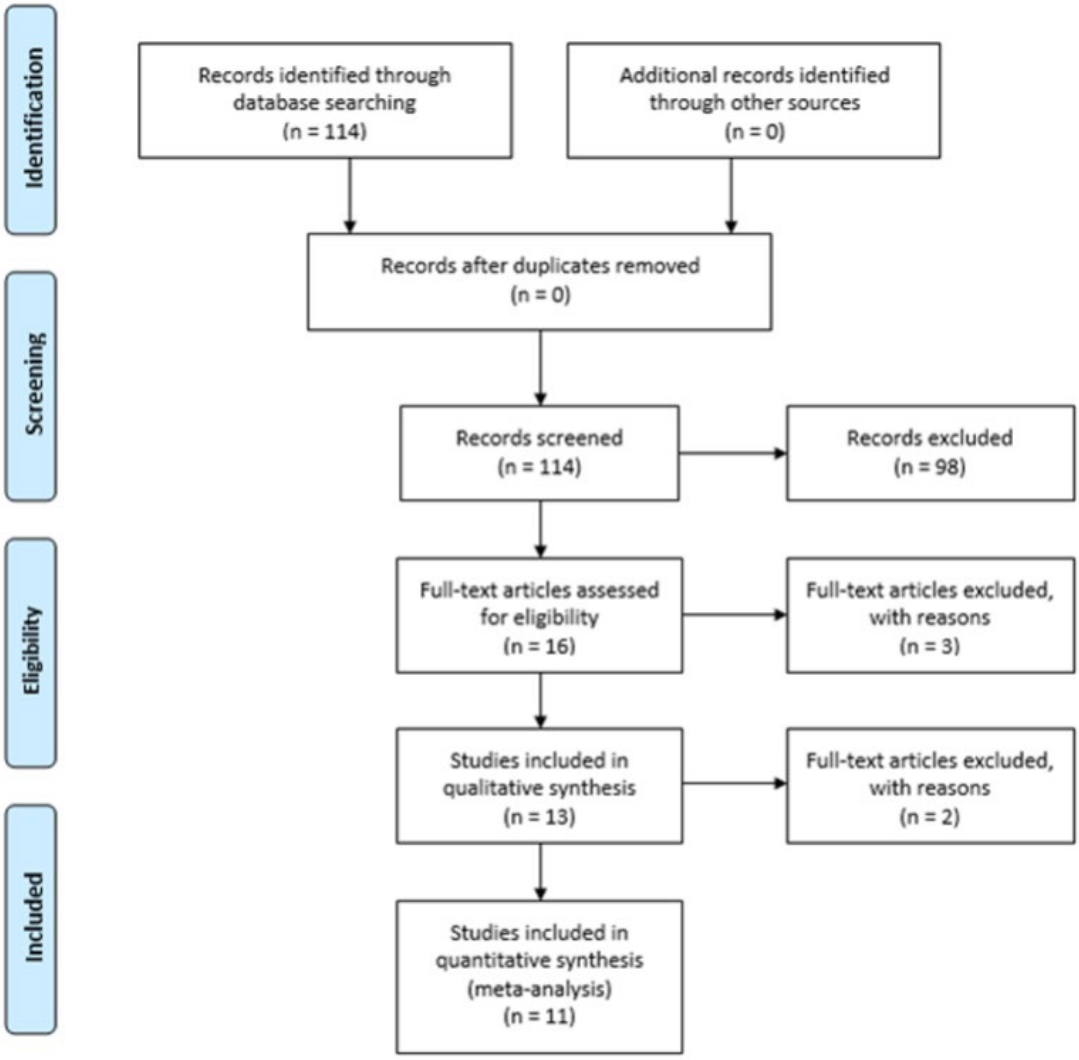

Figure 6.1: PRISMA flow diagram detailing the search and selection process employed during the systematic literature search and review. Reasons for exclusion at eligibility include: 1) the trial had not been conducted; 2) osteosarcoma patient data could not be extracted; and 3) frontline treatment history of patients were not described.

and one paper from each institution was excluded to avoid the duplication of patient data, as it was not possible to identify which patients had been included in both studies. The two studies selected for inclusion (Yu *et al.*, 2014; Lee *et al.*, 2016) had more recent publication dates, a longer study duration and a larger number of participants.

6.3.1.2 Quality assessment

To assess the quality of the retrospective studies, a set of 5 questions was compiled from different quality assessment tools including the NIH Study Quality Assessment Tool for Cohort Studies (National Heart, Blood and Lung Institute, 2017) and the Critical Appraisal Skills Programme checklist for cohort studies (Critical Appraisal Skills Programme, 2018). The questions were as follows: (1) Were the participants a representative sample of the target population, only patients with relapsed or refractory osteosarcoma who had undergone previous standard chemotherapy regimen and receiving combination of GEMDOX treatment were considered as representative sample; (2) Were there clearly defined inclusion and exclusion criteria; (3) Were the outcomes of interest and length of follow up clearly defined; (4) Were the reasons for discontinuation of treatment and loss to follow up documented; (5) Was valid statistical analysis of the data performed. The quality of each paper was assessed by two independent researchers, and any disagreements were resolved by a third party. None of the studies had scored highly for risk of bias for any of the 5 questions. Four of the 11 studies determined to have a low risk of bias across the 5 questions. The remaining 7 studies scored either a low risk or unclear risk of bias. In overall, the risk of bias for all the eligible studies included in this review was low (Table 6.2).

Table 6.2 Result of quality assessment of the 11 studies included in this review.

Author/ Year	Q1	Q2	Q2	Q4	Q5
(Fox *et al.*, 2012)	Low	Unclear	Unclear	Low	Unclear
(Gosiengfiao *et al.*, 2012)	Unclear	Low	Low	Low	Unclear
(He *et al.*, 2013)	Low	Low	Low	Low	Low
(Lee *et al.*, 2016)	Low	Low	Low	Unclear	Low
(Mora *et al.*, 2009)	Unclear	Unclear	Low	Low	Unclear
(Navid *et al.*, 2008)	Low	Low	Low	Low	Unclear
(Palmerini *et al.*, 2016)	Low	Low	Low	Low	Low
(Rapkin *et al.*, 2012)	Unclear	Unclear	Low	Low	Low
(Takahashi *et al.*, 2017)	Unclear	Low	Low	Low	Low
(Xu, Guo and Xie, 2018)	Low	Low	Low	Low	Low
(Yu *et al.*, 2014)	Low	Low	Low	Low	Low

6.3.1.3 Characteristic and summary of response data of included studies

Eleven studies published between 2008 – 2018 with a total of 197 evaluable patients met the inclusion criteria for this review (Fig. 6.1). Ten of the studies were retrospective reviews, whilst one study (Fox *et al.*, 2012) was a Phase II single-arm study. No data was available for the number of previous cycles of chemotherapy that patients received, or their grade of cancer. Due to loss to follow up, the inclusion of patients with different types of sarcomas, not all data was extractable for all studies. Patient characteristics

including weighted mean age, sex, and histology for all included patients in the review are summarised in Table 6.3.

Table 6.3 Summary of the patient characteristics included in the review.

	All Participants	Data Availability
No. of Participants	197	100%
Weighted Mean Age	18.37 years	100%
Sex	67 males & 45 females	57%
Histology	Conventional – 93% Other – 7%	50%

The doses of gemcitabine and docetaxel that were administered in each study and the patient response outcomes across all studies were collated in Covidence software (Babineau, 2014) and summarised in Table 6.4. Out of all 197 patients, 2.03% experienced a complete response to treatment, 8.63% of patients experienced a partial response, 23.86% of patients had stable disease and 65.48% experienced disease progression (Table 6.3). Overall, the proportion of patients who responded to GEMDOX treatment (experiencing either a complete response, partial response, or stable disease) was 34.52%, whilst the proportion of patients who did not respond to GEMDOX treatment (experienced progressive disease) was 65.48% (Table 6.4).

Table 6.4 Summary of the doses and response data for the 197 patients included in the review. Proportion of patients who responded to GEMDOX treatment (CR + PR + SD) was 34.52%, whilst the proportion of patients who did not respond to GEMDOX treatment (PD) was 65.48%.

Author/Year		Dosage Used		Treatment Response			
	No. of Patients	Gemcitabine (mg/m^2)	Docetaxel (mg/m^2)	Complete Response	Partial Response	Stable Disease	Progressive Disease
(Fox *et al.*, 2012)	14	675	75	0	1	3	10
(Gosiengfiao *et al.*, 2012)	2	675	75/100	0	1	1	0
(He *et al.*, 2013)	23	1000	75	0	3	8	12
(Lee *et al.*, 2016)	28	675/900	100	3	1	4	20
(Mora *et al.*, 2009)	1	1000	100	0	0	1	0
(Navid *et al.*, 2008)	10	675	75/100	0	3	1	6
(Palmerini *et al.*, 2016)	35	675/900	75	0	6	14	15
(Rapkin *et al.*, 2012)	6	675	75	1	0	2	3
(Takahashi *et al.*, 2017)	5	900	70	0	0	4	1
(Xu, Guo and Xie, 2018)	52	1000	75	0	0	5	47
(Yu *et al.*, 2014)	21	675	75	0	2	4	15
Percentage				2.03%	8.63%	23.86%	65.48%

6.3.1.4 Toxicity data

The incidence of toxicities and adverse reactions of patients to the combination therapy of GEMDOX treatment was recorded across all the studies included in this review according to the Common Terminology Criteria for Adverse Events (Jeong *et al.*, 2020). Data for the grade 3 and 4 toxicities are summarised in Table 6.5, including neutropenia, thrombocytopenia, anaemia, and neuropathy. Across all the studies, toxicity data of 133 patients of the total 197 patients were available to extract. Grade 3 – 4 neutropenia and thrombocytopenia were present in 36.0% and 35.3% of the total patients respectively. While grade 3 – 4 anaemia determined in 18.04% of the total patients. No studies reported any incidence of severe neuropathy.

Table 6.5 Summary of the toxicity data included in the review study.

Author/ Year	Discontinue due to toxicity	Grade 3/4 Neutropenia	Grade 3/4 Thrombocytopenia	Grade 3/4 Anaemia	Grade 3/4 Neuropathy
(Fox *et al.*, 2012)	0	-	-	-	-
(Gosiengfiao *et al.*, 2012)	0	2	0	1	0
(He *et al.*, 2013)	0	10	1	1	0
(Lee *et al.*, 2016)	3	11	7	0	0
(Mora *et al.*, 2009)	0	0	0	0	0
(Navid *et al.*, 2008)	-	-	-	-	-
(Palmerini *et al.*, 2016)	1	-	-	-	-
(Rapkin *et al.*, 2012)	0	3	2	2	0
(Takahashi *et al.*, 2017)	0				
(Xu, Guo and Xie, 2018)	0	22	28	16	0
(Yu *et al.*, 2014)	0	0	9	4	0
Total	**4**	**48**	**47**	**24**	**0**

6.3.1.5 Survival data of included studies

Complete survival data was available for 5 of the 11 studies. The median PFS for the studies ranged from 1-3 months, with 3 individual patients presenting with a duration of response that lasted a minimum of 12 months. The median overall survival ranged from 6 to 9 months, with the longest documented survival of an individual patient of being 69 months (Navid *et al.*, 2008). Sixteen patients from Lee *et al.*'s study were still alive 1 year after receiving GEMDOX treatment. Due to the variety of reporting measures employed by the researchers, we were unable to perform statistical analysis on the survival data.

6.3.1.6 Response to GEMDOX treatment is dependent on age

Participants response data were grouped according to age to determine if the age of participants affects the response to GEMDOX treatment. Five of the studies included in the study (Mora *et al.*, 2009; Gosiengfiao *et al.*, 2012; Rapkin *et al.*, 2012; Lee *et al.*, 2016; Palmerini *et al.*, 2016) had a median participant age of <18. Three studies had a median participant age of ≥18 years (Fox *et al.*, 2012; He *et al.*, 2013; Xu, Guo and Xie, 2018). The response data for all participants in these two age groups were added to produce a total count of participants who responded to GEMDOX treatment (CR + PR + SD) and a total count of participants who did not respond to GEMDOX treatment (PD). A chi-squared test of association was performed to determine the association between the response to GEMDOX treatment and the participant age. Results show the response to GEMDOX treatment was determined to be dependent on the age of participants, as 47.2% of patients from these studies with a median age of <18 years responded to GEMDOX treatment compared to 22.5% of patients from the papers with a median age of ≥18, X^2 (1, N = 161) = 10.94, $p < 0.05$ (Fig. 6.2A).

6.3.1.7 Response to GEMDOX treatment is dependent on gender

Participants response data were grouped according to gender to determine if the gender of participants affects the response to GEMDOX treatment. Due to the incomplete data recorded according to the gender of the participants in the studies, two groups of studies were categorised into "Equal Gender" and "More Males" for the comparison. Two studies (Fox *et al.*, 2012; Xu, Guo and Xie, 2018) included for the group of "Equal Gender" as they had an approximately equal number of male and female participants: 42.9% and 57.1%, and 55.8% and 44.2% males and females, respectively. Another two studies (He *et al.*, 2013; Yu *et al.*, 2014) included for the group of "More Males" as they had approximately 50% more male than female participants in their studies: 65.2% and 34.8%, and 71.4% and 28.6% males and females, respectively. The response data for all participants in these two age groups were added to produce a total count of participants who responded to GEMDOX treatment (CR + PR + SD) and a total count of participants who did not respond to GEMDOX treatment (PD). Chi square test of association was performed to determine the association between response to GEMDOX treatment and gender of participant. Result has shown the response to GEMDOX treatment was determined to be dependent on the gender of the participants by Chi-square test. 13.6% of patients from the studies with similar numbers of male and female participants responded to GEMDOX treatment, compared to 38.6% of patients from the studies with more male participants, X^2 (1, N = 110) = 9.14, $p < 0.05$ (Fig. 6.2B).

6.3.1.8 Response to GEMDOX treatment is not dependent on gemcitabine doses

Across all 11 studies included in this review, 3 different doses of gemcitabine were administered: 675, 900 or 1000 mg/m^2 (Table 6.3). Only one study (Takahashi *et al.*, 2017) administered gemcitabine at a dose of 900 mg/m^2. Three papers included in this review (Mora *et al.*, 2009; He *et al.*, 2013; Xu, Guo and Xie, 2018) administered gemcitabine at a dose of 1000 mg/m^2. Five papers (Navid *et al.*, 2008; Fox *et al.*, 2012; Gosiengfiao *et al.*, 2012; Rapkin *et al.*, 2012; Yu *et al.*, 2014) administered gemcitabine at a dose of 675 mg/m^2 (Table 6.3). Due to the number of patients treated with 900 mg/m^2 of gemcitabine was insufficient for Chi-square analysis, the comparison has been made between the response data for patients treated with 675 mg/m^2 and 1,000 mg/m^2 of gemcitabine. The response data for all participants in these two age groups were added to produce a total count of participants who responded to GEMDOX treatment (CR + PR + SD) and a total count of participants who did not respond to GEMDOX treatment (PD). A chi-squared test of association was performed to determine the association between the response rate of GEMDOX treatment and doses of gemcitabine. Results show no significant association between the dose of gemcitabine and the response of patients to GEMDOX treatment, X^2 (1, N = 88) = 1.41, p > 0.05 (Fig. 6.2C).

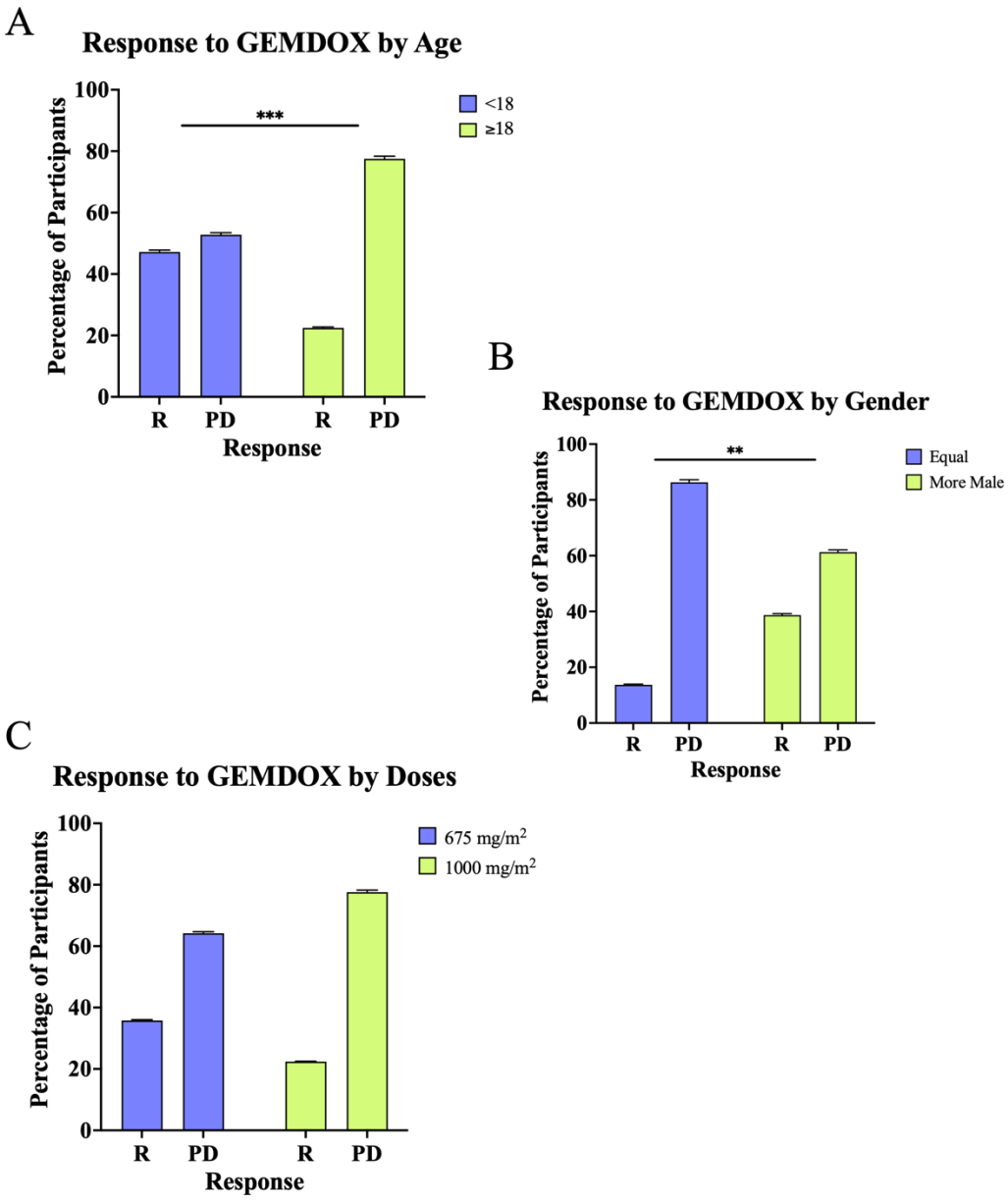

Figure 6.2: Response to combination of GEMDOX regimen. (A) Response to combination of GEMDOX regimen by (A) age, (B) gender, and (C) doses. Percentage of participants on y-axis and the response of the participants on x-axis. R represents participants who responded to the treatment (complete response, partial response, and stable disease) and PD represents not responded (progressive disease). Data are presented as percentage + 95% CI, ** = $p<0.01$, *** = $p<0.001$, X^2.

6.3.1.9 Incidence of toxicity is not dependent on age, gender, and dose of gemcitabine.

Across the 7 studies for which toxicity data was available, there were 119 cases of grade 3 or 4 haematological toxicities (Table 6.4). To determine whether incidence of grade 3-4 toxicity was associated with the age of participants, two of the 3 studies with a median participant age ≥18 years had toxicity data available (He *et al.*, 2013; Xu, Guo and Xie, 2018). Each of the 4 toxicities were analysed independently. The total counts for each of the recorded toxicities was calculated for each age group and a Chi-square test of association was performed to determine whether there was an association between the age of the participants and the incidence of grade 3-4 toxicities. No significant association was found between the age of the participants and the incidence of grade 3-4 toxicities, X^2 (2, N=105) = 3.84, p > 0.05 (Fig. 6.3A). Only one study (Xu, Guo and Xie, 2018) had a similar number of male and female participants and toxicity data available. Both (He *et al.*, 2013; Yu *et al.*, 2014) with roughly double the number of male participants than female, had toxicity data available. Chi-square analysis determined no significant association between sex and the incidence of grade 3-4 toxicities, X^2 (2, N = 91) = 0.40, p > 0.05 (Fig. 6.3B). Of the studies where patients had received gemcitabine at a dose of 1000 mg/m^2 and 675 mg/m^2, 2 and 3 studies respectively had toxicity data available. Chi-square analysis determined no significant association between the dose of gemcitabine and the incidence of grade 3-4 toxicities, X^2 (2, N = 101) = 2.87, p > 0.05 (Fig. 6.3C).

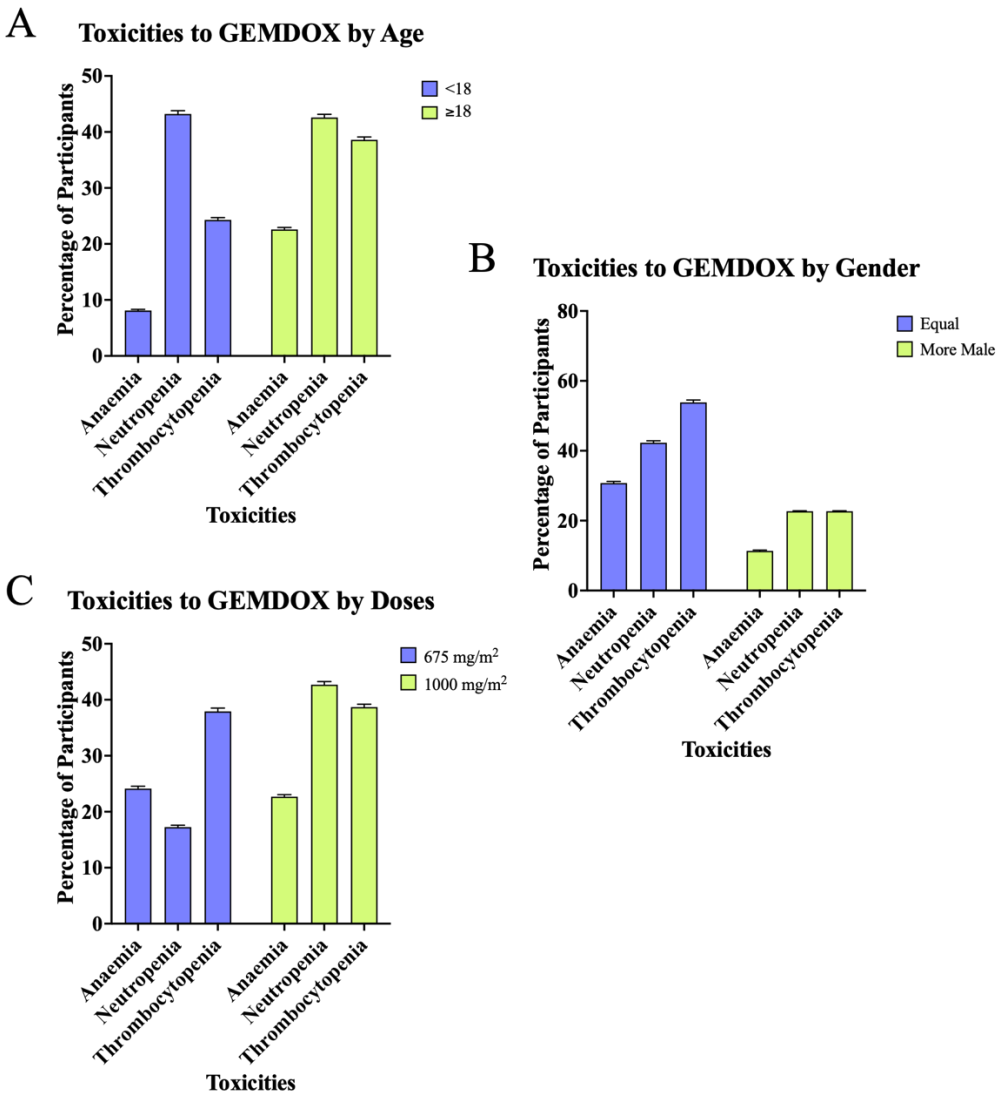

Figure 6.3 Toxicities to the combination treatment of GEMDOX regimen. (A) Percentage of patients who <18 or ≥18 years who experienced grade 3 or 4 toxicities. (B) Percentage of patients from the studies with equal numbers of male and female participants, and 50% more male participants who experienced grade 3 or 4 toxicities. (C) Percentage of patients who received 675 or 1000 mg/m^2 of gemcitabine who experienced grade 3 or 4 toxicities. Data are presented as percentage + 95% CI, $p > 0.05$, X^2.

6.3.2 In vitro study

6.3.2.1 Sensitivity profile of gemcitabine and docetaxel

Developed resistant models of MG-63 and HOS-143B including single-agent and multi-agent induced sublines were used for this *in vitro* study to determine their sensitivity profile of gemcitabine and docetaxel. Figure 6.4 shows the sensitivity profile of gemcitabine and docetaxel determined on resistant sublines of MG-63 and HOS-143B expressed as a fold change. Across all the resistant sublines of MG-63, only MG-63/DOXR8 showed a significant increase of resistance to gemcitabine with 2.44 ± 0.26-fold ($p=0.001$) compared to parental control MG-63 as shown in Figure 6.4A. MG-63/CISR8 also exhibited a trend in increasing resistance to gemcitabine with 2.01 ± 0.56-fold but was not significant ($p > 0.05$). For docetaxel, only MG-63/TRIR8 showed an increase trend of resistant compared to MG-63 with 1.73 ± 0.61-fold ($p > 0.05$). However, MG-63/DOXR8 and MG-63/MTXR8 showed a decrease resistant trend to docetaxel with 0.88 ± 0.32-fold ($p > 0.05$) and 0.83 ± 0.18-fold ($p > 0.05$) respectively (Fig. 6.4A).

In Figure 6.4B, the resistant sublines of HOS-143B did not show significant changes of sensitivity to the gemcitabine drug. The fold change determined on the resistant models were between the range of 0.68 – 1.40-fold ($p > 0.05$) compared to parental control HOS-143B. However, for the docetaxel drug profile, HOS-143B/MTXR8 exhibited a significant increase of resistant fold to docetaxel with 2.32 ± 0.17-fold ($p=0.005$) compared to HOS-143B (Fig. 6.4B). HOS-143B/DOXR8 and HOS-143B/TRIR8 showed an increase resistant trend to docetaxel with 1.35 ± 0.17-fold ($p > 0.05$) and 1.49 ± 0.36-fold ($p > 0.05$) respectively. Conversely, HOS-143B/CISR8 showed a decrease resistant trend to docetaxel with 0.73 ± 0.16-fold ($p > 0.05$) (Fig. 6.4B).

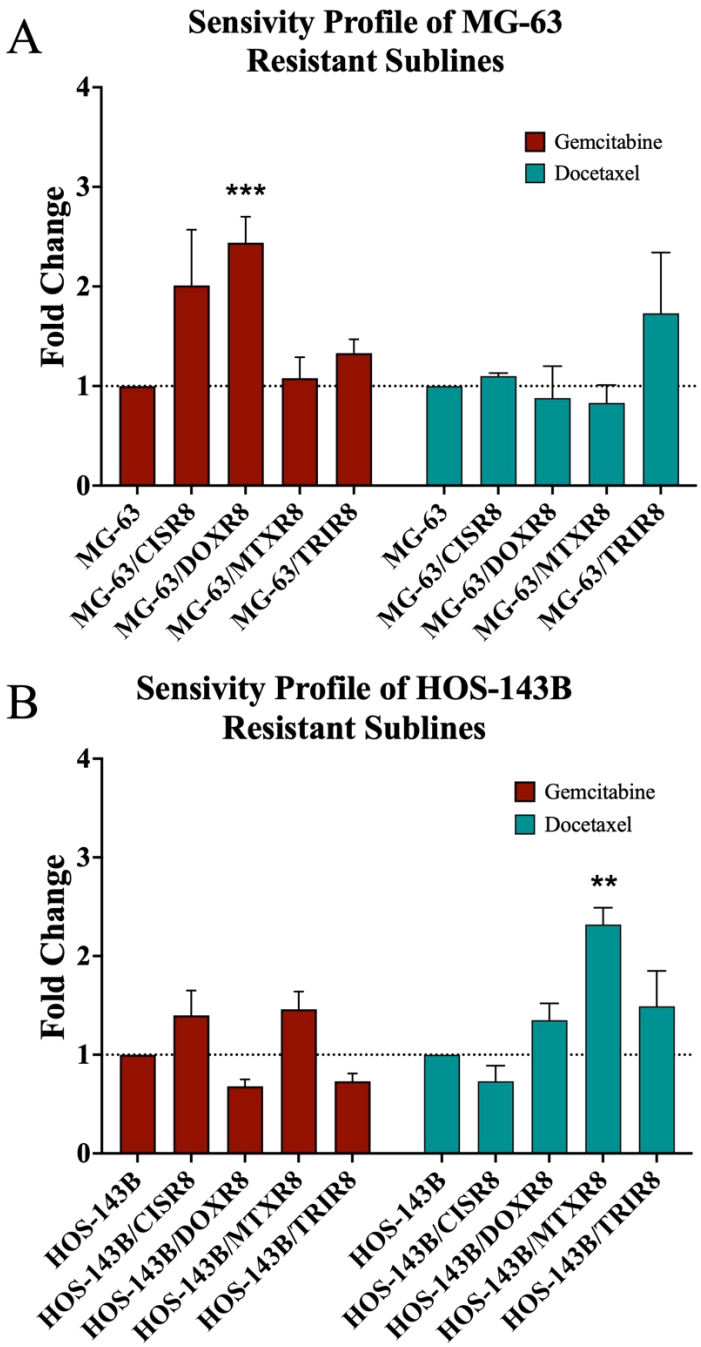

Figure 6.4: Sensitivity profile of gemcitabine and docetaxel on resistant sublines of MG-63 and HOS-143B. Cytotoxicity assays were performed to determine the fold change of the gemcitabine and docetaxel of (A) MG-63 resistant sublines comparing to parental cell line MG-63, and (B) HOS-143B resistant sublines comparing to parent cell line HOS-143B. Data represents in fold change and error bars represent SEM (n=3). ** = $p<0.01$, *** = $p<0.001$, Two sample *t*-test.

6.3.2.2 Sensitivity profile of combination of gemcitabine and docetaxel

The sensitivity profile of combination of gemcitabine and docetaxel was also performed by cytotoxicity assay on resistant sublines of MG-63 and HOS-143B as shown in Figure 6.5. The fold change was determined compared to the parental control to investigate the sensitivity of the resistant models on the combination treatment of gemcitabine and docetaxel.

Figure 6.5A has shown the resistant sublines MG-63/DOXR8 exhibited a significant fold resistant to the combination of gemcitabine and docetaxel with 2.50 ± 0.53-fold ($p=0.04$) compared to the parental control MG-63. MG-63/CISR8 and MG-63/TRIR8 showed an increase trend of resistant with 1.14 ± 0.14-fold ($p > 0.05$) and 1.30 ± 0.22-fold ($p > 0.05$) respectively. In contrast, MG-63/MTXR8 showed a trend of sensitivity to the combination of gemcitabine and docetaxel with 0.62 ± 0.09-fold ($p > 0.05$) as shown in Figure 6.5A.

For HOS-143B resistant sublines, HOS-143B/MTXR8 and HOS-143B/TRIR8 both showed a significant fold resistant to the combination of drugs with 2.09 ± 0.32-fold ($p=0.017$) and 2.44 ± 0.41-fold ($p=0.013$) respectively comparing to parental control HOS-143B (Fig. 6.5B). HOS-143B/CISR8 was determined to show an increase trend of resistant to the combination of drugs with 1.16 ± 0.26-fold ($p > 0.05$) compared to HOS-143B. HOS-143B/DOXR8 showed a similar IC_{50} value with HOS-143B with 0.99 ± 0.22-fold ($p > 0.05$) as shown in Figure 6.5B.

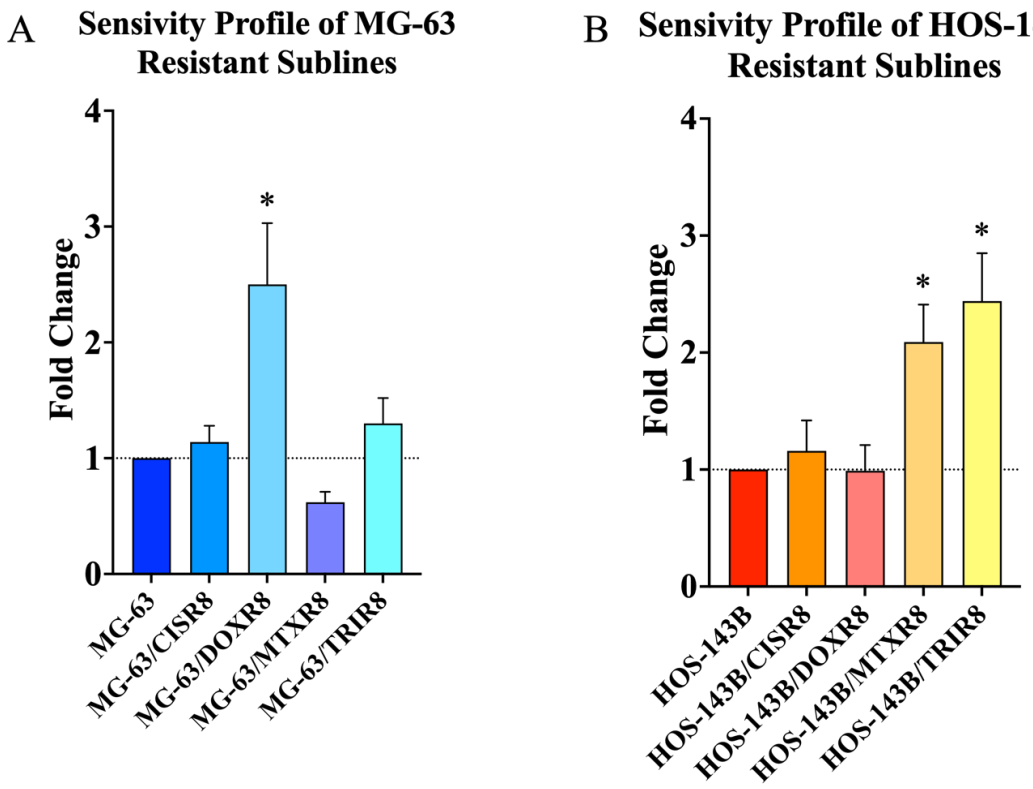

Figure 6.5: Sensitivity profile of combination of gemcitabine and docetaxel on resistant sublines of MG-63 and HOS-143B. Cytotoxicity assays were performed to determine the fold change of the combination of gemcitabine and docetaxel of (A) MG-63 resistant sublines comparing to parental cell line MG-63, and (B) HOS-143B resistant sublines comparing to parent cell line HOS-143B. Data represents in fold change and error bars represent SEM (n=3). * = $p<0.05$, ** = $p<0.01$, Two sample *t*-test.

6.3.2.3 Correlation analysis

Correlation between the IC_{50} value of doxorubicin, docetaxel, combination of gemcitabine and docetaxel, and the expression of P-gp was analysed as shown in Figure 6.6 and 6.7. The correlation analysis was performed by Pearson correlation (Nahler, 2009). A moderate correlation was shown between the IC_{50} value of doxorubicin and combination of gemcitabine and docetaxel in HOS-143B resistant sublines, $r = 0.532$ (Fig. 6.6). A strong correlation was shown between the IC_{50} value of doxorubicin and the gene expression of P-gp in HOS-143B resistant sublines, $r = 0.941$ (Fig. 6.6). Furthermore, a strong correlation was also shown between the IC_{50} value of docetaxel and the gene expression of P-gp in MG-63 resistant sublines, $r = 0.875$ (Fig. 6.7).

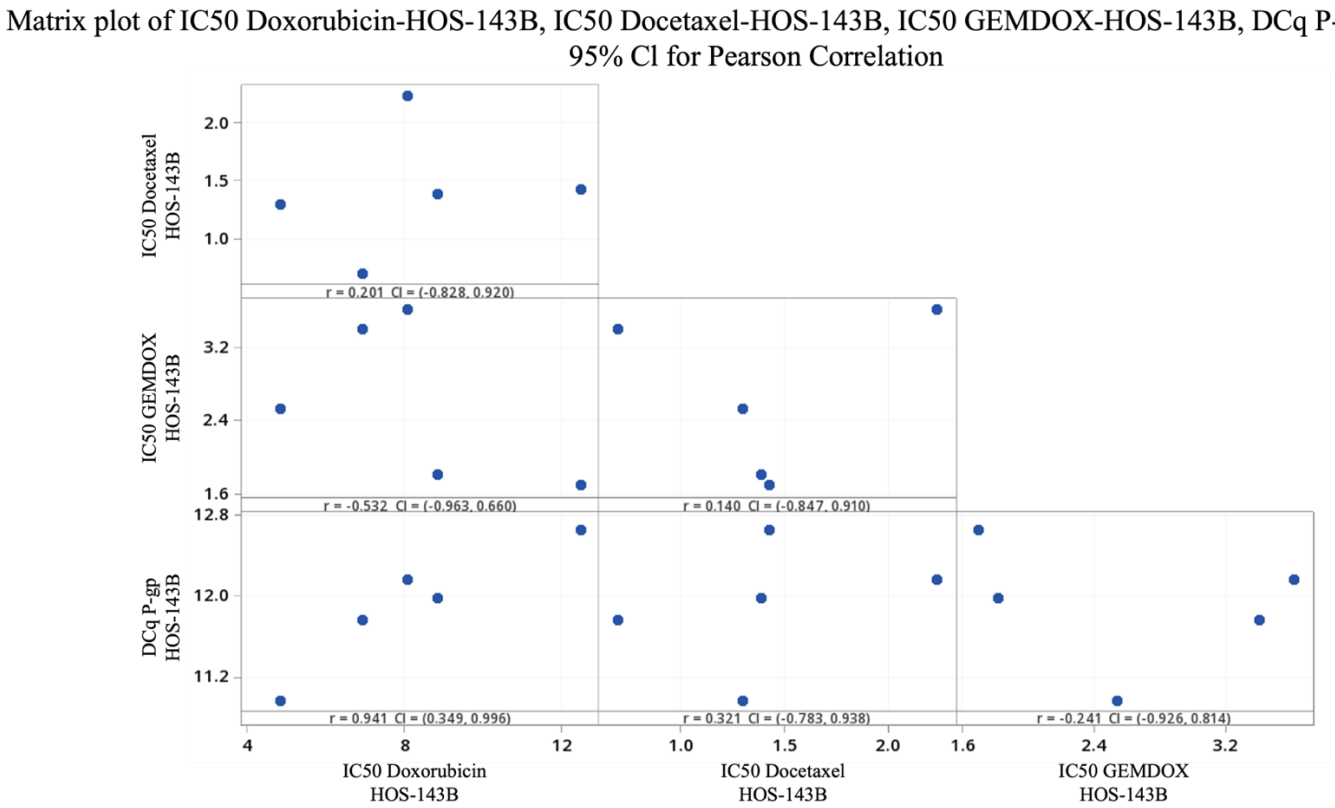

Figure 6.6: Correlation analysis on HOS-143B resistant sublines. Correlation was performed between the IC_{50} value of doxorubicin, docetaxel, combination of gemcitabine and docetaxel, and the gene expression of P-gp. $r > 0.5$ moderate correlation, $r > 0.7$ strong correlation, Pearson correlation test.

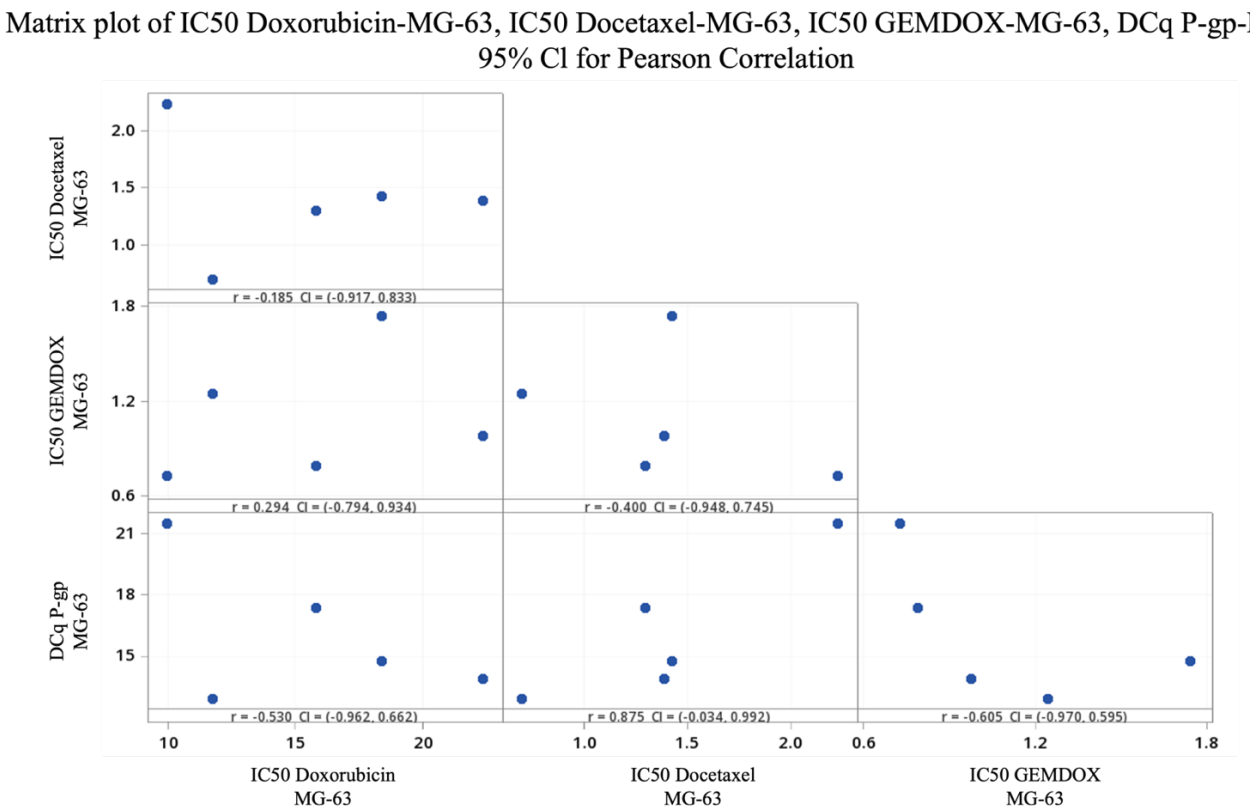

Figure 6.7: Correlation analysis on MG-63 resistant sublines. Correlation was performed between the IC_{50} value of doxorubicin, docetaxel, combination of gemcitabine and docetaxel, and the gene expression of P-gp. $r > 0.5$ moderate correlation, $r > 0.7$ strong correlation, Pearson correlation test.

6.4 Discussion

6.4.1 Systematic review study

6.4.1.1 Response data

This systematic review study focused on investigating the efficacy of gemcitabine and docetaxel combination chemotherapy on osteosarcoma patients as the second-line therapy as it has emerged as a potential alternative treatment in the past 10 years. Many retrospective studies from several institutions had been performed on this combination treatment, however, there remains a lack of strong conclusive evidence on the efficacy of this combination treatment for relapsed osteosarcoma patients and survival outcomes remained unclear. Therefore, the aim of this systematic review was to determine the efficacy of gemcitabine and docetaxel combination treatment for relapsed osteosarcoma patients, and to determine if the efficacy was associated with the characteristics of patients such as age, sex, and also the drug doses administered for gemcitabine.

The prognosis of primary osteosarcoma disease was found to be worse in older patients than younger patients, mainly due to lower drug doses administered due to intolerance of chemotherapy toxicities and the higher prevalence of tumour in axial locations (Durfee, Mohammed and Luu, 2016). In this systematic review study, the gemcitabine and docetaxel combination regimen also showed a similar result as the result of Chi-squared analysis determined a significant difference between the response of age <18 compared to ≥18 (Fig. 6.2A). The analysis also shown a total number of 34 patients in the group of age <18 had responded to the treatment compared to an expected count of 24.15, while total number of 20 patients in the group of age ≥18 had responded to the treatment compared to an expected count of 29.85. The responded patients in the analysis included patients experienced a complete response, partial response, and a stable disease. Therefore, this result has indicated that a higher number of patients with age <18 has

responded to the combination of GEMDOX regimen than the patients with age ≥18. Thus, combination of gemcitabine and docetaxel regimen has a higher efficacy in younger patients (<18 years) as a second-line therapy for relapsed osteosarcoma.

The gender of the patients was also determined to have a different prognosis and overall survival for primary osteosarcoma treated with conventional chemotherapy treatment. Studies have indicated female patients showed a better prognosis compared to male patients (Scranton *et al.*, 1975; Petrilli *et al.*, 1991; Smeland *et al.*, 2019). The result of the Chi-squared analysis in this systematic review study also determined a significant difference of number of patients responded to GEMDOX regimen between the gender of male and female patients as shown in Figure 6.2B. However, the result showed a higher number of male patients responded to the treatment than female patients in the eligible studies included in this review. The total number of patients in the group of "Equal Gender" responded to the treatment was 9 compared to the expected number of 15.6, and the total number of patients in the group "More Males" was 17 compared to the expected number of 10.4. This indicated that more males' patients had responded to the combination of GEMDOX treatment, which suggests the efficacy of this treatment as the second-line therapy for relapsed osteosarcoma patients was higher in male compared to female patients. In addition, the *in vitro* result from the resistant models developed form MG-63 and HOS-143B cell lines are showing MG-63 resistant models were generally more sensitive to GEMDOX therapy compared to HOS-143B resistant models, where only one model (MG-63/DOXR8) from MG-63 being resistant compared to two models (HOS-143B/MTXR8 and HOS-143B/TRIR8) from HOS-143B. MG-63 cell line was established from 14-year old male and HOS-143B was originally derived from a 13-year old Caucasian female (Pautke *et al.,* 2004; Luu *et al.,* 2005)

However, this analysis has been performed by categorising the eligible studies into "Equal Gender" and "More Males" due to the lack of information of the patients included in the studies. Therefore, the number of the gender of the patients in each sub-group was only represented by percentage and no accurate number of male and female patients were able to extract for comparison. Furthermore, there was none of the included eligible studies included only male or female patients and the response data was also not reported based on the gender of the patients. For example, the study from Lee *et al.* included total number of 28 patients with high number of patients responded to the treatment but the exact number of male or female patients responded was unknown and unable to extract accurately for analysis (Lee *et al.*, 2016). The contrasting result seen in our systematic review where more male patients responded to GEMDOX regimen compared to other literature could also be due to the different regimen the patients had received previously during their first-line therapy treatment, including single-agent cisplatin and MAP therapy (Scranton *et al.*, 1975; Petrilli *et al.*, 1991; Smeland *et al.*, 2019). Therefore, as there are no established prognostic factors for relapsed patients who received combination of GEMDOX regimen in osteosarcoma patients, our findings could be important for identifying the prognostic factors for this subset of patients.

The included eligible studies in this systematic review study have used three different doses of gemcitabine in the GEMDOX regimen as shown in Table 6.4, including the lowest 675 mg/m^2, 900 mg/m^2, and the highest 1,000 mg/m^2. The lowest (675 mg/m^2) and the highest (1,000 mg/m^2) were used to compare the response of the patients by Chi-squared analysis in this systematic review study with the hypothesis of greater difference between doses may translate into greater difference in response. However, the analysis result indicate there was no significant association between the dose of gemcitabine used in GEMDOX regimen and the response of the patients as shown in Figure 6.2C. Even

though, some other variables may be affecting the comparison analysis such as the dose of docetaxel patients received, and the reduced dose of gemcitabine due to adverse effects. However, all the original doses of gemcitabine used in each of the studies was reported to be the same across all the included eligible studies. Therefore, the availability and complete response data that are able to extract based on the doses of gemcitabine increases the confidence on the findings and our Chi-squared analysis result.

There was no significant association between the doses of gemcitabine used and the response of the patients (Fig. 6.4C). This suggests that the doses of gemcitabine used at 675 mg/m^2 contributed the same efficacy as the doses at 1,000 mg/m^2. Therefore, patients may benefit more from the gemcitabine doses at 675 mg/m^2 to reduce the exposure of the cytotoxic agent which causes the adverse effect. The doses of gemcitabine and docetaxel recommended by the NHS for the treatment of sarcomas is 675 mg/m^2 of gemcitabine and 75 mg/m^2 of docetaxel, with the indication of increasing these doses to 900 mg/m^2 and 100 mg/m^2, respectively if the standard dose is well tolerated (National Health Service, 2016). Currently there are no studies performed to investigate the efficacy of gemcitabine with the dose higher than 1,000 mg/m^2 and if this dose of gemcitabine is tolerable by patients.

6.4.1.2 Toxicity data

The most common adverse effects reported on the GEMDOX regime are haematological toxicities include neutropenia, thrombocytopenia, and anaemia with 36%, 35.3%, and 18.04% of the total patients, respectively as shown Table 6.5. The association between three of these reported toxicities and the characteristic of the patients was investigated by Chi-squared analysis in this systematic review. A study from Ferrari *et al.* has indicated that children below the age of 14 years and female patients experienced a higher incidence of grade 4 thrombocytopenia and neutropenia with MAP + I regimen (Ferrari *et al.*, 2009).

However, the Chi-squared analysis performed in this review study shows no significant association between the incidences of grade 3 and 4 toxicities (neutropenia, thrombocytopenia, and anaemia) reported on GEMDOX regimen and the characteristics of the patients (age, gender, and doses of gemcitabine) as shown in Figure 6.3.

6.4.2. *In vitro* study

The developed osteosarcoma resistant sublines from MG-63 and HOS-143B by single-agent and multi-agent were used in this study to simulate the similar clinical condition where relapsed osteosarcoma patients received the standard chemotherapy regimen before. The cytotoxicity effect of individual gemcitabine and docetaxel were shown to remain constant on most of the resistant models compared to their respective parental control, except for MG-63/DOXR8 and HOS-143B/MTXR8 (Figure 6.4). MG-63/DOXR8 showed a significant fold resistant to gemcitabine compared to MG-63 and HOS-143B/MTXR8 showed a significant fold resistant to docetaxel compared to HOS-143B. This suggests that osteosarcoma cells with acquired doxorubicin or methotrexate resistance is likely to be cross resistant to gemcitabine. Furthermore, due to their significant fold resistant showing on MG-63/DOXR8 to gemcitabine and HOS-143B/MTXR8 to docetaxel, they both also demonstrated significant fold resistant to the combination of both of the drugs (Fig. 6.5). Moreover, another resistant model HOS-143B/TRIR8 without showing fold resistant to both gemcitabine and docetaxel, is showing a fold resistant to the combination of the drugs (Fig. 6.5).

Only 3 out of 8 of the osteosarcoma resistant sublines were determined to have significant fold resistance to the combination of gemcitabine and docetaxel. This suggests that most of the developed resistant sublines remained comparably sensitive to the combination of gemcitabine and docetaxel compared to their parental control MG-63 and HOS-143B.

Therefore, this result also indicates patients who acquire drug resistance to the combination treatment of cisplatin, doxorubicin, and methotrexate, will have a high potential to remain an equivalent sensitivity to the combination treatment of gemcitabine and docetaxel especially with cisplatin resistance, where MG-63/CISR8 and HOS-143B/CISR8 both showed resistance to the GEMDOX combination.

Moreover, as docetaxel is one of the substrates of P-gp (Shirakawa *et al.*, 1999), a correlation analysis was performed between the IC_{50} value of doxorubicin, docetaxel, combination of gemcitabine and docetaxel, and the gene expression of P-gp. The correlation analysis result shown in Figures 6.6 and 6.7 determine a strong correlation between IC_{50} value of doxorubicin and the gene expression of P-gp in HOS-143B resistant sublines, r = 0.914 (Fig. 6.6), and between IC_{50} value of docetaxel and P-gp expression in MG-63 resistant sublines, r = 0.875 (Fig. 6.7). The strong correlation between the IC_{50} value of docetaxel and P-gp expression suggests that docetaxel is one of the substrates of P-gp in the cells. This also indicates that osteosarcoma cells with acquired doxorubicin resistant with overexpression of P-gp are cross resistant to docetaxel. In contrast, there is no strong or medium correlation between the P-gp expression and IC_{50} value of GEMDOX. However, the cross resistance of docetaxel through P-gp could potentially reduce the efficacy of the GEMDOX combination treatment especially for patients with overexpression of P-gp.

6.5 Conclusion

This systematic review study has determined the age and gender of the patients will have a prognostic effect on the GEMDOX regimen as the second-line treatment for relapsed osteosarcoma. Moreover, the age and gender of the patients, and the doses used for GEMDOX regime did not affect the incidence of toxicities. Lastly, most of the

osteosarcoma resistant sublines have remained a similar sensitivity to either single-agent gemcitabine, docetaxel, and the combination of both, which indicates that the GEMDOX treatment has a high potential for efficacy in relapsed osteosarcoma patients especially those with cisplatin resistance.

Chapter 7: General discussion

7.1 Discussion

7.1.1 Establishment of multi-agent osteosarcoma resistant models

Developing resistant osteosarcoma cell lines is one approach to understand the resistant mechanisms that may occur in osteosarcoma patients. The aim is to discover a counter strategy to reverse or overcome the drug resistance in osteosarcoma cells. Various osteosarcoma resistant models have been developed in several studies with different chemotherapeutic agents, mainly cisplatin (Perego *et al.*, 1999; Han *et al.*, 2014; Jiang *et al.*, 2017; Song *et al.*, 2017; Zhao, Zhang and Zhang, 2021), doxorubicin (Oda *et al.*, 2000; Niu *et al.*, 2010; Roncuzzi, Pancotti and Baldini, 2014; Buondonno *et al.*, 2019), and methotrexate (Serra *et al.*, 2004; Yin *et al.*, 2007; Li *et al.*, 2009; Wang and Li, 2014; Ding *et al.*, 2018), as they are the main chemotherapeutic drugs used in the treatment (Whelan *et al.*, 2015). However, none of the resistant models are clinically-relevant which represent the patients who receive the chemotherapy treatment in the clinical setting. Furthermore, all the current resistant models published in the literature were developed by using only single agents, which decreases the accuracy of these resistant models to patients who received a combination of chemotherapeutic drugs. Therefore, one of the aims of this project was to establish clinically relevant osteosarcoma resistant models by using single and multi-agents to overcome the challenge faced in laboratory investigation, which is the absence of a more accurate resistant models to study in osteosarcoma.

In this study, clinically relevant osteosarcoma models were successfully developed from MG-63 and HOS-143B cell lines and categorised into single-agent and multi-agent resistant models. The result shown in Figure 3.8 indicates that single-agent resistant models showed a higher fold resistance compared to multi-agent resistant models in both MG-63 and HOS-143B. This also suggests that the current use of combination of drugs in the treatment process for osteosarcoma patients reduces the risk of acquiring high

levels of drug resistance in the tumour cells (Whelan *et al.*, 2015). Even if the tumour cells acquire the resistant mechanisms, the fold resistant acquired will be lower compared to receiving a single-drug treatment. Furthermore, the major difference between the osteosarcoma cell lines MG-63 and HOS-143B is their different metastatic potential. The hypothesis was that the cell line with higher metastatic potential (HOS-143B) would acquire a faster and higher fold of resistant to the drugs. However, during the development process, there was no major difference between the two cell lines in acquiring resistance to all of the selecting agents including single and multi-agent induced method as shown in Figure 3.7.

Cisplatin has been shown to inhibit various types of tumours including osteosarcoma by cross-linking DNA to interfere with mitosis and promote apoptosis (Dasari and Tchounwou, 2014). Doxorubicin inhibits the synthesis of DNA in the cells by intercalating DNA (Carvalho *et al.*, 2009). Methotrexate also inhibits the synthesis of DNA by inhibiting dihydrofolate reductase (Genestier *et al.*, 2000). All three of these drugs have their own mechanisms of action in inhibiting the cancer cells growth. In this study, even though the multi-agent resistant models (MG-63/TRIR8 and HOS-143B/TRIR8) exhibited resistance to the combination of drugs, however they did not show any acquired resistance to the single-agent drugs of cisplatin, doxorubicin, or methotrexate (Table 4.1). This led us to investigate the apoptosis profile of these multi-agent resistant models and the results had shown that the MG-63/TRIR8 was more resistant to cisplatin and methotrexate, and HOS-143B/TRI was more resistant to doxorubicin and methotrexate compared to their respective parental control cell lines. This interesting findings with different selected resistant mechanisms observed in between MG-63/TRIR8 and HOS-143B/TRIR8 has directed us to refer back to the sensitivity profile of the parental cell lines MG-63 and HOS-143B. MG-63 was

determined to have a lower IC_{50} value of cisplatin (0.19 ± 0.07 μg/mL) compared to HOS-143B (0.38 ± 0.34 μg/mL), HOS-143B was indicated to have a lower IC_{50} value of doxorubicin (3.43 ± 0.21 ng/mL) compared to MG-63 (7.68 ± 1.78 ng/mL), and they both have approximately similar IC_{50} value of methotrexate at 11.57 ± 7.78 ng/mL for MG-63 and 12.56 ± 2.68 ng/mL for HOS-143B. This suggests that the osteosarcoma cell lines MG-63 was initially more sensitivity to cisplatin and HOS-143B was initially more sensitive to doxorubicin. After the multiple rounds of treatment with combination of drugs, even though no resistance was seen in the multi-agent resistant models to single drugs, but the osteosarcoma cells appear to acquire their resistance mechanism based on their most sensitive drug. Therefore, the resistance of MG-63/TRIR8 was determined to be compensated more from cisplatin and methotrexate resistant mechanisms, while HOS-143B/TRIR8 was complimented largely from doxorubicin and methotrexate according to the apoptosis result (Fig. 4.13).

A study from Ma *et al.* has investigated the synergy effect of three of these drugs compared to single drug by co-delivering them into the osteosarcoma cells MG-63 and Saos-2. Their results determined that the hydrogel coloaded with three of the drugs demonstrated a lower IC_{50} value compared to single drug, which indicated the combination of the drugs exhibited synergistic effects on the cytotoxicity against Sao-2 and MG-63 cells (Ma *et al.*, 2015). The combination actions of these drugs to multiple targets could be the possible mechanisms for the synergistic effect of cisplatin, doxorubicin, and methotrexate in osteosarcoma cells and this synergistic effect were then enhanced the sensitivity of osteosarcoma cells and reduced the possibility of drug resistance (Jhaveri, Deshpande and Torchilin, 2014). These findings also explain the lower fold resistance in our multi-agent resistant models compared to single agent resistant models in Chapter 3. It is also noteworthy to mention that the drug

concentrations used were different in developing the single and multi-agent resistant models. As shown in Figure 3.1, the drug concentrations used to establish single-agent resistant models were relatively higher compared to multi-agent resistant models due to the cytotoxicity effect of multiple drugs are not tolerable in the osteosarcoma cells. This might also result in the lower fold resistance acquired in the multi-agent resistant models than the single-agent resistant models.

7.1.2 Association of drug resistance to EMT progression

Drug resistance has been widely reported to be associated with EMT in various cancer types including bladder cancer, pancreatic cancer, and breast cancer (Arumugam *et al.*, 2009; McConkey *et al.*, 2009; Huang, Li and Ren, 2015) but the mechanisms is still elusive. EMT is a biological process that involves the transition of an epithelial cell into mesenchymal cell phenotype via multiple biochemical changes including enhanced invasiveness and migratory capacity (Kalluri and Neilson, 2003). In this study, we determined the increased migration and invasion rate in MG-63 resistant models compared to parental control MG-63, especially MG-63/CISR8, MG-63/MTXR8, and MG-63/TRIR8 (Fig. 4.5 & 4.6). This increased migration and invasion rate in MG-63 resistant models was determined to be EMT-mediated as shown in Figure 4.10B, where the expression of EMT transcription factors ZEB1 and mesenchymal biomarkers (N-CAD) showed an increasing trend in the MG-63 resistant models compared to parental control. However, a contrasting finding was demonstrated in the HOS-143B resistant models with reduced migration and invasion rate, and it was suggested to be caused by MET (reverse of EMT) as the gene expression of E-CAD tended to be upregulated trend and N-CAD tended to be a downregulated trend in all the HOS-143B resistance models (Fig. 4.10C). Even though HOS-143B resistant models acquired resistance to all three of the drugs in the single-agent resistant models, they did not experience EMT progression

as shown in MG-63 resistant models. Instead, they had been under the transition from a more mesenchymal cell type to epithelial phenotype. This has suggested that the acquisition of drug resistance in osteosarcoma cells is not necessarily associated with EMT progression and enhanced migration and invasion rate of the cells.

The EMT progression of MG-63 resistant models could also be observed in the morphology changes determined in Figure 4.1. Even though parental cell line MG-63 originally showed a spindle-like fibroblast structure of the cells, the MG-63 resistant models showed a more elongated and thinner spindle-like fibroblast cell morphology with enlarged nuclear compared to MG-63 especially MG-63/CISR8 (Fig. 4.1B). Morphological changes on cells underwent EMT was widely reported in various types of cancer cells which was associated with various biological changes resulted in the morphological alteration from a cuboidal shape (epithelial) to a spindle-like structure (mesenchymal) (Smith and Bhowmick, 2016). Conversely in HOS-143B parental cell line, the cells were originally showed a mix types of cell morphology with cuboidal and spindle-like structure (Fig. 4.2A). Resistant models of HOS-143B/CISR8 and HOS-143B/DOXR8 did not show a significant morphological change compared to HOS-143B (Fig. 4.2B & C), however HOS-143B/MTXR8 and HOS-143B/TRIR8 showed a more irregular cells shape and enlarged structure (Fig. 4.2 D & E). This morphological changes on HOS-143B/MTXR8 and HOS-143B/TRIR8 may be associated with their migratory capacity of the cells as the migration rate were significantly decreased in these two resistant models compared to HOS-143B (Fig. 4.5C & D).

7.1.3 P-gp is the dominant resistant mechanisms for doxorubicin

As discussed in Chapter 4, overexpression of P-gp was observed in all the resistant models of MG-63 and HOS-143B except for MG-63/MTXR8 and HOS-143B/MTXR8

(Fig. 4.8). Across all single-agent induced resistant models, cisplatin, and doxorubicin-induced models of MG-63 and HOS-143B expressed upregulation of P-gp protein compared to their parental cell lines. Both of the multi-agent induced resistant models also exhibited similar overexpression level of P-gp protein. This suggested that only chemotherapeutic drugs cisplatin and doxorubicin were able to induce the overexpression of P-gp protein but not methotrexate. Based on the mechanisms of actions of three of these drugs, cisplatin and doxorubicin are known to interfere with the DNA of the cells directly to prevent synthesis of DNA and induced apoptosis, however methotrexate prevents the DNA synthesis indirectly by inhibition of the formation of purines and pyrimidines (Genestier *et al.*, 2000; Carvalho *et al.*, 2009; Dasari and Tchounwou, 2014). This suggests that the different strategy of mechanisms of action of the drugs in inhibiting the DNA synthesis either directly or indirectly could be the major factors on inducing the overexpression of P-gp in osteosarcoma.

Moreover, even though P-gp protein was overexpressed in resistant models induced by cisplatin, however it had not provided any cytotoxicity advantage to the cell as shown in Figure 4.7A, where elacridar as the P-gp inhibitor was unable to reverse the cytotoxicity effect of cisplatin. This suggests that the upregulation of P-gp protein by cisplatin was most likely due to the generalised stress response as cisplatin is not the substrate of P-gp (Hamaguchi *et al.*, 1993). Furthermore, the expression of P-gp could also be modulated by the formation of reactive oxygen species (ROS), which are produced in the response to cisplatin (Berndtsson *et al.*, 2007). Since the doxorubicin drug also generated free radical-mediated oxidative to damage the DNA within the cells (Sritharan and Sivalingam, 2021), this has again justified the observation of upregulated P-gp expression in cisplatin and doxorubicin induced resistant models in osteosarcoma cells but not methotrexate.

7.2.4 Potential therapeutic targets to overcoming resistant mechanisms

PCR arrays results in Chapter 5 has shown the most deregulated genes are HIF1A and SPHK1 across all the resistant models of MG-63 and HOS-143B. The selected genes on PCR arrays were based on the most recent reported literature with an association with the resistant mechanisms to each drug. Figure 5.4 also shows the protein expression of SPHK1 was significantly upregulated in MG-63/CISR8 and HOS-143B/CISR8. Sphingosine-1-phosphate (S1P), the product of SPHK1 was determined to play an important role in the regulation of cell proliferation and survival (Spiegel and Milstien, 2003; Maceyka *et al.*, 2012). Furthermore, ceramide as another product of SPHK1 was also found to be associated with cell cycle arrest, senescence, and cell death (Obeid *et al.*, 1993; Venable *et al.*, 1995; Nava *et al.*, 2000). SPHK1 sits in between the junction of ceramide and S1P, responsible in controlling the level of these pro-survival lipid S1P and pro-apoptotic lipids ceramide (Pulkoski-Gross and Obeid, 2018).

S1P as the product of SPHK1 was discovered to be transported out from the cell by several members of ABC transporter family including P-gp (Mitra *et al.*, 2006). Several studies have been performed to determine the correlation between the expression of SPHK1 and P-gp on cancer cells. In this study, a similar result was found where a strong and medium correlation has been determined between the expression of SPHK1 and P-gp in HOS-143B and MG-63 resistant cells, respectively (Fig. 5.5). HL-60 cells, a doxorubicin-sensitive leukaemia cell demonstrated SPHK1 inhibition but chemoresistant HL-60 cells, which expresses the P-gp had determined to exhibit SPHK1 activity (Bonhoure *et al.*, 2006). Another drug resistant prostate cancer cell PC3 also showed an elevated expression of SPHK1 receptor and exhibited higher level of SPHK1 activity (Akao *et al.*, 2006). A study by Pilorget *et al.* has determined the upregulation of SPHK1 stimulated the expression of P-gp in brain endothelial cell RBE4. They also found that

the P-gp activity stimulated by SPHK1 is mediated by the S1P receptors on the surface of the cells (Pilorget *et al.*, 2007). Moreover, an increased sensitivity of cisplatin was determined on SGC7901/DDP, a cisplatin-resistant gastric cancer cell line with the pre-treatment with SPHK inhibitor (SKI-II) (Zhu *et al.*, 2012). A significant association was also found in between the downregulated expression of SPHK1 and downregulated expression P-gp on SGC7901/DDP (Zhu *et al.*, 2012). These findings have once again justified the overexpression of P-gp on our cisplatin-resistant models (MG-63/CISR8 and HOS-143B/CISR8) was not due to the efflux of cisplatin through P-gp. In this study, the upregulation of P-gp on MG-63/CISR8 and HOS-143B/CISR8 was suggested to be stimulated by the overexpression of SPHK1 determined in Figure 5.4.

PCR arrays result had shown the upregulation of HIF1A gene on all the resistant models except HOS-143B/TRIR8 (Table 5.4 & 5.3) but the HIF1A protein was not determined due to the unstable structure of proteins under normoxic condition as discussed in Chapter 5. HIF1A as the master regulator of hypoxic condition has been widely studied in cancer cells and evidence has shown that the activity and expression of HIF1A can be modulated by SPHK1 (Ader *et al.*, 2008). Study by Ader *et al.* has also indicated a significant increase of SPHK1 activity before the HIF1A accumulation on PC-3 prostate and U87 glioblastoma cell models (Ader *et al.*, 2008). However, the activation of SPHK1 in low oxygen condition is yet unknown. Since SPHK1 and HIF1A both play an important in drug resistant as they were reported to be upregulated in various resistant cancer cells, understanding the correlation between SPHK1 and HIF1A and the mechanisms involve in the activation of both of the gene under hypoxic condition could serve as a potential therapeutic target for osteosarcoma.

7.2.5 Gemcitabine and docetaxel as a treatment for relapsed osteosarcoma

The systematic review in Chapter 6 has discussed about the combination of gemcitabine and docetaxel as a second-line treatment for relapsed osteosarcoma. The result has determined that the response of GEMDOX treatment on relapsed osteosarcoma patients are dependent on age, gender, but not dependent on the doses of gemcitabine. To further investigate the efficacy of gemcitabine and docetaxel on this subject, cytotoxicity profile of these drugs was investigated in our developed osteosarcoma resistant models. The developed osteosarcoma models could be used to represent patients with relapsed osteosarcoma with previously administered single or multi-agent chemotherapy.

The results have shown that across all the resistant models of MG-63, only MG-63/DOXR8 with doxorubicin resistance was determined to have a significant fold resistant to gemcitabine (Fig. 6.6A). Across HOS-143B resistant models, only HOS-143B/MTXR8 indicated significant fold resistant to docetaxel (Fig. 6.6B). These two resistant models also have been shown to be resistant to the combination of gemcitabine and docetaxel with another resistant subline HOS-143B/TRIR8 (Fig. 6.7). These findings indicate osteosarcoma cells with doxorubicin and methotrexate resistance are likely to be resistant to the combination of gemcitabine and docetaxel. Conversely, osteosarcoma cells with cisplatin resistance remain a comparably sensitive to gemcitabine and docetaxel as their parental cell lines.

Several resistant mechanisms of gemcitabine has been reported in various cancer cell types, including dysregulation of proteins involves in gemcitabine metabolism pathways and the overexpression of drug efflux pumps such as ABC transporter family proteins (Zhou *et al.*, 2010; Chen *et al.*, 2012). Furthermore, EMT has been reported to be involved in gemcitabine resistant mechanism via the activation of Wnt signalling pathway, which

increased the EMT activator ZEB1 transcription factor in mantle cell lymphoma (Sánchez-Tilló *et al.*, 2014). Another study by Quint *et al*. also determined a similar result in their developed gemcitabine resistant pancreatic cancer cells, which showed the upregulation of EMT biomarker in both Capan-1 and Panc-1 cells (Quint *et al.*, 2012). Likewise, a study by Wang *et al.* also determined the association of EMT in gemcitabine resistance in pancreatic cancer cells. Wang *et al.* also found the overexpression of HIF1A in gemcitabine resistant pancreatic cells and the inhibition of HIF1A successfully reversed the EMT progression and therefore suggesting HIF1A was critically involved in gemcitabine resistant mediated EMT in pancreatic cells (Wang *et al.*, 2014). These findings explain the significant increased resistance of gemcitabine in the MG-63 resistant models but not HOS-143B resistant models, as the MG-63 resistant sublines underwent EMT progression when acquiring the drug resistance but conversely HOS-143B resistant sublines underwent MET progression. It will also be important for future research to investigate the correlation between Wnt pathway, HIF1A, and EMT in osteosarcoma cells to overcome gemcitabine resistance.

Several resistant mechanisms of docetaxel have been identified, including alteration in tubulin subunits (Giannakakou *et al.*, 2000), activation of the MDR gene (Chen *et al.*, 2000), and mutation of genes in the ABC transporter family (Murray *et al.*, 2012). Docetaxel resistant sublines MCF7/DOC was determined to highly express the ABCB1 mRNA compared to MCF7, suggesting P-gp as the product of ABCB1, mediated the efflux of docetaxel (Li *et al.*, 2014). This docetaxel-resistant subline MCF7/DOC also exhibited a cross resistant to paclitaxel, doxorubicin, and methotrexate. In this study, methotrexate resistant subline HOS-143B/MTXR8 was determined to be significantly resistant to docetaxel across all other resistant sublines. Studies suggested the elevated ABCB1 gene, which produces P-gp to be responsible in docetaxel resistance (Chen *et al.*,

2000; Murray *et al.*, 2012; Li *et al.*, 2014). However, HOS-143B/MTXR8 did not show an elevated expression of P-gp protein and ABCB1 mRNA (Fig. 4.8) compared to HOS-143B. This suggests the P-gp protein is not the dominant resistant mechanisms for docetaxel in our osteosarcoma cells. Moreover, the correlation between the methotrexate and docetaxel resistant mechanisms is yet still unknown.

7.2.6 Overall research findings

The schematic diagram in Figure 7.1 shows the overall research findings on MG-63 and HOS-143B resistant models developed in this study. After the drug development, the resistant models of MG-63 and HOS-143B were overexpressed with P-gp glycoprotein compared to parental control. In addition, the expression of HIF1A and SPHK1 genes were upregulated in most of the resistant models of MG-63 and HOS-143B. There are evidence showing that the upregulation of SPHK1 could result in the increased expression of P-gp (Mitra *et al.*, 2006). Moreover, the interplay between SPHK1 and HIF1A also play an important role in regulation the drug resistance (Ader *et al.*, 2008). The overexpression of P-gp in the resistant models could also result in conferring resistant to the GEMDOX therapy, especially the doxorubicin and methotrexate resistant models (Fig. 6.5). However, the systematic review and pre-clinical *in vitro* study show that most of the resistant models still retained a comparable sensitivity to GEMDOX therapy compared to parental cell lines which show the efficacy of this combination treatment for relapsed patients. Furthermore, the plasticity event of EMT/MET processes showed in the resistant models are believed to be involved in the activation of tumour metastasis, where EMT activation promotes tumour cells dissemination and invasion from primary tumour site, while MET activation to support metastatic outgrowth in distant organs (56). The distinctive activation of EMT and MET from these two resistant model cell lines could demonstrate a different state of metastasis. MG-63 resistant models with the activation of

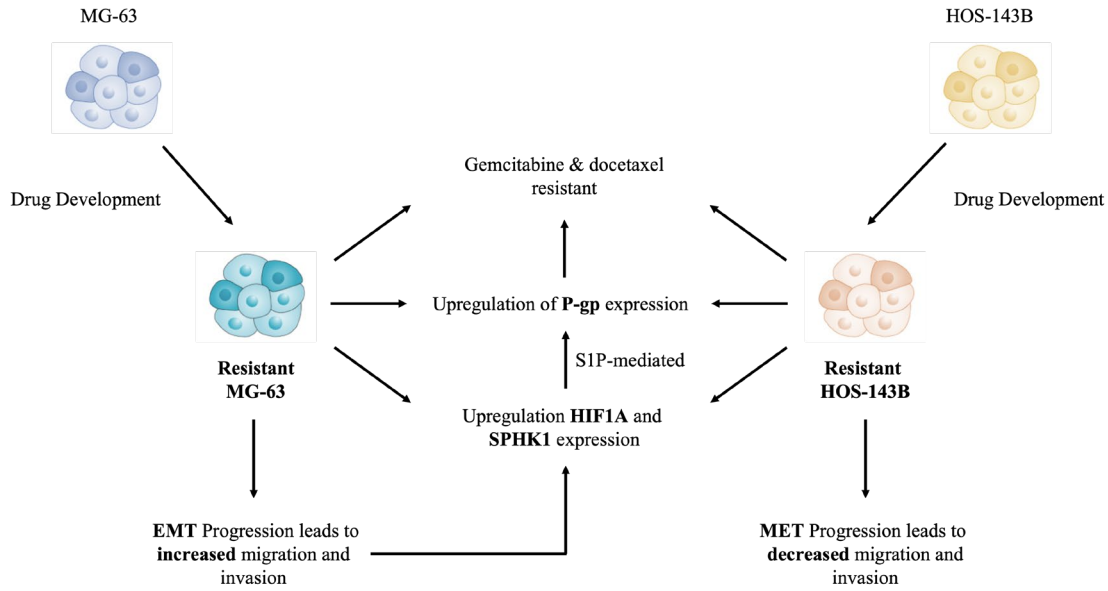

Figure 7.1: Schematic diagram of the overall characteristic and molecular changes of resistant osteosarcoma sublines. Drug resistance acquired in osteosarcoma exhibited morphological changes and alteration of migration and invasion assay mediated by EMT progression. The upregulation of SPHK1 and HIF1A in resistant cells mediated the upregulation of P-gp protein in cisplatin-treated resistant sublines. The gemcitabine and docetaxel resistance were mediated by the EMT progression and the expression of P-gp.

EMT could represent the primary tumour cells gradually dissemination, and HOS-143B resistant models are the tumour cells arriving in distant organs.

7.2 Future directions

7.2.1 Identify the effect of genes knockdown on osteosarcoma resistant cells

This study has determined two genes that are upregulated in both resistant osteosarcoma cell lines, which are SPHK1 and HIF1A. The protein level of SPHK1 has been determined to be significantly increased in cisplatin and doxorubicin-resistant models (Fig. 5.4A & B). However, due to the nature of the HIF1A protein, the expression level was not able to be determined. HIF1A protein level can be determined to set up the cell culture either under hypoxic condition or treating with hydroxylase inhibitor (Mizobuchi *et al.*, 2008; Gupta and Wish, 2017). After confirming the increasing expression of protein level in resistant osteosarcoma models, HIF1A could also be a good gene candidate to perform knockdown experiment to investigate the effect.

Gene knockdown experiment could be performed by CRISPR or RNA interference (siRNA) (Shan, 2010; Harrison *et al.*, 2014). Since both of the genes were shown to be associated with each other and contribute to the chemoresistance in cancer cells (Ader *et al.*, 2008), knocking down one of the genes in the osteosarcoma resistant cells could provide a good model to further study the inter-related molecular changes between two of the genes to understand the downstream mechanism pathway involved. Furthermore, since significant upregulation protein expression of SPHK1 was determined in MG-63/CISR8 and MG-63/DOXR8, they both could be used to perform the SPHK1 knockdown, and the sensitivity of cisplatin could then be assessed to find out if SPHK1 has a direct contributory effect in osteosarcoma cells to cisplatin. Moreover, since strong and medium correlation was determined between the expression of SPHK1 and P-gp in

this study, the expression level of P-gp could also be assessed after the knockdown of SPHK1 to determine if it is the effect of the overexpression of P-gp in cisplatin resistant cells.

7.2.2 Clinical implication of GEMDOX regimen

In in study, the review chapter has provided a clear outline for the important future avenues of investigation with regards to GEMDOX treatment for relapsed osteosarcoma. The study has also highlighted the need for a randomised Phase II clinical trial into the efficacy of GEMDOX therapy for the treatment of relapsed osteosarcoma. Since the studies included in the systematic review are mainly retrospective with a lack of accurate information about the treatment history of the patients, it would be important to have a clinical trial to compared GEMDOX therapy to conventional MAP therapy for this cohort of patient, as MAP remains the recommended second-line treatment. Furthermore, the incidence of severe toxicities associated with this regimen were relatively low, it would also be beneficial to determine if a higher dose of both gemcitabine and docetaxel are tolerated by patients, and whether they result in a greater treatment efficacy.

Furthermore, clinical samples from relapsed osteosarcoma patients in clinical trials could be collected and cultured in laboratory to establish relapsed osteosarcoma cells for study purposes. The relapsed or recurrent osteosarcoma cells could be used to study the resistant mechanisms towards GEMDOX therapy. In this study, the sensitivity of gemcitabine, docetaxel, and the combination of both have been determined in developed resistant osteosarcoma cells. The results have shown MG-63/DOXR8 is resistant to gemcitabine and HOS-143B/MTXR8 is resistant to docetaxel, they both also show resistant to the combination of both drugs (Fig. 6.4). Since the doxorubicin and methotrexate-resistant could decrease the efficacy of GEMDOX therapy in relapsed osteosarcoma cells,

investigating the molecular profile of these two resistant models related to gemcitabine and docetaxel resistant mechanism could identify the biomarker for relapsed osteosarcoma patient. Moreover, comparison between the established relapsed osteosarcoma cells and these two resistant models could also help with understanding the resistant mechanisms or pathway towards GEMDOX therapy.

7.3 Limitations

One of the limitations of this study is the application of two different platforms for qPCR analysis. In this study, both SYBR Green and Taqman qPCR gene expression assays were used in investigating the targeted gene expression in the resistant models compared to parental cell lines. The mechanisms of these two different platforms are slightly different. Taqman qPCR used a fluorogenic single-stranded oligonucleotide probe that binds only the DNA sequence between the two PCR primers, therefore only specific PCR product can generate a fluorescent signal (Holland *et al.,* 1991). SYBR Green qPCR is widely used because of the ease in designing the assay and its relatively low setup and running costs. Unlike Taqman fluorescent probes, SYBR Green dye intercalates into double-stranded DNA to monitor the amplification of the target gene specifically initiated by gene-specific primers (Schneeberger *et al*., 1995). One drawback of SYBR Green assay is that the dye is nonspecific, which can generate false positive signals if nonspecific products or primer-dimers are present in the assay. The other drawback of the SYBR Green assay is that the length of the amplicon also affects the intensity of the amplification.

7.4 Conclusions

Overall, this study has successfully established multi-agent resistant osteosarcoma models to fill the gap of not having a true representative resistant model with possible underlying molecular changes modulates by combination of chemotherapeutic drugs within a single cell population. This study also determines the alteration of migratory and invasion capability in resistant osteosarcoma cells is associated with EMT and MET progression. However, the drug resistance acquired is not always associated with increased migration and invasion in osteosarcoma cells.

This study also indicates that the overexpression of P-gp protein in osteosarcoma-resistant models is mainly mediated by cisplatin and doxorubicin, but the cytotoxicity effect of cisplatin is unable to reverse by elacridar on cisplatin-mediated P-gp protein. This concludes that P-gp is only the dominant resistant mechanism of doxorubicin and the cisplatin-mediated P-gp expression is mainly due to the formation of S1P, the product of SPHK1. Furthermore, the overexpression of SPHK1 and HIF1A and their correlation suggests further study are required as they have great potential to serve as a new therapeutic target for osteosarcoma. Additionally, this study also indicates the gemcitabine and docetaxel combination treatment will have a high potential efficacy for relapsed osteosarcoma patients especially with cisplatin resistance.

Finally, these clinically relevant osteosarcoma cell lines with exhibited characteristic and molecular changes have proven them as an invaluable tool to study drug resistant mechanisms in osteosarcoma cell lines. These resistant models could be further utilised in future studies with great potential to further explore the mechanism and pathway involve in drug resistance for osteosarcoma.

References

Abraham-Juárez, M.J. (2019) 'Western Blot in Maize', *BIO-PROTOCOL*, 9(11). doi:10.21769/BioProtoc.3257.

Acloque, H. *et al.* (2009) 'Epithelial-mesenchymal transitions: the importance of changing cell state in development and disease', *The Journal of Clinical Investigation*, 119(6), pp. 1438–1449. doi:10.1172/JCI38019.

Adamski, J. *et al.* (2013) 'Hypoxia-induced cytotoxic drug resistance in osteosarcoma is independent of HIF-1Alpha', *PloS One*, 8(6), p. e65304. doi:10.1371/journal.pone.0065304.

Ader, I. *et al.* (2008) 'Sphingosine kinase 1: a new modulator of hypoxia inducible factor 1alpha during hypoxia in human cancer cells', *Cancer Research*, 68(20), pp. 8635–8642. doi:10.1158/0008-5472.CAN-08-0917.

Ader, I. *et al.* (2015) 'Neutralizing S1P inhibits intratumoral hypoxia, induces vascular remodelling and sensitizes to chemotherapy in prostate cancer', *Oncotarget*, 6(15), pp. 13803–13821. doi:10.18632/oncotarget.3144.

Adler, V. *et al.* (1999) 'Regulation of JNK signaling by GSTp', *The EMBO journal*, 18(5), pp. 1321–1334. doi:10.1093/emboj/18.5.1321.

Akao, Y. *et al.* (2006) 'High expression of sphingosine kinase 1 and S1P receptors in chemotherapy-resistant prostate cancer PC3 cells and their camptothecin-induced up-regulation', *Biochemical and Biophysical Research Communications*, 342(4), pp. 1284–1290. doi:10.1016/j.bbrc.2006.02.070.

Alderden, R.A., Hall, M.D. and Hambley, T.W. (2006) 'The Discovery and Development of Cisplatin', *Journal of Chemical Education*, 83(5), p. 728. doi:10.1021/ed083p728.

Ali, S. *et al.* (2019) 'Cisplatin Synergistically Enhances Antitumor Potency of Conditionally Replicating Adenovirus via p53 Dependent or Independent Pathways in Human Lung Carcinoma', *International Journal of Molecular Sciences*, 20(5), p. 1125. doi:10.3390/ijms20051125.

Almasan, A. *et al.* (1995) 'Deficiency of retinoblastoma protein leads to inappropriate S-phase entry, activation of E2F-responsive genes, and apoptosis', *Proceedings of the National Academy of Sciences of the United States of America*, 92(12), pp. 5436–5440. doi:10.1073/pnas.92.12.5436.

Alvarez, M. *et al.* (1995) 'Generation of a drug resistance profile by quantitation of mdr-1/P-glycoprotein in the cell lines of the National Cancer Institute Anticancer Drug Screen', *The Journal of Clinical Investigation*, 95(5), pp. 2205–2214. doi:10.1172/JCI117910.

Alves, A.C. *et al.* (2017) 'Influence of doxorubicin on model cell membrane properties: insights from in vitro and in silico studies', *Scientific Reports*, 7(1), p. 6343. doi:10.1038/s41598-017-06445-z.

Ambudkar, S.V. *et al.* (1999) 'Biochemical, cellular, and pharmacological aspects of the multidrug transporter', *Annual Review of Pharmacology and Toxicology*, 39, pp. 361–398. doi:10.1146/annurev.pharmtox.39.1.361.

Ando, K. *et al.* (2013) 'Current therapeutic strategies and novel approaches in osteosarcoma', *Cancers*, 5(2), pp. 591–616. doi:10.3390/cancers5020591.

Andresen, KelliJ. *et al.* (2004) 'Imaging features of low-grade central osteosarcoma of the long bones and pelvis', *Skeletal Radiology*, 33(7). doi:10.1007/s00256-004-0796-4.

Andrews, P.A. *et al.* (1988) 'cis-Diamminedichloroplatinum(II) accumulation in sensitive and resistant human ovarian carcinoma cells', *Cancer Research*, 48(1), pp. 68–73.

Arany, I. and Safirstein, R.L. (2003) 'Cisplatin nephrotoxicity', *Seminars in Nephrology*, 23(5), pp. 460–464. doi:10.1016/s0270-9295(03)00089-5.

Arcamone, F. *et al.* (1969) 'Adriamycin, 14-hydroxydaunomycin, a new antitumor antibiotic from S. peucetius var. caesius', *Biotechnology and Bioengineering*, 11(6), pp. 1101–1110. doi:10.1002/bit.260110607.

Arumugam, T. *et al.* (2009) 'Epithelial to mesenchymal transition contributes to drug resistance in pancreatic cancer', *Cancer Research*, 69(14), pp. 5820–5828. doi:10.1158/0008-5472.CAN-08-2819.

Asada, N., Tsuchiya, H. and Tomita, K. (1999) 'De novo deletions of p53 gene and wild-type p53 correlate with acquired cisplatin-resistance in human osteosarcoma OST cell line.', *Anticancer research*, 19(6B), pp. 5131–5137.

Babineau, J. (2014) 'Product review: Covidence (systematic review software)', *Journal of the Canadian Health Libraries Association*, 68–71.

Bacci, G. *et al.* (2001) 'Telangiectatic osteosarcoma of the extremity: Neoadjuvant chemotherapy in 24 cases', *Acta Orthopaedica Scandinavica*, 72(2), pp. 167–172. doi:10.1080/000164701317323426.

Bacci, G. *et al.* (2002) 'High Dose Ifosfamide in Combination with High Dose Methotrexate, Adriamycin and Cisplatin in the Neoadjuvant Treatment of Extremity Osteosarcoma: Preliminary Results of an Italian Sarcoma Group/Scandinavian Sarcoma

Group Pilot Study', *Journal of Chemotherapy*, 14(2), pp. 198–206. doi:10.1179/joc.2002.14.2.198.

Bacci, G. (2003) 'Neoadjuvant chemotherapy for osteosarcoma of the extremities with metastases at presentation: recent experience at the Rizzoli Institute in 57 patients treated with cisplatin, doxorubicin, and a high dose of methotrexate and ifosfamide', *Annals of Oncology*, 14(7), pp. 1126–1134. doi:10.1093/annonc/mdg286.

Bacci, G. *et al.* (2006) 'Bone metastases in osteosarcoma patients treated with neoadjuvant or adjuvant chemotherapy The Rizzoli experience in 52 patients', *Acta Orthopaedica*, 77(6), pp. 938–943. doi:10.1080/17453670610013268.

Baker, J. *et al.* (2009) 'Docetaxel-related side effects and their management', *European Journal of Oncology Nursing: The Official Journal of European Oncology Nursing Society*, 13(1), pp. 49–59. doi:10.1016/j.ejon.2008.10.003.

Bakiri, L. *et al.* (2015) 'Fra-1/AP-1 induces EMT in mammary epithelial cells by modulating Zeb1/2 and TGFβ expression', *Cell Death and Differentiation*, 22(2), pp. 336–350. doi:10.1038/cdd.2014.157.

Barpe, D.R., Rosa, D.D. and Froehlich, P.E. (2010) 'Pharmacokinetic evaluation of doxorubicin plasma levels in normal and overweight patients with breast cancer and simulation of dose adjustment by different indexes of body mass', *European Journal of Pharmaceutical Sciences: Official Journal of the European Federation for Pharmaceutical Sciences*, 41(3–4), pp. 458–463. doi:10.1016/j.ejps.2010.07.015.

Bartke, T. *et al.* (2001) 'p53 upregulates cFLIP, inhibits transcription of NF-kappaB-regulated genes and induces caspase-8-independent cell death in DLD-1 cells', *Oncogene*, 20(5), pp. 571–580. doi:10.1038/sj.onc.1204124.

Barton-Burke, M. (1999) ‘Gemcitabine: a pharmacologic and clinical overview’, *Cancer Nursing*, 22(2), pp. 176–183. doi:10.1097/00002820-199904000-00011.

Beretta, G.L. *et al.* (2004) ‘Cellular pharmacology of cisplatin in relation to the expression of human copper transporter CTR1 in different pairs of cisplatin-sensitive and -resistant cells’, *Biochemical Pharmacology*, 68(2), pp. 283–291. doi:10.1016/j.bcp.2004.03.022.

Berndtsson, M. *et al.* (2007) ‘Acute apoptosis by cisplatin requires induction of reactive oxygen species but is not associated with damage to nuclear DNA’, *International Journal of Cancer*, 120(1), pp. 175–180. doi:10.1002/ijc.22132.

Bertino, J.R. *et al.* (1996) ‘Resistance mechanisms to methotrexate in tumors’, *Stem Cells (Dayton, Ohio)*, 14(1), pp. 5–9. doi:10.1002/stem.140005.

Bertoni, F., Bacchini, P. and Fabbri, N. (1993) ‘Osteosarcoma. Low-grade intraosseous-type osteosarcoma, histologically resembling parosteal osteosarcoma, fibrous dysplasia, and desmoplastic fibroma’, p. 8.

Biedler, J.L. and Riehm, H. (1970) ‘Cellular resistance to actinomycin D in Chinese hamster cells in vitro: cross-resistance, radioautographic, and cytogenetic studies’, *Cancer Research*, 30(4), pp. 1174–1184.

Bielack, S. *et al.* (2009) ‘Osteosarcoma: ESMO Clinical Recommendations for diagnosis, treatment and follow-up’, *Annals of Oncology*, 20(Supplement 4), pp. iv137–iv139. doi:10.1093/annonc/mdp154.

Bielack, S.S. *et al.* (1989) ‘Platinum disposition after intraarterial and intravenous infusion of cisplatin for osteosarcoma. Cooperative Osteosarcoma Study Group COSS’,

Cancer Chemotherapy and Pharmacology, 24(6), pp. 376–380. doi:10.1007/BF00257446.

Bielack, S.S. *et al.* (2002) 'Prognostic Factors in High-Grade Osteosarcoma of the Extremities or Trunk: An Analysis of 1,702 Patients Treated on Neoadjuvant Cooperative Osteosarcoma Study Group Protocols', *Journal of Clinical Oncology*, 20(3), pp. 776–790. doi:10.1200/JCO.2002.20.3.776.

Bielack, S.S. *et al.* (2008) 'Bone tumors in adolescents and young adults', *Current Treatment Options in Oncology*, 9(1), pp. 67–80. doi:10.1007/s11864-008-0057-1.

Bonhoure, E. *et al.* (2006) 'Overcoming MDR-associated chemoresistance in HL-60 acute myeloid leukemia cells by targeting sphingosine kinase-1', *Leukemia*, 20(1), pp. 95–102. doi:10.1038/sj.leu.2404023.

Borst, P. *et al.* (2000) 'A Family of Drug Transporters: the Multidrug Resistance-Associated Proteins', *JNCI Journal of the National Cancer Institute*, 92(16), pp. 1295–1302. doi:10.1093/jnci/92.16.1295.

Borst, P. and Schinkel, A.H. (2013) 'P-glycoprotein ABCB1: a major player in drug handling by mammals', *The Journal of Clinical Investigation*, 123(10), pp. 4131–4133. doi:10.1172/JCI70430.

Bouquerel, P. *et al.* (2016) 'Essential role for SphK1/S1P signaling to regulate hypoxia-inducible factor 2α expression and activity in cancer', *Oncogenesis*, 5, p. e209. doi:10.1038/oncsis.2016.13.

Braasch, D.A. and Corey, D.R. (2001) 'Locked nucleic acid (LNA): fine-tuning the recognition of DNA and RNA', *Chemistry & Biology*, 8(1), pp. 1–7. doi:10.1016/s1074-5521(00)00058-2.

Brabec, V. and Kasparkova, J. (2005) 'Modifications of DNA by platinum complexes. Relation to resistance of tumors to platinum antitumor drugs', *Drug Resistance Updates: Reviews and Commentaries in Antimicrobial and Anticancer Chemotherapy*, 8(3), pp. 131–146. doi:10.1016/j.drup.2005.04.006.

Brabletz, S. and Brabletz, T. (2010) 'The ZEB/miR-200 feedback loop--a motor of cellular plasticity in development and cancer?', *EMBO reports*, 11(9), pp. 670–677. doi:10.1038/embor.2010.117.

Braig, S. *et al.* (2011) 'CTGF is overexpressed in malignant melanoma and promotes cell invasion and migration', *British Journal of Cancer*, 105(2), pp. 231–238. doi:10.1038/bjc.2011.226.

Brigstock, D.R. *et al.* (2003) 'Proposal for a unified CCN nomenclature', *Molecular pathology: MP*, 56(2), pp. 127–128. doi:10.1136/mp.56.2.127.

de Bruin, M. *et al.* (1999) 'Reversal of resistance by GF120918 in cell lines expressing the ABC half-transporter, MXR', *Cancer Letters*, 146(2), pp. 117–126. doi:10.1016/s0304-3835(99)00182-2.

Buondonno, I. *et al.* (2019) 'Endoplasmic reticulum-targeting doxorubicin: a new tool effective against doxorubicin-resistant osteosarcoma', *Cellular and molecular life sciences: CMLS*, 76(3), pp. 609–625. doi:10.1007/s00018-018-2967-9.

Burchenal, J.H. and Robinson, E. (1950) 'The induction of resistance to 4-amino-N10-methylpteroylglutamic acid in a strain of transmitted mouse leukemia', *Science (New York, N.Y.)*, 111(2875), p. 116. doi:10.1126/science.111.2875.116.

Burk, U. *et al.* (2008) 'A reciprocal repression between ZEB1 and members of the miR-200 family promotes EMT and invasion in cancer cells', *EMBO reports*, 9(6), pp. 582–589. doi:10.1038/embor.2008.74.

Busschots, S. *et al.* (2015a) 'Carboplatin and taxol resistance develops more rapidly in functional BRCA1 compared to dysfunctional BRCA1 ovarian cancer cells', *Experimental Cell Research*, 336(1), pp. 1–14. doi:10.1016/j.yexcr.2014.12.001.

Busschots, S. *et al.* (2015b) 'Non-invasive and non-destructive measurements of confluence in cultured adherent cell lines', *MethodsX*, 2, pp. 8–13. doi:10.1016/j.mex.2014.11.002.

Cai, Z. *et al.* (2020) 'The Skp2 Pathway: A Critical Target for Cancer Therapy', *Seminars in Cancer Biology*, 67(Pt 2), pp. 16–33. doi:10.1016/j.semcancer.2020.01.013.

Callaghan, R. *et al.* (2008) 'P-glycoprotein: so many ways to turn it on', *Journal of Clinical Pharmacology*, 48(3), pp. 365–378. doi:10.1177/0091270007311568.

Camuzard, O. *et al.* (2019) 'Role of autophagy in osteosarcoma', *Journal of Bone Oncology*, 16, p. 100235. doi:10.1016/j.jbo.2019.100235.

Carrle, D. and Bielack, S.S. (2006) 'Current strategies of chemotherapy in osteosarcoma', *International Orthopaedics*, 30(6), pp. 445–451. doi:10.1007/s00264-006-0192-x.

Carvalho, C. *et al.* (2009) 'Doxorubicin: the good, the bad and the ugly effect', *Current Medicinal Chemistry*, 16(25), pp. 3267–3285. doi:10.2174/092986709788803312.

Casali, P.G. *et al.* (2018) 'Bone sarcomas: ESMO-PaedCan-EURACAN Clinical Practice Guidelines for diagnosis, treatment and follow-up', *Annals of Oncology: Official Journal of the European Society for Medical Oncology*, 29(Suppl 4), pp. iv79–iv95. doi:10.1093/annonc/mdy310.

Chan, H.S.L. *et al.* (1997) 'P-glycoprotein Expression: Critical Determinant in the Response to Osteosarcoma Chemotherapy', *JNCI Journal of the National Cancer Institute*, 89(22), pp. 1706–1715. doi:10.1093/jnci/89.22.1706.

Chang, C.-J. *et al.* (2011) 'p53 regulates epithelial-mesenchymal transition and stem cell properties through modulating miRNAs', *Nature Cell Biology*, 13(3), pp. 317–323. doi:10.1038/ncb2173.

Chatterjee, N. and Walker, G.C. (2017) 'Mechanisms of DNA damage, repair, and mutagenesis', *Environmental and Molecular Mutagenesis*, 58(5), pp. 235–263. doi:10.1002/em.22087.

Chen, G.K. *et al.* (2000) 'MDR 1 activation is the predominant resistance mechanism selected by vinblastine in MES-SA cells', *British Journal of Cancer*, 83(7), pp. 892–898. doi:10.1054/bjoc.2000.1371.

Chen, H.H.W. and Kuo, M.T. (2010) 'Role of glutathione in the regulation of Cisplatin resistance in cancer chemotherapy', *Metal-Based Drugs*, 2010, p. 430939. doi:10.1155/2010/430939.

Chen, J. *et al.* (2010) 'Constitutively nuclear FOXO3a localization predicts poor survival and promotes Akt phosphorylation in breast cancer', *PloS One*, 5(8), p. e12293. doi:10.1371/journal.pone.0012293.

Chen, J. *et al.* (2018) 'Deletion of sphingosine kinase 1 inhibits liver tumorigenesis in diethylnitrosamine-treated mice', *Oncotarget*, 9(21), pp. 15635–15649. doi:10.18632/oncotarget.24583.

Chen, L. *et al.* (2009) 'Effect of hypoxia-inducible factor-1alpha silencing on the sensitivity of human brain glioma cells to doxorubicin and etoposide', *Neurochemical Research*, 34(5), pp. 984–990. doi:10.1007/s11064-008-9864-9.

Chen, M. *et al.* (2012) 'Expression and promoter methylation analysis of ATP-binding cassette genes in pancreatic cancer', *Oncology Reports*, 27(1), pp. 265–269. doi:10.3892/or.2011.1475.

Chen, P. *et al.* (2017) 'Artesunate Decreases β-Catenin Expression, Cell Proliferation and Apoptosis Resistance in the MG-63 Human Osteosarcoma Cell Line', *Cellular Physiology and Biochemistry*, 43(5), pp. 1939–1949. doi:10.1159/000484118.

Chen, P.-P. *et al.* (2007) 'Expression of Cyr61, CTGF, and WISP-1 correlates with clinical features of lung cancer', *PloS One*, 2(6), p. e534. doi:10.1371/journal.pone.0000534.

Chico, I. *et al.* (2001) 'Phase I study of infusional paclitaxel in combination with the P-glycoprotein antagonist PSC 833', *Journal of Clinical Oncology: Official Journal of the American Society of Clinical Oncology*, 19(3), pp. 832–842. doi:10.1200/JCO.2001.19.3.832.

Chou, A.J. and Gorlick, R. (2006) 'Chemotherapy resistance in osteosarcoma: current challenges and future directions', *Expert Review of Anticancer Therapy*, 6(7), pp. 1075–1085. doi:10.1586/14737140.6.7.1075.

Clarke, S.J. and Rivory, L.P. (1999) 'Clinical pharmacokinetics of docetaxel', *Clinical Pharmacokinetics*, 36(2), pp. 99–114. doi:10.2165/00003088-199936020-00002.

Clementi, M.E. *et al.* (2003) 'Doxorubicin-derived metabolites induce release of cytochrome C and inhibition of respiration on cardiac isolated mitochondria.', *Anticancer research*, 23(3B), pp. 2445–2450.

Cole, S.P. *et al.* (1992) 'Overexpression of a transporter gene in a multidrug-resistant human lung cancer cell line', *Science (New York, N.Y.)*, 258(5088), pp. 1650–1654. doi:10.1126/science.1360704.

Collins, T.J. (2007) 'ImageJ for microscopy', *BioTechniques*, 43(1S), pp. S25–S30. doi:10.2144/000112517.

Comerford, K.M. *et al.* (2002) 'Hypoxia-inducible factor-1-dependent regulation of the multidrug resistance (MDR1) gene', *Cancer Research*, 62(12), pp. 3387–3394.

Cordon-Cardo, C. *et al.* (1989) 'Multidrug-resistance gene (P-glycoprotein) is expressed by endothelial cells at blood-brain barrier sites', *Proceedings of the National Academy of Sciences of the United States of America*, 86(2), pp. 695–698. doi:10.1073/pnas.86.2.695.

Cortés-Funes, H. and Coronado, C. (2007) 'Role of anthracyclines in the era of targeted therapy', *Cardiovascular Toxicology*, 7(2), pp. 56–60. doi:10.1007/s12012-007-0015-3.

Cox, J. and Weinman, S. (2016) 'Mechanisms of doxorubicin resistance in hepatocellular carcinoma', *Hepatic Oncology*, 3(1), pp. 57–59. doi:10.2217/hep.15.41.

Crews, K.R. *et al.* (2004) 'High-dose methotrexate pharmacokinetics and outcome of children and young adults with osteosarcoma', *Cancer*, 100(8), pp. 1724–1733. doi:10.1002/cncr.20152.

Critical Appraisal Skills Programme (2018) 'CASP Checklists'. Available at: CASP Checklists.

Cronstein, B.N. and Aune, T.M. (2020) ‘Methotrexate and its mechanisms of action in inflammatory arthritis’, *Nature Reviews. Rheumatology*, 16(3), pp. 145–154. doi:10.1038/s41584-020-0373-9.

Cronstein, B.N., Naime, D. and Ostad, E. (1993) ‘The antiinflammatory mechanism of methotrexate. Increased adenosine release at inflamed sites diminishes leukocyte accumulation in an in vivo model of inflammation.’, *Journal of Clinical Investigation*, 92(6), pp. 2675–2682. doi:10.1172/JCI116884.

Cuvillier, O. *et al.* (2010) ‘Activation of sphingosine kinase-1 in cancer: implications for therapeutic targeting’, *Current Molecular Pharmacology*, 3(2), pp. 53–65. doi:10.2174/1874467211003020053.

Damron, T.A., Ward, W.G. and Stewart, A. (2007) ‘Osteosarcoma, Chondrosarcoma, and Ewing??s Sarcoma: National Cancer Data Base Report’, *Clinical Orthopaedics and Related Research*, 459, pp. 40–47. doi:10.1097/BLO.0b013e318059b8c9.

Dasari, S. and Tchounwou, P.B. (2014) ‘Cisplatin in cancer therapy: molecular mechanisms of action’, *European Journal of Pharmacology*, 740, pp. 364–378. doi:10.1016/j.ejphar.2014.07.025.

Dass, C.R. *et al.* (2007) ‘A novel orthotopic murine model provides insights into cellular and molecular characteristics contributing to human osteosarcoma’, *Clinical & Experimental Metastasis*, 23(7–8), pp. 367–380. doi:10.1007/s10585-006-9046-6.

De Las Rivas, J. *et al.* (2021) ‘Cancer drug resistance induced by EMT: novel therapeutic strategies’, *Archives of Toxicology*, 95(7), pp. 2279–2297. doi:10.1007/s00204-021-03063-7.

Degenhardt, K. *et al.* (2006) 'Autophagy promotes tumor cell survival and restricts necrosis, inflammation, and tumorigenesis', *Cancer Cell*, 10(1), pp. 51–64. doi:10.1016/j.ccr.2006.06.001.

DeLaney, T.F. *et al.* (2005) 'Radiotherapy for local control of osteosarcoma', *International Journal of Radiation Oncology*Biology*Physics*, 61(2), pp. 492–498. doi:10.1016/j.ijrobp.2004.05.051.

Delepine, N. *et al.* (1988) 'Importance of age and methotrexate dosage: prognosis in children and young adults with high-grade osteosarcomas', *Biomedicine & Pharmacotherapy = Biomedecine & Pharmacotherapie*, 42(4), pp. 257–262.

Dempke, W.C. *et al.* (1992) 'Mechanisms associated with the expression of cisplatin resistance in a human ovarian tumor cell line following exposure to fractionated X-irradiation in vitro', *Carcinogenesis*, 13(7), pp. 1209–1215. doi:10.1093/carcin/13.7.1209.

Derdak, Z. *et al.* (2008) 'The mitochondrial uncoupling protein-2 promotes chemoresistance in cancer cells', *Cancer Research*, 68(8), pp. 2813–2819. doi:10.1158/0008-5472.CAN-08-0053.

Desjardins, P. and Conklin, D. (2010) 'NanoDrop microvolume quantitation of nucleic acids', *Journal of Visualized Experiments: JoVE*, (45), p. 2565. doi:10.3791/2565.

Desoize, B. and Madoulet, C. (2002) 'Particular aspects of platinum compounds used at present in cancer treatment', *Critical Reviews in Oncology/Hematology*, 42(3), pp. 317–325. doi:10.1016/s1040-8428(01)00219-0.

Devaney, K., Vinh, T.N. and Sweet, D.E. (1993) 'Small cell osteosarcoma of bone: An immunohistochemical study with differential diagnostic considerations', *Human Pathology*, 24(11), pp. 1211–1225. doi:10.1016/0046-8177(93)90218-6.

Deyrup, A.T. *et al.* (2007) 'Sarcomas arising in Paget disease of bone: a clinicopathologic analysis of 70 cases', *Archives of Pathology & Laboratory Medicine*, 131(6), pp. 942–946. doi:10.1043/1543-2165(2007)131[942:SAIPDO]2.0.CO;2.

Díaz-Martín, J. *et al.* (2014) 'A core microRNA signature associated with inducers of the epithelial-to-mesenchymal transition', *The Journal of Pathology*, 232(3), pp. 319–329. doi:10.1002/path.4289.

Diepenbruck, M. and Christofori, G. (2016) 'Epithelial–mesenchymal transition (EMT) and metastasis: yes, no, maybe?', *Current Opinion in Cell Biology*, 43, pp. 7–13. doi:10.1016/j.ceb.2016.06.002.

Ding, L., Li, R., Han, X., *et al.* (2017) 'Inhibition of Skp2 suppresses the proliferation and invasion of osteosarcoma cells', *Oncology Reports*, 38(2), pp. 933–940. doi:10.3892/or.2017.5713.

Ding, L., Li, R., Sun, R., *et al.* (2017) 'S-phase kinase-associated protein 2 promotes cell growth and motility in osteosarcoma cells', *Cell Cycle (Georgetown, Tex.)*, 16(16), pp. 1547–1555. doi:10.1080/15384101.2017.1346760.

Ding, L. *et al.* (2018) 'S-phase kinase-associated protein 2 is involved in epithelial-mesenchymal transition in methotrexate-resistant osteosarcoma cells', *International Journal of Oncology*, 52(6), pp. 1841–1852. doi:10.3892/ijo.2018.4345.

Ding, Z. *et al.* (2010) 'Expression and significance of hypoxia-inducible factor-1 alpha and MDR1/P-glycoprotein in human colon carcinoma tissue and cells', *Journal of Cancer*

Research and Clinical Oncology, 136(11), pp. 1697–1707. doi:10.1007/s00432-010-0828-5.

Doroshow, J.H. (1986) 'Role of hydrogen peroxide and hydroxyl radical formation in the killing of Ehrlich tumor cells by anticancer quinones', *Proceedings of the National Academy of Sciences of the United States of America*, 83(12), pp. 4514–4518. doi:10.1073/pnas.83.12.4514.

Doyle, L.A. *et al.* (1998) 'A multidrug resistance transporter from human MCF-7 breast cancer cells', *Proceedings of the National Academy of Sciences of the United States of America*, 95(26), pp. 15665–15670. doi:10.1073/pnas.95.26.15665.

Duffaud, F. *et al.* (2012) 'A phase II trial of second-line pemetrexed in adults with advanced/metastatic osteosarcoma', *European Journal of Cancer (Oxford, England: 1990)*, 48(4), pp. 564–570. doi:10.1016/j.ejca.2011.12.015.

Durfee, R.A., Mohammed, M. and Luu, H.H. (2016) 'Review of Osteosarcoma and Current Management', *Rheumatology and Therapy*, 3(2), pp. 221–243. doi:10.1007/s40744-016-0046-y.

Eastman, A. (1987) 'Cross-linking of glutathione to DNA by cancer chemotherapeutic platinum coordination complexes', *Chemico-Biological Interactions*, 61(3), pp. 241–248. doi:10.1016/0009-2797(87)90004-4.

Eckford, P.D.W. and Sharom, F.J. (2009) 'ABC efflux pump-based resistance to chemotherapy drugs', *Chemical Reviews*, 109(7), pp. 2989–3011. doi:10.1021/cr9000226.

Eisenhauer, E.A. *et al.* (2009) 'New response evaluation criteria in solid tumours: revised RECIST guideline (version 1.1)', *European Journal of Cancer (Oxford, England: 1990)*, 45(2), pp. 228–247. doi:10.1016/j.ejca.2008.10.026.

Eliseev, R.A. *et al.* (2008) 'Runx2-mediated activation of the Bax gene increases osteosarcoma cell sensitivity to apoptosis', *Oncogene*, 27(25), pp. 3605–3614. doi:10.1038/sj.onc.1211020.

Errani, C. *et al.* (2011) 'Palliative therapy for osteosarcoma', *Expert Review of Anticancer Therapy*, 11(2), pp. 217–227. doi:10.1586/era.10.172.

Eyre, R. *et al.* (2009) 'Epidemiology of bone tumours in children and young adults', *Pediatric Blood & Cancer*, 53(6), pp. 941–952. doi:10.1002/pbc.22194.

Fan, Y. *et al.* (2008) 'Regulation of programmed cell death by NF-kappaB and its role in tumorigenesis and therapy', *Advances in Experimental Medicine and Biology*, 615, pp. 223–250. doi:10.1007/978-1-4020-6554-5_11.

Fanelli, M. *et al.* (2016) 'Targeting ABCB1 and ABCC1 with their Specific Inhibitor CBT-1® can Overcome Drug Resistance in Osteosarcoma', *Current Cancer Drug Targets*, 16(3), pp. 261–274. doi:10.2174/1568009616666151106120434.

Fanelli, M. *et al.* (2020) 'Cisplatin Resistance in Osteosarcoma: In vitro Validation of Candidate DNA Repair-Related Therapeutic Targets and Drugs for Tailored Treatments', *Frontiers in Oncology*, 10, p. 331. doi:10.3389/fonc.2020.00331.

Fantappiè, O. *et al.* (2007) 'P-glycoprotein mediates celecoxib-induced apoptosis in multiple drug-resistant cell lines', *Cancer Research*, 67(10), pp. 4915–4923. doi:10.1158/0008-5472.CAN-06-3952.

Fassbinder-Orth, C.A. (2014) 'Methods for quantifying gene expression in ecoimmunology: from qPCR to RNA-Seq', *Integrative and Comparative Biology*, 54(3), pp. 396–406. doi:10.1093/icb/icu023.

Fellenberg, J. *et al.* (2003) 'Identification of drug-regulated genes in osteosarcoma cells', *International Journal of Cancer*, 105(5), pp. 636–643. doi:10.1002/ijc.11135.

Ferguson, W.S. and Goorin, A.M. (2001) 'Current Treatment of Osteosarcoma', *Cancer Investigation*, 19(3), pp. 292–315. doi:10.1081/CNV-100102557.

Ferrari, S. *et al.* (2003) 'Postrelapse Survival in Osteosarcoma of the Extremities: Prognostic Factors for Long-Term Survival', *Journal of Clinical Oncology*, 21(4), pp. 710–715. doi:10.1200/JCO.2003.03.141.

Ferrari, S. *et al.* (2005) 'Neoadjuvant Chemotherapy With High-Dose Ifosfamide, High-Dose Methotrexate, Cisplatin, and Doxorubicin for Patients With Localized Osteosarcoma of the Extremity: A Joint Study by the Italian and Scandinavian Sarcoma Groups', *Journal of Clinical Oncology*, 23(34), pp. 8845–8852. doi:10.1200/JCO.2004.00.5785.

Ferrari, S. *et al.* (2009) 'Sex- and age-related chemotherapy toxicity in patients with non-metastatic osteosarcoma', *Journal of Chemotherapy (Florence, Italy)*, 21(2), pp. 205–210. doi:10.1179/joc.2009.21.2.205.

Ferrari, S. and Palmerini, E. (2007) 'Adjuvant and neoadjuvant combination chemotherapy for osteogenic sarcoma', *Current Opinion in Oncology*, 19(4), pp. 341–346. doi:10.1097/CCO.0b013e328122d73f.

Figgitt, D.P. and Wiseman, L.R. (2000) 'Docetaxel: an update of its use in advanced breast cancer', *Drugs*, 59(3), pp. 621–651. doi:10.2165/00003495-200059030-00015.

Fishel, M.L. and Kelley, M.R. (2007) 'The DNA base excision repair protein Ape1/Ref-1 as a therapeutic and chemopreventive target', *Molecular Aspects of Medicine*, 28(3–4), pp. 375–395. doi:10.1016/j.mam.2007.04.005.

Fletcher, C.D.M., World Health Organization and International Agency for Research on Cancer (eds) (2013) *WHO classification of tumours of soft tissue and bone*. 4th ed. Lyon: IARC Press (World Health Organization classification of tumours).

Flintoff, W.F. *et al.* (2004) 'Functional analysis of altered reduced folate carrier sequence changes identified in osteosarcomas', *Biochimica Et Biophysica Acta*, 1690(2), pp. 110–117. doi:10.1016/j.bbadis.2004.05.008.

Florea, A.-M. and Büsselberg, D. (2006) 'Occurrence, use and potential toxic effects of metals and metal compounds', *BioMetals*, 19(4), pp. 419–427. doi:10.1007/s10534-005-4451-x.

Florea, A.-M. and Büsselberg, D. (2011) 'Cisplatin as an anti-tumor drug: cellular mechanisms of activity, drug resistance and induced side effects', *Cancers*, 3(1), pp. 1351–1371. doi:10.3390/cancers3011351.

Fogli, S., Nieri, P. and Breschi, M.C. (2004) 'The role of nitric oxide in anthracycline toxicity and prospects for pharmacologic prevention of cardiac damage', *FASEB journal: official publication of the Federation of American Societies for Experimental Biology*, 18(6), pp. 664–675. doi:10.1096/fj.03-0724rev.

Fojo, A.T. *et al.* (1987) 'Expression of a multidrug-resistance gene in human tumors and tissues', *Proceedings of the National Academy of Sciences of the United States of America*, 84(1), pp. 265–269. doi:10.1073/pnas.84.1.265.

Fox, E. *et al.* (2012) 'Phase II study of sequential gemcitabine followed by docetaxel for recurrent Ewing sarcoma, osteosarcoma, or unresectable or locally recurrent chondrosarcoma: results of Sarcoma Alliance for Research Through Collaboration Study 003', *The Oncologist*, 17(3), p. 321. doi:10.1634/theoncologist.2010-0265.

Fox, E. and Bates, S.E. (2007) 'Tariquidar (XR9576): a P-glycoprotein drug efflux pump inhibitor', *Expert Review of Anticancer Therapy*, 7(4), pp. 447–459. doi:10.1586/14737140.7.4.447.

Franke, M. *et al.* (2011) 'Solitary skeletal osteosarcoma recurrence. Findings from the Cooperative Osteosarcoma Study Group', *Pediatric Blood & Cancer*, 56(5), pp. 771–776. doi:10.1002/pbc.22864.

Franken, N.A.P. *et al.* (2006) 'Clonogenic assay of cells in vitro', *Nature Protocols*, 1(5), pp. 2315–2319. doi:10.1038/nprot.2006.339.

French, K.J. *et al.* (2006) 'Antitumor activity of sphingosine kinase inhibitors', *The Journal of Pharmacology and Experimental Therapeutics*, 318(2), pp. 596–603. doi:10.1124/jpet.106.101345.

Fuja, D.G. *et al.* (2018) 'Transglutaminase-2 promotes metastatic and stem-like phenotypes in osteosarcoma', *American Journal of Cancer Research*, 8(9), pp. 1752–1763.

Fujii, R. *et al.* (1994) 'Active efflux system for cisplatin in cisplatin-resistant human KB cells', *Japanese Journal of Cancer Research: Gann*, 85(4), pp. 426–433. doi:10.1111/j.1349-7006.1994.tb02376.x.

Gachechiladze, M. *et al.* (2019) 'Sphingosine kinase-1 predicts overall survival outcomes in non-small cell lung cancer patients treated with carboplatin and navelbine', *Oncology Letters*, 18(2), pp. 1259–1266. doi:10.3892/ol.2019.10447.

Gault, C.R. and Obeid, L.M. (2011) 'Still benched on its way to the bedside: sphingosine kinase 1 as an emerging target in cancer chemotherapy', *Critical Reviews in Biochemistry and Molecular Biology*, 46(4), pp. 342–351. doi:10.3109/10409238.2011.597737.

Gayan, S., Teli, A. and Dey, T. (2017) 'Inherent aggressive character of invasive and non-invasive cells dictates the in vitro migration pattern of multicellular spheroid', *Scientific Reports*, 7(1), p. 11527. doi:10.1038/s41598-017-10078-7.

Geller, D.S. and Gorlick, R. (2010) 'Osteosarcoma: A Review of Diagnosis, Management, and Treatment Strategies', *O s t e o s a r co m a*, p. 14.

Genestier, L. *et al.* (2000) 'Mechanisms of action of methotrexate', *Immunopharmacology*, 47(2), pp. 247–257. doi:10.1016/S0162-3109(00)00189-2.

Germann, U.A. (1996) 'P-glycoprotein--a mediator of multidrug resistance in tumour cells', *European Journal of Cancer (Oxford, England: 1990)*, 32A(6), pp. 927–944. doi:10.1016/0959-8049(96)00057-3.

Germann, U.A. *et al.* (1997) 'Chemosensitization and drug accumulation effects of VX-710, verapamil, cyclosporin A, MS-209 and GF120918 in multidrug resistant HL60/ADR cells expressing the multidrug resistance-associated protein MRP', *Anti-Cancer Drugs*, 8(2), pp. 141–155. doi:10.1097/00001813-199702000-00005.

Gerrand, C. *et al.* (2016) 'UK guidelines for the management of bone sarcomas', *Clinical Sarcoma Research*, 6, p. 7. doi:10.1186/s13569-016-0047-1.

Gewirtz, D.A. (1999) ‘A critical evaluation of the mechanisms of action proposed for the antitumor effects of the anthracycline antibiotics adriamycin and daunorubicin’, *Biochemical Pharmacology*, 57(7), pp. 727–741. doi:10.1016/s0006-2952(98)00307-4.

Giannakakou, P. *et al.* (2000) ‘A common pharmacophore for epothilone and taxanes: molecular basis for drug resistance conferred by tubulin mutations in human cancer cells’, *Proceedings of the National Academy of Sciences of the United States of America*, 97(6), pp. 2904–2909. doi:10.1073/pnas.040546297.

Gillet, J.-P. and Gottesman, M.M. (2010) ‘Mechanisms of multidrug resistance in cancer’, *Methods in Molecular Biology (Clifton, N.J.)*, 596, pp. 47–76. doi:10.1007/978-1-60761-416-6_4.

Göker, E. *et al.* (1995) ‘Amplification of the dihydrofolate reductase gene is a mechanism of acquired resistance to methotrexate in patients with acute lymphoblastic leukemia and is correlated with p53 gene mutations’, *Blood*, 86(2), pp. 677–684.

Goldman, I.D. and Matherly, L.H. (1985) ‘The cellular pharmacology of methotrexate’, *Pharmacology & Therapeutics*, 28(1), pp. 77–102. doi:10.1016/0163-7258(85)90083-x.

Gosiengfiao, Y. *et al.* (2012) ‘Gemcitabine with or without docetaxel and resection for recurrent osteosarcoma: the experience at Children’s Memorial Hospital’, *Journal of Pediatric Hematology/Oncology*, 34(2), pp. e63-65. doi:10.1097/MPH.0b013e3182331ee8.

Gottesman, M.M., Fojo, T. and Bates, S.E. (2002) ‘Multidrug resistance in cancer: role of ATP-dependent transporters’, *Nature Reviews. Cancer*, 2(1), pp. 48–58. doi:10.1038/nrc706.

Gottesman, M.M. and Ling, V. (2006) 'The molecular basis of multidrug resistance in cancer: the early years of P-glycoprotein research', *FEBS letters*, 580(4), pp. 998–1009. doi:10.1016/j.febslet.2005.12.060.

Greenburg, G. and Hay, E.D. (1982) 'Epithelia suspended in collagen gels can lose polarity and express characteristics of migrating mesenchymal cells', *The Journal of Cell Biology*, 95(1), pp. 333–339. doi:10.1083/jcb.95.1.333.

Greene, R.F. *et al.* (1983) 'Plasma Pharmacokinetics of Adriamycin and Adriamycinol: Implications for the Design of in Vitro Experiments and Treatment Protocols', p. 6.

Gregory, P.A. *et al.* (2008) 'The miR-200 family and miR-205 regulate epithelial to mesenchymal transition by targeting ZEB1 and SIP1', *Nature Cell Biology*, 10(5), pp. 593–601. doi:10.1038/ncb1722.

Grignani, G. *et al.* (2012) 'A phase II trial of sorafenib in relapsed and unresectable high-grade osteosarcoma after failure of standard multimodal therapy: an Italian Sarcoma Group study', *Annals of Oncology: Official Journal of the European Society for Medical Oncology*, 23(2), pp. 508–516. doi:10.1093/annonc/mdr151.

Grignani, G. *et al.* (2015) 'Sorafenib and everolimus for patients with unresectable high-grade osteosarcoma progressing after standard treatment: a non-randomised phase 2 clinical trial', *The Lancet. Oncology*, 16(1), pp. 98–107. doi:10.1016/S1470-2045(14)71136-2.

Guminski, A.D. *et al.* (2006) 'MRP2 (ABCC2) and cisplatin sensitivity in hepatocytes and human ovarian carcinoma', *Gynecologic Oncology*, 100(2), pp. 239–246. doi:10.1016/j.ygyno.2005.08.046.

Günes, D.A. *et al.* (2009) 'Co-application of arsenic trioxide (As2O3) and cisplatin (CDDP) on human SY-5Y neuroblastoma cells has differential effects on the intracellular calcium concentration ([Ca2+]i) and cytotoxicity', *Neurotoxicology*, 30(2), pp. 194–202. doi:10.1016/j.neuro.2008.12.001.

Guo, M. *et al.* (2014) 'Hypoxia promotes migration and induces CXCR4 expression via HIF-1α activation in human osteosarcoma', *PloS One*, 9(3), p. e90518. doi:10.1371/journal.pone.0090518.

Guo, W. *et al.* (1999) 'Mechanisms of Methotrexate Resistance in Osteosarcoma', p. 8.

Gupta, G.P. and Massagué, J. (2006) 'Cancer metastasis: building a framework', *Cell*, 127(4), pp. 679–695. doi:10.1016/j.cell.2006.11.001.

Gupta, N. and Wish, J.B. (2017) 'Hypoxia-Inducible Factor Prolyl Hydroxylase Inhibitors: A Potential New Treatment for Anemia in Patients With CKD', *American Journal of Kidney Diseases: The Official Journal of the National Kidney Foundation*, 69(6), pp. 815–826. doi:10.1053/j.ajkd.2016.12.011.

Hah, J., Goldinger, J.M. and Jung, C.Y. (1985) 'In situ assembly states of (Na+,K+)-pump ATPase in human erythrocytes. Radiation target size analyses', *The Journal of Biological Chemistry*, 260(26), pp. 14016–14019.

Haldar, S., Basu, A. and Croce, C.M. (1997) 'Bcl2 is the guardian of microtubule integrity', *Cancer Research*, 57(2), pp. 229–233.

Hamaguchi, K. *et al.* (1993) 'Cross-resistance to diverse drugs is associated with primary cisplatin resistance in ovarian cancer cell lines', *Cancer Research*, 53(21), pp. 5225–5232.

Han, T. *et al.* (2014) 'Establishment and characterization of a cisplatin-resistant human osteosarcoma cell line', *Oncology Reports*, 32(3), pp. 1133–1139. doi:10.3892/or.2014.3314.

Han, Z. and Shi, L. (2018) 'Long non-coding RNA LUCAT1 modulates methotrexate resistance in osteosarcoma via miR-200c/ABCB1 axis', *Biochemical and Biophysical Research Communications*, 495(1), pp. 947–953. doi:10.1016/j.bbrc.2017.11.121.

Hansen, M.F., Seton, M. and Merchant, A. (2006) 'Osteosarcoma in Paget's Disease of Bone', *Journal of Bone and Mineral Research*, 21(S2), pp. P58–P63. doi:10.1359/jbmr.06s211.

Harrison, M.M. *et al.* (2014) 'A CRISPR view of development', *Genes & Development*, 28(17), pp. 1859–1872. doi:10.1101/gad.248252.114.

Hartford, C.M. *et al.* (2006) 'Osteosarcoma among children aged 5 years or younger: the St. Jude Children's Research Hospital experience', *Journal of Pediatric Hematology/Oncology*, 28(1), pp. 43–47.

Hata, A.N., Engelman, J.A. and Faber, A.C. (2015) 'The BCL2 Family: Key Mediators of the Apoptotic Response to Targeted Anticancer Therapeutics', *Cancer Discovery*, 5(5), pp. 475–487. doi:10.1158/2159-8290.CD-15-0011.

Hatoum, D. *et al.* (2017) 'Mammalian sphingosine kinase (SphK) isoenzymes and isoform expression: challenges for SphK as an oncotarget', *Oncotarget*, 8(22), pp. 36898–36929. doi:10.18632/oncotarget.16370.

Hattinger, C.M. *et al.* (2003) 'Genomic imbalances associated with methotrexate resistance in human osteosarcoma cell lines detected by comparative genomic

hybridization-based techniques', *European Journal of Cell Biology*, 82(9), pp. 483–493. doi:10.1078/0171-9335-00336.

Hattinger, C.M. *et al.* (2010) 'Emerging drugs for high-grade osteosarcoma', *Expert Opinion on Emerging Drugs*, 15(4), pp. 615–634. doi:10.1517/14728214.2010.505603.

Hauben, E.I. *et al.* (2006) 'Clinico-histologic parameters of osteosarcoma patients with late relapse', *European Journal of Cancer*, 42(4), pp. 460–466. doi:10.1016/j.ejca.2005.09.032.

He, A. *et al.* (2013) 'Comparison of pirarubicin-based versus gemcitabine-docetaxel chemotherapy for relapsed and refractory osteosarcoma: a single institution experience', *International Journal of Clinical Oncology*, 18(3), pp. 498–505. doi:10.1007/s10147-012-0409-5.

He, H., Ni, J. and Huang, J. (2014) 'Molecular mechanisms of chemoresistance in osteosarcoma (Review)', *Oncology Letters*, 7(5), pp. 1352–1362. doi:10.3892/ol.2014.1935.

Heffernan-Stroud, L.A. and Obeid, L.M. (2013) 'Sphingosine kinase 1 in cancer', *Advances in Cancer Research*, 117, pp. 201–235. doi:10.1016/B978-0-12-394274-6.00007-8.

van der Heijden, J.W. *et al.* (2007) 'Drug Insight: resistance to methotrexate and other disease-modifying antirheumatic drugs--from bench to bedside', *Nature Clinical Practice. Rheumatology*, 3(1), pp. 26–34. doi:10.1038/ncprheum0380.

Hensley, M.L. *et al.* (2002) 'Gemcitabine and docetaxel in patients with unresectable leiomyosarcoma: results of a phase II trial', *Journal of Clinical Oncology: Official*

Journal of the American Society of Clinical Oncology, 20(12), pp. 2824–2831. doi:10.1200/JCO.2002.11.050.

Hensley, M.L. (2010) 'Update on gemcitabine and docetaxel combination therapy for primary and metastatic sarcomas':, *Current Opinion in Oncology*, 22(4), pp. 356–361. doi:10.1097/CCO.0b013e32833aafef.

Herbst, R.S. and Khuri, F.R. (2003) 'Mode of action of docetaxel - a basis for combination with novel anticancer agents', *Cancer Treatment Reviews*, 29(5), pp. 407–415. doi:10.1016/s0305-7372(03)00097-5.

Heremans, H. *et al.* (1978) 'In vitro cultivation of human tumor tissues. II. Morphological and virological characterization of three cell lines', *Oncology*, 35(6), pp. 246–252. doi:10.1159/000225298.

Hewitt, K.M. *et al.* (2008) 'Parosteal osteosarcoma: Case report and review of the literature', *Head & Neck*, 30(1), pp. 122–126. doi:10.1002/hed.20658.

Higgins, C.F. *et al.* (1997) 'Structure of the multidrug resistance P-glycoprotein', *Seminars in Cancer Biology*, 8(3), pp. 135–142. doi:10.1006/scbi.1997.0067.

Himmelstein, K.J. *et al.* (1981) 'Clinical kinetics of intact cisplatin and some related species', *Clinical Pharmacology and Therapeutics*, 29(5), pp. 658–664. doi:10.1038/clpt.1981.91.

Holland, B. *et al.* (2003) *ABC proteins: from bacteria to man.* Elsevier.

Höllt, V. *et al.* (1992) 'Stereoisomers of calcium antagonists which differ markedly in their potencies as calcium blockers are equally effective in modulating drug transport by P-glycoprotein', *Biochemical Pharmacology*, 43(12), pp. 2601–2608. doi:10.1016/0006-2952(92)90149-d.

Holohan, C. *et al.* (2013) 'Cancer drug resistance: an evolving paradigm', *Nature Reviews. Cancer*, 13(10), pp. 714–726. doi:10.1038/nrc3599.

Hou, C.-H. *et al.* (2009) 'Bone morphogenetic protein-2 enhances the motility of chondrosarcoma cells via activation of matrix metalloproteinase-13', *Bone*, 44(2), pp. 233–242. doi:10.1016/j.bone.2008.09.021.

Hromas, R.A. *et al.* (1987) 'Glutathione depletion reverses cisplatin resistance in murine L1210 leukemia cells', *Cancer Letters*, 34(1), pp. 9–13. doi:10.1016/0304-3835(87)90067-x.

Hsieh, Y.-F. *et al.* (2013) 'Transglutaminase 2 contributes to apoptosis induction in Jurkat T cells by modulating Ca2+ homeostasis via cross-linking RAP1GDS1', *PloS One*, 8(12), p. e81516. doi:10.1371/journal.pone.0081516.

Huang, G., Mills, L. and Worth, L.L. (2007) 'Expression of human glutathione S-transferase P1 mediates the chemosensitivity of osteosarcoma cells', *Molecular Cancer Therapeutics*, 6(5), pp. 1610–1619. doi:10.1158/1535-7163.MCT-06-0580.

Huang, J. *et al.* (2012) 'HMGB1 Promotes Drug Resistance in Osteosarcoma', *Cancer Research*, 72(1), pp. 230–238. doi:10.1158/0008-5472.CAN-11-2001.

Huang, Jun *et al.* (2012) 'Targeting HMGB1-mediated autophagy as a novel therapeutic strategy for osteosarcoma', *Autophagy*, 8(2), pp. 275–277. doi:10.4161/auto.8.2.18940.

Huang, J., Li, H. and Ren, G. (2015) 'Epithelial-mesenchymal transition and drug resistance in breast cancer (Review)', *International Journal of Oncology*, 47(3), pp. 840–848. doi:10.3892/ijo.2015.3084.

Huang, Y.-M. *et al.* (2009) 'The metastasectomy and timing of pulmonary metastases on the outcome of osteosarcoma patients', *Clinical Medicine. Oncology*, 3, pp. 99–105. doi:10.4137/cmo.s531.

Hubaux, R. *et al.* (2015) 'Microtubule affinity-regulating kinase 2 is associated with DNA damage response and cisplatin resistance in non-small cell lung cancer', *International Journal of Cancer*, 137(9), pp. 2072–2082. doi:10.1002/ijc.29577.

Hui, R.C.-Y. *et al.* (2008) 'Doxorubicin activates FOXO3a to induce the expression of multidrug resistance gene ABCB1 (MDR1) in K562 leukemic cells', *Molecular Cancer Therapeutics*, 7(3), pp. 670–678. doi:10.1158/1535-7163.MCT-07-0397.

Hwang, J.Y. *et al.* (2008) 'Clinical and biological significance of tissue transglutaminase in ovarian carcinoma', *Cancer Research*, 68(14), pp. 5849–5858. doi:10.1158/0008-5472.CAN-07-6130.

Iida, K. *et al.* (2003) 'Effect of retinoblastoma tumor suppressor gene expression on chemosensitivity of human osteosarcoma cell lines', *Oncology Reports*, 10(6), pp. 1961–1965.

Imanishi, S. *et al.* (2014) 'Constitutive activation of the ATM/BRCA1 pathway prevents DNA damage-induced apoptosis in 5-azacytidine-resistant cell lines', *Biochemical Pharmacology*, 89(3), pp. 361–369. doi:10.1016/j.bcp.2014.03.008.

Ishikawa, T. (1992) 'The ATP-dependent glutathione S-conjugate export pump', *Trends in Biochemical Sciences*, 17(11), pp. 463–468. doi:10.1016/0968-0004(92)90489-v.

Ishikawa, T. and Ali-Osman, F. (1993) 'Glutathione-associated cis-diamminedichloroplatinum(II) metabolism and ATP-dependent efflux from leukemia cells. Molecular characterization of glutathione-platinum complex and its biological

significance.', *Journal of Biological Chemistry*, 268(27), pp. 20116–20125. doi:10.1016/S0021-9258(20)80702-9.

Jabeen, S. *et al.* (2015) 'Impact of genetic variants of RFC1, DHFR and MTHFR in osteosarcoma patients treated with high-dose methotrexate', *The Pharmacogenomics Journal*, 15(5), pp. 385–390. doi:10.1038/tpj.2015.11.

Jaffe, N. *et al.* (1983) 'Osteosarcoma: intra-arterial treatment of the primary tumor with cis-diammine-dichloroplatinum II (CDP). Angiographic, pathologic, and pharmacologic studies', *Cancer*, 51(3), pp. 402–407. doi:10.1002/1097-0142(19830201)51:3<402::aid-cncr2820510308>3.0.co;2-p.

Jaffe, N. *et al.* (2002) 'Can cure in patients with osteosarcoma be achieved exclusively with chemotherapy and abrogation of surgery?', *Cancer*, 95(10), pp. 2202–2210. doi:10.1002/cncr.10944.

Jaffe, N. (2009) 'Osteosarcoma: review of the past, impact on the future. The American experience', *Cancer Treatment and Research*, 152, pp. 239–262. doi:10.1007/978-1-4419-0284-9_12.

Janeway, K.A. and Grier, H.E. (2010) 'Sequelae of osteosarcoma medical therapy: a review of rare acute toxicities and late effects', *The Lancet. Oncology*, 11(7), pp. 670–678. doi:10.1016/S1470-2045(10)70062-0.

Jemal, A. *et al.* (2011) 'Global cancer statistics', *CA: a cancer journal for clinicians*, 61(2), pp. 69–90. doi:10.3322/caac.20107.

Jensen, G.A. *et al.* (2001) 'A comparison of the solution structures of an LNA:DNA duplex and the unmodified DNA:DNA duplex', *Journal of the Chemical Society, Perkin Transactions 2*, (7), pp. 1224–1232. doi:10.1039/b008431j.

Jeong, S.-Y. *et al.* (2020) 'The Current Status of Clinical Research Involving Microneedles: A Systematic Review', *Pharmaceutics*, 12(11), p. E1113. doi:10.3390/pharmaceutics12111113.

Jhaveri, A., Deshpande, P. and Torchilin, V. (2014) 'Stimuli-sensitive nanopreparations for combination cancer therapy', *Journal of Controlled Release: Official Journal of the Controlled Release Society*, 190, pp. 352–370. doi:10.1016/j.jconrel.2014.05.002.

Ji, C. *et al.* (2010) 'Exogenous cell-permeable C6 ceramide sensitizes multiple cancer cell lines to Doxorubicin-induced apoptosis by promoting AMPK activation and mTORC1 inhibition', *Oncogene*, 29(50), pp. 6557–6568. doi:10.1038/onc.2010.379.

Jiang, B., Yan, L. and Wu, Q. (2019) '*ABCB1* (C1236T) Polymorphism Affects P-Glycoprotein-Mediated Transport of Methotrexate, Doxorubicin, Actinomycin D, and Etoposide', *DNA and Cell Biology*, 38(5), pp. 485–490. doi:10.1089/dna.2018.4583.

Jiang, K. *et al.* (2017) 'Autophagic degradation of FOXO3a represses the expression of PUMA to block cell apoptosis in cisplatin-resistant osteosarcoma cells', *American Journal of Cancer Research*, 7(7), pp. 1407–1422.

Johnson, D.G. *et al.* (1993) 'Expression of transcription factor E2F1 induces quiescent cells to enter S phase', *Nature*, 365(6444), pp. 349–352. doi:10.1038/365349a0.

Johnson, K. *et al.* (1999) 'Parosteal osteosarcoma of a metatarsal with intramedullary invasion', *Skeletal Radiology*, 28(2), pp. 111–115. doi:10.1007/s002560050485.

Johnson, R.A., Ince, T.A. and Scotto, K.W. (2001) 'Transcriptional repression by p53 through direct binding to a novel DNA element', *The Journal of Biological Chemistry*, 276(29), pp. 27716–27720. doi:10.1074/jbc.C100121200.

Kager, L. *et al.* (2003) 'Primary metastatic osteosarcoma: presentation and outcome of patients treated on neoadjuvant Cooperative Osteosarcoma Study Group protocols', *Journal of Clinical Oncology: Official Journal of the American Society of Clinical Oncology*, 21(10), pp. 2011–2018. doi:10.1200/JCO.2003.08.132.

Kager, L. *et al.* (2010) 'Osteosarcoma in very young children: Experience of the Cooperative Osteosarcoma Study Group', *Cancer*, 116(22), pp. 5316–5324. doi:10.1002/cncr.25287.

Kalluri, R. and Neilson, E.G. (2003) 'Epithelial-mesenchymal transition and its implications for fibrosis', *The Journal of Clinical Investigation*, 112(12), pp. 1776–1784. doi:10.1172/JCI20530.

Kartalou, M. and Essigmann, J.M. (2001) 'Mechanisms of resistance to cisplatin', *Mutation Research*, 478(1–2), pp. 23–43. doi:10.1016/s0027-5107(01)00141-5.

Kaur, H. *et al.* (2006) 'Thermodynamic, counterion, and hydration effects for the incorporation of locked nucleic acid nucleotides into DNA duplexes', *Biochemistry*, 45(23), pp. 7347–7355. doi:10.1021/bi060307w.

Ke, Q. and Costa, M. (2006) 'Hypoxia-inducible factor-1 (HIF-1)', *Molecular Pharmacology*, 70(5), pp. 1469–1480. doi:10.1124/mol.106.027029.

Kelly, R.J. *et al.* (2011) 'A pharmacodynamic study of docetaxel in combination with the P-glycoprotein antagonist tariquidar (XR9576) in patients with lung, ovarian, and cervical cancer', *Clinical Cancer Research: An Official Journal of the American Association for Cancer Research*, 17(3), pp. 569–580. doi:10.1158/1078-0432.CCR-10-1725.

Kempf-Bielack, B. *et al.* (2005) 'Osteosarcoma relapse after combined modality therapy: an analysis of unselected patients in the Cooperative Osteosarcoma Study Group (COSS)', *Journal of Clinical Oncology: Official Journal of the American Society of Clinical Oncology*, 23(3), pp. 559–568. doi:10.1200/JCO.2005.04.063.

Kessel, D., Botterill, V. and Wodinsky, I. (1968) 'Uptake and retention of daunomycin by mouse leukemic cells as factors in drug response', *Cancer Research*, 28(5), pp. 938–941.

Kim, H.J. *et al.* (2013) 'Cytoprotective role of autophagy during paclitaxel-induced apoptosis in Saos-2 osteosarcoma cells', *International Journal of Oncology*, 42(6), pp. 1985–1992. doi:10.3892/ijo.2013.1884.

King, M.P. and Attardi, G. (1996) 'Isolation of human cell lines lacking mitochondrial DNA', *Methods in Enzymology*, 264, pp. 304–313. doi:10.1016/s0076-6879(96)64029-4.

Klein, M.J. and Siegal, G.P. (2006) 'Osteosarcoma: Anatomic and Histologic Variants', *American Journal of Clinical Pathology*, 125(4), pp. 555–581. doi:10.1309/UC6KQHLD9LV2KENN.

Korpal, M. *et al.* (2008) 'The miR-200 family inhibits epithelial-mesenchymal transition and cancer cell migration by direct targeting of E-cadherin transcriptional repressors ZEB1 and ZEB2', *The Journal of Biological Chemistry*, 283(22), pp. 14910–14914. doi:10.1074/jbc.C800074200.

Krishna, R. and Mayer, L.D. (2000) 'Multidrug resistance (MDR) in cancer. Mechanisms, reversal using modulators of MDR and the role of MDR modulators in influencing the pharmacokinetics of anticancer drugs', *European Journal of Pharmaceutical Sciences: Official Journal of the European Federation for Pharmaceutical Sciences*, 11(4), pp. 265–283. doi:10.1016/s0928-0987(00)00114-7.

Kruh, G.D. *et al.* (2001) 'MRP Subfamily Transporters and Resistance to Anticancer Agents', *Journal of Bioenergetics and Biomembranes; New York*, 33(6), pp. 493–501. doi:http://dx.doi.org/10.1023/A:1012827221844.

Kubo, M. *et al.* (1998) 'Expression of fibrogenic cytokines in desmoplastic malignant melanoma', *The British Journal of Dermatology*, 139(2), pp. 192–197. doi:10.1046/j.1365-2133.1998.02354.x.

Kuo, M.T. *et al.* (2002) 'Induction of human MDR1 gene expression by 2-acetylaminofluorene is mediated by effectors of the phosphoinositide 3-kinase pathway that activate NF-kappaB signaling', *Oncogene*, 21(13), pp. 1945–1954. doi:10.1038/sj.onc.1205117.

Kusunoki, N. *et al.* (1998) 'Inhibitory effects of a cyclosporin derivative, SDZ PSC 833, on transport of doxorubicin and vinblastine via human P-glycoprotein', *Japanese Journal of Cancer Research: Gann*, 89(11), pp. 1220–1228. doi:10.1111/j.1349-7006.1998.tb00518.x.

Lage, H. (2008) 'An overview of cancer multidrug resistance: a still unsolved problem', *Cellular and molecular life sciences: CMLS*, 65(20), pp. 3145–3167. doi:10.1007/s00018-008-8111-5.

Lamouille, S., Xu, J. and Derynck, R. (2014) 'Molecular mechanisms of epithelial-mesenchymal transition', *Nature Reviews. Molecular Cell Biology*, 15(3), pp. 178–196. doi:10.1038/nrm3758.

Lamplot, J.D. *et al.* (2013) 'The Current and Future Therapies for Human Osteosarcoma', *Current Cancer Therapy Reviews*, 9(1), pp. 55–77. doi:10.2174/1573394711309010006.

Lauzier, A. *et al.* (2012) 'Transglutaminase 2 cross-linking activity is linked to invadopodia formation and cartilage breakdown in arthritis', *Arthritis Research & Therapy*, 14(4), p. R159. doi:10.1186/ar3899.

Law, L.W. (1951) 'Resistance in leukemic cells to a guanine analog, 8-azaguanine', *Proceedings of the Society for Experimental Biology and Medicine. Society for Experimental Biology and Medicine (New York, N.Y.)*, 78(2), pp. 499–502. doi:10.3181/00379727-78-19118.

Lee, J.A. *et al.* (2016) 'Higher Gemcitabine Dose Was Associated With Better Outcome of Osteosarcoma Patients Receiving Gemcitabine-Docetaxel Chemotherapy', *Pediatric Blood & Cancer*, 63(9), pp. 1552–1556. doi:10.1002/pbc.26058.

Lei, Z.-N. *et al.* (2020) 'Establishment and Characterization of a Topotecan Resistant Non-small Cell Lung Cancer NCI-H460/TPT10 Cell Line', *Frontiers in Cell and Developmental Biology*, 8, p. 607275. doi:10.3389/fcell.2020.607275.

Leonard, G.D., Fojo, T. and Bates, S.E. (2003) 'The role of ABC transporters in clinical practice', *The Oncologist*, 8(5), pp. 411–424. doi:10.1634/theoncologist.8-5-411.

Letai, A.G. (2008) 'Diagnosing and exploiting cancer's addiction to blocks in apoptosis', *Nature Reviews. Cancer*, 8(2), pp. 121–132. doi:10.1038/nrc2297.

Leu, K.M. *et al.* (2004) 'Laboratory and clinical evidence of synergistic cytotoxicity of sequential treatment with gemcitabine followed by docetaxel in the treatment of sarcoma', *Journal of Clinical Oncology: Official Journal of the American Society of Clinical Oncology*, 22(9), pp. 1706–1712. doi:10.1200/JCO.2004.08.043.

Levin, J.D. *et al.* (2006) 'Position-dependent effects of locked nucleic acid (LNA) on DNA sequencing and PCR primers', *Nucleic Acids Research*, 34(20), p. e142. doi:10.1093/nar/gkl756.

Levine, B. and Kroemer, G. (2008) 'Autophagy in the pathogenesis of disease', *Cell*, 132(1), pp. 27–42. doi:10.1016/j.cell.2007.12.018.

Li, C. *et al.* (2018) 'TGM2 knockdown reverses cisplatin chemoresistance in osteosarcoma', *International Journal of Molecular Medicine*, 42(4), pp. 1799–1808. doi:10.3892/ijmm.2018.3753.

Li, J. *et al.* (2006) 'Knockdown of hypoxia-inducible factor-1alpha in breast carcinoma MCF-7 cells results in reduced tumor growth and increased sensitivity to methotrexate', *Biochemical and Biophysical Research Communications*, 342(4), pp. 1341–1351. doi:10.1016/j.bbrc.2006.02.094.

Li, Ji *et al.* (2009) 'Diallyl trisulfide reverses drug resistance and lowers the ratio of CD133+ cells in conjunction with methotrexate in a human osteosarcoma drug-resistant cell subline', *Molecular Medicine Reports*, 2(2), pp. 245–252. doi:10.3892/mmr_00000091.

Li, W. *et al.* (1995) 'Lack of functional retinoblastoma protein mediates increased resistance to antimetabolites in human sarcoma cell lines', *Proceedings of the National Academy of Sciences of the United States of America*, 92(22), pp. 10436–10440. doi:10.1073/pnas.92.22.10436.

Li, W. *et al.* (2014) 'Association of ABCB1, β tubulin I, and III with multidrug resistance of MCF7/DOC subline from breast cancer cell line MCF7', *Tumour Biology: The Journal of the International Society for Oncodevelopmental Biology and Medicine*, 35(9), pp. 8883–8891. doi:10.1007/s13277-014-2101-z.

Li, X. *et al.* (2007) '[Expressions of ERCC2 and ERCC4 genes in osteosarcoma and peripheral blood lymphocytes and their clinical significance]', *Beijing Da Xue Xue Bao. Yi Xue Ban = Journal of Peking University. Health Sciences*, 39(5), pp. 467–471.

Lim, J. and Thiery, J.P. (2012) 'Epithelial-mesenchymal transitions: insights from development', *Development (Cambridge, England)*, 139(19), pp. 3471–3486. doi:10.1242/dev.071209.

Lin, P.P. and Patel, S. (2013) 'Osteosarcoma', in Lin, P.P. and Patel, S. (eds) *Bone Sarcoma*. Boston, MA: Springer US, pp. 75–97. doi:10.1007/978-1-4614-5194-5_5.

Lippert, B. (ed.) (1999) *Cisplatin: Chemistry and Biochemistry of a Leading Anticancer Drug*. 1st edn. Wiley. doi:10.1002/9783906390420.

Lippert, T.H., Ruoff, H.-J. and Volm, M. (2008) 'Intrinsic and acquired drug resistance in malignant tumors. The main reason for therapeutic failure', *Arzneimittel-Forschung*, 58(6), pp. 261–264. doi:10.1055/s-0031-1296504.

Liu, J. *et al.* (2020) 'Establishment and characterization of a docetaxel-resistant human prostate cancer cell line', *Oncology Letters*, 20(5), p. 230. doi:10.3892/ol.2020.12093.

Liu, L. *et al.* (2008) 'Hypoxia-inducible factor-1 alpha contributes to hypoxia-induced chemoresistance in gastric cancer', *Cancer Science*, 99(1), pp. 121–128. doi:10.1111/j.1349-7006.2007.00643.x.

Liu, T. *et al.* (2016) 'Targeting *ABCB1 (MDR1)* in multi-drug resistant osteosarcoma cells using the CRISPR-Cas9 system to reverse drug resistance', *Oncotarget*, 7(50). doi:10.18632/oncotarget.13148.

Livak, K.J. and Schmittgen, T.D. (2001) 'Analysis of relative gene expression data using real-time quantitative PCR and the 2(-Delta Delta C(T)) Method', *Methods (San Diego, Calif.)*, 25(4), pp. 402–408. doi:10.1006/meth.2001.1262.

Loh, C.-Y. *et al.* (2019) 'The E-Cadherin and N-Cadherin Switch in Epithelial-to-Mesenchymal Transition: Signaling, Therapeutic Implications, and Challenges', *Cells*, 8(10), p. E1118. doi:10.3390/cells8101118.

Longhi, A. *et al.* (2006) 'Primary bone osteosarcoma in the pediatric age: State of the art', *Cancer Treatment Reviews*, 32(6), pp. 423–436. doi:10.1016/j.ctrv.2006.05.005.

Lønning, P.E. and Knappskog, S. (2013) 'Mapping genetic alterations causing chemoresistance in cancer: identifying the roads by tracking the drivers', *Oncogene*, 32(46), pp. 5315–5330. doi:10.1038/onc.2013.48.

Losada, A. *et al.* (2004) 'Establishment and characterisation of a human carcinoma cell line with acquired resistance to Aplidin', *British Journal of Cancer*, 91(7), pp. 1405–1413. doi:10.1038/sj.bjc.6602166.

Lu, M. *et al.* (2004) 'Dual effects of glutathione-S-transferase pi on As2O3 action in prostate cancer cells: enhancement of growth inhibition and inhibition of apoptosis', *Oncogene*, 23(22), pp. 3945–3952. doi:10.1038/sj.onc.1207500.

Luetke, A. *et al.* (2014) 'Osteosarcoma treatment – Where do we stand? A state of the art review', *Cancer Treatment Reviews*, 40(4), pp. 523–532. doi:10.1016/j.ctrv.2013.11.006.

Luft, F.C. (2008) 'CCN2, the connective tissue growth factor', *Journal of Molecular Medicine (Berlin, Germany)*, 86(1), pp. 1–3. doi:10.1007/s00109-007-0287-x.

Lv, J. *et al.* (2014) ‘miRNA expression patterns in chemoresistant breast cancer tissues’, *Biomedicine & Pharmacotherapy = Biomedecine & Pharmacotherapie*, 68(8), pp. 935–942. doi:10.1016/j.biopha.2014.09.011.

Ma, H. *et al.* (2015) ‘Localized Co-delivery of Doxorubicin, Cisplatin, and Methotrexate by Thermosensitive Hydrogels for Enhanced Osteosarcoma Treatment’, *ACS applied materials & interfaces*, 7(49), pp. 27040–27048. doi:10.1021/acsami.5b09112.

Maceyka, M. *et al.* (2012) ‘Sphingosine-1-phosphate signaling and its role in disease’, *Trends in Cell Biology*, 22(1), pp. 50–60. doi:10.1016/j.tcb.2011.09.003.

Machioka, K. *et al.* (2018) ‘Establishment and characterization of two cabazitaxel-resistant prostate cancer cell lines’, *Oncotarget*, 9(22), pp. 16185–16196. doi:10.18632/oncotarget.24609.

Mackey, J.R. *et al.* (1998) ‘Functional nucleoside transporters are required for gemcitabine influx and manifestation of toxicity in cancer cell lines’, *Cancer Research*, 58(19), pp. 4349–4357.

Maiuri, M.C. *et al.* (2007) ‘Self-eating and self-killing: crosstalk between autophagy and apoptosis’, *Nature Reviews. Molecular Cell Biology*, 8(9), pp. 741–752. doi:10.1038/nrm2239.

Maki, R.G. (2007) ‘Gemcitabine and docetaxel in metastatic sarcoma: past, present, and future’, *The Oncologist*, 12(8), pp. 999–1006. doi:10.1634/theoncologist.12-8-999.

Maki, R.G. *et al.* (2007) ‘Randomized phase II study of gemcitabine and docetaxel compared with gemcitabine alone in patients with metastatic soft tissue sarcomas: results of sarcoma alliance for research through collaboration study 002 [corrected]’, *Journal of*

Clinical Oncology: Official Journal of the American Society of Clinical Oncology, 25(19), pp. 2755–2763. doi:10.1200/JCO.2006.10.4117.

Malavaud, B. *et al.* (2010) 'Sphingosine kinase-1 activity and expression in human prostate cancer resection specimens', *European Journal of Cancer (Oxford, England: 1990)*, 46(18), pp. 3417–3424. doi:10.1016/j.ejca.2010.07.053.

Marchandet, L. *et al.* (2021) 'Mechanisms of Resistance to Conventional Therapies for Osteosarcoma', *Cancers*, 13(4), p. 683. doi:10.3390/cancers13040683.

Marcove, R.C. *et al.* (1970) 'Osteogenic sarcoma under the age of twenty-one. A review of one hundred and forty-five operative cases', *The Journal of Bone and Joint Surgery. American Volume*, 52(3), pp. 411–423.

Martin, A. and Clynes, M. (1993) 'Comparison of 5 microplate colorimetric assays for in vitro cytotoxicity testing and cell proliferation assays', *Cytotechnology*, 11(1), pp. 49–58. doi:10.1007/BF00749057.

Marulanda, G.A. *et al.* (2008) 'Orthopedic surgery options for the treatment of primary osteosarcoma', *Cancer Control: Journal of the Moffitt Cancer Center*, 15(1), pp. 13–20. doi:10.1177/107327480801500103.

Matenia, D. and Mandelkow, E.-M. (2009) 'The tau of MARK: a polarized view of the cytoskeleton', *Trends in Biochemical Sciences*, 34(7), pp. 332–342. doi:10.1016/j.tibs.2009.03.008.

Mazzanti, R. *et al.* (2009) 'Down-regulation of the HGF/MET autocrine loop induced by celecoxib and mediated by P-gp in MDR-positive human hepatocellular carcinoma cell line', *Biochemical Pharmacology*, 78(1), pp. 21–32. doi:10.1016/j.bcp.2009.03.013.

McAllister, R.M. *et al.* (1971) 'Cultivation in vitro of cells derived from a human osteosarcoma', *Cancer*, 27(2), pp. 397–402. doi:10.1002/1097-0142(197102)27:2<397::AID-CNCR2820270224>3.0.CO;2-X.

McConkey, D.J. *et al.* (2009) 'Role of epithelial-to-mesenchymal transition (EMT) in drug sensitivity and metastasis in bladder cancer', *Cancer Metastasis Reviews*, 28(3–4), pp. 335–344. doi:10.1007/s10555-009-9194-7.

McDermott, M. *et al.* (2014) 'In vitro Development of Chemotherapy and Targeted Therapy Drug-Resistant Cancer Cell Lines: A Practical Guide with Case Studies', *Frontiers in Oncology*, 4. doi:10.3389/fonc.2014.00040.

Merimsky, O. *et al.* (2000) 'Gemcitabine in bone sarcoma resistant to Doxorubicin-based chemotherapy', *Sarcoma*, 4(1–2), pp. 7–10. doi:10.1155/S1357714X00000025.

Merlin, J.L. *et al.* (1994) 'Comparative evaluation of S9788, verapamil, and cyclosporine A in K562 human leukemia cell lines and in P-glycoprotein-expressing samples from patients with hematologic malignancies', *Blood*, 84(1), pp. 262–269.

Meyers, P.A. *et al.* (2005) 'Osteosarcoma: a randomized, prospective trial of the addition of ifosfamide and/or muramyl tripeptide to cisplatin, doxorubicin, and high-dose methotrexate', *Journal of Clinical Oncology: Official Journal of the American Society of Clinical Oncology*, 23(9), pp. 2004–2011. doi:10.1200/JCO.2005.06.031.

Mirabello, L., Troisi, R.J. and Savage, S.A. (2009) 'International osteosarcoma incidence patterns in children and adolescents, middle ages and elderly persons', *International Journal of Cancer*, 125(1), pp. 229–234. doi:10.1002/ijc.24320.

Misaghi, A. *et al.* (2018) 'Osteosarcoma: a comprehensive review', *SICOT-J*, 4, p. 12. doi:10.1051/sicotj/2017028.

Mistry, P. *et al.* (1993) 'Effect of buthionine sulfoximine on PtII and PtIV drug accumulation and the formation of glutathione conjugates in human ovarian-carcinoma cell lines', *International Journal of Cancer*, 55(5), pp. 848–856. doi:10.1002/ijc.2910550526.

Mitra, P. *et al.* (2006) 'Role of ABCC1 in export of sphingosine-1-phosphate from mast cells', *Proceedings of the National Academy of Sciences of the United States of America*, 103(44), pp. 16394–16399. doi:10.1073/pnas.0603734103.

Mizobuchi, H. *et al.* (2008) 'Hypoxia markers in human osteosarcoma: an exploratory study', *Clinical Orthopaedics and Related Research*, 466(9), pp. 2052–2059. doi:10.1007/s11999-008-0328-y.

Mizushima, N. (2007) 'Autophagy: process and function', *Genes & Development*, 21(22), pp. 2861–2873. doi:10.1101/gad.1599207.

Mohseny, A.B. *et al.* (2011) 'Functional characterization of osteosarcoma cell lines provides representative models to study the human disease', *Laboratory Investigation*, 91(8), pp. 1195–1205. doi:10.1038/labinvest.2011.72.

Mora, J. *et al.* (2009) 'Treatment of relapsed/refractory pediatric sarcomas with gemcitabine and docetaxel', *Journal of Pediatric Hematology/Oncology*, 31(10), pp. 723–729. doi:10.1097/MPH.0b013e3181b2598c.

Morgan, S.L. *et al.* (1990) 'The effect of folic acid supplementation on the toxicity of low-dose methotrexate in patients with rheumatoid arthritis', *Arthritis & Rheumatism*, 33(1), pp. 9–18. doi:10.1002/art.1780330102.

Morgan, S.L. (1994) ‘Supplementation with Folic Acid during Methotrexate Therapy for Rheumatoid Arthritis: A Double-Blind, Placebo-Controlled Trial’, *Annals of Internal Medicine*, 121(11), p. 833. doi:10.7326/0003-4819-121-11-199412010-00002.

Morgan, S.L. *et al.* (1998) ‘Folic acid supplementation prevents deficient blood folate levels and hyperhomocysteinemia during longterm, low dose methotrexate therapy for rheumatoid arthritis: implications for cardiovascular disease prevention’, *The Journal of Rheumatology*, 25(3), pp. 441–446.

Morin, P.J. (2003) ‘Drug resistance and the microenvironment: nature and nurture’, *Drug Resistance Updates: Reviews and Commentaries in Antimicrobial and Anticancer Chemotherapy*, 6(4), pp. 169–172. doi:10.1016/s1368-7646(03)00059-1.

Morrow, J.J. *et al.* (2018) ‘Positively selected enhancer elements endow osteosarcoma cells with metastatic competence’, *Nature Medicine*, 24(2), pp. 176–185. doi:10.1038/nm.4475.

Muller, P.A.J. and Vousden, K.H. (2013) ‘p53 mutations in cancer’, *Nature Cell Biology*, 15(1), pp. 2–8. doi:10.1038/ncb2641.

Murphey, M.D. *et al.* (2004) ‘Imaging of Periosteal Osteosarcoma: Radiologic-Pathologic Comparison’, *Radiology*, 233(1), pp. 129–138. doi:10.1148/radiol.2331030326.

Murphree, A.L. and Benedict, W.F. (1984) ‘Retinoblastoma: clues to human oncogenesis’, *Science (New York, N.Y.)*, 223(4640), pp. 1028–1033. doi:10.1126/science.6320372.

Murray, S. *et al.* (2012) 'Taxane resistance in breast cancer: mechanisms, predictive biomarkers and circumvention strategies', *Cancer Treatment Reviews*, 38(7), pp. 890–903. doi:10.1016/j.ctrv.2012.02.011.

Nagourney, R.A. *et al.* (2008) 'Carboplatin plus gemcitabine repeating doublet therapy in recurrent breast cancer', *Clinical Breast Cancer*, 8(5), pp. 432–435. doi:10.3816/CBC.2008.n.052.

Nahler, G. (2009) 'Pearson correlation coefficient', in Nahler, G., *Dictionary of Pharmaceutical Medicine*. Vienna: Springer Vienna, pp. 132–132. doi:10.1007/978-3-211-89836-9_1025.

Nakajima, H. *et al.* (1997) 'Small cell osteosarcoma of bone', p. 12.

Nardinocchi, L. *et al.* (2009) 'Inhibition of HIF-1alpha activity by homeodomain-interacting protein kinase-2 correlates with sensitization of chemoresistant cells to undergo apoptosis', *Molecular Cancer*, 8, p. 1. doi:10.1186/1476-4598-8-1.

Nathrath, M. *et al.* (2002) '[Expression of genes of potential importance in the response to chemotherapy in osteosarcoma patients]', *Klinische Padiatrie*, 214(4), pp. 230–235. doi:10.1055/s-2002-33189.

National Cancer Institute (2017) 'Common Terminology Criteria for Adverse Events (CTCAE)'. Available at: https://ctep.cancer.gov/protocoldevelopment/electronic_applications/docs/CTCAE_v5_Quick_Reference_8.5x11.pdf.

National Health Service (2016) 'DOcetaxel-Gemcitabine'. Available at: https://www.uhs.nhs.uk/Media/SUHTExtranet/Services/Chemotherapy-SOPs/Sarcoma/Docetaxel-Gemcitabinev1.2.pdf.

National Heart, Blood and Lung Institute (2017) 'NIH Study Quality Assessment Tool for Cohort Studies'. Available at: https://www.nhlbi.nih.gov/health-topics/study-quality-assessment-tools.

Nava, V.E. *et al.* (2000) 'Sphingosine enhances apoptosis of radiation-resistant prostate cancer cells', *Cancer Research*, 60(16), pp. 4468–4474.

Navid, F. *et al.* (2008) 'Combination of gemcitabine and docetaxel in the treatment of children and young adults with refractory bone sarcoma', *Cancer*, 113(2), pp. 419–425. doi:10.1002/cncr.23586.

Nesher, G. and Moore, T.L. (1990) 'The in vitro effects of methotrexate on peripheral blood mononuclear cells: Modulation by methyl donors and spermidine', *Arthritis & Rheumatism*, 33(7), pp. 954–959. doi:10.1002/art.1780330706.

Nieto, M.A. (2013) 'Epithelial plasticity: a common theme in embryonic and cancer cells', *Science (New York, N.Y.)*, 342(6159), p. 1234850. doi:10.1126/science.1234850.

Nieto, M.A. *et al.* (2016) 'EMT: 2016', *Cell*, 166(1), pp. 21–45. doi:10.1016/j.cell.2016.06.028.

Nieto, M.A. and Cano, A. (2012) 'The epithelial–mesenchymal transition under control: Global programs to regulate epithelial plasticity', *Seminars in Cancer Biology*, 22(5–6), pp. 361–368. doi:10.1016/j.semcancer.2012.05.003.

Nitiss, J.L. (2009) 'Targeting DNA topoisomerase II in cancer chemotherapy', *Nature Reviews. Cancer*, 9(5), pp. 338–350. doi:10.1038/nrc2607.

Niu, B.-H. *et al.* (2010) 'The establishment and characterization of adriamycin-resistant cell lines derived from Saos-2', *Medical Science Monitor*, 16(6), pp. BR184–BR192.

Noonan, K.E. *et al.* (1990) 'Quantitative analysis of MDR1 (multidrug resistance) gene expression in human tumors by polymerase chain reaction', *Proceedings of the National Academy of Sciences of the United States of America*, 87(18), pp. 7160–7164. doi:10.1073/pnas.87.18.7160.

Obeid, L.M. *et al.* (1993) 'Programmed cell death induced by ceramide', *Science (New York, N.Y.)*, 259(5102), pp. 1769–1771. doi:10.1126/science.8456305.

Ochs, J.J. *et al.* (1978) 'cis-Dichlorodiammineplatinum (II) in advanced osteogenic sarcoma', *Cancer Treatment Reports*, 62(2), pp. 239–245.

Oda, Y. *et al.* (2000) 'Establishment of new multidrug-resistant human osteosarcoma cell lines.', *Oncology Reports*, 7(4), pp. 859–925. doi:10.3892/or.7.4.859.

Ohsumi, Y. and Mizushima, N. (2004) 'Two ubiquitin-like conjugation systems essential for autophagy', *Seminars in Cell & Developmental Biology*, 15(2), pp. 231–236. doi:10.1016/j.semcdb.2003.12.004.

Onder, T.T. *et al.* (2008) 'Loss of E-Cadherin Promotes Metastasis via Multiple Downstream Transcriptional Pathways', *Cancer Research*, 68(10), pp. 3645–3654. doi:10.1158/0008-5472.CAN-07-2938.

Osborn, M.T. and Chambers, T.C. (1996) 'Role of the stress-activated/c-Jun NH2-terminal protein kinase pathway in the cellular response to adriamycin and other chemotherapeutic drugs', *The Journal of Biological Chemistry*, 271(48), pp. 30950–30955. doi:10.1074/jbc.271.48.30950.

Ottaviani, G. and Jaffe, N. (2009) 'The Epidemiology of Osteosarcoma', in *Pediatric and Adolescent Osteosarcoma*. Springer, Boston, MA (Cancer Treatment and Research), pp. 3–13. doi:10.1007/978-1-4419-0284-9_1.

Ottaviano, L. *et al.* (2010) 'Molecular characterization of commonly used cell lines for bone tumor research: A trans-European EuroBoNet effort', *Genes, Chromosomes and Cancer*, 49(1), pp. 40–51. doi:10.1002/gcc.20717.

Overholtzer, M. *et al.* (2003) 'The presence of p53 mutations in human osteosarcomas correlates with high levels of genomic instability', *Proceedings of the National Academy of Sciences of the United States of America*, 100(20), pp. 11547–11552. doi:10.1073/pnas.1934852100.

Ozaki, T. *et al.* (2002) 'Osteosarcoma of the spine: Experience of the Cooperative Osteosarcoma Study Group', *Cancer*, 94(4), pp. 1069–1077. doi:10.1002/cncr.10258.

Palmeira, A. *et al.* (2012) 'Three decades of P-gp inhibitors: skimming through several generations and scaffolds', *Current Medicinal Chemistry*, 19(13), pp. 1946–2025. doi:10.2174/092986712800167392.

Palmerini, E. *et al.* (2016) 'Gemcitabine and docetaxel in relapsed and unresectable high-grade osteosarcoma and spindle cell sarcoma of bone', *BMC cancer*, 16, p. 280. doi:10.1186/s12885-016-2312-3.

Pan, G. *et al.* (1990) 'Osteosarcoma: MR imaging after preoperative chemotherapy', *Radiology*, 174(2), pp. 517–526. doi:10.1148/radiology.174.2.2296660.

Pan, K.L., Chan, W.H. and Chia, Y.Y. (2010) 'Initial Symptoms and Delayed Diagnosis of Osteosarcoma around the Knee Joint', *Journal of Orthopaedic Surgery*, 18(1), pp. 55–57. doi:10.1177/230949901001800112.

Panayotopoulou, E.G. *et al.* (2017) 'Targeting of apoptotic pathways by SMAC or BH3 mimetics distinctly sensitizes paclitaxel-resistant triple negative breast cancer cells', *Oncotarget*, 8(28), pp. 45088–45104. doi:10.18632/oncotarget.15125.

Park, H. *et al.* (2015) 'Genomic alterations in BCL2L1 and DLC1 contribute to drug sensitivity in gastric cancer', *Proceedings of the National Academy of Sciences of the United States of America*, 112(40), pp. 12492–12497. doi:10.1073/pnas.1507491112.

Park, H.J. *et al.* (2018) 'The PARP inhibitor olaparib potentiates the effect of the DNA damaging agent doxorubicin in osteosarcoma', *Journal of experimental & clinical cancer research: CR*, 37(1), p. 107. doi:10.1186/s13046-018-0772-9.

Park, K.-S. *et al.* (2010) 'Transglutaminase 2 as a cisplatin resistance marker in non-small cell lung cancer', *Journal of Cancer Research and Clinical Oncology*, 136(4), pp. 493–502. doi:10.1007/s00432-009-0681-6.

Parker, R.J. *et al.* (1991) 'Acquired cisplatin resistance in human ovarian cancer cells is associated with enhanced repair of cisplatin-DNA lesions and reduced drug accumulation', *The Journal of Clinical Investigation*, 87(3), pp. 772–777. doi:10.1172/JCI115080.

Pasello, M. *et al.* (2008) 'Overcoming glutathione S-transferase P1-related cisplatin resistance in osteosarcoma', *Cancer Research*, 68(16), pp. 6661–6668. doi:10.1158/0008-5472.CAN-07-5840.

Patel, S.R. *et al.* (1997) 'High-dose ifosfamide in bone and soft tissue sarcomas: results of phase II and pilot studies--dose-response and schedule dependence', *Journal of Clinical Oncology: Official Journal of the American Society of Clinical Oncology*, 15(6), pp. 2378–2384. doi:10.1200/JCO.1997.15.6.2378.

Patiño-García, A. *et al.* (2009) 'Methotrexate in pediatric osteosarcoma: response and toxicity in relation to genetic polymorphisms and dihydrofolate reductase and reduced folate carrier 1 expression', *The Journal of Pediatrics*, 154(5), pp. 688–693. doi:10.1016/j.jpeds.2008.11.030.

Pautier, P. *et al.* (2012) 'Randomized multicenter and stratified phase II study of gemcitabine alone versus gemcitabine and docetaxel in patients with metastatic or relapsed leiomyosarcomas: a Federation Nationale des Centres de Lutte Contre le Cancer (FNCLCC) French Sarcoma Group Study (TAXOGEM study)', *The Oncologist*, 17(9), pp. 1213–1220. doi:10.1634/theoncologist.2011-0467.

Pautke, C. *et al.* (2004) 'Characterization of osteosarcoma cell lines MG-63, Saos-2 and U-2 OS in comparison to human osteoblasts', *Anticancer Research*, 24(6), pp. 3743–3748.

Pawłowska, J. *et al.* (2003) 'Differential ability of cytostatics from anthraquinone group to generate free radicals in three enzymatic systems: NADH dehydrogenase, NADPH cytochrome P450 reductase, and xanthine oxidase', *Oncology Research*, 13(5), pp. 245–252. doi:10.3727/096504003108748294.

Peinado, H., Olmeda, D. and Cano, A. (2007) 'Snail, Zeb and bHLH factors in tumour progression: an alliance against the epithelial phenotype?', *Nature Reviews. Cancer*, 7(6), pp. 415–428. doi:10.1038/nrc2131.

Peltier, L.F. (1985) 'Historical note on bone and soft tissue sarcoma', *Journal of Surgical Oncology*, 30(4), pp. 201–205. doi:10.1002/jso.2930300403.

Perbal, B. (2004) 'CCN proteins: multifunctional signalling regulators', *Lancet (London, England)*, 363(9402), pp. 62–64. doi:10.1016/S0140-6736(03)15172-0.

Perego, P. *et al.* (1999) 'A novel trinuclear platinum complex overcomes cisplatin resistance in an osteosarcoma cell system', *Molecular Pharmacology*, 55(3), pp. 528–534.

Perkins, N.D. (2012) 'The diverse and complex roles of NF-κB subunits in cancer', *Nature Reviews. Cancer*, 12(2), pp. 121–132. doi:10.1038/nrc3204.

Petrilli, A.S. *et al.* (1991) 'Increased survival, limb preservation, and prognostic factors for osteosarcoma', *Cancer*, 68(4), pp. 733–737. doi:10.1002/1097-0142(19910815)68:4<733::aid-cncr2820680412>3.0.co;2-0.

Pfisterer, J. *et al.* (2006) 'Gemcitabine plus carboplatin compared with carboplatin in patients with platinum-sensitive recurrent ovarian cancer: an intergroup trial of the AGO-OVAR, the NCIC CTG, and the EORTC GCG', *Journal of Clinical Oncology: Official Journal of the American Society of Clinical Oncology*, 24(29), pp. 4699–4707. doi:10.1200/JCO.2006.06.0913.

Philip, B. *et al.* (2013) 'HIF expression and the role of hypoxic microenvironments within primary tumours as protective sites driving cancer stem cell renewal and metastatic progression', *Carcinogenesis*, 34(8), pp. 1699–1707. doi:10.1093/carcin/bgt209.

Pilorget, A. *et al.* (2007) 'Modulation of P-glycoprotein function by sphingosine kinase-1 in brain endothelial cells: Sphingosine kinase-1 stimulates P-gp transport activity', *Journal of Neurochemistry*, 100(5), pp. 1203–1210. doi:10.1111/j.1471-4159.2006.04295.x.

Pinkel, D. (1958) 'The use of body surface area as a criterion of drug dosage in cancer chemotherapy', *Cancer Research*, 18(7), pp. 853–856.

Plunkett, W., Huang, P. and Gandhi, V. (1995) 'Preclinical characteristics of gemcitabine', *Anti-Cancer Drugs*, 6 Suppl 6, pp. 7–13. doi:10.1097/00001813-199512006-00002.

Polyak, K. and Weinberg, R.A. (2009) 'Transitions between epithelial and mesenchymal states: acquisition of malignant and stem cell traits', *Nature Reviews. Cancer*, 9(4), pp. 265–273. doi:10.1038/nrc2620.

PosthumaDeBoer, J., van Royen, B.J. and Helder, M.N. (2013) ‘Mechanisms of therapy resistance in osteosarcoma: a review’, *Oncology Discovery*, 1(1), p. 8. doi:10.7243/2052-6199-1-8.

Press, M.F. *et al.* (2011) ‘Alteration of topoisomerase II-alpha gene in human breast cancer: association with responsiveness to anthracycline-based chemotherapy’, *Journal of Clinical Oncology: Official Journal of the American Society of Clinical Oncology*, 29(7), pp. 859–867. doi:10.1200/JCO.2009.27.5644.

Pulkoski-Gross, M.J. and Obeid, L.M. (2018) ‘Molecular mechanisms of regulation of sphingosine kinase 1’, *Biochimica Et Biophysica Acta. Molecular and Cell Biology of Lipids*, 1863(11), pp. 1413–1422. doi:10.1016/j.bbalip.2018.08.015.

Pyne, N.J. and Pyne, S. (2010) ‘Sphingosine 1-phosphate and cancer’, *Nature Reviews. Cancer*, 10(7), pp. 489–503. doi:10.1038/nrc2875.

Qi, W.-X. *et al.* (2012) ‘Efficacy and safety of gemcitabine-docetaxel combination therapy for recurrent or refractory high-grade osteosarcoma in China: a retrospective study of 18 patients’, *Japanese Journal of Clinical Oncology*, 42(5), pp. 427–431. doi:10.1093/jjco/hys030.

Qiagen (2021) ‘QuantiNova LNA PCR Handbook’. Available at: https://www.qiagen.com/gb/resources/download.aspx?id=84bcc325-6b64-43a2-8143-3bbc84a4bc5f&lang=en.

Qin, X.Q. *et al.* (1995) ‘The transcription factor E2F-1 is a downstream target of RB action’, *Molecular and Cellular Biology*, 15(2), pp. 742–755. doi:10.1128/MCB.15.2.742.

Quint, K. *et al.* (2012) 'Pancreatic cancer cells surviving gemcitabine treatment express markers of stem cell differentiation and epithelial-mesenchymal transition', *International Journal of Oncology*, 41(6), pp. 2093–2102. doi:10.3892/ijo.2012.1648.

Rada, M. *et al.* (2018) 'Inhibitor of apoptosis proteins (IAPs) mediate collagen type XI alpha 1-driven cisplatin resistance in ovarian cancer', *Oncogene*, 37(35), pp. 4809–4820. doi:10.1038/s41388-018-0297-x.

Rapkin, L. *et al.* (2012) 'Gemcitabine and docetaxel (GEMDOX) for the treatment of relapsed and refractory pediatric sarcomas', *Pediatric Blood & Cancer*, 59(5), pp. 854–858. doi:10.1002/pbc.24101.

Reck, M. *et al.* (2009) 'Phase III trial of cisplatin plus gemcitabine with either placebo or bevacizumab as first-line therapy for nonsquamous non-small-cell lung cancer: AVAil', *Journal of Clinical Oncology: Official Journal of the American Society of Clinical Oncology*, 27(8), pp. 1227–1234. doi:10.1200/JCO.2007.14.5466.

Ren, X. and Su, C. (2020) 'Sphingosine kinase 1 contributes to doxorubicin resistance and glycolysis in osteosarcoma', *Molecular Medicine Reports*, 22(3), pp. 2183–2190. doi:10.3892/mmr.2020.11295.

Rhee, M.S. *et al.* (1993) 'Acquisition of resistance to antifolates caused by enhanced gamma-glutamyl hydrolase activity', *Cancer Research*, 53(10 Suppl), pp. 2227–2230.

Ringel, I. and Horwitz, S.B. (1991) 'Studies with RP 56976 (taxotere): a semisynthetic analogue of taxol', *Journal of the National Cancer Institute*, 83(4), pp. 288–291. doi:10.1093/jnci/83.4.288.

Rodriguez, L.G., Wu, X. and Guan, J.-L. (2004) 'Wound-Healing Assay', in Guan, J.-L., *Cell Migration*. New Jersey: Humana Press, pp. 023–030. doi:10.1385/1-59259-860-9:023.

Roncuzzi, L., Pancotti, F. and Baldini, N. (2014) 'Involvement of HIF-1α activation in the doxorubicin resistance of human osteosarcoma cells', *Oncology Reports*, 32(1), pp. 389–394. doi:10.3892/or.2014.3181.

Rosen, G. *et al.* (1979) 'Primary osteogenic sarcoma: the rationale for preoperative chemotherapy and delayed surgery', *Cancer*, 43(6), pp. 2163–2177. doi:10.1002/1097-0142(197906)43:6<2163::aid-cncr2820430602>3.0.co;2-s.

Rosen, G. (1985) 'Preoperative (neoadjuvant) chemotherapy for osteogenic sarcoma: a ten year experience', *Orthopedics*, 8(5), pp. 659–664. doi:10.3928/0147-7447-19850501-19.

Rosen, G. *et al.* (1994) 'Synovial sarcoma. Uniform response of metastases to high dose ifosfamide', *Cancer*, 73(10), pp. 2506–2511. doi:10.1002/1097-0142(19940515)73:10<2506::aid-cncr2820731009>3.0.co;2-s.

Rosen, G. and Nirenberg, A. (1985) 'Neoadjuvant chemotherapy for osteogenic sarcoma: a five year follow-up (T-10) and preliminary report of new studies (T-12)', *Progress in Clinical and Biological Research*, 201, pp. 39–51.

Rosenberg, B. (1980) *Nucleic Acid-Metal Ion Interactions*. Spiro, T.G., Ed. New York, NY, USA: John Wiley & Sons, Inc.

Ryan, K.M., Phillips, A.C. and Vousden, K.H. (2001) 'Regulation and function of the p53 tumor suppressor protein', *Current Opinion in Cell Biology*, 13(3), pp. 332–337. doi:10.1016/s0955-0674(00)00216-7.

Saeter, G. *et al.* (1991) 'Treatment of osteosarcoma of the extremities with the T-10 protocol, with emphasis on the effects of preoperative chemotherapy with single-agent high-dose methotrexate: a Scandinavian Sarcoma Group study.', *Journal of Clinical Oncology*, 9(10), pp. 1766–1775. doi:10.1200/JCO.1991.9.10.1766.

Sánchez-Tilló, E. *et al.* (2014) 'The EMT activator ZEB1 promotes tumor growth and determines differential response to chemotherapy in mantle cell lymphoma', *Cell Death and Differentiation*, 21(2), pp. 247–257. doi:10.1038/cdd.2013.123.

Savagner, P. (2010) 'The epithelial-mesenchymal transition (EMT) phenomenon', *Annals of Oncology: Official Journal of the European Society for Medical Oncology*, 21 Suppl 7, pp. vii89-92. doi:10.1093/annonc/mdq292.

Schajowicz, F., Sissons, H.A. and Sobin, L.H. (1995) 'The World Health Organization's histologic classification of bone tumors. A commentary on the second edition', *Cancer*, 75(5), pp. 1208–1214. doi:10.1002/1097-0142(19950301)75:5<1208::AID-CNCR2820750522>3.0.CO;2-F.

Schiefler, C. *et al.* (2014) 'Inhibition of SphK1 reduces radiation-induced migration and enhances sensitivity to cetuximab treatment by affecting the EGFR / SphK1 crosstalk', *Oncotarget*, 5(20), pp. 9877–9888. doi:10.18632/oncotarget.2436.

Schinkel, A.H. *et al.* (1994) 'Disruption of the mouse mdr1a P-glycoprotein gene leads to a deficiency in the blood-brain barrier and to increased sensitivity to drugs', *Cell*, 77(4), pp. 491–502. doi:10.1016/0092-8674(94)90212-7.

Schweitzer, B.I., Dicker, A.P. and Bertino, J.R. (1990) 'Dihydrofolate reductase as a therapeutic target', *FASEB journal: official publication of the Federation of American Societies for Experimental Biology*, 4(8), pp. 2441–2452. doi:10.1096/fasebj.4.8.2185970.

Scotlandi, K., Picci, P. and Kovar, H. (2009) 'Targeted therapies in bone sarcomas', *Current Cancer Drug Targets*, 9(7), pp. 843–853. doi:10.2174/156800909789760410.

Scotto, K.W. (2003) 'Transcriptional regulation of ABC drug transporters', *Oncogene*, 22(47), pp. 7496–7511. doi:10.1038/sj.onc.1206950.

Scranton, P.E. *et al.* (1975) 'Prognostic factors in osteosarcoma. A review of 20 year's experience at the University of Pittsburgh Health Center Hospitals', *Cancer*, 36(6), pp. 2179–2191. doi:10.1002/cncr.2820360936.

Sedletska, Y., Giraud-Panis, M.-J. and Malinge, J.-M. (2005) 'Cisplatin is a DNA-damaging antitumour compound triggering multifactorial biochemical responses in cancer cells: importance of apoptotic pathways', *Current Medicinal Chemistry. Anti-Cancer Agents*, 5(3), pp. 251–265. doi:10.2174/1568011053765967.

Serra, M. (2004) 'Analysis of dihydrofolate reductase and reduced folate carrier gene status in relation to methotrexate resistance in osteosarcoma cells', *Annals of Oncology*, 15(1), pp. 151–160. doi:10.1093/annonc/mdh004.

Serra, M. *et al.* (2004) 'Analysis of dihydrofolate reductase and reduced folate carrier gene status in relation to methotrexate resistance in osteosarcoma cells', *Annals of Oncology: Official Journal of the European Society for Medical Oncology*, 15(1), pp. 151–160. doi:10.1093/annonc/mdh004.

Shah, N. and Dizon, D.S. (2009) 'New-generation platinum agents for solid tumors', *Future Oncology (London, England)*, 5(1), pp. 33–42. doi:10.2217/14796694.5.1.33.

Shan, G. (2010) 'RNA interference as a gene knockdown technique', *The International Journal of Biochemistry & Cell Biology*, 42(8), pp. 1243–1251. doi:10.1016/j.biocel.2009.04.023.

Sharom, F.J. (2011) 'The P-glycoprotein multidrug transporter', *Essays in Biochemistry*, 50(1), pp. 161–178. doi:10.1042/bse0500161.

Shen, M. *et al.* (2019) 'Inhibition of ATM reverses EMT and decreases metastatic potential of cisplatin-resistant lung cancer cells through JAK/STAT3/PD-L1 pathway', *Journal of experimental & clinical cancer research: CR*, 38(1), p. 149. doi:10.1186/s13046-019-1161-8.

Shida, D. *et al.* (2008) 'Targeting SphK1 as a new strategy against cancer', *Current Drug Targets*, 9(8), pp. 662–673. doi:10.2174/138945008785132402.

Shiloh, Y. and Ziv, Y. (2013) 'The ATM protein kinase: regulating the cellular response to genotoxic stress, and more', *Nature Reviews. Molecular Cell Biology*, 14(4), pp. 197–210.

Shirakawa, K. *et al.* (1999) 'Interaction of docetaxel ("Taxotere") with human P-glycoprotein', *Japanese Journal of Cancer Research: Gann*, 90(12), pp. 1380–1386. doi:10.1111/j.1349-7006.1999.tb00723.x.

Shiroky, J.B. *et al.* (1993) 'Low-dose methotrexate with leucovorin (folinic acid) in the management of rheumatoid arthritis. results of a multicenter randomized, double-blind, placebo-controlled trial', *Arthritis & Rheumatism*, 36(6), pp. 795–803. doi:10.1002/art.1780360609.

Shpilka, T., Mizushima, N. and Elazar, Z. (2012) 'Ubiquitin-like proteins and autophagy at a glance', *Journal of Cell Science*, 125(Pt 10), pp. 2343–2348. doi:10.1242/jcs.093757.

Siddik, Z.H. (2003) 'Cisplatin: mode of cytotoxic action and molecular basis of resistance', *Oncogene*, 22(47), pp. 7265–7279. doi:10.1038/sj.onc.1206933.

Simpson, S. *et al.* (2017) 'Comparative review of human and canine osteosarcoma: morphology, epidemiology, prognosis, treatment and genetics', *Acta Veterinaria Scandinavica*, 59(1), p. 71. doi:10.1186/s13028-017-0341-9.

Singer, C.F. *et al.* (2006) 'Tissue array-based expression of transglutaminase-2 in human breast and ovarian cancer', *Clinical & Experimental Metastasis*, 23(1), pp. 33–39. doi:10.1007/s10585-006-9015-0.

Sirotnak, F.M. (1987) 'Determinants of resistance to antifolates: biochemical phenotypes, their frequency of occurrence and circumvention', *NCI monographs: a publication of the National Cancer Institute*, (5), pp. 27–35.

Slansky, J.E. *et al.* (1993) 'A protein synthesis-dependent increase in E2F1 mRNA correlates with growth regulation of the dihydrofolate reductase promoter', *Molecular and Cellular Biology*, 13(3), pp. 1610–1618. doi:10.1128/mcb.13.3.1610-1618.1993.

Smeland, S. *et al.* (2019) 'Survival and prognosis with osteosarcoma: outcomes in more than 2000 patients in the EURAMOS-1 (European and American Osteosarcoma Study) cohort', *European Journal of Cancer (Oxford, England: 1990)*, 109, pp. 36–50. doi:10.1016/j.ejca.2018.11.027.

Smith, B.N. and Bhowmick, N.A. (2016) 'Role of EMT in Metastasis and Therapy Resistance', *Journal of Clinical Medicine*, 5(2), p. E17. doi:10.3390/jcm5020017.

Song, B.S. *et al.* (2014) 'Gemcitabine and docetaxel for the treatment of children and adolescents with recurrent or refractory osteosarcoma: Korea Cancer Center Hospital experience', *Pediatric Blood & Cancer*, 61(8), pp. 1376–1381. doi:10.1002/pbc.25035.

Song, L. *et al.* (2017) 'Silencing LPAATβ inhibits tumor growth of cisplatin-resistant human osteosarcoma in vivo and in vitro', *International Journal of Oncology*, 50(2), pp. 535–544. doi:10.3892/ijo.2016.3820.

de Sousa Cavalcante, L. and Monteiro, G. (2014) 'Gemcitabine: metabolism and molecular mechanisms of action, sensitivity and chemoresistance in pancreatic cancer', *European Journal of Pharmacology*, 741, pp. 8–16. doi:10.1016/j.ejphar.2014.07.041.

Sparreboom, A. *et al.* (1997) 'Limited oral bioavailability and active epithelial excretion of paclitaxel (Taxol) caused by P-glycoprotein in the intestine', *Proceedings of the National Academy of Sciences of the United States of America*, 94(5), pp. 2031–2035. doi:10.1073/pnas.94.5.2031.

Spiegel, S. and Milstien, S. (2003) 'Sphingosine-1-phosphate: an enigmatic signalling lipid', *Nature Reviews. Molecular Cell Biology*, 4(5), pp. 397–407. doi:10.1038/nrm1103.

Sritharan, S. and Sivalingam, N. (2021) 'A comprehensive review on time-tested anticancer drug doxorubicin', *Life Sciences*, 278, p. 119527. doi:10.1016/j.lfs.2021.119527.

Steffen, J.A. and Stolzmann, W.M. (1969) 'Studies on in vitro lymphocyte proliferation in cultures synchronized by the inhibition of DNA synthesis. I. Variability of S plus G2 periods of first generation cells', *Experimental Cell Research*, 56(2), pp. 453–460. doi:10.1016/0014-4827(69)90039-1.

Stordal, B. *et al.* (2012) 'Resistance to Paclitaxel in a Cisplatin-Resistant Ovarian Cancer Cell Line Is Mediated by P-Glycoprotein', *PLoS ONE*. Edited by A.J.R. Bishop, 7(7), p. e40717. doi:10.1371/journal.pone.0040717.

Stordal, B.K., Davey, M.W. and Davey, R.A. (2006) 'Oxaliplatin induces drug resistance more rapidly than cisplatin in H69 small cell lung cancer cells', *Cancer Chemotherapy and Pharmacology*, 58(2), pp. 256–265. doi:10.1007/s00280-005-0148-7.

Sun, X. *et al.* (2022) 'The anti-osteosarcoma cell activity by the sphingosine kinase 1 inhibitor SKI-V', *Cell Death Discovery*, 8(1), p. 48. doi:10.1038/s41420-022-00838-4.

Sung, H. *et al.* (2021) 'Global Cancer Statistics 2020: GLOBOCAN Estimates of Incidence and Mortality Worldwide for 36 Cancers in 185 Countries', *CA: a cancer journal for clinicians*, 71(3), pp. 209–249. doi:10.3322/caac.21660.

Susa, M. *et al.* (2009) 'Doxorubicin loaded Polymeric Nanoparticulate Delivery System to overcome drug resistance in osteosarcoma', *BMC Cancer*, 9(1). doi:10.1186/1471-2407-9-399.

Susa, M. *et al.* (2010) 'Inhibition of ABCB1 (MDR1) expression by an siRNA nanoparticulate delivery system to overcome drug resistance in osteosarcoma', *PloS One*, 5(5), p. e10764. doi:10.1371/journal.pone.0010764.

Swain, S.M., Whaley, F.S. and Ewer, M.S. (2003) 'Congestive heart failure in patients treated with doxorubicin: a retrospective analysis of three trials', *Cancer*, 97(11), pp. 2869–2879. doi:10.1002/cncr.11407.

Swinehart, D.F. (1962) 'The Beer-Lambert Law', *Journal of Chemical Education*, 39(7), p. 333. doi:10.1021/ed039p333.

Szakács, G. *et al.* (2004) 'Predicting drug sensitivity and resistance: profiling ABC transporter genes in cancer cells', *Cancer Cell*, 6(2), pp. 129–137. doi:10.1016/j.ccr.2004.06.026.

Szakács, G. *et al.* (2006) 'Targeting multidrug resistance in cancer', *Nature Reviews. Drug Discovery*, 5(3), pp. 219–234. doi:10.1038/nrd1984.

Ta, H.T. *et al.* (2009) 'Osteosarcoma treatment: state of the art', *Cancer Metastasis Reviews*, 28(1–2), pp. 247–263. doi:10.1007/s10555-009-9186-7.

Takahashi, Masanobu *et al.* (2017) 'Efficacy and safety of gemcitabine plus docetaxel in Japanese patients with unresectable or recurrent bone and soft tissue sarcoma: Results from a single-institutional analysis', *PloS One*, 12(5), p. e0176972. doi:10.1371/journal.pone.0176972.

Takeda, M. *et al.* (2007) 'The establishment of two paclitaxel-resistant prostate cancer cell lines and the mechanisms of paclitaxel resistance with two cell lines', *The Prostate*, 67(9), pp. 955–967. doi:10.1002/pros.20581.

Tegze, B. *et al.* (2012) 'Parallel evolution under chemotherapy pressure in 29 breast cancer cell lines results in dissimilar mechanisms of resistance', *PloS One*, 7(2), p. e30804. doi:10.1371/journal.pone.0030804.

van Tellingen, O. *et al.* (2003) 'P-glycoprotein and Mrp1 collectively protect the bone marrow from vincristine-induced toxicity in vivo', *British Journal of Cancer*, 89(9), pp. 1776–1782. doi:10.1038/sj.bjc.6601363.

Tew, K.D. (1994) 'Glutathione-associated enzymes in anticancer drug resistance', *Cancer Research*, 54(16), pp. 4313–4320.

Tewey, K.M. *et al.* (1984) 'Adriamycin-induced DNA damage mediated by mammalian DNA topoisomerase II', *Science (New York, N.Y.)*, 226(4673), pp. 466–468. doi:10.1126/science.6093249.

Thiery, J.P. *et al.* (2009) 'Epithelial-Mesenchymal Transitions in Development and Disease', *Cell*, 139(5), pp. 871–890. doi:10.1016/j.cell.2009.11.007.

Thomas, H. and Coley, H.M. (2003) 'Overcoming multidrug resistance in cancer: an update on the clinical strategy of inhibiting p-glycoprotein', *Cancer Control: Journal of the Moffitt Cancer Center*, 10(2), pp. 159–165. doi:10.1177/107327480301000207.

Thorn, C.F. *et al.* (2011) 'Doxorubicin pathways: pharmacodynamics and adverse effects', *Pharmacogenetics and Genomics*, 21(7), pp. 440–446. doi:10.1097/FPC.0b013e32833ffb56.

Tian, H. and Cronstein, B.N. (2007) 'Understanding the mechanisms of action of methotrexate: implications for the treatment of rheumatoid arthritis', *Bulletin of the NYU hospital for joint diseases*, 65(3), pp. 168–173.

Tiwari, N. *et al.* (2013) 'Sox4 is a master regulator of epithelial-mesenchymal transition by controlling Ezh2 expression and epigenetic reprogramming', *Cancer Cell*, 23(6), pp. 768–783. doi:10.1016/j.ccr.2013.04.020.

Tolstrup, N. *et al.* (2003) 'OligoDesign: Optimal design of LNA (locked nucleic acid) oligonucleotide capture probes for gene expression profiling', *Nucleic Acids Research*, 31(13), pp. 3758–3762. doi:10.1093/nar/gkg580.

Townsend, D.M. and Tew, K.D. (2003) 'The role of glutathione-S-transferase in anti-cancer drug resistance', *Oncogene*, 22(47), pp. 7369–7375. doi:10.1038/sj.onc.1206940.

Townsend, D.M., Tew, K.D. and Tapiero, H. (2003) 'The importance of glutathione in human disease', *Biomedicine & Pharmacotherapy = Biomedecine & Pharmacotherapie*, 57(3–4), pp. 145–155. doi:10.1016/s0753-3322(03)00043-x.

Trédan, O. *et al.* (2007) 'Drug resistance and the solid tumor microenvironment', *Journal of the National Cancer Institute*, 99(19), pp. 1441–1454. doi:10.1093/jnci/djm135.

Tsai, H.-C. *et al.* (2014) 'CCN2 enhances resistance to cisplatin-mediating cell apoptosis in human osteosarcoma', *PloS One*, 9(3), p. e90159. doi:10.1371/journal.pone.0090159.

Tsai, H.-C. *et al.* (2019) 'CCN2 promotes drug resistance in osteosarcoma by enhancing ABCG2 expression', *Journal of Cellular Physiology*, 234(6), pp. 9297–9307. doi:10.1002/jcp.27611.

Tsang, R.Y., Al-Fayea, T. and Au, H.-J. (2009) 'Cisplatin overdose: toxicities and management', *Drug Safety*, 32(12), pp. 1109–1122. doi:10.2165/11316640-000000000-00000.

Tsuchiya, H. *et al.* (2000) 'Sensitization and caffeine potentiation of cisplatin cytotoxicity resulting from introduction of wild-type p53 gene in human osteosarcoma', *Anticancer Research*, 20(1A), pp. 235–242.

Turel, M.K. *et al.* (2012) 'Primary telangiectatic osteosarcoma of the cervical spine', *Journal of Neurosurgery: Spine*, 16(4), pp. 373–378. doi:10.3171/2011.12.SPINE111037.

Ullah, M.F. (2008) 'Cancer multidrug resistance (MDR): a major impediment to effective chemotherapy', *Asian Pacific journal of cancer prevention: APJCP*, 9(1), pp. 1–6.

Unni, K., Dahlin, D. and Beabout, J. (1976) 'Periosteal osteogenic sarcoma', 37, p. 10.

Unnim, K., Mcleodm, R. and Pritcharmdd, D. (1977) 'Intraosseous well-differentiated osteosarcoma', p. 11.

Varamo, C. *et al.* (2019) 'Establishment and Characterization of a New Intrahepatic Cholangiocarcinoma Cell Line Resistant to Gemcitabine', *Cancers*, 11(4), p. E519. doi:10.3390/cancers11040519.

Venable, M.E. *et al.* (1995) 'Role of ceramide in cellular senescence', *The Journal of Biological Chemistry*, 270(51), pp. 30701–30708. doi:10.1074/jbc.270.51.30701.

Vermorken, J.B. *et al.* (1984) 'Pharmacokinetics of free and total platinum species after short-term infusion of cisplatin', *Cancer Treatment Reports*, 68(3), pp. 505–513.

Viscarra, T. *et al.* (2019) 'Functional and transcriptomic characterization of carboplatin-resistant A2780 ovarian cancer cell line', *Biological Research*, 52(1), p. 13. doi:10.1186/s40659-019-0220-0.

Wadayama, B. *et al.* (1994) 'Mutation spectrum of the retinoblastoma gene in osteosarcomas', *Cancer Research*, 54(11), pp. 3042–3048.

Waghray, D. and Zhang, Q. (2018) 'Inhibit or Evade Multidrug Resistance P-Glycoprotein in Cancer Treatment', *Journal of Medicinal Chemistry*, 61(12), pp. 5108–5121. doi:10.1021/acs.jmedchem.7b01457.

Wang, D. *et al.* (2019) 'Visfatin is involved in the cisplatin resistance of osteosarcoma cells via upregulation of Snail and Zeb1', *Cancer Biology & Therapy*, 20(7), pp. 999–1006. doi:10.1080/15384047.2019.1591675.

Wang, D., Luo, M. and Kelley, M.R. (2004) 'Human apurinic endonuclease 1 (APE1) expression and prognostic significance in osteosarcoma: enhanced sensitivity of osteosarcoma to DNA damaging agents using silencing RNA APE1 expression inhibition', *Molecular Cancer Therapeutics*, 3(6), pp. 679–686.

Wang, G. *et al.* (2012) 'Novel roles of Skp2 E3 ligase in cellular senescence, cancer progression, and metastasis', *Chinese Journal of Cancer*, 31(4), pp. 169–177. doi:10.5732/cjc.011.10319.

Wang, J. and Li, G. (2015) 'Mechanisms of methotrexate resistance in osteosarcoma cell lines and strategies for overcoming this resistance', *Oncology Letters*, 9(2), pp. 940–944. doi:10.3892/ol.2014.2773.

Wang, J.J. and Li, G.J. (2014) 'Relationship between RFC gene expression and intracellular drug concentration in methotrexate-resistant osteosarcoma cells', *Genetics and molecular research: GMR*, 13(3), pp. 5313–5321. doi:10.4238/2014.July.24.10.

Wang, R. *et al.* (2014) 'Gemcitabine Resistance is Associated with Epithelial-Mesenchymal Transition and Induction of HIF-1α in Pancreatic Cancer Cells', *Current Cancer Drug Targets*, 14(4), pp. 407–417. doi:10.2174/1568009614666140226114015.

Wang, S. *et al.* (2018) 'Triple Negative Breast Cancer Depends on Sphingosine Kinase 1 (SphK1)/Sphingosine-1-Phosphate (S1P)/Sphingosine 1-Phosphate Receptor 3 (S1PR3)/Notch Signaling for Metastasis', *Medical Science Monitor: International Medical Journal of Experimental and Clinical Research*, 24, pp. 1912–1923. doi:10.12659/msm.905833.

Wang, W. *et al.* (2015) 'Transglutaminase-2 is Involved in Cell Apoptosis of Osteosarcoma Cell Line U2OS Under Hypoxia Condition', *Cell Biochemistry and Biophysics*, 72(1), pp. 283–288. doi:10.1007/s12013-014-0451-1.

Wang, X., Zhang, H. and Chen, X. (2019) 'Drug resistance and combating drug resistance in cancer', *Cancer Drug Resistance* [Preprint]. doi:10.20517/cdr.2019.10.

Warmann, S. *et al.* (2002) 'MDR1 modulators improve the chemotherapy response of human hepatoblastoma to doxorubicin in vitro', *Journal of Pediatric Surgery*, 37(11), pp. 1579–1584. doi:10.1053/jpsu.2002.36188.

Weber, A.M. and Ryan, A.J. (2015) 'ATM and ATR as therapeutic targets in cancer', *Pharmacology & Therapeutics*, 149, pp. 124–138. doi:10.1016/j.pharmthera.2014.12.001.

Wei, L. *et al.* (2006) '[Expression of MDR1 and GST-pi in osteosarcoma and soft tissue sarcoma and their correlation with chemotherapy resistance]', *Zhonghua Zhong Liu Za Zhi [Chinese Journal of Oncology]*, 28(6), pp. 445–448.

Wei, X. *et al.* (2020) 'MARK2 enhances cisplatin resistance via PI3K/AKT/NF-κB signaling pathway in osteosarcoma cells', *American Journal of Translational Research*, 12(5), pp. 1807–1823.

Weidemann, A. and Johnson, R.S. (2008) 'Biology of HIF-1alpha', *Cell Death and Differentiation*, 15(4), pp. 621–627. doi:10.1038/cdd.2008.12.

Weiss, A. *et al.* (2007) 'Telangiectatic osteosarcoma: The St. Jude Children's Research Hospital's experience', *Cancer*, 109(8), pp. 1627–1637. doi:10.1002/cncr.22574.

Weiss, R.B. (1992) 'The anthracyclines: will we ever find a better doxorubicin?', *Seminars in Oncology*, 19(6), pp. 670–686.

Wen, J. *et al.* (2015) 'Autophagy inhibition re-sensitizes pulse stimulation-selected paclitaxel-resistant triple negative breast cancer cells to chemotherapy-induced apoptosis', *Breast Cancer Research and Treatment*, 149(3), pp. 619–629. doi:10.1007/s10549-015-3283-9.

Wen, X.-M. *et al.* (2019) 'Establishment and molecular characterization of decitabine-resistant K562 cells', *Journal of Cellular and Molecular Medicine*, 23(5), pp. 3317–3324. doi:10.1111/jcmm.14221.

Wenger, C. *et al.* (1999) 'Expression and differential regulation of connective tissue growth factor in pancreatic cancer cells', *Oncogene*, 18(4), pp. 1073–1080. doi:10.1038/sj.onc.1202395.

Westhoff, M.-A. and Fulda, S. (2009) 'Adhesion-mediated apoptosis resistance in cancer', *Drug Resistance Updates: Reviews and Commentaries in Antimicrobial and Anticancer Chemotherapy*, 12(4–5), pp. 127–136. doi:10.1016/j.drup.2009.08.001.

Whelan, J.S. *et al.* (2015) 'EURAMOS-1, an international randomised study for osteosarcoma: results from pre-randomisation treatment', *Annals of Oncology: Official Journal of the European Society for Medical Oncology*, 26(2), pp. 407–414. doi:10.1093/annonc/mdu526.

Wilfinger, W.W., Mackey, K. and Chomczynski, P. (1997) 'Effect of pH and ionic strength on the spectrophotometric assessment of nucleic acid purity', *BioTechniques*, 22(3), pp. 474–476, 478–481. doi:10.2144/97223st01.

Wilson, W.H. *et al.* (1995) 'Phase I and pharmacokinetic study of the multidrug resistance modulator dexverapamil with EPOCH chemotherapy', *Journal of Clinical Oncology: Official Journal of the American Society of Clinical Oncology*, 13(8), pp. 1985–1994. doi:10.1200/JCO.1995.13.8.1985.

Wittig, J.C. *et al.* (2002) 'Osteosarcoma: a multidisciplinary approach to diagnosis and treatment', *American Family Physician*, 65(6), pp. 1123–1132.

Wold, L.E. *et al.* (1984) 'High-grade surface osteosarcomas*':, *The American Journal of Surgical Pathology*, 8(3), pp. 181–186. doi:10.1097/00000478-198403000-00003.

Wong, H.L. *et al.* (2006) 'Simultaneous delivery of doxorubicin and GG918 (Elacridar) by new polymer-lipid hybrid nanoparticles (PLN) for enhanced treatment of multidrug-resistant breast cancer', *Journal of Controlled Release: Official Journal of the Controlled Release Society*, 116(3), pp. 275–284. doi:10.1016/j.jconrel.2006.09.007.

Wong, R.P.C. *et al.* (2007) 'p53-R273H gains new function in induction of drug resistance through down-regulation of procaspase-3', *Molecular Cancer Therapeutics*, 6(3), pp. 1054–1061. doi:10.1158/1535-7163.MCT-06-0336.

Wu, T., Gu, X. and Cui, H. (2021) 'Emerging Roles of SKP2 in Cancer Drug Resistance', *Cells*, 10(5), p. 1147. doi:10.3390/cells10051147.

Wu, X. *et al.* (2012) 'Expressions of p53, c-MYC, BCL-2 and apoptotic index in human osteosarcoma and their correlations with prognosis of patients', *Cancer Epidemiology*, 36(2), pp. 212–216. doi:10.1016/j.canep.2011.08.002.

Wu, Z.-Z., Lu, H.-P. and Chao, C.C.-K. (2010) 'Identification and functional analysis of genes which confer resistance to cisplatin in tumor cells', *Biochemical Pharmacology*, 80(2), pp. 262–276. doi:10.1016/j.bcp.2010.03.029.

Xiao, X. *et al.* (2018) 'HSP90AA1-mediated autophagy promotes drug resistance in osteosarcoma', *Journal of experimental & clinical cancer research: CR*, 37(1), p. 201. doi:10.1186/s13046-018-0880-6.

Xie, D. *et al.* (2001) 'Elevated levels of connective tissue growth factor, WISP-1, and CYR61 in primary breast cancers associated with more advanced features', *Cancer Research*, 61(24), pp. 8917–8923.

Xu, J., Guo, W. and Xie, L. (2018) 'Combination of gemcitabine and docetaxel: a regimen overestimated in refractory metastatic osteosarcoma?', *BMC cancer*, 18(1), p. 987. doi:10.1186/s12885-018-4872-x.

Xu, L. *et al.* (2020) 'The inhibition of MARK2 suppresses cisplatin resistance of osteosarcoma stem cells by regulating DNA damage and repair', *Journal of Bone Oncology*, 23, p. 100290. doi:10.1016/j.jbo.2020.100290.

Xu, Z., Mei, J. and Tan, Y. (2017) 'Baicalin attenuates DDP (cisplatin) resistance in lung cancer by downregulating MARK2 and p-Akt', *International Journal of Oncology*, 50(1), pp. 93–100. doi:10.3892/ijo.2016.3768.

Yamamoto, S. *et al.* (2009) 'Actinin-4 gene amplification in ovarian cancer: a candidate oncogene associated with poor patient prognosis and tumor chemoresistance', *Modern Pathology: An Official Journal of the United States and Canadian Academy of Pathology, Inc*, 22(4), pp. 499–507. doi:10.1038/modpathol.2008.234.

Yan, X.-D. *et al.* (2007) 'Biological comparison of ovarian cancer resistant cell lines to cisplatin and Taxol by two different administrations', *Oncology Reports*, 17(5), pp. 1163–1169.

Yang, C. *et al.* (2014) 'High-mobility group nucleosome-binding domain 5 increases drug resistance in osteosarcoma through upregulating autophagy', *Tumour Biology: The Journal of the International Society for Oncodevelopmental Biology and Medicine*, 35(7), pp. 6357–6363. doi:10.1007/s13277-014-1833-0.

Yang, J. *et al.* (2010) 'APEX1 gene amplification and its protein overexpression in osteosarcoma: correlation with recurrence, metastasis, and survival', *Technology in Cancer Research & Treatment*, 9(2), pp. 161–169. doi:10.1177/153303461000900205.

Yang, R. *et al.* (2003) 'Sequence alterations in the reduced folate carrier are observed in osteosarcoma tumor samples', *Clinical Cancer Research: An Official Journal of the American Association for Cancer Research*, 9(2), pp. 837–844.

Yang, R. *et al.* (2008) 'Polymorphisms and methylation of the reduced folate carrier in osteosarcoma', *Clinical Orthopaedics and Related Research*, 466(9), pp. 2046–2051. doi:10.1007/s11999-008-0323-3.

Yang, T.-T., Sinai, P. and Kain, S.R. (1996) 'An Acid Phosphatase Assay for Quantifying the Growth of Adherent and Nonadherent Cells', *Analytical Biochemistry*, 241(1), pp. 103–108. doi:10.1006/abio.1996.0383.

Yao, C. *et al.* (2012) 'Co-administration phenoxodiol with doxorubicin synergistically inhibit the activity of sphingosine kinase-1 (SphK1), a potential oncogene of osteosarcoma, to suppress osteosarcoma cell growth both in vivo and in vitro', *Molecular Oncology*, 6(4), pp. 392–404. doi:10.1016/j.molonc.2012.04.002.

Yao, C. *et al.* (2020) 'The therapeutic value of the SphK1-targeting microRNA-3677 in human osteosarcoma cells', *Aging*, 12(6), pp. 5399–5410. doi:10.18632/aging.102961.

Yasko, A.W. (2009) 'Surgical management of primary osteosarcoma', *Cancer Treatment and Research*, 152, pp. 125–145. doi:10.1007/978-1-4419-0284-9_6.

Yin, J. *et al.* (2007) 'Bufalin induces apoptosis in human osteosarcoma U-2OS and U-2OS methotrexate300-resistant cell lines', *Acta Pharmacologica Sinica*, 28(5), pp. 712–720. doi:10.1111/j.1745-7254.2007.00559.x.

Yin, Z. *et al.* (2000) 'Glutathione S-transferase p elicits protection against H2O2-induced cell death via coordinated regulation of stress kinases', *Cancer Research*, 60(15), pp. 4053–4057.

Ying, W. *et al.* (2012) 'ER-/ER+ breast cancer cell lines exhibited different resistance to paclitaxel through pulse selection', *Medical Oncology (Northwood, London, England)*, 29(2), pp. 495–502. doi:10.1007/s12032-011-9889-9.

Yoshikawa, A. *et al.* (1997) 'A mechanism of cisplatin action: antineoplastic effect through inhibition of neovascularization.', *The Kobe journal of medical sciences*, 43(3–4), pp. 109–120.

You, Y. *et al.* (2006) 'Design of LNA probes that improve mismatch discrimination', *Nucleic Acids Research*, 34(8), p. e60. doi:10.1093/nar/gkl175.

Youle, R.J. and Strasser, A. (2008) 'The BCL-2 protein family: opposing activities that mediate cell death', *Nature Reviews. Molecular Cell Biology*, 9(1), pp. 47–59. doi:10.1038/nrm2308.

Young, L. *et al.* (2010) 'Detection of Mycoplasma in cell cultures', *Nature Protocols*, 5(5), pp. 929–934. doi:10.1038/nprot.2010.43.

Yu, D. *et al.* (2019) 'Methotrexate, doxorubicin, and cisplatinum regimen is still the preferred option for osteosarcoma chemotherapy: A meta-analysis and clinical observation', *Medicine*, 98(19), p. e15582. doi:10.1097/MD.0000000000015582.

Yu, W.-X. *et al.* (2014) 'Comparison of pemetrexed plus cisplatin with gemcitabine plus docetaxel in refractory/metastatic osteosarcoma: Clinical outcomes from a retrospective database monitored in a single institute', *Oncology Letters*, 8(5), pp. 2243–2248. doi:10.3892/ol.2014.2472.

Yu, Y. *et al.* (2019) 'Establishment and characterization of the gemcitabine-resistant human pancreatic cancer cell line SW1990/gemcitabine', *Oncology Letters*, 18(3), pp. 3065–3071. doi:10.3892/ol.2019.10627.

Zeng, H. *et al.* (2001) 'Transport of methotrexate (MTX) and folates by multidrug resistance protein (MRP) 3 and MRP1: effect of polyglutamylation on MTX transport', *Cancer Research*, 61(19), pp. 7225–7232.

Zhang, F. *et al.* (2017) 'Simultaneous targeting of ATM and Mcl-1 increases cisplatin sensitivity of cisplatin-resistant non-small cell lung cancer', *Cancer Biology & Therapy*, 18(8), pp. 606–615. doi:10.1080/15384047.2017.1345391.

Zhang, H. *et al.* (2018) 'Silencing Lin28 promotes apoptosis in colorectal cancer cells by upregulating let-7c targeting of antiapoptotic BCL2L1', *Molecular Medicine Reports*, 17(4), pp. 5143–5149. doi:10.3892/mmr.2018.8483.

Zhang, P., Sun, Y. and Ma, L. (2015) 'ZEB1: at the crossroads of epithelial-mesenchymal transition, metastasis and therapy resistance', *Cell Cycle (Georgetown, Tex.)*, 14(4), pp. 481–487. doi:10.1080/15384101.2015.1006048.

Zhang, T. *et al.* (2015) 'The ATM inhibitor KU55933 sensitizes radioresistant bladder cancer cells with DAB2IP gene defect', *International Journal of Radiation Biology*, 91(4), pp. 368–378. doi:10.3109/09553002.2015.1001531.

Zhang, W. *et al.* (2015) 'Knockdown of autophagy-related protein 6, Beclin-1, decreases cell growth, invasion, and metastasis and has a positive effect on chemotherapy-induced cytotoxicity in osteosarcoma cells', *Tumor Biology*, 36(4), pp. 2531–2539. doi:10.1007/s13277-014-2868-y.

Zhang, Y. *et al.* (2018) 'Progress in the chemotherapeutic treatment of osteosarcoma', *Oncology Letters*, 16(5), pp. 6228–6237. doi:10.3892/ol.2018.9434.

Zhang, Y. and Weinberg, R.A. (2018) ‘Epithelial-to-mesenchymal transition in cancer: complexity and opportunities’, *Frontiers of Medicine*, 12(4), pp. 361–373. doi:10.1007/s11684-018-0656-6.

Zhang, Y.-K. *et al.* (2017) ‘Establishment and characterization of arsenic trioxide resistant KB/ATO cells’, *Acta Pharmaceutica Sinica. B*, 7(5), pp. 564–570. doi:10.1016/j.apsb.2017.04.001.

Zhang, Z. *et al.* (2009) ‘Expression of Beclin1 in osteosarcoma and the effects of down-regulation of autophagy on the chemotherapeutic sensitivity’, *Journal of Huazhong University of Science and Technology. Medical Sciences = Hua Zhong Ke Ji Da Xue Xue Bao. Yi Xue Ying De Wen Ban = Huazhong Keji Daxue Xuebao. Yixue Yingdewen Ban*, 29(6), pp. 737–740. doi:10.1007/s11596-009-0613-3.

Zhao, H.-C. *et al.* (2007) ‘p53-expressing conditionally replicative adenovirus CNHK500-p53 against hepatocellular carcinoma in vitro’, *World Journal of Gastroenterology*, 13(5), pp. 683–691. doi:10.3748/wjg.v13.i5.683.

Zhao, L., Zhang, W. and Zhang, F. (2021) ‘Poncirin downregulates ATP-binding cassette transporters to enhance cisplatin sensitivity in cisplatin-resistant osteosarcoma cells’, *Phytotherapy research: PTR*, 35(1), pp. 278–288. doi:10.1002/ptr.6798.

Zhao, Y. *et al.* (2009) ‘Enhanced chemosensitivity of drug-resistant osteosarcoma cells by lentivirus-mediated Bcl-2 silencing’, *Biochemical and Biophysical Research Communications*, 390(3), pp. 642–647. doi:10.1016/j.bbrc.2009.10.020.

Zheng, T. *et al.* (2010) ‘Nutlin-3 cooperates with doxorubicin to induce apoptosis of human hepatocellular carcinoma cells through p53 or p73 signaling pathways’, *Journal of Cancer Research and Clinical Oncology*, 136(10), pp. 1597–1604. doi:10.1007/s00432-010-0817-8.

Zhou, J. *et al.* (2010) 'Modulation of the ribonucleotide reductase-antimetabolite drug interaction in cancer cell lines', *Journal of Nucleic Acids*, 2010, p. 597098. doi:10.4061/2010/597098.

Zhu, H. *et al.* (2005) 'Involvement of hypoxia-inducible factor-1-alpha in multidrug resistance induced by hypoxia in HepG2 cells', *Journal of experimental & clinical cancer research: CR*, 24(4), pp. 565–574.

Zhu, K.-P. *et al.* (2015) 'Long noncoding RNA expression profiles of the doxorubicin-resistant human osteosarcoma cell line MG63/DXR and its parental cell line MG63 as ascertained by microarray analysis', *International Journal of Clinical and Experimental Pathology*, 8(8), pp. 8754–8773.

Zhu, Z.-A. *et al.* (2012) 'Reversion of multidrug resistance by SKI-II in SGC7901/DDP cells and exploration of underlying mechanisms', *Asian Pacific journal of cancer prevention: APJCP*, 13(2), pp. 625–631. doi:10.7314/apjcp.2012.13.2.625.

Appendix 1

Middlesex University London

Natural Science REC

The Burroughs
Hendon
London NW4 4BT

Main Switchboard: 0208 411 5000

08/05/2018

APPLICATION NUMBER: 4088

Dear Kaan Low

Re your application title: Drug Resistance Osteosarcoma Cell Lines

Supervisor: Britta Frank Helen Hills Roberts Stordal

Co-investigators/collaborators:

Thank you for submitting your application. I can confirm that your application has been given approval from the date of this letter by the Natural Science REC.

Although your application has been approved, the reviewers of your application may have made some useful comments on your application. Please look at your online application again to check whether the reviewers have added any comments for you to look at.

Also, please note the following:

1. Please ensure that you contact your supervisor/research ethics committee (REC) if any changes are made to the research project which could affect your ethics approval. There is an Amendment sub-form on MORE that can be completed and submitted to your REC for further review.

2. You must notify your supervisor/REC if there is a breach in data protection management or any issues that arise that may lead to a health and safety concern or conflict of interests.

3. If you require more time to complete your research, i.e., beyond the date specified in your application, please complete the Extension sub-form on MORE and submit it your REC for review.

4. Please quote the application number in any correspondence.

5. It is important that you retain this document as evidence of research ethics approval, as it may be required for submission to external bodies (e.g., NHS, grant awarding bodies) or as part of your research report, dissemination (e.g., journal articles) and data management plan.

6. Also, please forward any other information that would be helpful in enhancing our application form and procedures - please contact MOREsupport@mdx.ac.uk to provide feedback.

Good luck with your research.

Yours sincerely

Chair Mr Adam Choonara

Natural Science REC